Multipurpose Modular UAV with Combat, Transport, Surveillance, and Decoy Capabilities

a report presented to

The Faculty of the Department of Aerospace Engineering

San José State University

in partial fulfillment of the requirements for

Master of Science in Aerospace Engineering

by

Jason Sagara

May 2024

Approved by

Mr. Sean Montgomery

Faculty Advisor

San José State University

ABSTRACT

Multipurpose Modular UAV with Combat, Transport, Surveillance, and Decoy Capabilities

Jason Sagara

As the aerospace industry continues to grow, it will become necessary to cut costs in spending to continue its growth. A UAV that can accomplish various missions by changing its configuration with a modular approach would reduce overall spending when compared to using a different UAV for each mission. To validate this, certain aspects of the aircraft such as landing gear location were shared across configurations while other aspects were varied depending on the mission type. This was accomplished by using the methods for aircraft design described by Roskam and Raymer in their respective textbooks. Models and calculations were completed with assistance from the following programs: OpenVSP, RDS, XFLR5, and MATLAB.

ACKNOWLEDGEMENTS

I would like to thank Professor Sean Montgomery for his assistance during the project. His feedback and encouragement, even from the first week of working on this project, was helpful in completing this project. I would also like to thank my family for their continued support of my education during my pursuit of a master's degree.

Table of Contents

List of Figures xii
List of Tables xiv
Symbols..... xvi
1. Mission Specification and Comparative Study..... 1
  1.1 Introduction 1
  1.2 Literature Review..... 1
  1.3 Project Objective 6
  1.4 Methodology 6
  1.5 Mission Specifications 6
    1.5.1 Mission Requirements 6
    1.5.2 Mission Profile..... 7
    1.5.3 Critical Mission Requirements 8
  1.6 Comparative Study of Similar Aircraft 8
  1.7 Discussion 9
2. Weight Sizing..... 10
  2.1 Initial Weight Sizing 10
  2.2 Discussion 12
  2.3 Conclusion..... 12
3. Performance Constraint Analysis 13
  3.1 Introduction 13
  3.2 Calculations..... 13
  3.3 Constraint Diagrams..... 14
  3.4 Discussion 16
  3.5 Conclusion..... 16
4. Configuration Selection 17
  4.1 Introduction 17
  4.2 Selection of Propulsion System 17
    4.2.1 Selection of Propulsion System Type..... 17
    4.2.2 Selection of Number of Engines..... 17
    4.2.3 Propeller Sizing..... 17
  4.3 Configuration Selection..... 18

4.3.1 Overall Configuration 18
4.3.2 Wing Configuration 18
4.3.3 Empennage Configuration 18
4.3.4 Landing Gear Disposition 19
4.3.5 Proposed Configuration 19
5. Fuselage Design 21
5.1 Introduction 21
5.2 Layout Design of Fuselage 21
5.3 Discussion 22
6. Wing Design 23
6.1 Introduction 23
6.2 Wing Planform Design 23
6.3 Airfoil Selection 23
6.4 Wing Sizing Calculations 25
6.5 Fuel Tank Dimensions 26
6.6 Wing Drawings 26
6.7 High Lift Devices 27
6.8 Discussion 29
7. Empennage Design 30
7.1 Introduction 30
7.2 Overall Empennage Design 30
7.3 Design of the Horizontal Stabilizer 32
7.4 Design of the Vertical Stabilizer 32
7.5 CAD Drawings 33
7.6 Discussion 35
8. Landing Gear Design 36
8.1 Introduction 36
8.2 Estimation of the Center of Gravity Location for the Aircraft 36
8.3 Landing Gear Design 36
8.3.1 Number, type and size of tires 36
8.3.2 Preliminary arrangement 36
8.3.3 Retraction feasibility 36

8.3.4 Clearance angles 37
8.4 Discussion 40
9. Weight and Balance Analysis 41
9.1 Introduction 41
9.2 Component Weight Breakdown 41
9.3 Center of Gravity Location for Various Loading Scenarios 43
9.4 Discussion 45
10. Stability and Control Analysis 46
10.1 Introduction 46
10.2 Static Margin 46
10.3 Discussion 47
11. Drag Polar Estimation 48
11.1 Introduction 48
11.2 Airplane Drag Polars and Low Speed Drag Increments 48
11.3 Discussion 50
12. Drawings, Environmental and Safety Considerations 51
12.1 Drawings 51
12.2 Environmental Considerations 51
12.3 Safety Considerations 52
13. Airplane Subsystem Arrangement 53
13.1 Flight Controls System 53
13.2 Propulsion System 53
13.3 Fuel System Layout Design 54
13.4 Hydraulic System Layout Design 56
13.5 Electrical System Layout Design 57
13.6 Environmental Control System 58
13.7 Ground Station Instrumentation and Avionics System 58
13.8 Escape System/Emergency System 59
13.9 Discussion 59
14. Initial Structural Arrangement 60
14.1 Introduction 60
14.2 Structural Drawings 60

14.3 Discussion 62
15. V-n Diagram 63
15.1 Introduction 63
15.2 V-n Diagrams 63
15.3 Discussion 65
16. Weight and Balance Analysis – Class II 66
16.1 Introduction 66
16.2 Component Weight Breakdown 66
16.3 CG Excursion Diagrams 71
16.4 Discussion 73
17. Stability and Control Analysis – Class II 74
17.1 Trim Diagram 74
17.2 Discussion 75
18. Drag Polar Estimation – Class II 76
18.1 Introduction 76
18.2 Component Drag Polar Buildup 76
18.3 Discussion 84
19. Installed Power Characteristics 85
19.1 Introduction 85
19.2 Installed Power 85
19.3 Discussion 85
20. Critical Performance Requirements 86
20.1 Mission Requirements 86
20.2 Performance Calculations 86
20.3 Discussion 89
21. Final 3-View and Subsystem Drawings 90
21.1 Final 3-View 90
22. Cost Analysis 98
22.1 Introduction 98
22.2 Design and Development Cost 98
22.3 Manufacturing Cost 98
22.4 Operating Cost 100

22.5 Discussion 101
23. Conclusions 102
23.1 Discussion 102
References 103
Appendix A – Constraint Diagram 106
A.1 Equations 106
A.2 Cargo 108
A.3 Combat 110
A.4 Surveillance 112
A.5 Decoy 114
Appendix B - Wing Design 116
B.1 Wing Design Equations 116
B.2 Cargo 116
B.3 Combat 116
B.4 Surveillance 117
B.5 Decoy 117
B.6 High Lift Devices Equations 118
B.7 Cargo 119
B.8 Combat 120
B.9 Surveillance 121
B.10 Decoy 122
Appendix C - Weight and Balance Analysis 123
C.1 Cargo 123
C.2 Combat 124
C.3 Surveillance 125
C.4 Decoy 126
Appendix D - Stability and Control Analysis 127
D.1 Cargo 127
D.2 Combat 128
D.3 Surveillance 129
D.4 Decoy 130
D.5 Landing gear tire sizing equation 131

D.6 Landing gear tire sizing for cargo 132
D.7 Landing gear tire sizing for combat 132
D.8 Landing gear tire sizing for surveillance 133
D.9 Landing gear tire sizing for decoy 133
Appendix E - Drag Polar Estimation 134
E.1 Equations 134
E.2 Cargo 135
E.3 Combat 136
E.4 Surveillance 137
E.5 Decoy 138
Appendix F - V-n Diagram 139
F.1 Equations 139
F.2 Cargo 140
F.3 Combat 141
F.4 Surveillance 142
F.5 Decoy 143
Appendix G - Weight and Balance Analysis Class II 144
G.1 Equations 144
G.2 Cargo 145
G.3 Combat 146
G.4 Surveillance 147
G.5 Decoy 148
Appendix H - Stability and Control Analysis 149
H.1 Equations 149
Appendix I - Drag Polar Estimation Class II 154
I.1 Equations 154
I.2 Cargo 155
I.3 Combat 156
I.4 Surveillance 157
I.5 Decoy 158
Appendix J - Installed Power 159
J.1 Equations 159

J.2 Values 160
Appendix K - Performance Calculations 161
K.1 Equations 161
K.2 Cargo 163
K.3 Combat 165
K.4 Surveillance 167
K.5 Decoy 169
Appenndix L - Cost Analysis 171
L.1 Equations 171
L.2 Results 177

List of Figures

Figure 1-1 Surveillance and decoy mission profile 7
Figure 1-2 Cargo and combat mission profile 8
Figure 5-1 Top view of the fuselage 21
Figure 5-2 Side view of the fuselage 21
Figure 6-1 NACA 23012 airfoil shape 23
Figure 6-2 NACA 23012 polar plots [28] 24
Figure 6-3 Wing of the cargo configuration 26
Figure 6-4 Wing of the combat configuration 26
Figure 6-5 Wing of the surveillance configuration 26
Figure 6-6 Wing of the decoy configuration 27
Figure 6-7 High lift devices on cargo wing 28
Figure 6-8 High lift devices on combat wing 28
Figure 6-9 High lift devices on surveillance wing 28
Figure 6-10 High lift devices on decoy wing 28
Figure 7-1 NACA 0012 airfoil shape 30
Figure 7-2 NACA 0012 polar plots [28] 31
Figure 7-3 Cargo Transport CAD model with empennages 33
Figure 7-4 Combat CAD model with empennages 34
Figure 7-5 Surveillance CAD model with empennages 34
Figure 7-6 Decoy CAD model with empennages 35
Figure 8-1 Landing gear in stowed configuration 37
Figure 8-2 Longitudinal tip over angle 38
Figure 8-3 Longitudinal ground clearance angle 39
Figure 8-4 Lateral ground clearance angle 39
Figure 8-5 Lateral tip over angle 40
Figure 9-1 Cargo CG locations for empty, payload and fuel, just payload, and just fuel loading scenarios 43
Figure 9-2 Combat CG locations for empty, payload and fuel, just payload, and just loading scenarios 44
Figure 9-3 Surveillance CG locations for empty, payload and fuel, just payload, and just loading scenarios 44
Figure 9-4 Decoy CG locations for payload and fuel, just payload, and just loading scenarios 45
Figure 11-1 C_l vs C_d plot 49
Figure 11-2 C_l vs angle of attack plot 50
Figure 12-1 Updated CAD model for the cargo configuration 51
Figure 13-1 Continental GSIO-520-D [32] 53
Figure 13-2 Fuel tanks for the cargo configuration 54
Figure 13-3 Fuel tanks for the combat configuration 55
Figure 13-4 Fuel tanks for the surveillance configuration 55
Figure 13-5 Fuel tanks for the decoy configuration 56
Figure 13-6 Hydraulic Lines 57

Figure 13-7 Battery locations.. 58
Figure 14-1 Fuselage internal array layout 60
Figure 14-2 Wing internal spar and rib layout.. 61
Figure 14-3 Horizontal stabilizer spar and rib layout 61
Figure 14-4 Vertical stabilizer spar and rib layout 62
Figure 15-1 V-n diagram for cargo configuration 63
Figure 15-2 V-n diagram for combat configuration 64
Figure 15-3 V-n diagram for surveillance configuration... 64
Figure 15-4 V-n diagram for decoy configuration... 65
Figure 16-1 Component breakdown by weight (cargo).. 67
Figure 16-2 Component breakdown by weight (combat)... 68
Figure 16-3 Component breakdown by weight (surveillance) 69
Figure 16-4 Component breakdown by weight (decoy) 70
Figure 16-5 CG excursion diagram for the cargo configuration...................................... 71
Figure 16-6 CG excursion diagram for the combat configuration................................... 72
Figure 16-7 CG excursion diagram for the surveillance configuration 72
Figure 16-8 CG excursion diagram for the decoy configuration..................................... 73
Figure 17-1 Trim diagram.. 74
Figure 17-2 C_{m_cg} vs C_L plot 75
Figure 18-1 Component breakdown by drag for cargo configuration 78
Figure 18-2 Component breakdown by drag for combat configuration 80
Figure 18-3 Component breakdown by drag for surveillance configuration................... 82
Figure 18-4 Component breakdown by drag for decoy configuration 84
Figure 20-1 Takeoff distance [27] 86
Figure 20-2 Landing distance [27]... 87
Figure 21-1 Final 3-view of the cargo configuration... 90
Figure 21-2 Final CAD model for the cargo configuration 91
Figure 21-3 Final 3-view of the combat configuration.. 92
Figure 21-4 Final CAD model for the combat configuration 93
Figure 21-5 Final 3-view of the surveillance configuration 94
Figure 21-6 Final CAD model for the surveillance configuration................................... 95
Figure 21-7 Final 3-view of the decoy configuration 96
Figure 21-8 Final CAD model for the decoy configuration 97
Figure 22-1 Selling price vs units produced (Raymer method)....................................... 99
Figure 22-2 Selling price vs units produced (Snorri method).. 99
Figure 22-3 Selling price vs units produced (Nicolai method)...................................... 100

List of Tables

Table 1.1 Performance parameters of BN-2 Islander [25] ... 8
Table 2.1 RDS input for cargo transport ... 10
Table 2.2 RDS input for combat ... 10
Table 2.3 RDS input for surveillance ... 11
Table 2.4 RDS input for decoy ... 11
Table 2.5 RDS initial weight sizing ... 12
Table 6.1 Wing sizing inputs ... 23
Table 6.2 Wing sizing results ... 25
Table 6.3 Fuel tank size ... 26
Table 6.4 High lift devices sizing ... 27
Table 6.5 Lift coefficients for various scenarios ... 27
Table 6.6 Flap deflection angles ... 27
Table 7.1 Horizontal stabilizer volume coefficients ... 32
Table 7.2 Horizontal stabilizer sizing results ... 32
Table 7.3 Vertical stabilizer volume coefficients ... 32
Table 7.4 Vertical stabilizer sizing results ... 32
Table 8.1 Clearance angles of cargo configuration ... 37
Table 8.2 Clearance angles of combat configuration ... 37
Table 8.3 Clearance angles of surveillance configuration ... 38
Table 8.4 Clearance angles of decoy configuration ... 38
Table 9.1 Component weight breakdown and CG locations for cargo configuration ... 41
Table 9.2 Component weight breakdown and CG locations for combat configuration ... 41
Table 9.3 Component weight breakdown and CG locations for surveillance configuration ... 42
Table 9.4 Component weight breakdown and CG locations for decoy configuration ... 42
Table 10.1 Stability of cargo configuration ... 46
Table 10.2 Stability of combat configuration ... 46
Table 10.3 Stability of surveillance configuration ... 47
Table 10.4 Stability of decoy configuration ... 47
Table 11.1 Drag estimation of cargo configuration ... 48
Table 11.2 Drag estimation of combat configuration ... 48
Table 11.3 Drag estimation of surveillance configuration ... 48
Table 11.4 Drag estimation of decoy configuration ... 49
Table 16.1 Weight breakdown of cargo configuration ... 66
Table 16.2 Weight breakdown of combat configuration ... 67
Table 16.3 Weight breakdown of surveillance configuration ... 68
Table 16.4 Weight breakdown of decoy configuration ... 69
Table 16.5 CG of various loading scenarios for cargo configuration ... 70
Table 16.6 CG of various loading scenarios for combat configuration ... 70
Table 16.7 CG of various loading scenarios for surveillance configuration ... 71
Table 16.8 CG of various loading scenarios for decoy configuration ... 71
Table 18.1 Class I drag estimation for cargo configuration ... 76

Table 18.2 Component drag build up for cargo configuration 77
Table 18.3 Class I drag estimation for combat configuration.. 78
Table 18.4 Component drag build up for combat configuration 79
Table 18.5 Class I drag estimation for surveillance configuration 80
Table 18.6 Component drag build up for surveillance configuration 81
Table 18.7 Class I drag estimation for decoy configuration 82
Table 18.8 Component drag build up for decoy configuration 83
Table 19.1 Installed power per engine 85
Table 19.2 Power available compared to power required 85
Table 20.1 Performance of cargo configuration 87
Table 20.2 Performance of combat configuration 88
Table 20.3 Performance of surveillance configuration 88
Table 20.4 Performance of decoy configuration 89
Table 21.1 Cargo configuration information 91
Table 21.2 Combat configuration information 93
Table 21.3 Surveillance configuration information 95
Table 21.4 Decoy configuration information 97
Table 22.1 Developmental cost estimation from Roskam 98
Table 22.2 Manufacturing cost estimation from Snorri 98
Table 22.3 Direct operating cost estimation from Roskam 100
Table 22.4 Direct operating cost comparison 100

Symbols

Symbol	Definition	Units (SI)
A	Aspect ratio	
b	Span	ft (m)
C	Chord	ft (m)
C_{fe}	Skin friction coefficient	
C_l	Coefficient of lift	
C_d	Coefficient of drag	
D	Drag	
h	Height	ft (m)
I_P	Power index	
L	Lift	
L_{HT}	Moment arm of the horizontal stabilizer	ft (m)
L_{VT}	Moment arm of the vertical stabilizer	ft (m)
P	Power	HP (KW)
S	Wing area	ft^2 (m^2)
v	Velocity	knot (km/h)
W	Weight	lb (kg)
Greek Symbols		
Δ	Change	
θ	Angle	°, rad
λ	Taper ratio	
ρ	Density	$slug/ft^3$ (kg/m^3)
σ	Air stream density	$slug/ft^3$ (kg/m^3)
Ψ	Lateral tip over angle	°, rad
Subscripts		
$()_{23}$	FAR 23 requirement	
$()_a$	Aft	
$()_f$	Forward	
$()_G$	Ground	
$()_H$	Horizontal tail	
$()_L$	Landing	
$()_{MAX}$	Maximum	
$()_{OPS}$	Operating	
$()_{REF}$	Reference area	ft^2 (m^2)
$()_S$	Stall	
$()_{SL}$	Sea level	
$()_{TO}$	Takeoff	
$()_V$	Vertical tail	

Symbol	**Definition**	**Units (SI)**
Subscripts		
$()_{WET}$	Wetted area	ft^2 (m^2)
$()_X$	X axis	
$()_Z$	Z axis	
Acronyms		
A/C	Air Conditioning	
AGM	Air to Ground Missile	
BFL	Balanced Field Length	
CAD	Computer Assisted Drawing	
CG	Center of Gravity	
CPI	Consumer Price Index	
CPU	Central Processing Unit	
DOC	Direct Operating Cost	
FAR	Federal Aviation Regulation	
FEA	Finite Element Analysis	
GPS	Global Positioning System	
I/O	Input/Output	
MAC	Mean Aerodynamic Chord	
OEI	One Engine Inoperable	
QDF	Quantity Discount Factor	
SM	Static Margin	
UAV	Unmanned Aerial Vehicle	
XNP	X-axis Neutral Point	

1. Mission Specification and Comparative Study

1.1 Introduction

As the aerospace industry grows, the design and manufacturing costs will similarly grow. The global aerospace industry is expected to grow an additional $80 billion in the next four years [1]. A study from 2004 showed that as the aerospace industry has matured, manufacturers were not able to develop all aspects of the aircraft in-house [2]. This led to other companies being contracted to focus on specific aspects of manufacturing. As a result of this, the supply chains would increase to account for the new companies that specialized in a specific aspect. The original equipment manufacturers used to be the focal point of the supply chains, but as the industry became more global, third parties were necessary to keep up with the workload and productivity. Third parties were then able to increase their market value as they became proficient at their specialized work. This has led to an overall lower financial risk as they became separate operating entities, but further increased costs in manufacturing [2]. To reduce overall spending on design and manufacturing, a multipurpose modular UAV will be designed that can be used across various types of missions. While not a new concept, modular UAVs are typically modular in their sensor setup or ability to combine with other UAVs to increase performance. The modular UAV that will be designed in this project will have a common fuselage with wings, avionics suites, cargo bay configurations, and empennages that will be swapped out depending on the mission profile. Similar to a camera that can swap lens, sensors, or outputs, this UAV will be able to change depending on what is required of it. This adaptability should prove useful in a military setting as the status quo can change in the blink of an eye. To incorporate a modular design, systems will need to be able to function independently for both software and hardware. This would make maintenance easier, and in turn make a modular design more reliable than a traditional one. Since the UAV will share aspects across all four designs, the overall cost during design and manufacturing should be lowered.

1.2 Literature Review

Introducing modularization can lead to oversizing and a possible increase in weight due to the interacting interfaces [3]. Lowering the weight can be achieved by changing materials (composites), reducing connection points for the modularization, or integrating additional uses through the structures [3]. When considering a multipurpose design, the separate purposes should be designed simultaneously and not consecutively. This results in a continuous exchange of information between the two instead of one being designed first and used as the baseline to adjust the second. This can be achieved by firmly defining the requirements early on so the proper constraints can be applied to both. After this, both designs can be harmonized to achieve a lightweight, modular aircraft. This can be done iteratively, with gradual changes being introduced. In a similar project, a morphing wing was designed to improve aerodynamic performance by varying the airfoil camber in varying operating conditions [4]. The morphing wing was created to be fully modular so aspects could be removed or replaced without the wing needing to be entirely reprinted. The morphing wing was comprised of five main sections: a spine, stringers, two skin surfaces, a tendon, and a trailing edge tab. The flexible spine was placed at the trailing edge of the airfoil. Stringers were placed span wise to provide additional support without increasing the stiffness in the direction of the morph. The morphing wing was able to change the lift coefficient by 0.55 with varying camber distribution [4]. While the article is focused more on varying the camber, this project is focused on swapping out the entirety of the wing for a different wing that would be more relevant to the specific mission. Another similar study was focused on designing a flexible, modular wing [5]. The wing was comprised of a single aluminum spar with four separate sections that connect to the main spar at a single point. This design was modular so the control surfaces could be altered between one and four surfaces. The main spar was connected to the additional surfaces by two pins at the mid span of the section. While the modular section of this wing in this article is different than the one planned for this project, the manner in which it is assembled and connected is similar.

While researching for modular UAVs that focused on the wing being modular, a relevant patent was found that described a modular monoplane. The UAV defined in this patent is capable of being used for reconnaissance, surveillance, and data acquisition [6]. Using a minimal amount of tools, this monoplane could be assembled to combine two sections of the fuselage, two horizontal stabilizers, and four wing sections. The UAV could also be altered to use either two or four wing sections depending on the mission profile. Being modular, the UAV could be disassembled for easier storage and being easily repairable as a damaged section can be switched out for a new one. The UAV is capable of carrying two standard volume weight boxes. The payload hatch can be increased to allow for easier loading and unloading. The UAV engine mount is long enough to account for various types of engines. The engine mount can also be lengthened to accommodate the center of gravity changes that may occur as a result of a heavier engine being used. Aside from being published in 2011, it does not appear that any additional updates or studies have been completed.

Similar studies have been conducted on varying the configurations for unmanned cargo aircraft. One study focused on just configurations with wing tunnel testing [7]. Three configurations were used in the testing for this study: a double trail boom fixed wing, a box wing, and a gyrocopter. Wind tunnel testing and dynamic simulations were performed to compare their performance in a cargo transport setting. However, each configuration used a different fuselage and didn't share many aspects between each configuration. Similar tests were performed, although the gyrocopter required a scaled down model for testing. Similar to this article, the UAV designed in this project will compare various configurations to justify the modular nature of the UAV. To reduce possible sources of error, the fuselage will remain the same across all four configurations. Another study focused on varying the wingspan in addition to changing the overall configuration [8]. In this study, five fixed-wing aircraft and two rotorcraft were chosen. For the fixed-wing aircraft, the convention of the wing span was varied. A conventional configuration, a canard configuration, a twin boom configuration, a biplane configuration, and a box wing configuration were used. For the rotorcraft, a helicopter and gyrocopter were compared with each other. The cruise drag coefficient, wing loading, wing area, maximum takeoff mass and fuel mass were generated and compared. For a cargo mission, the twin boom and box wing configurations were found to be better suited for transportation. The gyrocopter was the better performing of the rotorcraft. This study was further expanded upon by introducing a payload [9]. It used the same configurations from the previous study (conventional, canard, twin-boom, biplane, and box wing). Assuming a payload of one ton, and operating in the lower air space with low takeoff and landing distances. The flight performance data of the five were compared with each other in addition to the data of a helicopter and gyrocopter. Aside from the twin-boom, the fuselage was kept consistent across the other four configurations. It was found that for the fixed-wing aircraft, all were capable of completing the mission, but takeoff and landing distance requirements were not reached for all configurations. A means of fixing these issues is the introduction of supplementary electrically driven propellers. The gyrocopter outperformed the helicopter in testing. In the end, the box wing and twin-boom configurations were chosen for further investigations.

A main advantage in this modular UAV design is that the fuselage will remain constant across the four variations. A study from April 2023 showed that the fixtures used to manufacture parts of the fuselage can account for more than 50% of the workload for the production lifecycle [10]. Just designing and producing the fixtures for this can cost 10-20% of the overall production cost [10]. The sections of the fuselage that are manufactured separately and attached were shown as being comprised of 9 sections. Sections 1-2 are the cockpit, sections 3-4 are from the cockpit to the wing, section 5 is the wing location of the fuselage, sections 6-8 being the area immediately following the wing, with section 9 being the location of the stabilizers. Keeping sections of the fuselage as the baseline for the modularization will result in a lower manufacturing cost compared to other aircraft that require new fixture assemblies.

Incorporating a modular approach can also save costs during the design phase. Modular architecture allows for flexibility in designs and manufacturing by separating the components into independent modules [11]. Commonality across modular products allows for parts to be unified and to make manufacturing simpler. Stretch-based aircraft design allows for changes in the length of the fuselage, wings, or engine to be applied across the entirety of the design [11]. Increasing the fuselage length would in turn result in the main wing being stretched while maintaining the same aspect ratio. The horizontal and vertical stabilizers would be adjusted similarly. Stretching and replacing parts results in mutual, positive side effects that further optimize the design. Further optimization can be achieved by locking a specific requirement and increasing or decreasing another. The modular variants can be compared against these two variables to determine the optimal design for the stated requirements. Another study suggested that a modular approach requires a well-thought-out approach that may require additional planning during the design phase, but can bring reductions in cost and time in the long run [2]. Introducing modularity into the airframe lowers costs, allows for quick repairs, permit interconnected optimization, and enables wide customization [2]. A modular aircraft can be optimized for a specific mission or payload while being flexible enough to account for possible changes. Modularity can come at the cost of increasing weight, additional complexity, and reduced structural strength. It can also enable piecewise customization of the aircraft that would not be possible with a non-modular aircraft.

A modular design for a UAV allows for the ability to continually improve and adapt the system for various tasks. This can reduce the time and cost of development due to the nonspecific nature in which it is designed [12]. UAVs are traditionally complex with systems being intertwined and dependent on each other. A modular design can reduce complexity by having systems function independent of each other, and in turn reduce the chance of a singular point of failure being fatal. One particular study used a modular approach for the design of the landing module [12]. This allowed the UAV to have a traditional landing module or an amphibious one depending on the mission, increasing its possible coverage. Another study followed a similar approach, but the modularity was more incorporated into the design [13]. In this study, a modular UAV platform was designed to reduce development time between multiple missions. Three frames were designed to be used as the baseline for the modular commonality with each frame being bigger than the previous. The UAV legs were modularly designed so they could also be used to hold various equipment in addition to its traditional use. The legs could be swapped out for different missions or if damaged. The modular design allowed for a quick turnaround time during initial design and testing as various aspects could be adjusted if problems were found during testing. This came at the cost of requiring more electrical components as the modules need to be independent of each other to be truly modular [13].

A similar dissertation was found that focused on a multi-rotor UAV in the context of military operations [14]. The modular nature that this dissertation goes over is by changing aspects of the UAV to adjust the flight time, size, weight, and payload capabilities. The hardware that was changed included the motors, propellers, controllers, and batteries. These changes could be made quickly and easily without tools. The framework of the UAV was the focus of the modularity with the end user being able to pick a specific set of modules for their mission. While similar in nature, this dissertation was focused purely on cargo missions. One of the modular components of this project includes the avionics. A study into the history of modular avionics showed that a modular approach emphasizes change that can evolve and grow [15]. For the software, a layered modular architecture is used to hide hardware and programs from each other and enable code to be reused across the system. Programs can be updated or altered without impacting the entire CPU. Modular avionics in the Gulfstream G500/600 reduced the cables and parts for the system while increasing the redundancy and maintainability [15]. This was accomplished by portioning the software so multiple critical level applications could be run simultaneously on the same core processor [15]. Each I/O was decoupled so each system could function independently. Additional points of focus for modular avionics include dual use modules that while function independently, can combine their processing power to increase performance. Integrating these dual modules would require additional planning during the design phase, but could drastically increase the capabilities of the avionics [15].

In a military setting, the adaptability of a modular UAV would prove highly beneficial. When it comes to mission planning, adaptability is highly valued [16]. Enough so that missions are often planned assuming that the odds of completing every objective in a single mission is highly unlikely [16]. With such an unstable environment, a UAV that can be adjusted on the fly to better suit a new objective would be desirable. The safety of a UAV would also be highly valued as it removes the pilot from the cockpit of the aircraft. During operation Desert Storm, UAVs were successful in collecting intel in areas that would've been too dangerous for a human pilot [16]. Being able to closely monitor areas with hidden explosives without a possible loss of life is only achievable with a UAV.

The last focus of this review is centered on the reliability of modular systems. UAVs were reported to crash at higher percentage than manned aircraft [17]. This was a result of a lack of redundancy and poor reliability growth tests. Since military UAV are exposed to more threats as a result of being unmanned, they are shot down more often [17]. A cost analysis showed that because of this, the reliability of the UAV doesn't need to be as high as traditional aircraft. Costs of military UAV can range from $260,000 to $20,000,000 which is still much cheaper than an F-22 which is upwards of $100,000,000 [17]. This new context showed that military UAVs were much more reliable than initially thought of. Mechanical defects and communications errors were the most common cause of failure aside from external attacks, both of which can be addressed through redundancy. This redundancy could be addressed by a modular approach, as the components being swapped out must be able to function on their own without being too incorporated into other components. This can be accomplished on both a hardware and software level. For the hardware, a backplane bus can be used to separate power sources. For the software, a partitioning system is required to ensure that each program is fully isolated [18]. Components would be separated enough that a specific software could be updated independently even using a common CPU or I/O [18]. Modular architecture allows for ease of maintenance and reduction in the time between each maintenance intervals due to the increased fault visibility. This functional independence ensures that a failure in one system would not result in a similar failure in another. While each system should be physically separated, they still need to communicate with each other. This results in more computing resources being used just to communicate between these systems [19]. During the infancy of the UAV industry, this separation of systems led to payload sizes being only a few kilograms [19]. To find some kind of balance between independency and functionality, partitioning principles could be used for processing and communications. By allocating set amounts of processing power, a single processor could be used by multiple systems independently [19]. The processing modules could be added for additional capabilities or updated to improve software stability. Rather than completely overhauling the entire UAV, the processor could be swapped out or updated to improve the UAV. This would result in a lowering of operating and manufacturing costs [19].

This approach of physically separating systems could be found in a study that focused on a modular UAV with a multi-objective mission [20]. To carry out multiple types of missions, a modular design was used to carry multiple kinds of sensors to monitor various air pollutants [20]. A data fusion module was used to connect GPS coordinates with the collected data. Keeping this data onboard decreased the overall power consumption as there was no need to wirelessly transmit the data. Standardizing the design allowed for the sensors to be swapped out if a different kind of air pollutant needed to be monitored. The nature of the modular design in this study is similar to what is planned for the avionics and communications module. A surveillance mission would require a different set of sensors and avionics than a mission focused purely on transport.

Due to a lack of research in a UAV with modular wings that can be swapped out for better performance, another option for adjustable wings is in the form of a folding wing. In one particular study, the foldable wing was made up of two wing segments that could be expanded upon to a total of four wing segments [21]. Each wing was made up of a cantilevered inboard wing segment in addition to one or more outboard wing segments [21]. The segments were connected by torsional springs. The three wing configurations were tested at various fold angles and speeds to accurately model the physics of a folding wing. This study was continued to model the structural dynamics of the folding wing as well [22]. Additional studies were found on the topic of folding wings, including the flutter characteristics and manufacturing of a full size wing [23] [24]. Although these studies focused on a folding wing with a single segment that is foldable. Testing was performed to determine the vibration characteristics at first-order bending and first-order torsion. This was repeated for second-order testing in addition to testing at various folding angles. While still relatively new, folding wings are continuously being studied to one day be ready for real world use.

1.3 Project Objective

The focus of this project is to design a modular UAV that can be used across varying missions. The UAV will be used in a military setting. These missions include: surveillance, transport, combat, and decoy. The plan is to use a fuselage that is common across all four variations. The modular aspect will be focused on the wings, horizontal and vertical stabilizers, avionics suite, and internal configuration of the fuselage. Since the fuselage will be kept the same, the landing gear will have to be designed so that it provides proper support and balance across the four designs. More specifically, the location and type of landing gear will not change across configurations. This may result in some challenges but landing gear will be adjusted until the lateral and longitudinal stability of all four configurations is stable. The engine may be varied across the four designs, although it would require additional analysis before this decision is finalized. To justify the modular nature of the UAV, the aerodynamic performance of each variation will be compared for each mission type.

1.4 Methodology

To validate the four modular designs, XFLR5 and RDS-win will be used. XFLR5 focused primarily on the aerodynamic characteristics of the wing. The fuselage will remain the same across the four designs, which can be used in XFLR5, but is not necessary as that is not the focus of the program. The results across the four variations will be compared to show the differences in performance as specified by the mission. RDS-win will be used for initial sizing parameters. This program will help refine the sizing of the fuselage and wings once the missions have been specified. The fuel weight sizing and range can also be calculated in this software. The performance data from this program will also be used as a reference when getting finalized results from XFLR5. Both programs can output to .CSV files, making comparisons between the variations simple and straightforward.

1.5 Mission Specifications

1.5.1 Mission Requirements

To justify the modular design of the aircraft, separate mission requirements will be defined for each variation. The following mission types will be defined: combat, transport, surveillance, and decoy. Since some aspects of the aircraft will be shared amongst the configurations, some consistency among the configurations may prevent widely varying missions such as a long range mission, or a highly maneuverable mission. After defining the mission requirements and checking to see if they are achievable in RDS, a mission profile will be defined for each variation. The specific requirements are as follows:

- Cargo Transport
    - Carry 6 paratroopers (300 lb or 136 kg each) or an equivalent payload
    - Range: 1500 nmi (2778 km)
    - Cruise: 200 knots (371 km/h)
    - Service ceiling: 15000 ft (4570 m)
- Combat
    - 2 hardpoints
    - 4 AGM missiles (525 lb or 238 kg each)
    - Range: 1000 nmi (1852 km)
    - Cruise: 200 knots (371 km/h)
    - Service ceiling: 15000 ft (4570 m)
- Surveillance
    - Transmit collected data to command center
    - Endurance: 20 hours
    - Range: 2000 nmi (3704 km)
    - Cruise: 200 knots (371 km/h)
    - Service ceiling: 15000 ft (4570 m)
- Decoy
    - Jamming/interference capabilities
    - Range: 2000 nmi (3704 km)
    - Cruise: 200 knots (371 km/h)
    - Service ceiling: 15000 ft (4570 m)

1.5.2 Mission Profile

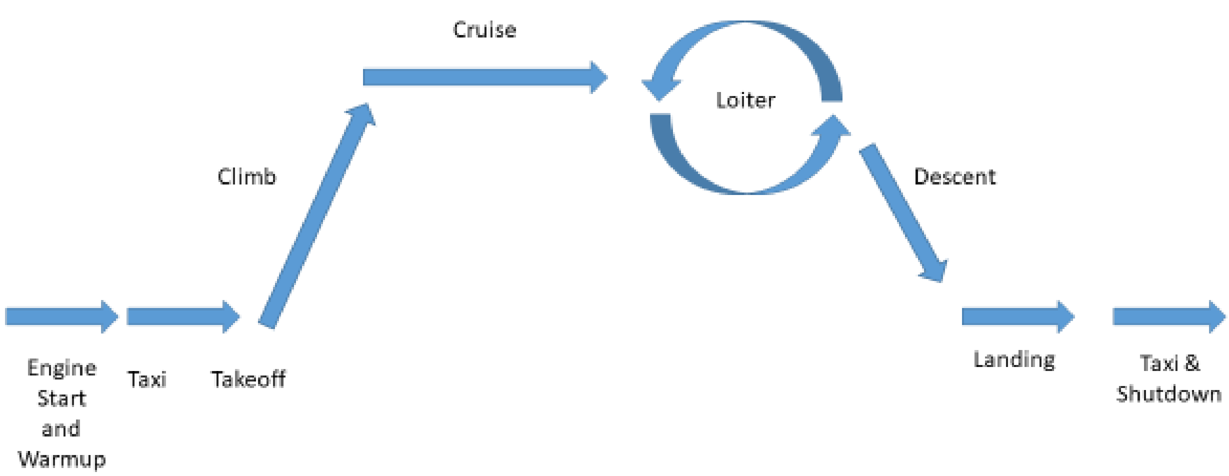

Figure 1-1 Surveillance and decoy mission profile

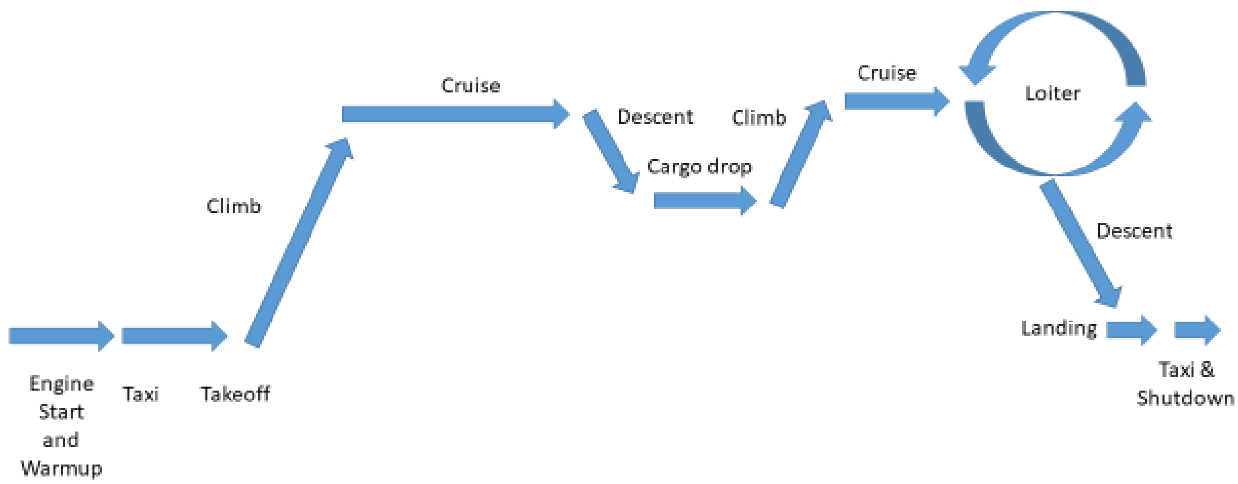

Figure 1-2 Cargo and combat mission profile

1.5.3 Critical Mission Requirements

While all the mission requirements will be used to shape the design of the aircraft, some of the requirements will take precedence over others. More specifically, the range, payload, and cruise requirements will be the most critical. Once these requirements have been met, the other mission requirements will be addressed should they have not already been met.

1.6 Comparative Study of Similar Aircraft

To begin the initial weight sizing, a baseline using similarly sized aircraft will be established. For a general baseline, a Britten-Norman BN-2 Islander will be used as a comparison.

Table 1.1 Performance parameters of BN-2 Islander [25]

Parameter	Value (SI units)
Capacity	1 crew, 9 paratroopers
Length	35.6 ft (10.9 m)
Wingspan	49.0 ft (14.9 m)
Height	13.7 ft (4.2 m)
Wing area	325 ft^2 (30.2 m^2)
Aspect Ratio	7.4
Empty weight	4114 lb (1866 kg)
Range	755 nmi (1398 km)
Cruise speed	130 knots (66.9 m/s)
Service ceiling	11300 ft (3.44 km)

1.7 Discussion

While the BN-2 isn't an exact match for what this project attains to design, it does provide similar aspects in the general profile of the fuselage and wings. Unlike the BN-2, there will be no crew onboard and there will only be room for 6 paratroopers in the cargo configuration. The wingspan and aspect ratio from the BN-2 will be used as a baseline for the cargo configuration and adjusted to meet the mission requirements. The weight, range, cruise speed, and service ceiling will be higher than the BN-2 which may in turn affect the other parameters. Since an exact comparison can't be made for the aircraft defined in this project, several different aircraft may be used as a basis for comparison. The mission profile defined in this chapter will continually be used a baseline for entire design process. Should the aircraft not meet these requirements, further design iterations may be necessary.

2. Weight Sizing

2.1 Initial Weight Sizing

Using the similar aircraft as a reference, the aircraft specifications along with the mission requirements will be used to define initial weight estimates. Using the program RDS, this data can be input along with educated estimations to get an initial idea for the fuel weight, mission sizing, and empty weight of the aircraft [26]. As the design process moves along, the updated data will replace the placeholder estimates to develop an accurate picture of the design. A twin piston propeller configuration was assumed for all 4 variations. The range length was adjusted among all four missions until the empty weights and gross weights were close in value among each other. The S_{WET}/S_{REF} values were estimated according to other aircraft specified in *Aircraft Design* [26]. A general value was initially chosen the wing loading, this value was then replaced by a more accurate wing loading after more aspects of the design were finalized. The following inputs were used to generate an initial sizing for each mission:

Table 2.1 RDS input for cargo transport

Input	Value
Estimated weight guess	7000 lb (3175 kg)
Passenger weight	1800 lb (816 kg)
Cargo weight	0 lb (0 kg)
S_{WET}/S_{REF}	5
Aspect ratio	7.5
Oswald efficiency	0.8
Wing loading	22.5 lb/ft^2 (110 kg/m^2)
Power loading	11 lb/HP (5.0 kg/HP)
Specific fuel consumption	0.4 lb/lb$_f$ h (0.04 kg/N h)
Propeller efficiency	0.8
Number of engines	2
Range	2000 nmi (3704 km)

Table 2.2 RDS input for combat

Input	Value
Estimated weight guess	7000 lb (3175 kg)
Passenger weight	0 lb (0 kg)
Cargo weight	2100 lb (953 kg)
S_{WET}/S_{REF}	5
Aspect ratio	8
Oswald efficiency	0.8
Wing loading	20 lb/ft^2 (98 kg/m^2)
Power loading	9 lb/HP (4.1 kg/HP)
Specific fuel consumption	0.4 lb/lb$_f$ h (0.04 kg/N h)
Propeller efficiency	0.8
Number of engines	2
Range	1500 nmi (2778 km)

Table 2.3 RDS input for surveillance

Input	Value
Estimated weight guess	7000 lb (3175 kg)
Passenger weight	0 lb (0 kg)
Cargo weight	1000 lb (454 kg)
S_{WET}/S_{REF}	4
Aspect ratio	10
Oswald efficiency	0.8
Wing loading	23 lb/ft^2 (112 kg/m^2)
Power loading	11 lb/HP (5.0 kg/HP)
Specific fuel consumption	0.4 lb/lb$_f$ h (0.04 kg/N h)
Propeller efficiency	0.8
Number of engines	2
Range	4500 nmi (8334 km)

Table 2.4 RDS input for decoy

Input	Value
Estimated weight guess	7000 lb (3175 kg)
Passenger weight	0 lb (0 kg)
Cargo weight	500 lb (227 kg)
S_{WET}/S_{REF}	5
Aspect ratio	7.5
Oswald efficiency	0.8
Wing loading	20 lb/ft^2 (98 kg/m^2)
Power loading	9 lb/HP (4.0 kg/HP)
Specific fuel consumption	0.4 lb/lb$_f$ h (0.04 kg/N h)
Propeller efficiency	0.8
Number of engines	2
Range	3500 nmi (6482 km)

From the output file, the following weights were calculated:

Table 2.5 RDS initial weight sizing

Output	Cargo	Combat	Surveillance	Decoy
Fuel weight	1830 lb (830 kg)	1494 lb (678 kg)	2563 lb (1163 kg)	2998 lb (1360 kg)
Empty weight	4536 lb (2057 kg)	3951 lb (1792 kg)	4169 lb (1891 kg)	3936 lb (1785 kg)
Payload weight	1800 lb (816 kg)	2100 lb (953 kg)	1000 lb (454 kg)	500 lb (227 kg)
Gross weight	8165 lb (3704 kg)	7545 lb (3422 kg)	7722 lb (3503 kg)	7434 lb (3372 kg)
Range	1388 nmi (2571 km)	1079 nmi (1998 km)	2536 nmi (4697 km)	2961 nmi (5484 km)

2.2 Discussion

The cargo transport variation is currently the heaviest with the decoy being the lightest. To bring the weight values closer together, the mission ranges were adjusted. The surveillance and decoy require much more fuel than the other two configurations. With this in mind, these missions may need to be changed if the stability analysis shows that this may be an issue. Since only the cargo and combat configurations carry payloads, the other two configurations made up for this weight difference by having more fuel. As the surveillance and decoy configurations don't have a mission required payload, additional weight was added to both configurations to account for additional avionics required to carry out these two missions. The surveillance has an additional 1000 lb added, while the decoy has an additional 500 lb.

2.3 Conclusion

During the initial sizing for the weight analysis, several placeholder values were used as a definitive value had not been calculated yet. As the constraint diagram was created, the placeholder values for wing loading and power loading were replaced. Once an appropriate engine had been chosen, the placeholder for specific fuel consumption was replaced. This resulted in weight sizing going through several iterations before the finalized values were calculated.

3. Performance Constraint Analysis

3.1 Introduction

In the previous chapter, an educated estimate was used for the wing loading. To get a more accurate idea of the capabilities of the aircraft, a constraint diagram was created using previously calculated data in addition to some assumptions. Across all four variations, sea level flight was assumed, with varying C_{L_MAX} values for landing and takeoff. These values were 1.7, 2.0, and 2.3 for landing, with the takeoff values being 1.4, 1.7, and 2.0. To start the matching graph, a landing distance requirement was necessary. For all four configurations, a distance of 1500 feet (457 meters) was used.

3.2 Calculations

The previously calculated data was used along with the formulas below to create a matching graph for each configuration [27]:

$$v_{SL} = \sqrt{\frac{2*(W/s)}{\rho*C_{Lmax}}} \tag{3.1}$$

$$S_{TOG} = \frac{(W/s)_{TO}*(W/P)_{TO}}{\sigma*C_{Lmax\_TO}} = TOP_{23} \tag{3.2}$$

$$S_{TOG} = 4.9 * TOP_{23} + 0.009(TOP_{23})^2 \tag{3.3}$$

$$S_{LG} = 0.265 v_{SL}^2 \tag{3.4}$$

$$I_p = [\frac{(W/s)}{\sigma*(W/P)}]^{1/3} \tag{3.5}$$

The landing constraint was calculated using the landing distance requirement along with the C_{L_MAX} values for landing, which is represented by the vertical line. From the landing requirement, the power loading could be determined by varying the wing loading. The wing loading was set at 20 lb/ft^2 (98 kg/m^2) and increased in increments of 10 lb/ft^2 (49 kg/m^2) until 60 lb/ft^2 (293 kg/m^2). OEI and AEO were also considered in the constraint diagrams. The final component of the matching graph is the cruise speed constraint. Assuming 200 knots (370 km/h) as the cruise velocity at a height of 10,000 feet (3048 km), the wing loading was varied from 0 lb/ft^2 (0 kg/m^2) to 70 lb/ft^2 (342 kg/m^2). The Excel formulas and calculations can be found in Appendix A.

3.3 Constraint Diagrams

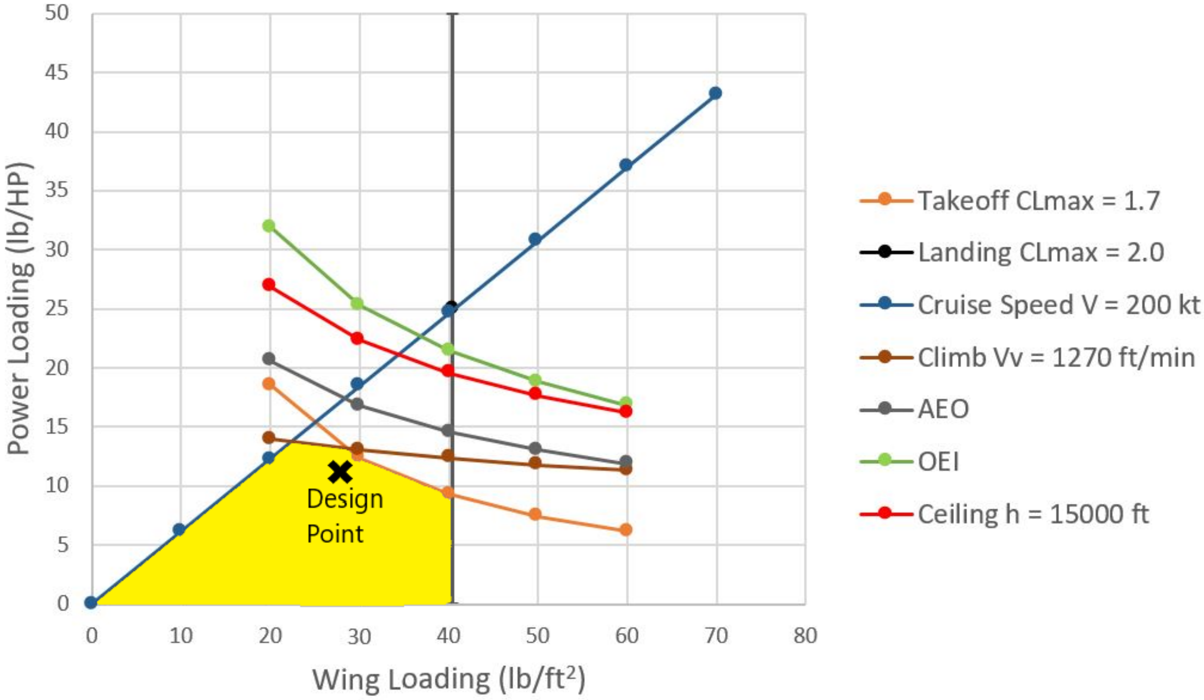

Figure 3-1 Matching graph for cargo configuration

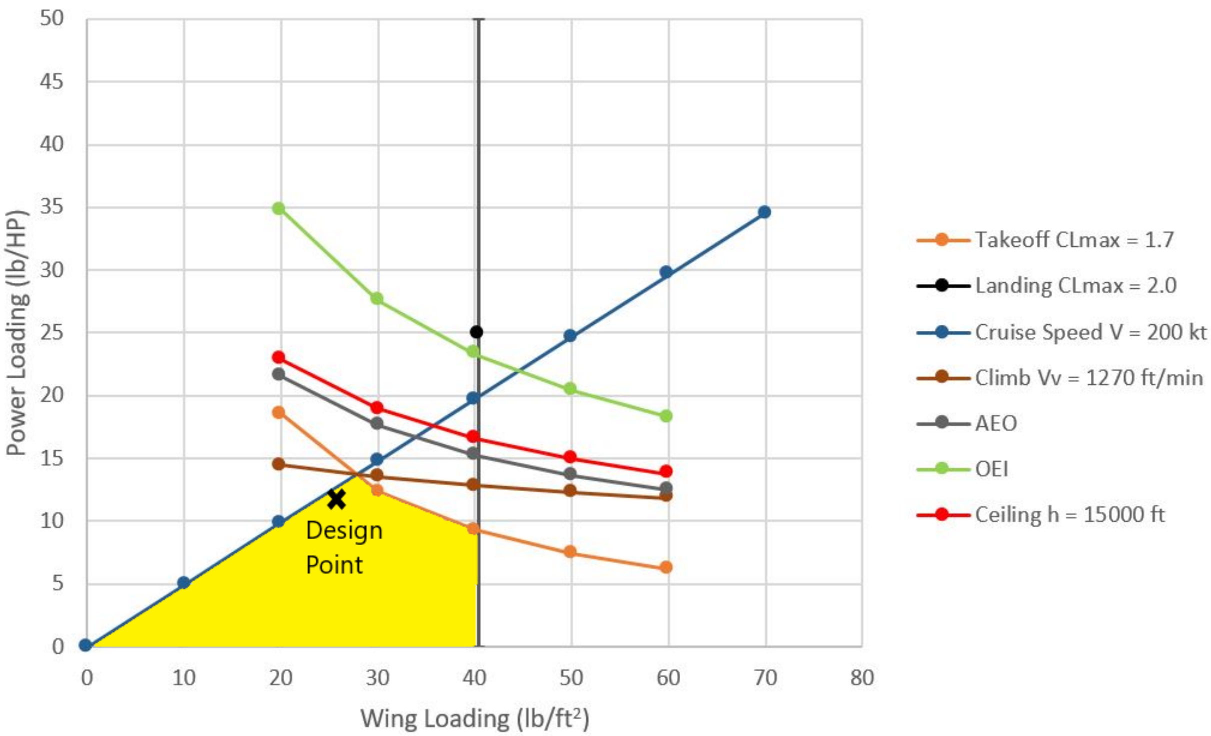

Figure 3-2 Matching graph for combat configuration

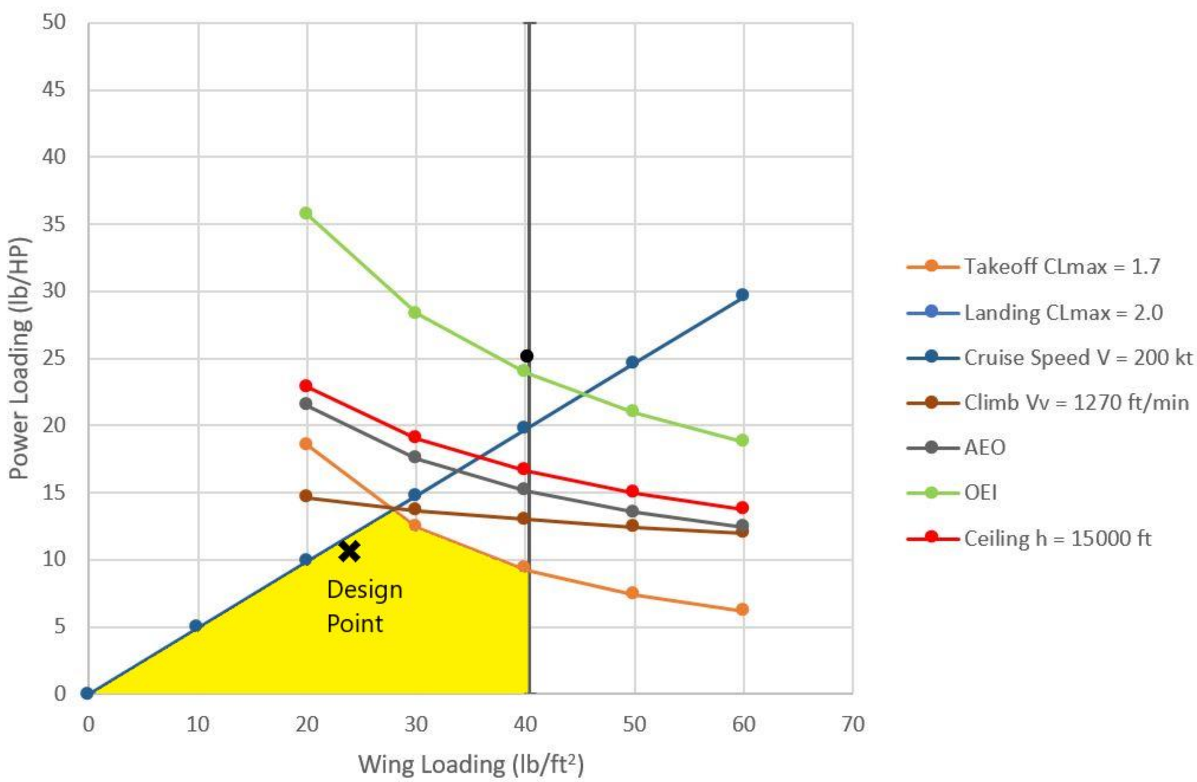

Figure 3-3 Matching graph for surveillance configuration

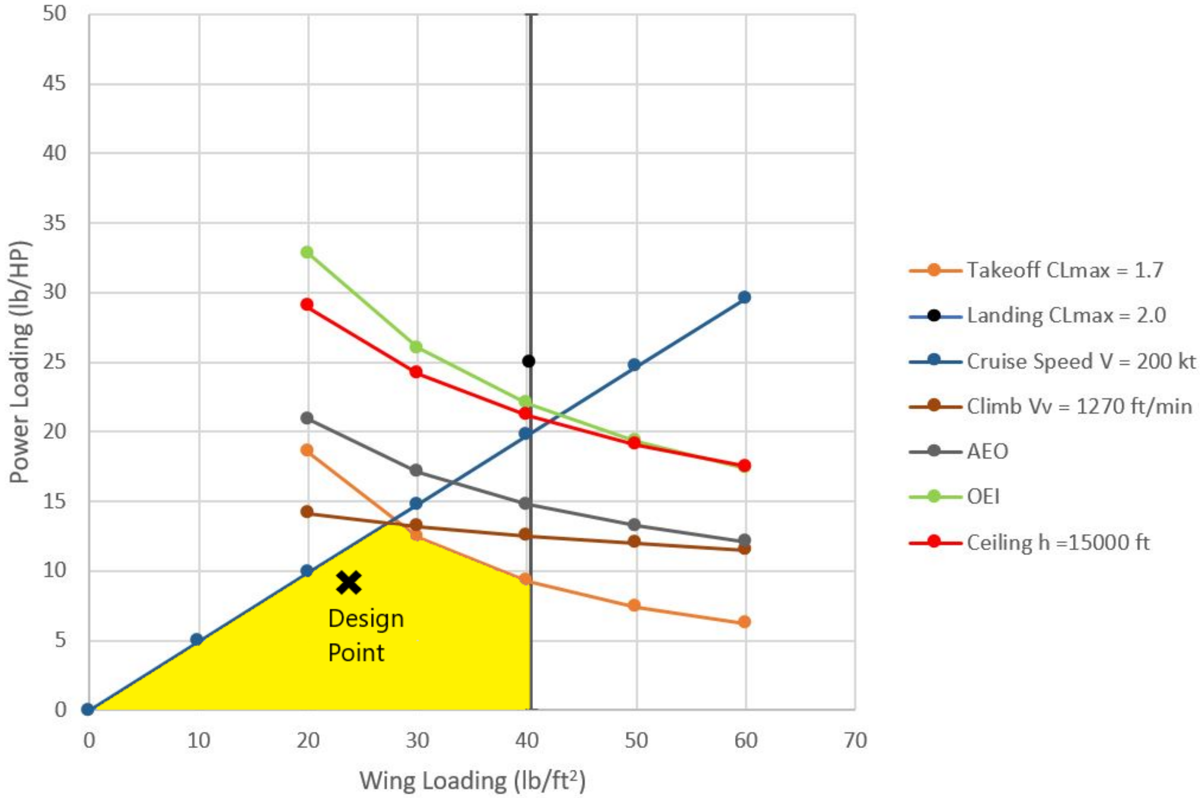

Figure 3-4 Matching graph for decoy configuration

3.4 Discussion

For the transport configuration, a wing loading of 28 lb/ft^2 (137 kg/m^2) was chosen along with a power loading of 11 lb/HP (6.7 kg/KW). For the combat configuration, a wing loading of 25 lb/ft^2 (122 kg/m^2) was chosen along with a power loading of 12.2 lb/HP (7.4 kg/KW). Even though a higher wing loading could've been chosen, this particular wing loading allows for the highest power loading. For the surveillance configuration, a wing loading of 23 lb/ft^2 (113 kg/m^2) was picked along with a power loading of 11 lb/HP (6.7 kg/KW). These chosen values were close to two different constraints, but should still be within acceptable values. For the decoy configuration, a wing loading of 24 lb/ft^2 (117 kg/m^2) was picked along with a power loading of 9 lb/HP (6.7 kg/KW). These values allow for takeoff even with less than optimal conditions.

3.5 Conclusion

In order to perform under various conditions, values such as C_{L_MAX} were varied to show the performance of the aircraft in different situations. These acted as constraints for the design of the aircraft. The two main constraints across all four configurations were the landing and takeoff curves. To prevent the plots from being cluttered, only the chosen values for landing and takeoff C_{L_MAX} were shown. Even with the least favorable C_{L_MAX} for landing and takeoff, the aircraft should still be capable of flight. Using the finalized values for wing loading and power loading, the placeholders used for the weight sizing can be replaced. The new weight sizing values were then used for the constraint diagrams to finalize these values as well.

4. Configuration Selection

4.1 Introduction

Now that the requirements and constraints of the aircraft have been decided upon, more aspects of the aircraft can be designed. This includes the various configurations of the wing, engine, empennage, and landing gear. Design parameters relating to the fuselage will be kept consistent across the configurations as the fuselage won't change across configurations. Other design parameters will be designed separately as each configuration has different requirements.

4.2 Selection of Propulsion System

4.2.1 Selection of Propulsion System Type

A piston engine was chosen for all the configurations. Earlier on in the design process, a turboprop was considered, but it ended up being too powerful for the aircraft. A Continental GTSIO-520-D was chosen as the engine for all four configurations. The 375 HP (280 KW) it generates is enough for all four aircraft. Using the power loading from the constraint diagram, the highest horsepower required was from the combat configurations. This was around 309 HP (230 KW).

4.2.2 Selection of Number of Engines

Twin engines were selected early on in the weight sizing. This was due to similar sized aircraft requiring two engines. Each engine will be mounted on the leading edge of the wing. The engines will be placed so that the propellers are far enough away from the fuselage to prevent a diminished airflow.

4.2.3 Propeller Sizing

Using similar aircraft as a reference, a propeller diameter of 90 inches (48 cm) was chosen. In the same vein, the number of propellers were chosen, resulting in a propeller number of 3. The height of the propellers from the ground will also be considered.

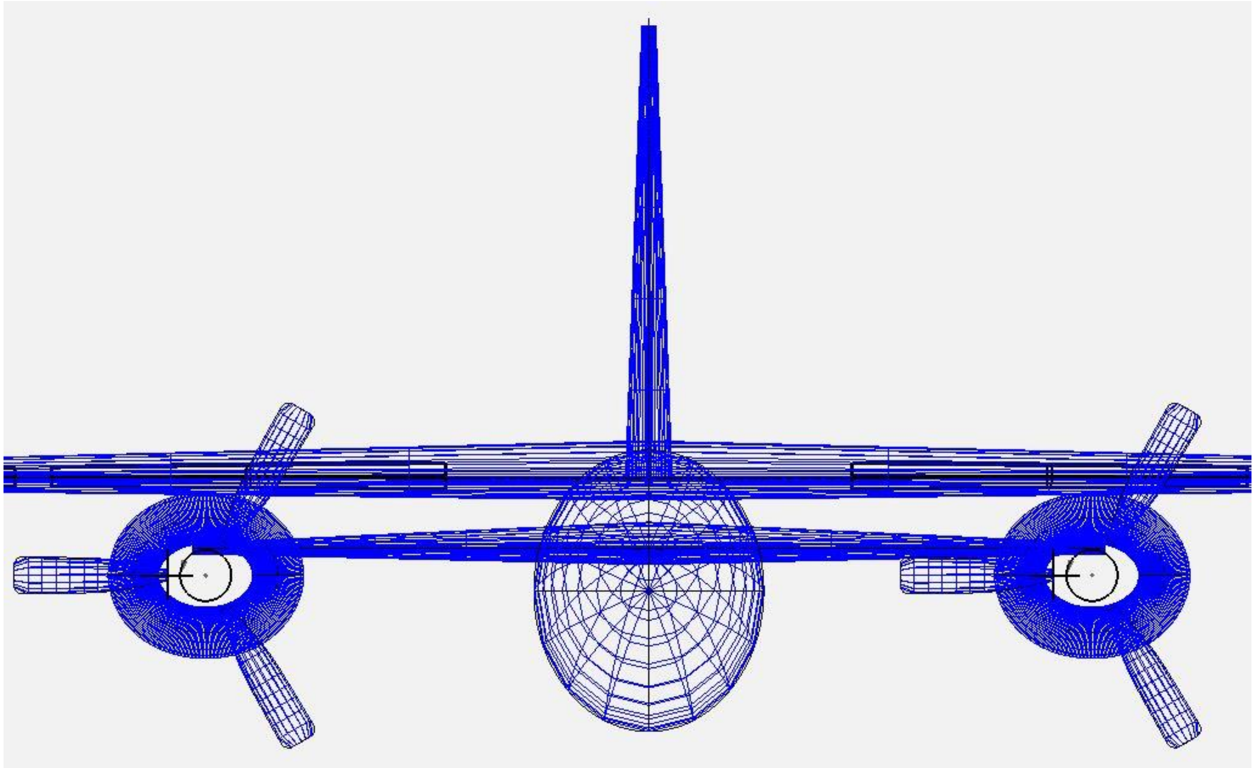

Figure 4-1 Front view with engines

4.3 Configuration Selection

4.3.1 Overall Configuration

All four configurations will use fairly conventional configurations as the innovative aspect of the design relates to the modularity of the aircraft.

4.3.2 Wing Configuration

The wings were kept fairly conventional with a slight sweep being used on the leading edges. Since each configuration has a different mission, the wings will be designed separately. High life devices for the wings will be kept to just flaps and ailerons.

4.3.3 Empennage Configuration

A vertical stabilizer and horizontal stabilizer will be used for all four configurations. Since the wing is different in each case, the empennage for each configuration will be designed separately according to the wing size. A conventional configuration will be common across all the configurations. Both the horizontal and vertical stabilizer will have swept edges.

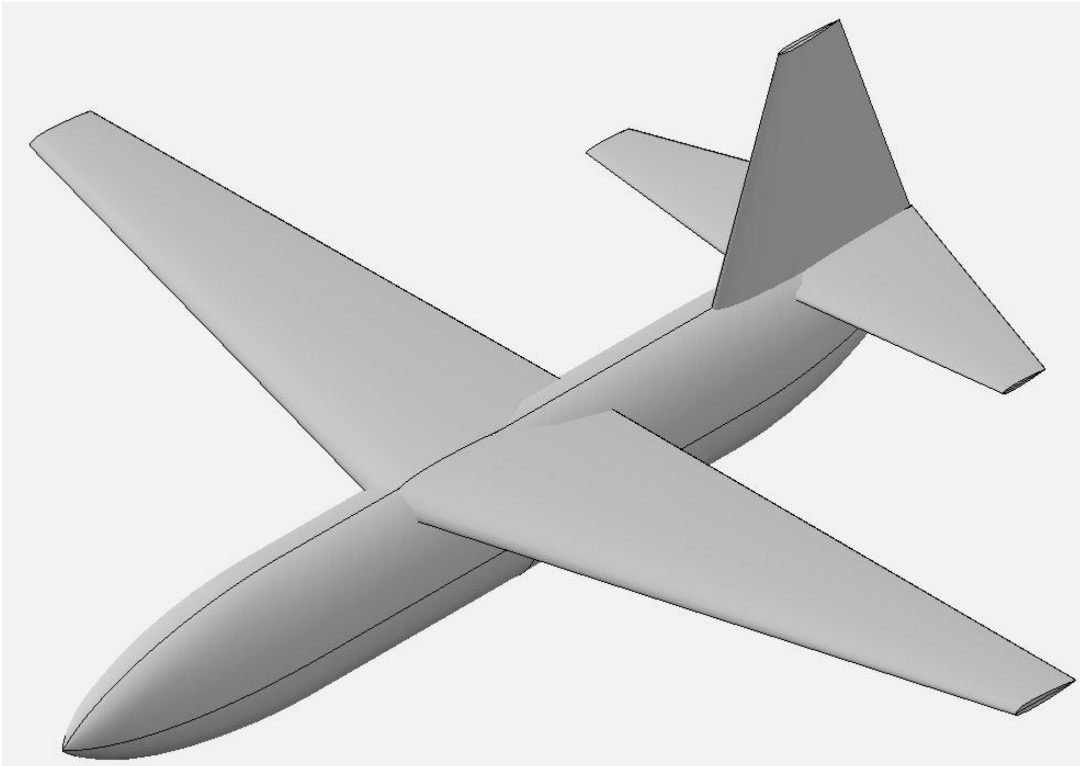

Figure 4-2 General empennage layout

4.3.4 Landing Gear Disposition

The main landing gear will be mounted on the fuselage near the main wing. To assist with the overall stability of the aircraft, the landing gear will extend beyond the width of the fuselage. A tricycle configuration was selected. The landing gear will be retractable due to the cruise requirement being 200 knots (370 km/h).

4.3.5 Proposed Configuration

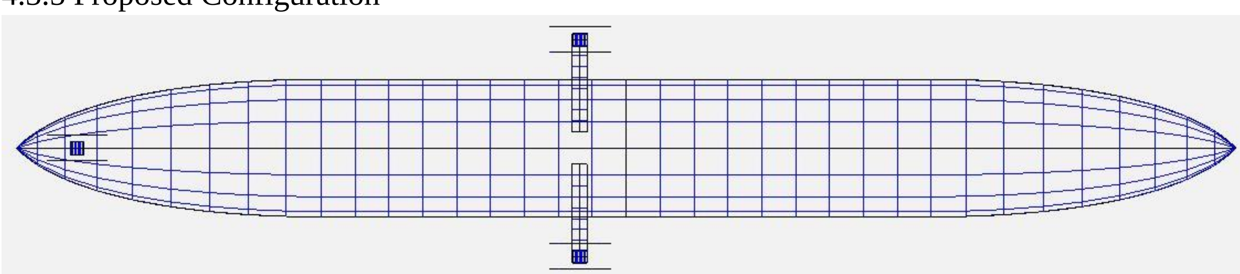

Figure 4-3 Landing gear locations (bottom view)

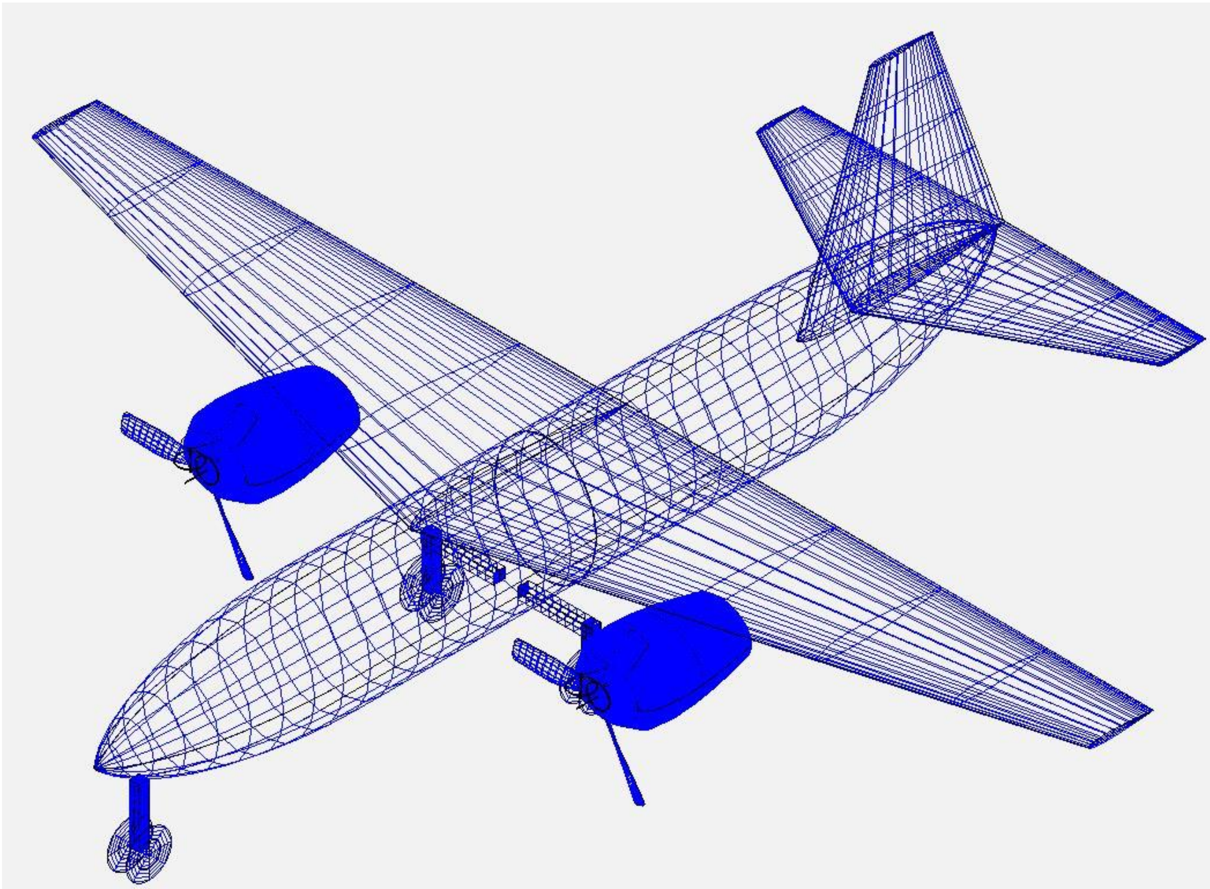

Figure 4-4 General configuration of the aircraft

5. Fuselage Design

5.1 Introduction

OpenVSP was used to create a model of the fuselage. The BN-2 was used as a baseline from which the fuselage was modified to better fit the needs of the mission requirements. This fuselage will be shared among all 4 variations. The fuselage has a length of 40 feet (12 m). The width of the cabin is 4.5 feet (1.4 m) with a height of 5.5 feet (1.7 m). To accurately represent the modular nature of the design, the wing, empennages, landing gear, and engines will be placed with the exact same coordinates across the 4 variations.

5.2 Layout Design of Fuselage

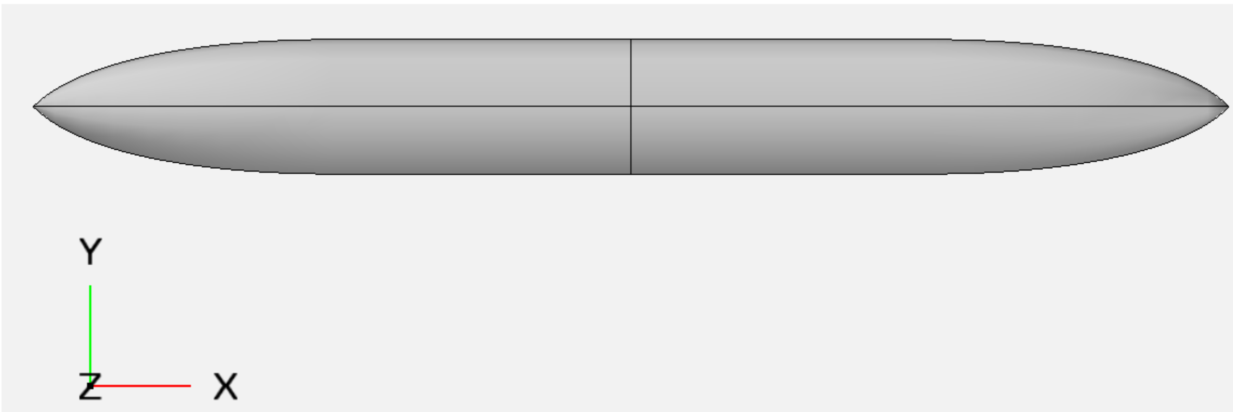

Figure 5-1 Top view of the fuselage

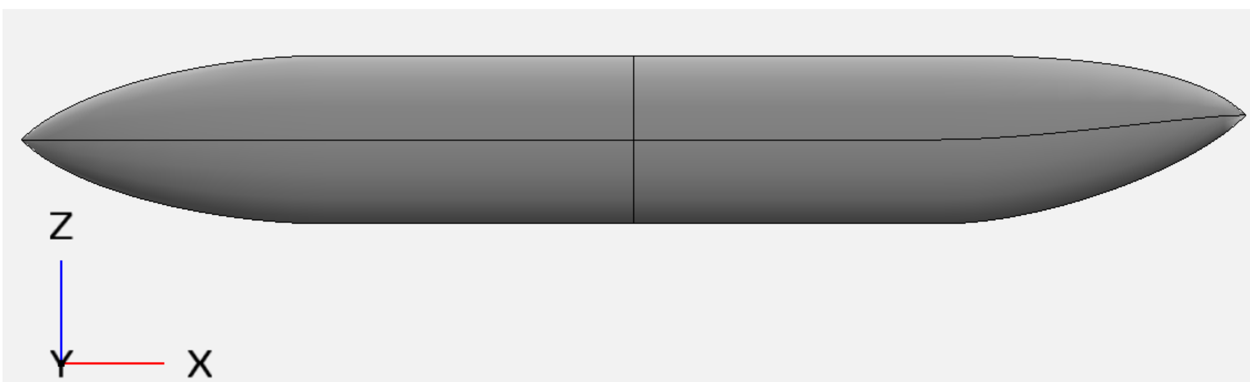

Figure 5-2 Side view of the fuselage

5.3 Discussion

The surveillance and decoy configurations don't have fuselage size requirements and only use the fuselage to store equipment and avionics. The payload for the combat configuration include the missiles which will be placed on the wings. To fit 6 paratroopers, 6 seats were modeled to fit the average adult. These seats are placed in two rows of three seats, facing each other. The dimensions of the fuselage allow for the seats and paratroopers to snuggly fit. While the fuselage will be shared amongst the four configurations, the internal layout will vary with each configuration. Since the aircraft is a UAV, the avionics can be freely moved inside the fuselage as necessary. The internal layout of the fuselage will be constrained by the overall CG of the aircraft.

6. Wing Design

6.1 Introduction

Using the values calculated during the weight sizing, the specifications of the wing can be decided upon and calculated. The takeoff weight, wing loading, and aspect ratios were used to size the wing. Keeping with the modular design, each configuration will use a different wing.

6.2 Wing Planform Design

A general taper ratio of 0.3 was selected for all 4 variations. The wing loading values were chosen based on the matching graph. A higher wing loading was used at the cost of a lower power loading. The values decided upon and calculated from the previous chapters are as follows:

Table 6.1 Wing sizing inputs

Value	Cargo	Combat	Surveillance	Decoy
W (weight)	8165 lb (3704 kg)	7545 lb (3422 kg)	7722 lb (3503 kg)	7434 lb (3372 kg)
W/S (wing loading)	28 lb/ft^2 (137 kg/m^2)	25 lb/ft^2 (122 kg/m^2)	23 lb/ft^2 (112 kg/m^2)	24 lb/ft^2 (117 kg/m^2)
A (aspect ratio)	7.5	8	10	7.5
λ (taper ratio)	0.3	0.3	0.3	0.3

6.3 Airfoil Selection

A NACA 23012 was chosen as the airfoil for the main wing and horizontal stabilizer. At this point during the design, an incidence angle of 0° and a twist angle of -2° will be used. A negative angle was used for washout. This airfoil will be used for all the configurations.

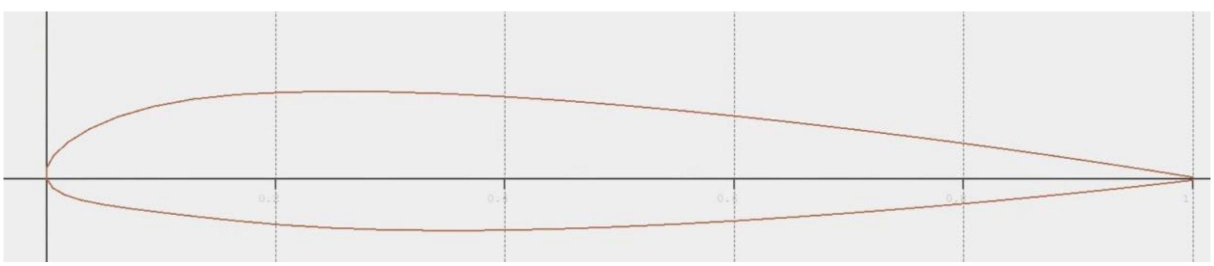

Figure 6-1 NACA 23012 airfoil shape

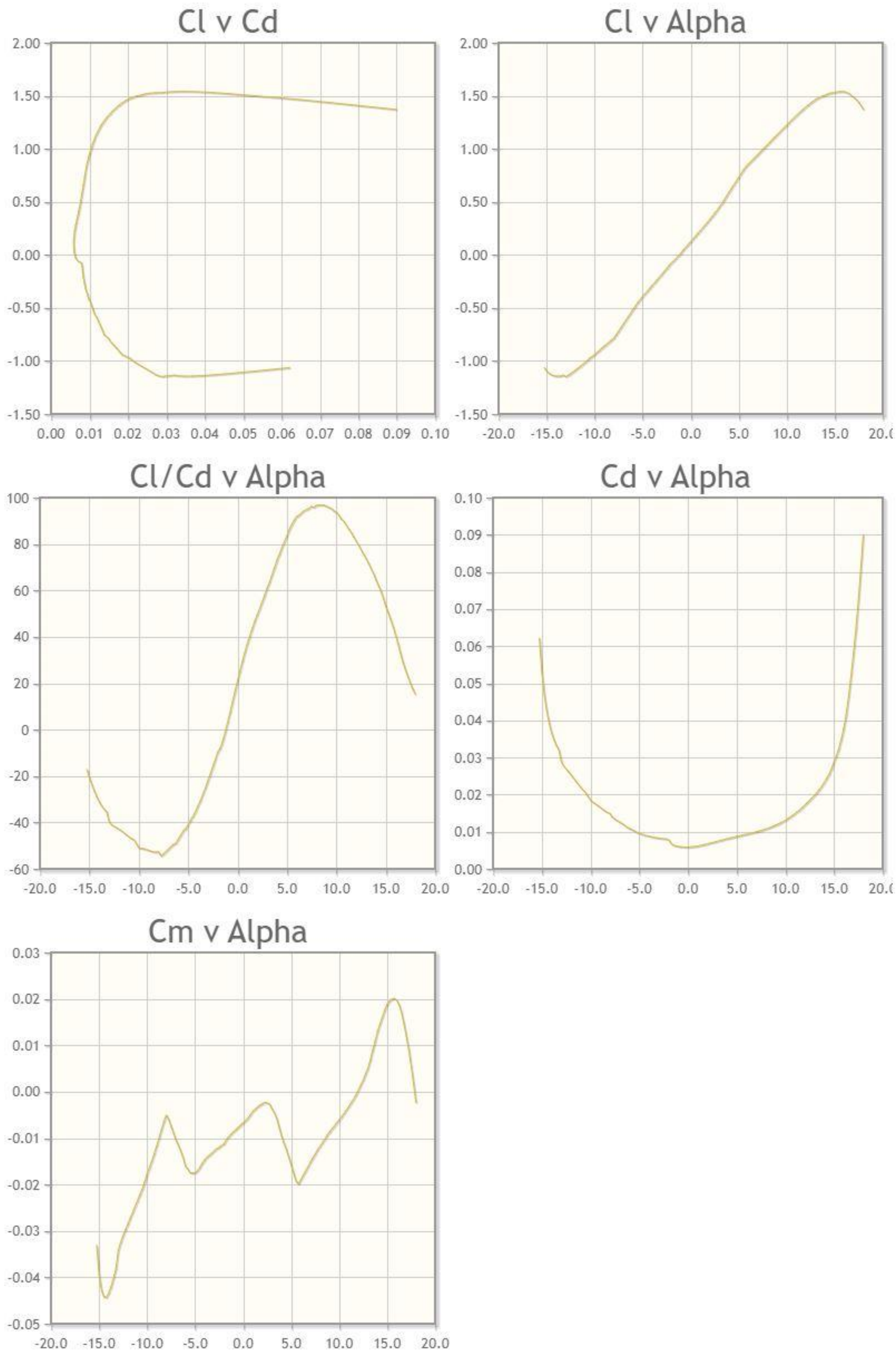

Figure 6-2 NACA 23012 polar plots [28]

6.4 Wing Sizing Calculations

Using Raymer as a reference, the following equations were used to get an initial estimate of the wing [26]:

$$S_{REF} = \frac{W}{W/S} \quad (4.1)$$

$$b = \sqrt{A * S_{REF}} \quad (4.2)$$

$$C_{root} = \frac{2 * S_{REF}}{b * (1+\lambda)} \quad (4.3)$$

$$C_{tip} = \lambda * C_{root} \quad (4.4)$$

$$MAC = \left(\frac{2}{3}\right) * C_{root} * \left(\frac{1+\lambda+\lambda^2}{1+\lambda}\right) \quad (4.5)$$

The calculated values were validated with the wing plotting tool from Aerotoolbox [29]. The data was near exact in both methods. The Excel formulas and calculations can be found in Appendix B. The results calculated from the equations described in Raymer are as follows [26]:

Table 6.2 Wing sizing results

Value	Cargo	Combat	Surveillance	Decoy
S_{REF} (reference wing area)	292 ft^2 (27.1 m^2)	302 ft^2 (28.1 m^2)	336 ft^2 (31.2 m^2)	310 ft^2 (28.8 m^2)
b (span)	46.8 ft (14.3 m)	49.1 ft (15.0 m)	57.9 ft (17.6 m)	48.2 ft (14.7 m)
C_{root}	9.59 ft (2.92 m)	9.45 ft (2.88 m)	8.91 ft (2.72 m)	9.89 ft (3.01 m)
C_{tip}	2.88 ft (0.88 m)	2.83 ft (0.86 m)	2.67 ft (0.81 m)	2.97 ft (0.91 m)
MAC	6.84 ft (2.08 m)	6.74 ft (2.05 m)	6.35 ft (1.94 m)	7.05 ft (2.15 m)
MAC y position	9.59 ft (2.92 m)	10.08 ft (3.07 m)	11.89 ft (3.62 m)	9.89 ft (3.01 m)
MAC x position	0.69 ft (0.21 m)	0.68 ft (0.21 m)	0.64 ft (0.20 m)	0.71 ft (0.22 m)
Quarter chord sweep	12º	11.5º	9º	12º
Leading edge sweep	15.87º	15.16º	11.99º	15.88º
Trailing edge sweep	-0.16º	0.06º	-0.2º	-0.17º

6.5 Fuel Tank Dimensions

The fuel for each configuration will be stored in the wings. To represent the fuel tanks, a box was designed in OpenVSP. To keep the aircraft stable, the fuel was split into two separate fuel tanks placed inside the wing. A1 fuel will be used which has a density of 6.76 lb/gal (0.81 g/ml). To denote the fuel tanks, they will be colored red in the wing drawings (see chapter 13.3).

Table 6.3 Fuel tank size

	Cargo	Combat	Surveillance	Decoy
Empty weight	4536 lb (2057 kg)	3951 lb (1792 kg)	4169 lb (1891 kg)	3936 lb (1785 kg)
Fuel weight	1830 lb (830 kg)	1494 lb (678 kg)	2563 lb (1163 kg)	2998 lb (1360 kg)
Fuel tank size	36.02 ft^3 (1.02 m^3)	29.66 ft^3 (0.84 m^3)	50.85 ft^3 (1.44 m^3)	59.33 ft^3 (1.68 m^3)

6.6 Wing Drawings

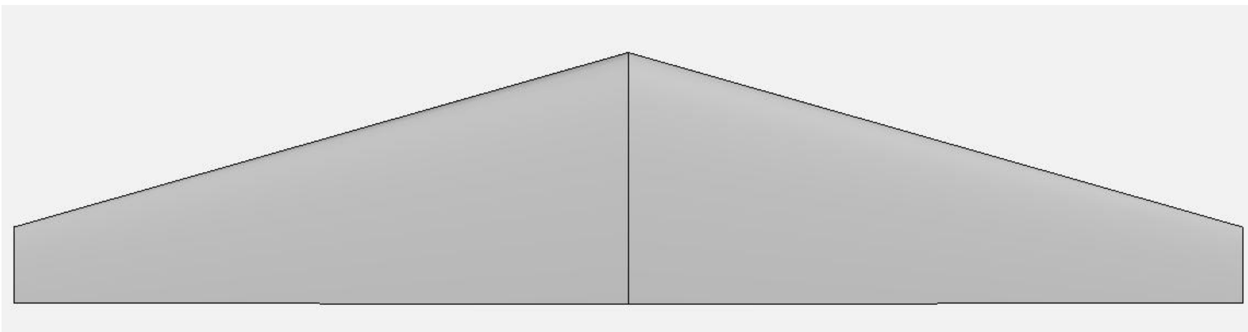

Figure 6-3 Wing of the cargo configuration

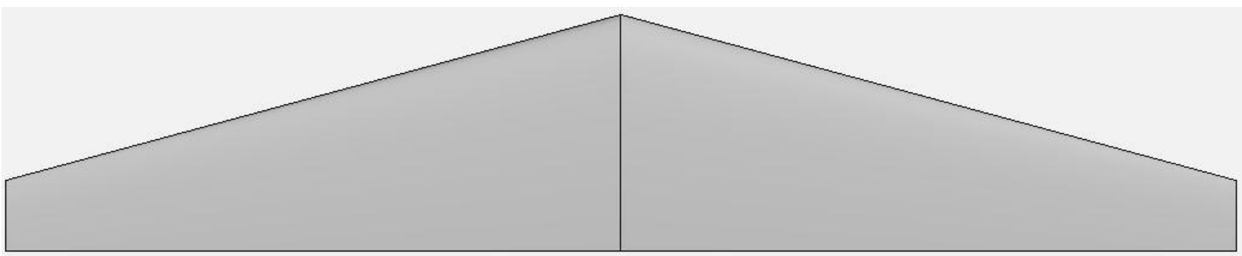

Figure 6-4 Wing of the combat configuration

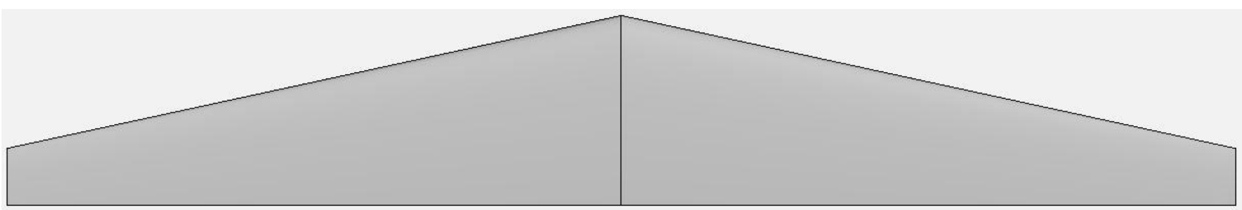

Figure 6-5 Wing of the surveillance configuration

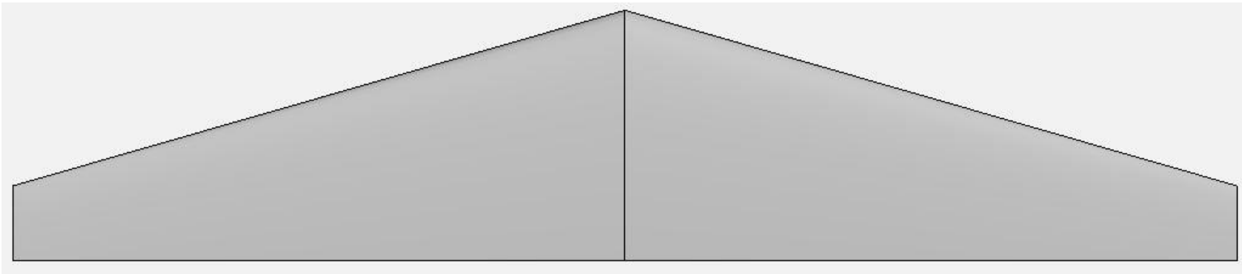

Figure 6-6 Wing of the decoy configuration

6.7 High Lift Devices

Flaps and ailerons were sized according to the methods described in Raymer and Roskam [26] [27]. Fowler flaps were chosen due to the benefits of increased drag and lower stall speeds. The landing ΔC_{L_max} required was around 0.65 for all the cargo, combat and decoy configurations. While the takeoff ΔC_{L_max} was around 0.33 for the same configurations. The surveillance was slightly higher at 0.81 and 0.49 respectively. The aileron and flaps take up around 30% of the chord.

Table 6.4 High lift devices sizing

	Cargo	Combat	Surveillance	Decoy
Flap start (% of span)	17.1	18.3	19.0	16.6
Flap end (% of span)	51.3	53.0	51.8	49.8
Aileron start (% of span)	52.3	54.0	52.8	50.8
Aileron end (% of span)	86.5	90.6	90.8	84.0

Table 6.5 Lift coefficients for various scenarios

	Cargo	Combat	Surveillance	Decoy
Clean C_{L_max}	1.60	1.60	1.62	1.60
Landing C_{L_max}	1.7	1.7	1.7	1.7
Takeoff C_{L_max}	2.0	2.0	2.0	2.0

Table 6.6 Flap deflection angles

Scenario	Flap deflection angle
Landing	15°
Takeoff	35°

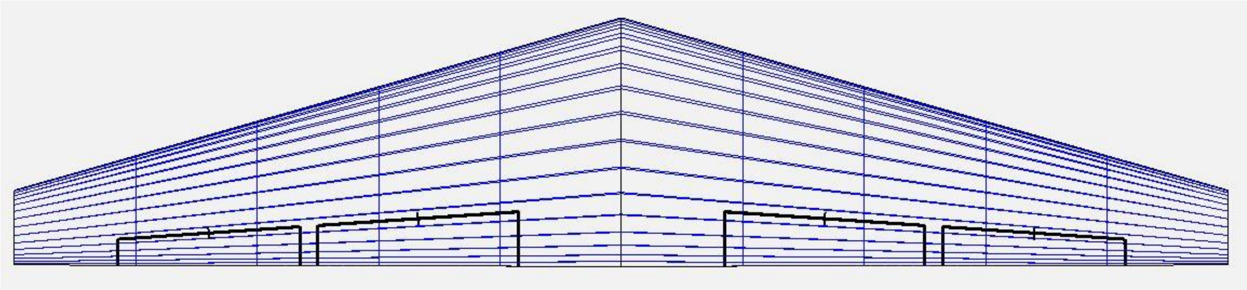

Figure 6-7 High lift devices on cargo wing

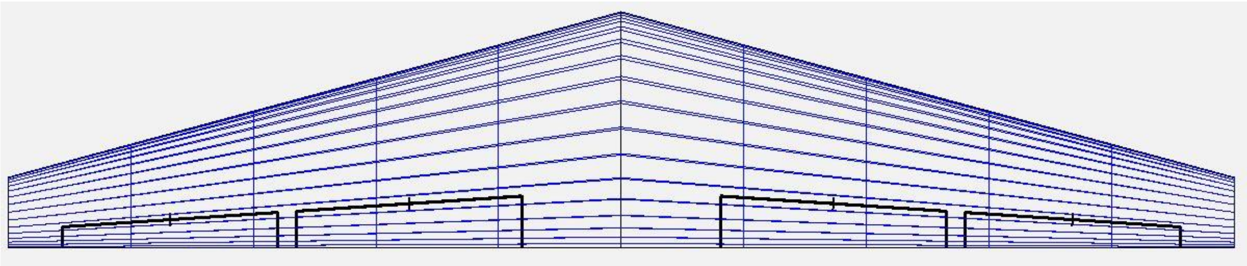

Figure 6-8 High lift devices on combat wing

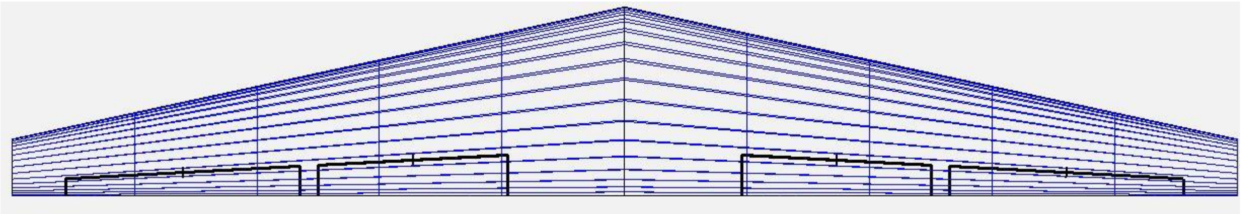

Figure 6-9 High lift devices on surveillance wing

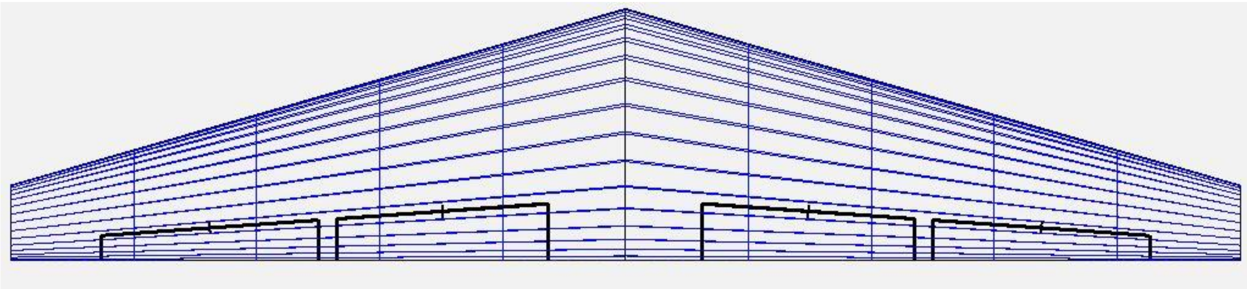

Figure 6-10 High lift devices on decoy wing

6.8 Discussion

The values from Table 6.2 were used to model the wings in OpenVSP. The wingspan, tip chord, and root chord were input into the program to start designing the wing. OpenVSP is able to calculate the reference area and angles of the wing, which were checked against the calculated values. These values along with the mean aerodynamic chord were close in value, validating the calculations. After this, the fuel tanks were modeled. Using the calculated fuel tank size, the boxes were modeled to fit the correct amount of fuel. To keep the center of gravity of the aircraft closer to the center, the fuel tanks were placed inside the wing near the center. All the configurations require two separate fuel tanks in each wing. The fuel tanks for each configuration were able to be placed inside the wings. This was checked from all angles to ensure that the dimensions of the fuel tanks didn't extend outside the wing dimensions. The internal spars and ribs for the wing were considered when placing the fuel in the wings. The flaps and aileron sizes were also taken into account when placing the fuel tanks. In the case of the surveillance and decoy configurations, the missions may need to be downsized to allow for a smaller tank size if the new shape can't fit the previously designed fuel tanks.

7. Empennage Design

7.1 Introduction

The horizontal and vertical stabilizers were sized according to the methods described in Raymer's textbook [26]. The volume coefficients were calculated using the following formulas:

$$V_h = \frac{S_h * L_{ht}}{S_{ref} * \bar{c}} \qquad (7.1)$$

$$V_v = \frac{S_v * L_{vt}}{S_{ref} * b} \qquad (7.2)$$

Using historical data for general aviation twin engines, the volume coefficient for the horizontal and vertical stabilizers were set at 0.8 and 0.07 respectively. The wing reference area, mean aerodynamic chord, and span were previously calculated and used during these calculations. A moment arm of 20 feet (6.1 m) was used for the horizontal stabilizers while the vertical stabilizer used a moment arm of 18 feet (5.5 m). These values were chosen to minimize the size of the stabilizers. Using the above equations, the reference area of the stabilizers could be calculated. After finalizing the aspect and taper ratios, the stabilizers could be sized.

7.2 Overall Empennage Design

Historical data was used to determine the aspect ratio and taper ratios for the empennage. For all four designs the aspect and taper ratios were kept consistent. The horizontal stabilizers use an aspect ratio of 4 and a taper ratio of 0.3. The vertical stabilizers use an aspect ratio of 1.5 and a taper ratio of 0.3. The horizontal stabilizer uses a symmetrical airfoil, more specifically a NACA 0012. This airfoil was used for all four configurations.

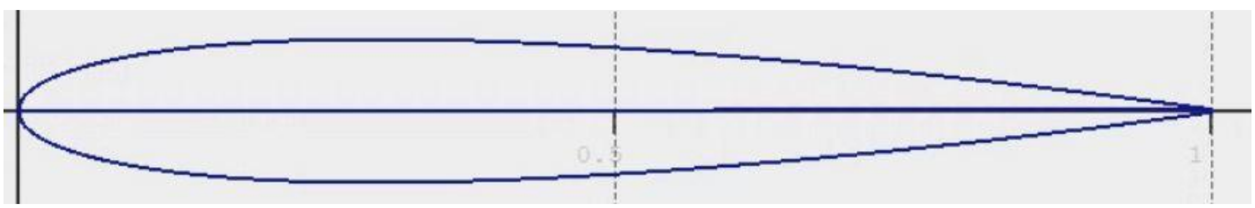

Figure 7-1 NACA 0012 airfoil shape

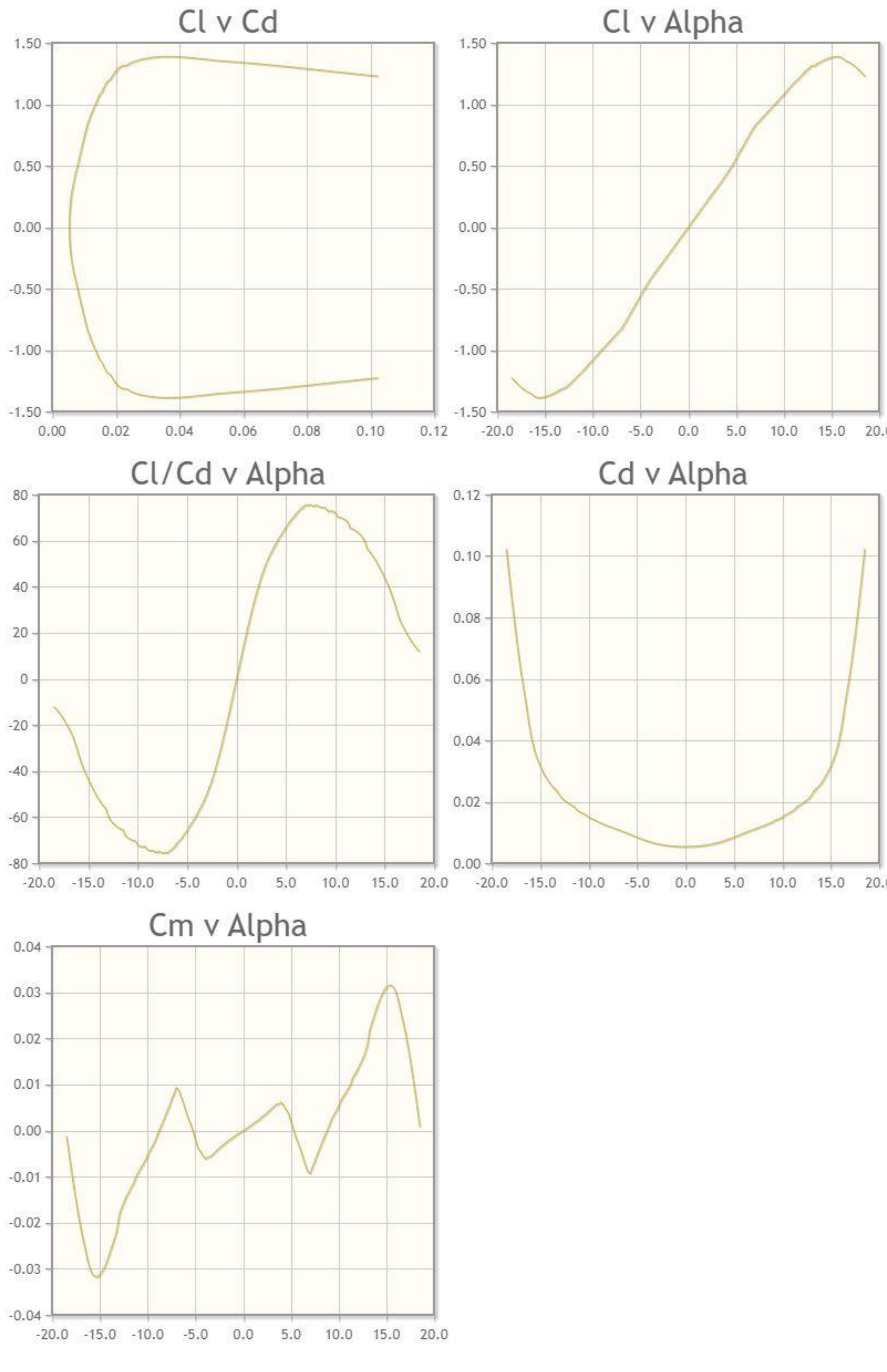

Figure 7-2 NACA 0012 polar plots [28]

7.3 Design of the Horizontal Stabilizer

Table 7.1 Horizontal stabilizer volume coefficients

	Cargo	Combat	Surveillance	Decoy
S_{REF}	292 ft^2 (27.1 m^2)	302 ft^2 (28.1 m^2)	336 ft^2 (31.2 m^2)	310 ft^2 (28.8 m^2)
b	46.8 ft (14.3 m)	49.1 ft (15.0 m)	57.9 ft (17.6 m)	48.2 ft (14.7 m)
c	6.84 ft (2.08 m)	6.74 ft (2.05 m)	6.35 ft (1.94 m)	7.05 ft (2.15 m)
L_{HT}	20 ft (6.10 m)	20 ft (6.10 m)	20 ft (6.10 m)	20 ft (6.10 m)
S_H	79.8 ft^2 (7.4 m^2)	81.4 ft^2 (7.6 m^2)	85.3 ft^2 (7.9 m^2)	87.2 ft^2 (8.1 m^2)

Table 7.2 Horizontal stabilizer sizing results

	Cargo	Combat	Surveillance	Decoy
Span	17.9 ft (5.5 m)	18.0 ft (5.5 m)	18.5 ft (5.6 m)	18.7 ft (5.7 m)
Root chord	6.9 ft (2.1 m)	6.9 ft (2.1 m)	7.1 ft (2.2 m)	7.2 ft (2.2 m)
Tip chord	2.1 ft (0.6 m)	2.1 ft (0.6 m)	2.1 ft (0.6 m)	2.2 ft (0.7 m)
MAC	4.9 ft (1.5 m)	5.0 ft (1.5 m)	5.1 ft (1.6 m)	5.1 ft (1.6 m)
Sweep angle	7.67°	7.67°	7.67°	7.67°

7.4 Design of the Vertical Stabilizer

Table 7.3 Vertical stabilizer volume coefficients

	Cargo	Combat	Surveillance	Decoy
S_{REF}	292 ft^2 (27.1 m^2)	302 ft^2 (28.1 m^2)	336 ft^2 (31.2 m^2)	310 ft^2 (28.8 m^2)
b	46.8 ft (14.3 m)	49.1 ft (15.0 m)	57.9 ft (17.6 m)	48.2 ft (14.7 m)
c	6.84 ft (2.08 m)	6.74 ft (2.05 m)	6.35 ft (1.94 m)	7.05 ft (2.15 m)
L_{VT}	18 ft (5.49 m)	18 ft (5.49 m)	18 ft (5.49 m)	18 ft (5.49 m)
S_V	53.1 ft^2 (4.9 m^2)	57.6 ft^2 (5.4 m^2)	75.6 ft^2 (7.0 m^2)	58.1 ft^2 (5.4 m^2)

Table 7.4 Vertical stabilizer sizing results

	Cargo	Combat	Surveillance	Decoy
Span	8.9 ft (2.7 m)	9.3 ft (2.8 m)	10.7 ft (3.3 m)	9.3 ft (2.8 m)
Root chord	9.2 ft (2.8 m)	9.5 ft (2.9 m)	10.9 ft (3.3 m)	9.6 ft (2.9 m)
Tip chord	2.8 ft (0.9 m)	2.9 ft (0.9 m)	3.3 ft (1.0 m)	2.9 ft (0.9 m)
MAC	6.5 ft (2.0 m)	6.8 ft (2.1 m)	7.8 ft (2.4 m)	6.8 ft (2.1 m)
Sweep angle	19.76°	19.73°	19.74°	19.76°

7.5 CAD Drawings

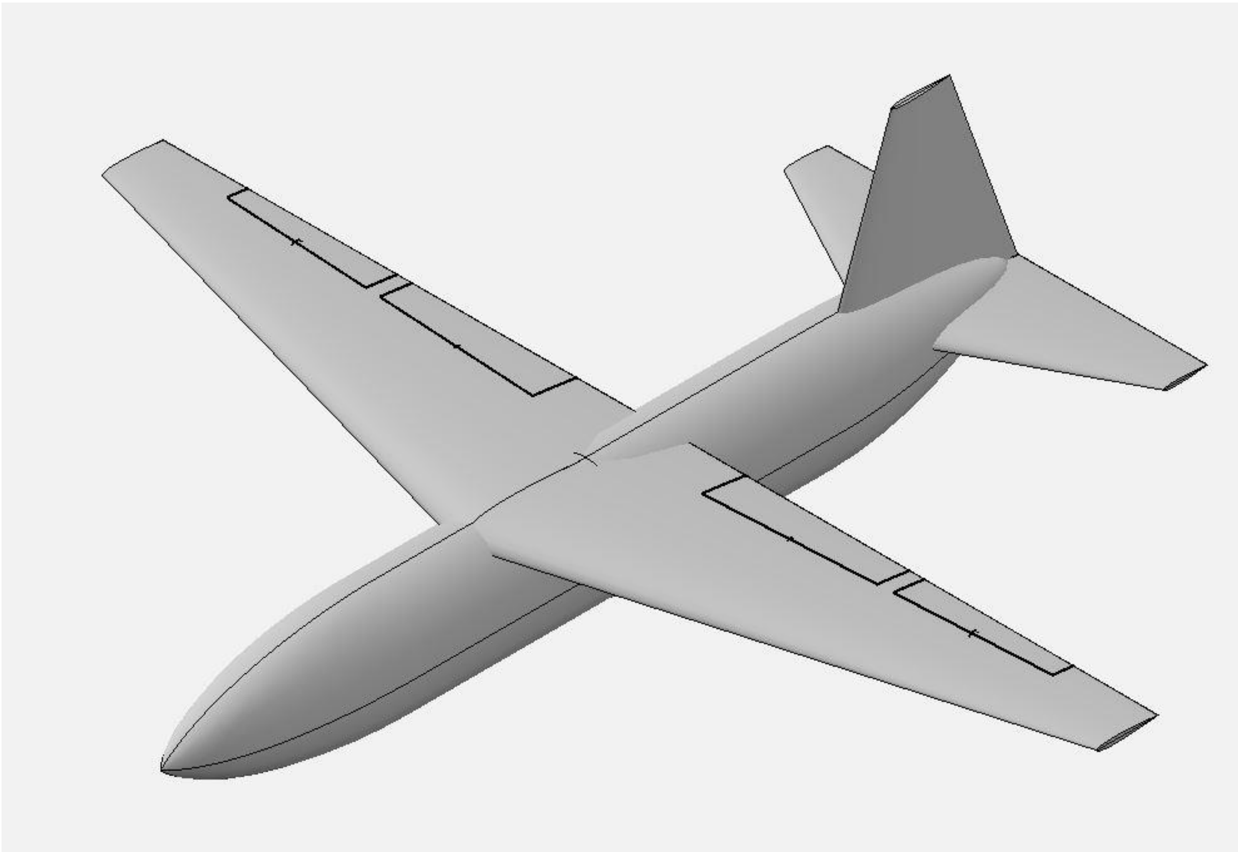

Figure 7-3 Cargo Transport CAD model with empennages

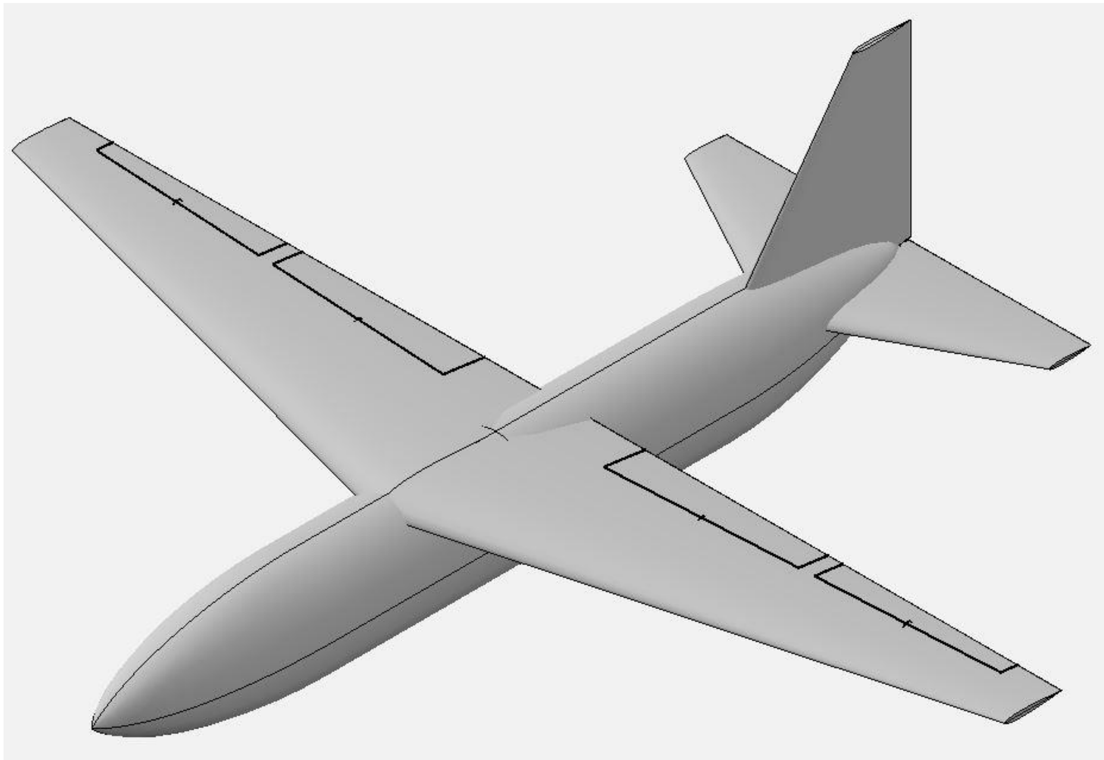

Figure 7-4 Combat CAD model with empennages

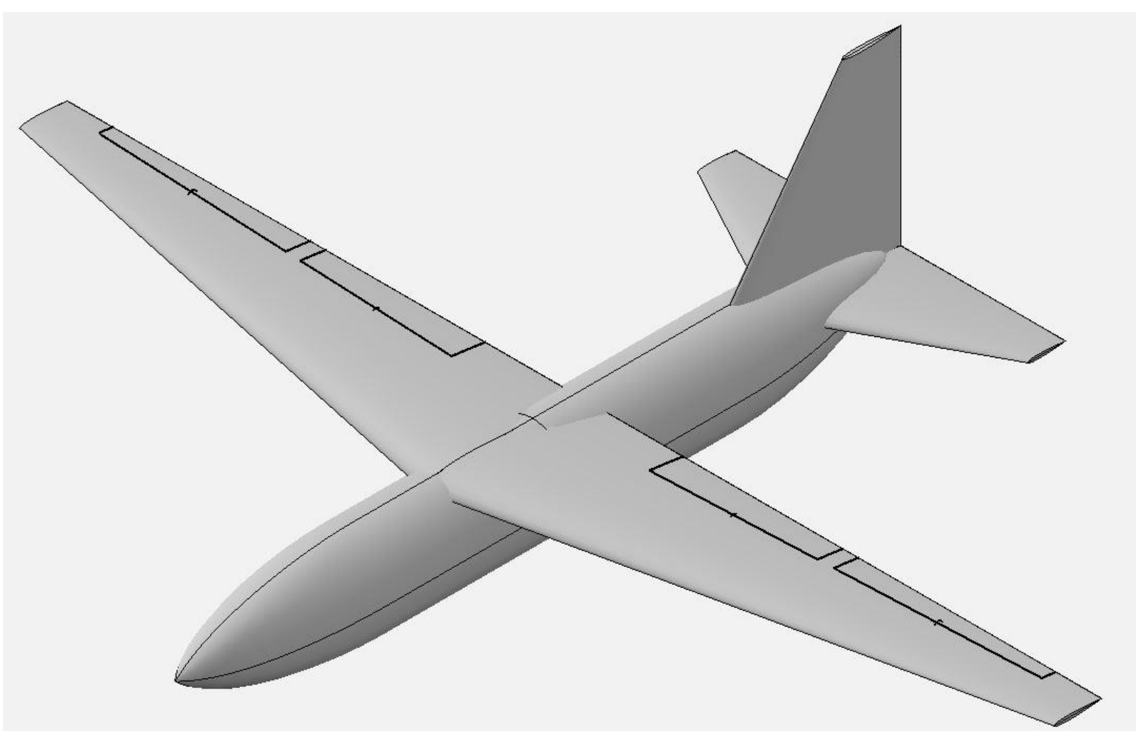

Figure 7-5 Surveillance CAD model with empennages

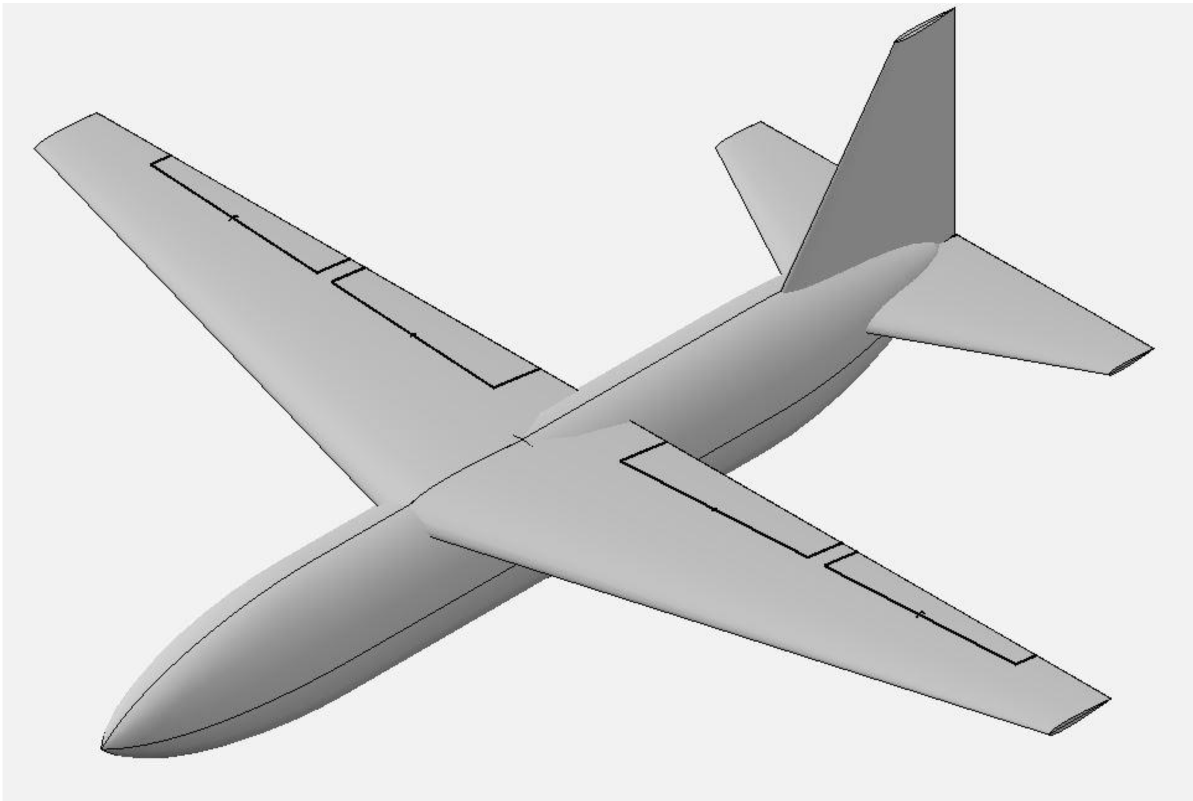

Figure 7-6 Decoy CAD model with empennages

7.6 Discussion

The horizontal and vertical stabilizers went through several iterations until the current design was achieved. In previous designs, the empennages were slightly larger than anticipated and resulted in much heavier stabilizers than was previously assumed. To reduce the sizing, the aspect ratio was slightly lowered and the moment arm between the main wing and empennages was increased. This was achieved by pushing the wing forward. Since the empennage sizing was based on the main wing, this meant the main wing had to be redesigned to further reduce the empennage size. A conventional empennage was used for simplicities sake. The area of the horizontal stabilizers were fairly close in size, with only a difference of 6 ft^2 (0.6 m^2) between the smallest and largest. If additional time was dedicated to the empennage design, a single horizontal stabilizer could've been designed and shared amongst the four configurations. This horizontal stabilizer would then be compared against the initially designed one to see if there was a negligible effect in overall performance. This could also have been applied to the vertical stabilizers, but the surveillance configuration would still need a separately sized one as it required a much bigger size.

8. Landing Gear Design

8.1 Introduction

A tricycle configuration was chosen for the aircraft early on in the design process. Due to the velocity achieved during cruise, a retractable landing gear would be more appropriate. The Excel formulas and calculations for this section can be found in Appendix D.

8.2 Estimation of the Center of Gravity Location for the Aircraft

In order to begin with a detail component weight breakdown, the locations of the landing gear need to be estimated. The location of the nose landing gear was picked to be in front of the wing, which is located 14 feet (4.3 m) from the nose. An estimate of 2 feet (0.6 m) was used for this landing gear. Due to the modular nature of the wings, it would be best for the main landing gear to be connected to the fuselage. For stability, it was assumed the main landing gear would be aft of the CG of the aircraft. An estimate of 18.5 feet (5.6 m) was used for the main landing gear.

8.3 Landing Gear Design

8.3.1 Number, type and size of tires

The main and nose landing gears will each use two tires for a total of six tires. They were sized according to Roskam where the maximum takeoff weight and internal pressure of the tires were used to determine the tire dimension [27]. The internal pressure was kept near 106 psi. The weight on the main landing gears was assumed to be 90% of the overall maximum takeoff gross weight. This was then divided by the total number of tires to determine the weight on each tire. Using these values, an estimated tire size came out to around 20 inches for the diameter and 7.3 inches for the width. Since the tire sizing was close among the four configurations, they will use the same tires. A type III 7.00-8 is the best fit considering the previously stated values.

	Cargo	Combat	Surveillance	Decoy
Weight	8165 lb (3704 kg)	7545 lb (3422 kg)	7722 lb (3503 kg)	7434 lb (3372 kg)
Weight per wheel	1837 lb (833 kg)	1698 lb (770 kg)	1737 lb (788 kg)	1673 lb (759 kg)
Diameter	20.8 in (52.8 cm)	20.2 in (51.3 cm)	20.4 in (51.8 cm)	20.1 in (51.1 cm)
Width	7.5 in (19.1 cm)	7.3 in (18.5 cm)	7.3 in (18.5 cm)	7.2 in (18.3 cm)
Pressure	106.4 psi (733.6 kPa)	106.8 psi (736.4 kPa)	106.2 psi (732.2 kPa)	106.1 psi (731.5 kPa)

8.3.2 Preliminary arrangement

Using the previously defined characteristics, an initial arrangement of the landing gear was created in the form of a CAD model (see Chapter 4.3).

8.3.3 Retraction feasibility

To simulate the retraction of the landing gear fitting within the fuselage, a separate part was added to the CAD model for the stowed configuration.

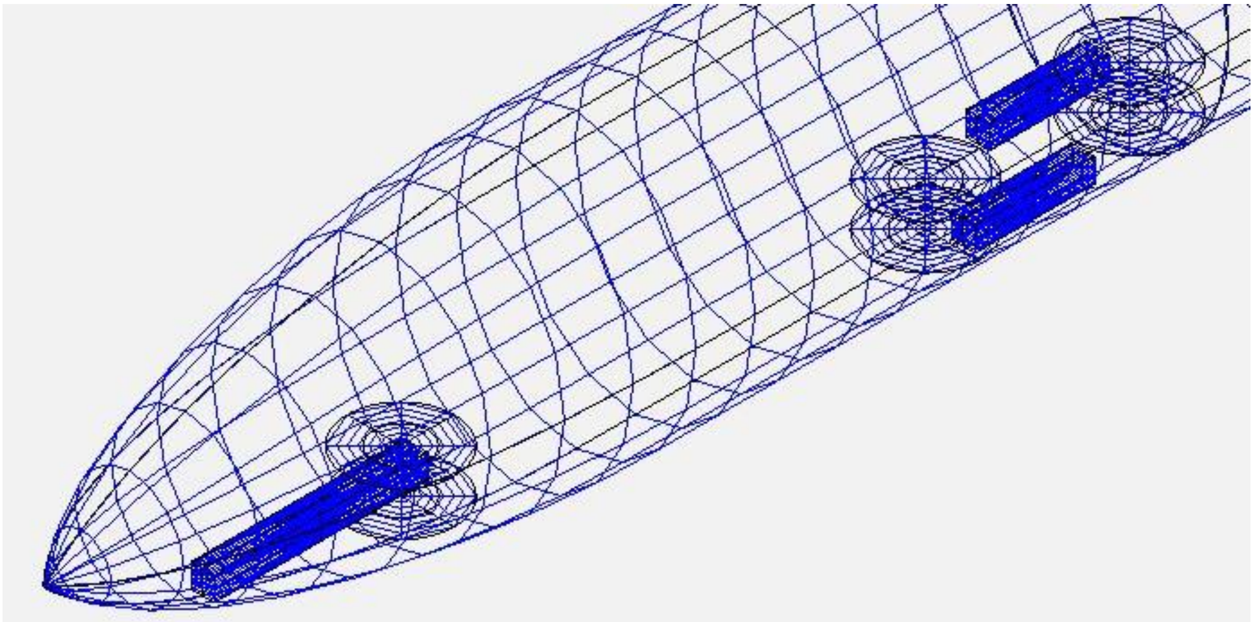

Figure 8-1 Landing gear in stowed configuration

8.3.4 Clearance angles

Table 8.1 Clearance angles of cargo configuration

Parameter	Value
θ_1 (longitudinal tip over angle)	13.5º
θ_2 (longitudinal ground clearance angle)	16.8º
θ_3 (lateral ground clearance angle)	5.4º
θ_4 (semi-apex angle)	14.8º
Ψ (lateral tip over angle)	54.8º

Table 8.2 Clearance angles of combat configuration

Parameter	Value
θ_1 (longitudinal tip over angle)	14.8º
θ_2 (longitudinal ground clearance angle)	16.7º
θ_3 (lateral ground clearance angle)	5.1º
θ_4 (semi-apex angle)	17.4º
Ψ (lateral tip over angle)	52.0º

Table 8.3 Clearance angles of surveillance configuration

Parameter	Value
θ_1 (longitudinal tip over angle)	14.6^o
θ_2 (longitudinal ground clearance angle)	16.7^o
θ_3 (lateral ground clearance angle)	4.1^o
θ_4 (semi-apex angle)	17.1^o
Ψ (lateral tip over angle)	49.5^o

Table 8.4 Clearance angles of decoy configuration

Parameter	Value
θ_1 (longitudinal tip over angle)	16.1^o
θ_2 (longitudinal ground clearance angle)	16.7^o
θ_3 (lateral ground clearance angle)	4.9^o
θ_4 (semi-apex angle)	17.1^o
Ψ (lateral tip over angle)	50.0^o

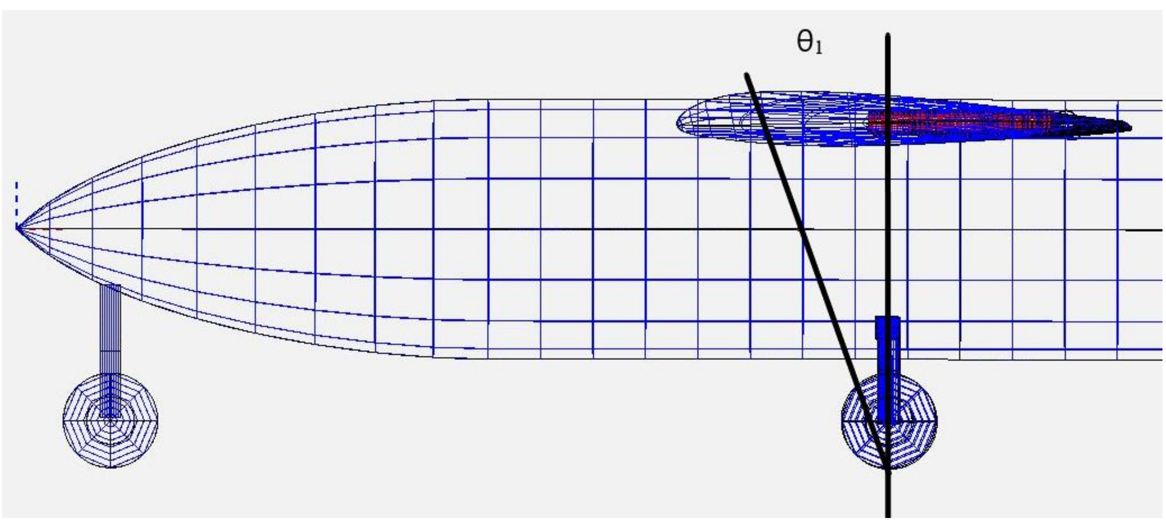

Figure 8-2 Longitudinal tip over angle

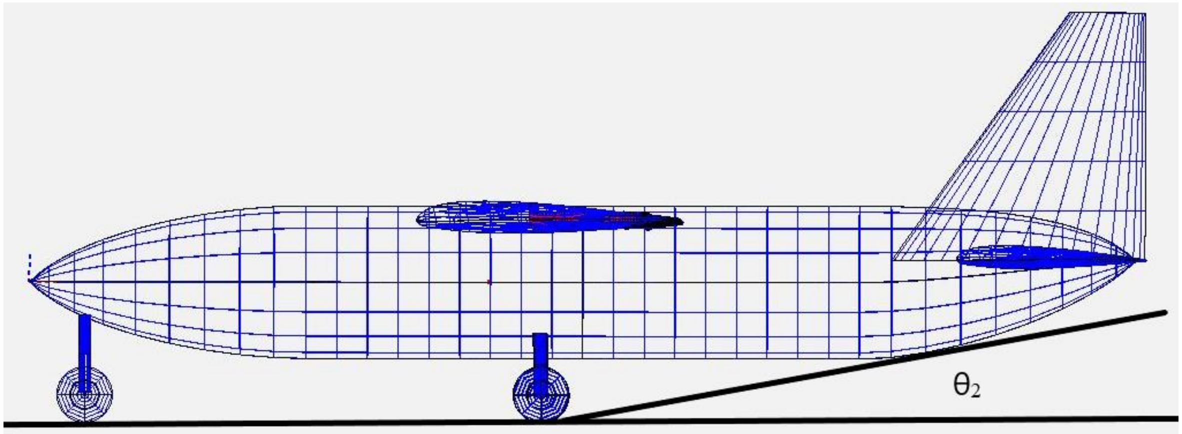

Figure 8-3 Longitudinal ground clearance angle

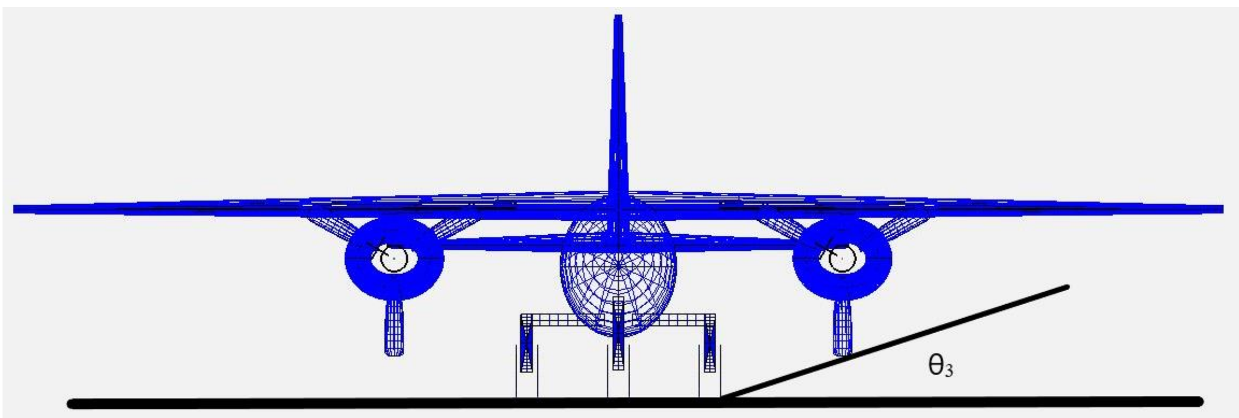

Figure 8-4 Lateral ground clearance angle

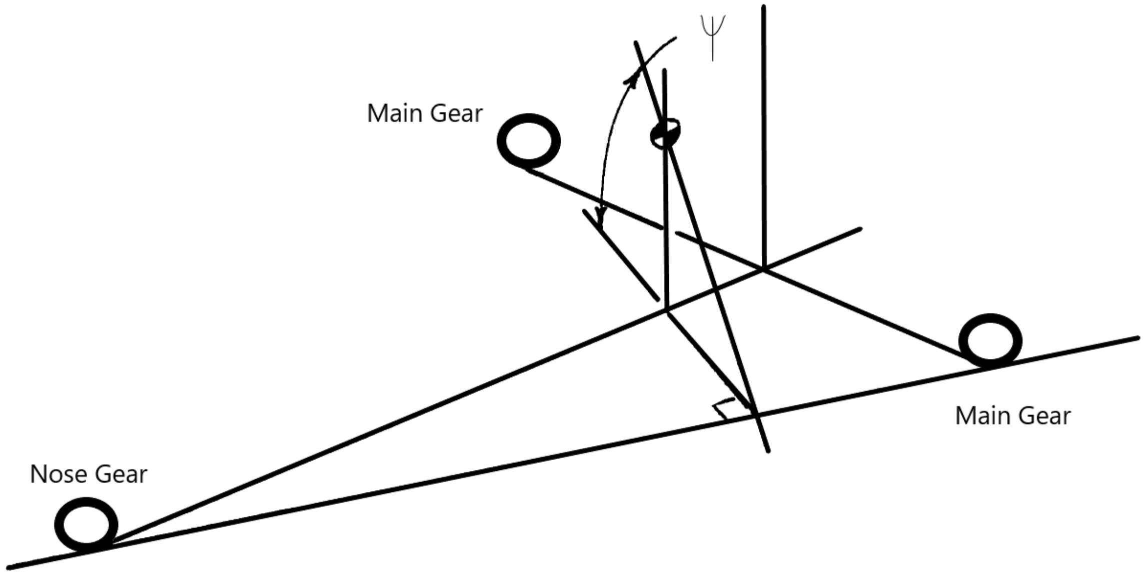

Figure 8-5 Lateral tip over angle

8.4 Discussion

A tricycle configuration was chosen due to other similarly sized aircraft having this layout. If additional time was devoted to the landing gear design, multiple landing gear configurations could've been designed and compared amongst each other to determine the optimal design. At first, a placeholder value was used for the center of gravity. This value was replaced by a center of gravity that was calculated for each configuration. This change required the landing gear to be moved to keep the clearance angles within acceptable values. The following were considered acceptable for a stable aircraft: longitudinal tip over angle around 15°, a longitudinal ground clearance angle of at least 15°, a lateral ground clearance angle of at least 5°, and a lateral tip over angle under 55°. A careful balance was required to keep the clearance angles within of near the accepted values. In the case of the surveillance configuration, it had a lower lateral ground clearance angle compared to the other three configurations. The location of the landing gear needed to be kept constant amongst the four configurations so the landing gear couldn't be moved too far away from configuration to configuration. While a higher lateral ground clearance angle would've been ideal, it was not low enough that another iteration was required.

9. Weight and Balance Analysis

9.1 Introduction

Now that more aspects of the design have been finalized, a more accurate weight can be calculated for the components. Using data such as the empty weight, maximum takeoff weight, fuel weight, and wing sizing, the necessary size of the components of the empty aircraft can be calculated.

9.2 Component Weight Breakdown

Using the methods described in Raymer's textbook, the component weight breakdown was calculated as follows [26]:

Table 9.1 Component weight breakdown and CG locations for cargo configuration

Component	Weight	X location
Wing	634 lb (288 kg)	17.4 ft (5.3 m)
Horizontal tail	102 lb (46 kg)	35.5 ft (10.8 m)
Vertical tail	65 lb (29 kg)	36.1 ft (11 m)
Fuselage	725 lb (329 kg)	15.6 ft (4.8 m)
Main landing gear	381 lb (173 kg)	22 ft (6.7 m)
Nose landing gear	103 lb (47 kg)	9 ft (2.7 m)
Installed engine	968 lb (439 kg)	16.9 ft (5.2 m)
Fuel systems	150 lb (68 kg)	16.9 ft (5.2 m)
Flight controls	114 lb (52 kg)	4 ft (1.2 m)
Hydraulics	81 lb (37 kg)	22 ft (6.7 m)
Electrical	324 lb (147 kg)	4 ft (1.2 m)
Avionics	403 lb (183 kg)	5 ft (1.5 m)
A/C and anti-ice	232 lb (105 kg)	5 ft (1.5 m)
Furnishings	357 lb (162 kg)	20 ft (6.1 m)

Table 9.2 Component weight breakdown and CG locations for combat configuration

Component	Weight	X location
Wing	654 lb (297 kg)	17.4 ft (5.3 m)
Horizontal tail	102 lb (46 kg)	35.5 ft (10.8 m)
Vertical tail	69 lb (31 kg)	36.2 ft (11 m)
Fuselage	728 lb (330 kg)	15.6 ft (4.8 m)
Main landing gear	259 lb (117 kg)	22 ft (6.7 m)
Nose landing gear	77 lb (35 kg)	9 ft (2.7 m)
Installed engine	968 lb (439 kg)	16.9 ft (5.2 m)
Fuel systems	129 lb (59 kg)	16.9 ft (5.2 m)
Flight controls	111 lb (50 kg)	4 ft (1.2 m)
Hydraulics	76 lb (34 kg)	22 ft (6.7 m)
Electrical	318 lb (144 kg)	4 ft (1.2 m)
Avionics	403 lb (183 kg)	5 ft (1.5 m)

Table 9.3 Component weight breakdown and CG locations for surveillance configuration

Component	Weight	X location
Wing	883 lb (401 kg)	17.2 ft (5.3 m)
Horizontal tail	104 lb (47 kg)	35.5 ft (10.8 m)
Vertical tail	85 lb (39 kg)	36.6 ft (11.2 m)
Fuselage	722 lb (327 kg)	15.6 ft (4.8 m)
Main landing gear	259 lb (117 kg)	22 ft (6.7 m)
Nose landing gear	77 lb (35 kg)	9 ft (2.7 m)
Installed engine	968 lb (439 kg)	16.9 ft (5.2 m)
Fuel systems	191 lb (87 kg)	16.9 ft (5.2 m)
Flight controls	112 lb (51 kg)	4 ft (1.2 m)
Hydraulics	73 lb (33 kg)	22 ft (6.7 m)
Electrical	225 lb (102 kg)	4 ft (1.2 m)
Avionics	403 lb (183 kg)	5 ft (1.5 m)

Table 9.4 Component weight breakdown and CG locations for decoy configuration

Component	Weight	X location
Wing	603 lb (274 kg)	17.6 ft (5.4 m)
Horizontal tail	102 lb (46 kg)	35.6 ft (10.9 m)
Vertical tail	66 lb (30 kg)	36.2 ft (11 m)
Fuselage	714 lb (324 kg)	15.6 ft (4.8 m)
Main landing gear	247 lb (112 kg)	22 ft (6.7 m)
Nose landing gear	75 lb (34 kg)	9 ft (2.7 m)
Installed engine	968 lb (439 kg)	16.9 ft (5.2 m)
Fuel systems	214 lb (97 kg)	16.9 ft (5.2 m)
Flight controls	99 lb (45 kg)	4 ft (1.2 m)
Hydraulics	69 lb (31 kg)	22 ft (6.7 m)
Electrical	341 lb (155 kg)	4 ft (1.2 m)
Avionics	403 lb (183 kg)	5 ft (1.5 m)

9.3 Center of Gravity Location for Various Loading Scenarios

To accurately model the center of gravity, various loading scenarios needed to be considered. This includes the aircraft with no fuel or no payload. In the case of the transport configuration, the CG at with both the payload and fuel was the same as when the fuel was removed at 16.6 feet (5.1 m) from the nose. With just the fuel, the CG moved to 15.6 feet (4.8 m). The combat configuration had a full payload and fuel CG at 15.8 feet (4.8 m). Removing the fuel brought the CG to 15.5 feet (4.7 m), with the CG shifting to 15.6 feet (4.8 m) after removing the payload. The surveillance configuration had a full fuel and payload configuration CG at 16.2 feet (4.9 m). Removing the fuel brought the CG to 16.4 feet (5.0 m). Due to the smaller payload, the CG moved to 15.8 feet (4.8 m) after removing the payload. The decoy has an even smaller payload which resulted in the full fuel and full payload in and the payload out to have the same CG at 15.8 feet (4.8 m). Removing the fuel shifted the CG to 15.5 feet (4.7 m). The largest movement out of all the configurations was attributed to the cargo configuration when the payload is added, moving the CG 1.3 feet (0.4 m).

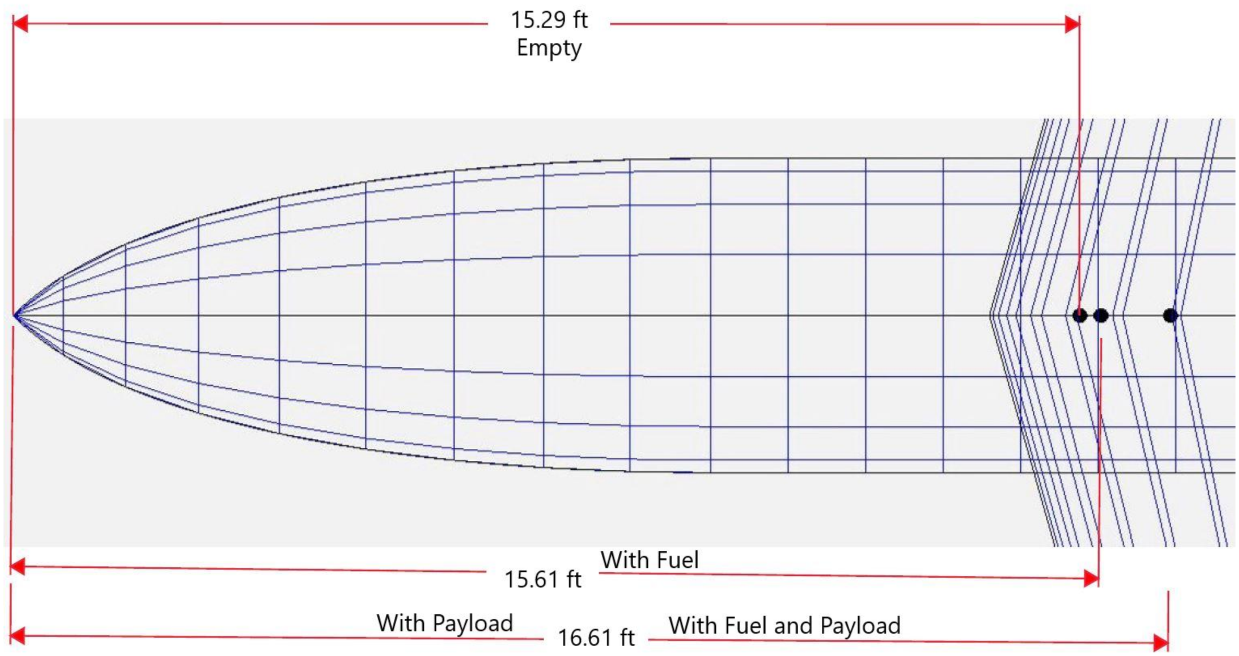

Figure 9-1 Cargo CG locations for empty, payload and fuel, just payload, and just fuel loading scenarios

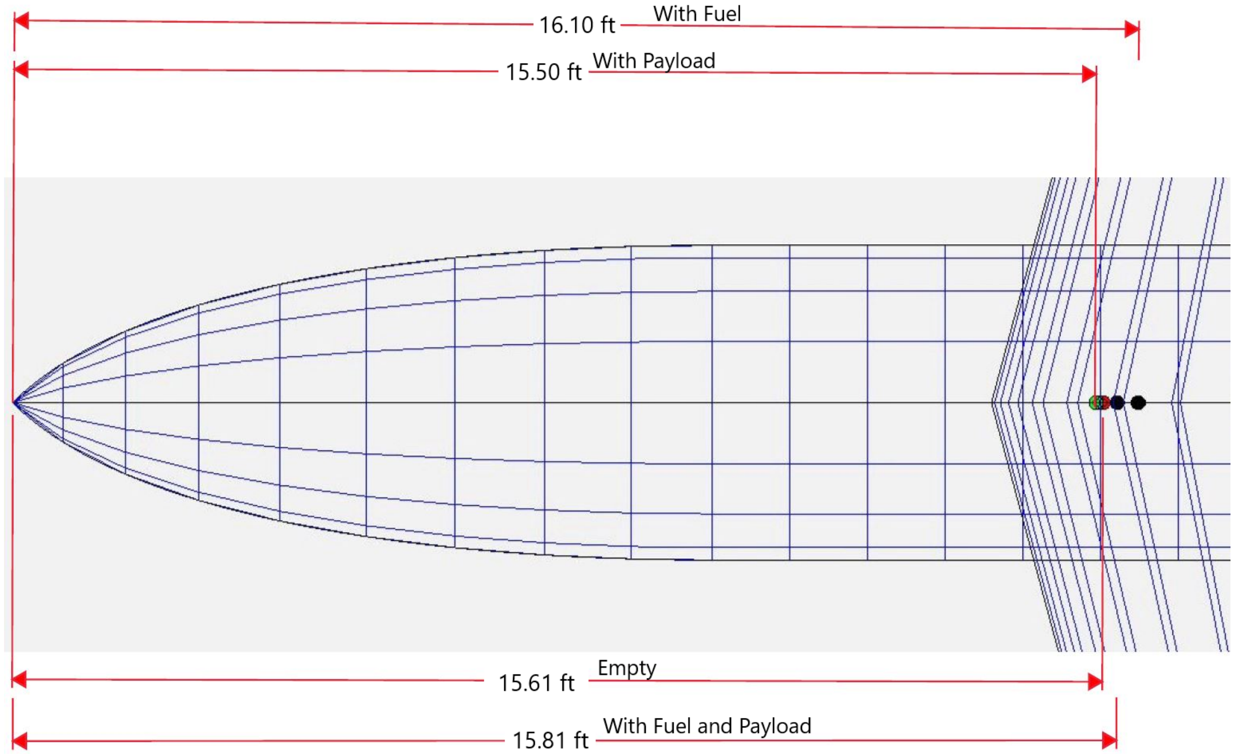

Figure 9-2 Combat CG locations for empty, payload and fuel, just payload, and just loading scenarios

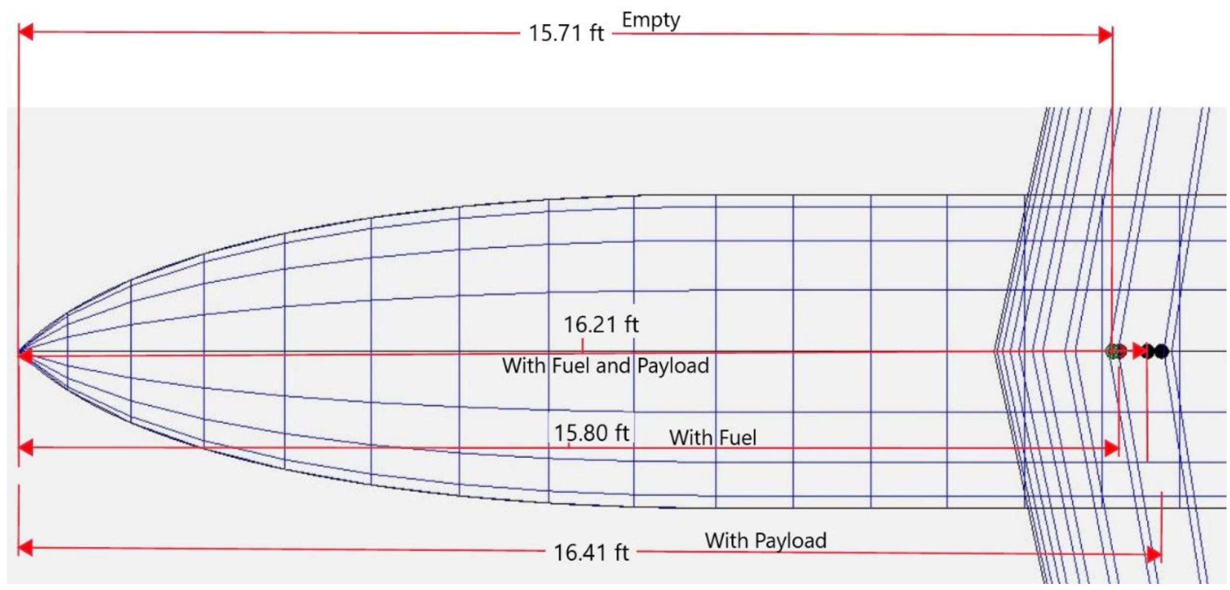

Figure 9-3 Surveillance CG locations for empty, payload and fuel, just payload, and just loading scenarios

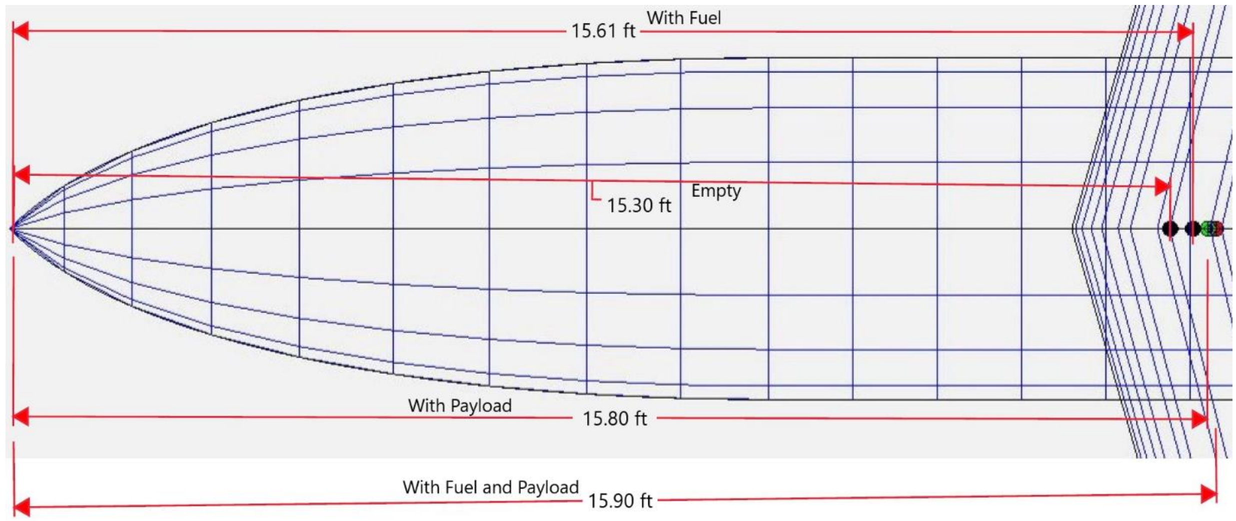

Figure 9-4 Decoy CG locations for payload and fuel, just payload, and just loading scenarios

9.4 Discussion

Using the CG locations from this chapter along with the neutral point of the aircraft, the overall stability can be determined. The weight breakdown from this chapter will be used as a reference for chapter 16, where a more detailed breakdown is defined. These values will need to be fairly similar with a 5% tolerance being used to determine if additional design iterations need to occur. The air conditioning and furnishings were only considered in the cargo configuration as the other three configurations will not be carrying passengers. This caused the cargo configuration to require an additional 590 lb. Due to this additional weight, these two extra components were placed near the nose and main wing so that the overall CG didn't widely vary amongst the configurations. Currently, the farthest the CG moves is 1.3 feet (0.4 m) aft. If necessary, further iterations on the design will occur. These changes will be noted. The Excel formulas and calculations for this section can be found in Appendix C.

10. Stability and Control Analysis

10.1 Introduction

Now that the forward and aft movement of the CG with various loading conditions has been calculated, the overall stability of the aircraft can be determined. Using XFLR5, the neutral point of the aircraft can be found. With these known values, the static margins can be calculated. In addition to this, the lateral and longitudinal stability angles can be found. These angles will show if the aircraft is able to remain stable in a neutral position. Should these values show a high degree of instability, some aspects of the aircraft may need to be adjusted. This includes: moving the position of the landing gear, moving internal components to move the CG, or moving the position of the wing and empennages.

10.2 Static Margin

Table 10.1 Stability of cargo configuration

Parameter	Value
XNP	17.6 ft (5.4 m)
XCG_f	15.3 ft (4.7 m)
XCG_a	16.6 ft (5.1 m)
SM_{f1}	33.63%
SM_{a1}	14.62%

Table 10.2 Stability of combat configuration

Parameter	Value
XNP	17.3 ft (5.3 m)
XCG_f	15.5 ft (4.7 m)
XCG_a	16.1 ft (4.9 m)
SM_{f1}	26.71%
SM_{a1}	17.80%

Table 10.3 Stability of surveillance configuration

Parameter	Value
XNP	17.3 ft (5.3 m)
XCG_f	15.7 ft (4.8 m)
XCG_a	16.4 ft (5.0 m)
SM_{f1}	24.72%
SM_{a1}	13.70%

Table 10.4 Stability of decoy configuration

Parameter	Value
XNP	17.5 ft (5.3 m)
XCG_f	15.3 ft (4.7 m)
XCG_a	15.9 ft (4.8 m)
SM_{f1}	30.92%
SM_{a1}	22.41%

10.3 Discussion

Due to slight differences in the wings between the configurations, the neutral point of the aircraft varied slightly. Between the largest and smallest neutral point was a difference of 0.3 ft (0.09 m). Across the four configurations, all the static margins are positive meaning each aircraft is statically stable. The Excel formulas and calculations for this section can be found in Appendix D. The static margins were calculated twice using two separate methods to ensure these values were correct. Across the board, the static margin values did not differ using another method.

11. Drag Polar Estimation

11.1 Introduction

At this point in the design, the characteristics of the wing have been finalized. Using the known values and OpenVSP, the wetted area of the wing can be found. This can be used to get an estimate of the initial drag that the aircraft will experience.

11.2 Airplane Drag Polars and Low Speed Drag Increments

Table 11.1 Drag estimation of cargo configuration

Parameter	Value
Cfe	0.0045
S_{wet}/S_{ref}	4.4
Clean CD_0	0.0198
Takeoff CD_0	0.0548
Landing CD_0	0.1048
Clean L/D_{max} at $C_L = 0.6$	15.4
Takeoff L/D_{max} at $C_L = 1.0$	9.0
Landing L/D_{max} at $C_L = 1.3$	6.3

Table 11.2 Drag estimation of combat configuration

Parameter	Value
Cfe	0.0045
S_{wet}/S_{ref}	4.3
Clean CD_0	0.0196
Takeoff CD_0	0.0546
Landing CD_0	0.1046
Clean L/D_{max} at $C_L = 0.6$	16.0
Takeoff L/D_{max} at $C_L = 1.0$	9.3
Landing L/D_{max} at $C_L = 1.4$	6.5

Table 11.3 Drag estimation of surveillance configuration

Parameter	Value
Cfe	0.0045
S_{wet}/S_{ref}	4.4
Clean CD_0	0.0197
Takeoff CD_0	0.0547
Landing CD_0	0.1047
Clean L/D_{max} at $C_L = 0.7$	17.9
Takeoff L/D_{max} at $C_L = 1.1$	10.4
Landing L/D_{max} at $C_L = 1.5$	7.2

Table 11.4 Drag estimation of decoy configuration

Parameter	Value
Cfe	0.0045
S_{wet}/S_{ref}	4.3
Clean CD_0	0.0196
Takeoff CD_0	0.0546
Landing CD_0	0.1046
Clean L/D_{max} at $C_L = 0.6$	15.5
Takeoff L/D_{max} at $C_L = 1.0$	9.0
Landing L/D_{max} at $C_L = 1.3$	6.3

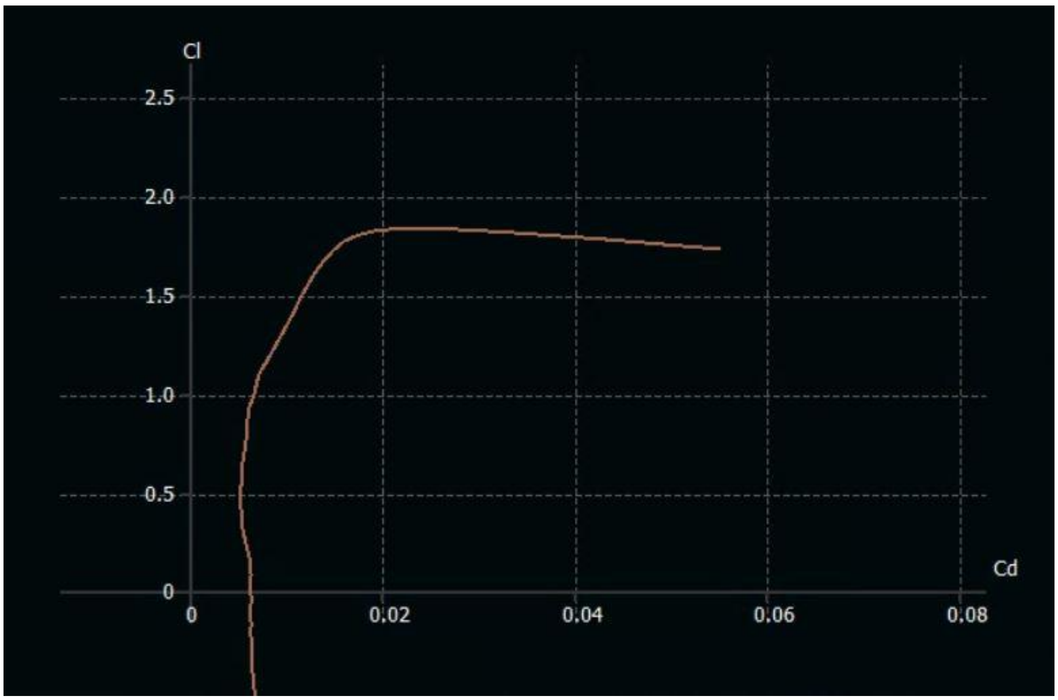

Figure 11-1 C_l vs C_d plot

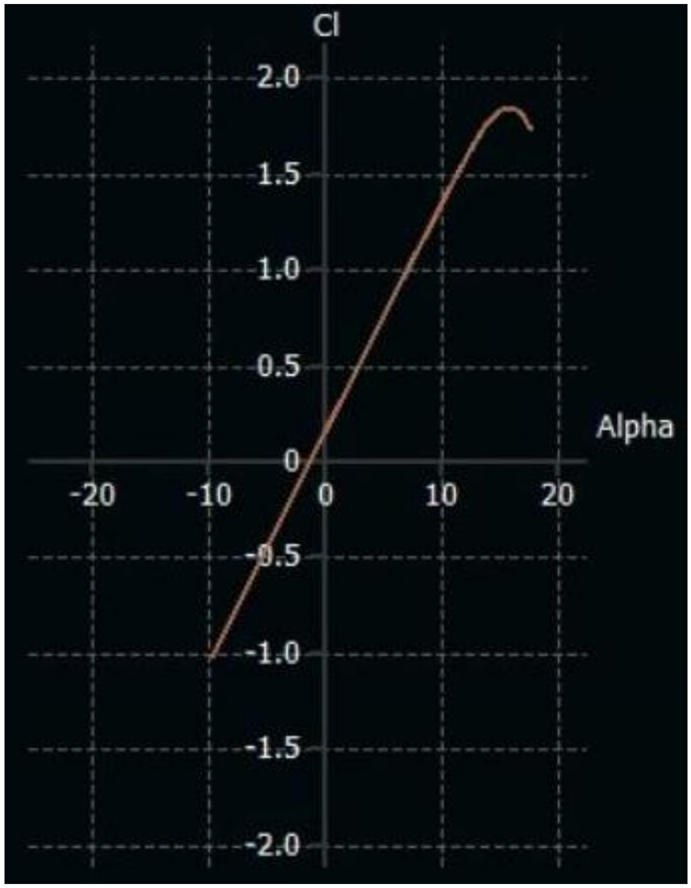

Figure 11-2 C_l vs angle of attack plot

11.3 Discussion

The Excel formulas and calculations for this section can be found in Appendix E. Raymer was used for the tables presented above, but Roskam was used as a reference to check the values. The skin friction coefficient was higher at 0.007 for Roskam, which in turn resulted in a higher CD_0 across the four configurations. In turn, this resulted in a lower clean L/D at cruise across the board. The cargo went from 15.4 to 12.4, the combat from 16 to 12.8, the surveillance from 17.9 to 14.2, and the decoy from 15.5 to 12.4. The results from Roskam will be used for the Class II drag polar estimation as there is not an equivalent section in Raymer. The Class I results for Roskam will also be presented in the Class II section.

12. Drawings, Environmental and Safety Considerations

12.1 Drawings

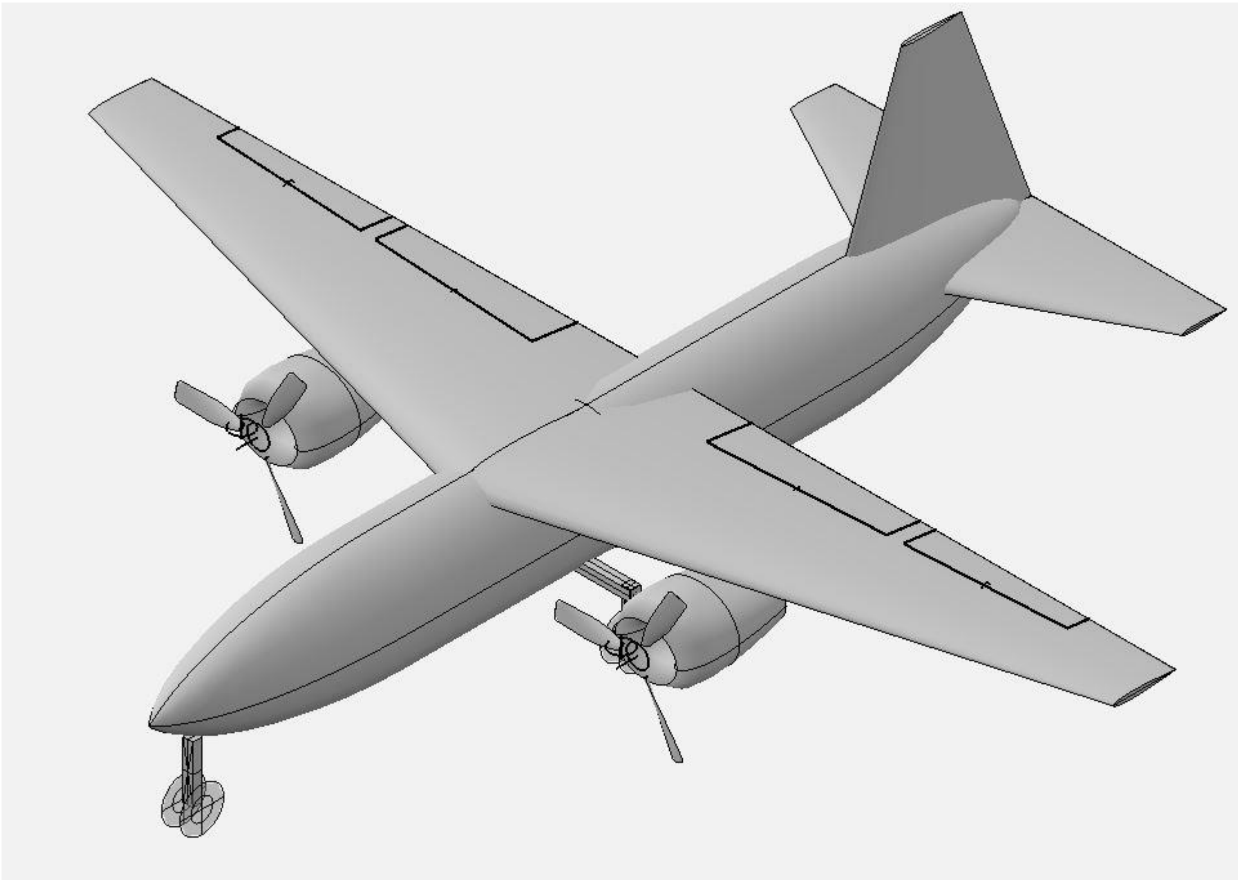

Figure 12-1 Updated CAD model for the cargo configuration

12.2 Environmental Considerations

To address aircraft that can only be used for a single type of missions, whether that is combat, transport, or surveillance, the aircraft designed in this project will be able to accomplish a variety of mission types. Instead of storing four separate aircraft, this design will only require a single aircraft to be stored along with the modular wings. Less materials will be used in addition to less manufacturing being required. By the end of the lifecycle of an aircraft, the components need to be stripped and recycled. Higher value parts that can be recycled include the engine and navigation systems. The cost of recycling an aircraft can reach into the $100,000s [30]. Any way in which the size of the aircraft can be reduced can lower overall costs, especially those related to recycling. By having only one fuselage and four sets of wings, smaller transport trucks can be used to send the materials to recycling plants, which reduces the carbon footprint. As the aeronautical industry grows, more airplanes will be created and then decommissioned over time. The aircraft recycling industry revenue has been estimated to be $6 billion [30]. It is expected that in the future, the recycling industry for aircraft will need to increase just as much as the aeronautical [30]. By creating a multi-mission aircraft, less materials will be required to build it, and less materials will be used to recycle it.

When it comes to recycling materials from an aircraft, 0.1% of the environmental emissions of an aircraft are related to recycling with the other 99.9% coming from operational use [30]. Recycling results in a net positive as the environmental emissions are low and reusing materials is good for the environment and can result in costs being reduced. At this time, there is not much in the way of recycling composite materials, but as the aeronautical industry continues to grow, it should be a matter of time before new recycling methods are developed.

12.3 Safety Considerations

During times of conflict, pilots would risk their lives by flying near enemy territories. The nature of the missions being in areas of conflict result in a higher probability of an accident or fatality [31]. Even ignoring fatal accidents, there's still the possibility of pilot error or environmental oversight that results in injuries or damage to the pilot or aircraft. Using a UAV instead of a traditional airplane means the pilot no longer has to physically be on the aircraft. By removing the pilots onboard, their safety is no longer tied to the safety of the aircraft. Safety features such as: an ejection seat, a parachute, GPS, or emergency supplies are no longer necessary and the associated costs with them can be diverted toward the communications for remote piloting.

13. Airplane Subsystem Arrangement

13.1 Flight Controls System

Since all four configurations will be unmanned, there is no need for a flight controls system. Instead, through the use of the control surfaces (flaps and ailerons), the hydraulic system, and the software, the pilot will be able to have full control over the aircraft. Sensors will be used to monitor the position of the control surfaces to ensure the correct positions for each stage of the mission. Since the aircraft is unmanned, the pilot and control system will need to interact remotely.

13.2 Propulsion System

The engine used in all four configurations is the Continental GSIO-520-D. It is a piston engine that is capable of 375 HP (280 KW) per engine. The highest required horsepower was for the combat configuration which required 309 HP (230 KW), and the lowest horsepower required being 222 HP (166 KW) for the surveillance configuration. It has a specific fuel consumption of 0.4 lb/(HP*h) (243 g/(KW*h)) and a weight of 484 lb (220 kg). With a length of 64 inches (1.6 m), a height of 27 inches (0.7 m) and a width of 34 inches (0.9 m), the engine will fit when mounted directly on the wings. In all four configurations, a twin engine setup will be used.

To select an engine for the aircraft, the required horsepower was one of the main deciding factors. During each stage of the engine selection, 5 engines were chosen based on this. From this list, the specific fuel consumption and weight were taken into account. Comparing these three factors, an engine was chosen. Due to the iterative process of the design, this comparison was done three times due to the required horsepower changing amongst iterations. The Continental GSIO-520-D was not the most powerful engine, but it had one of the lowest weights while being able to provide enough horsepower for all four configurations.

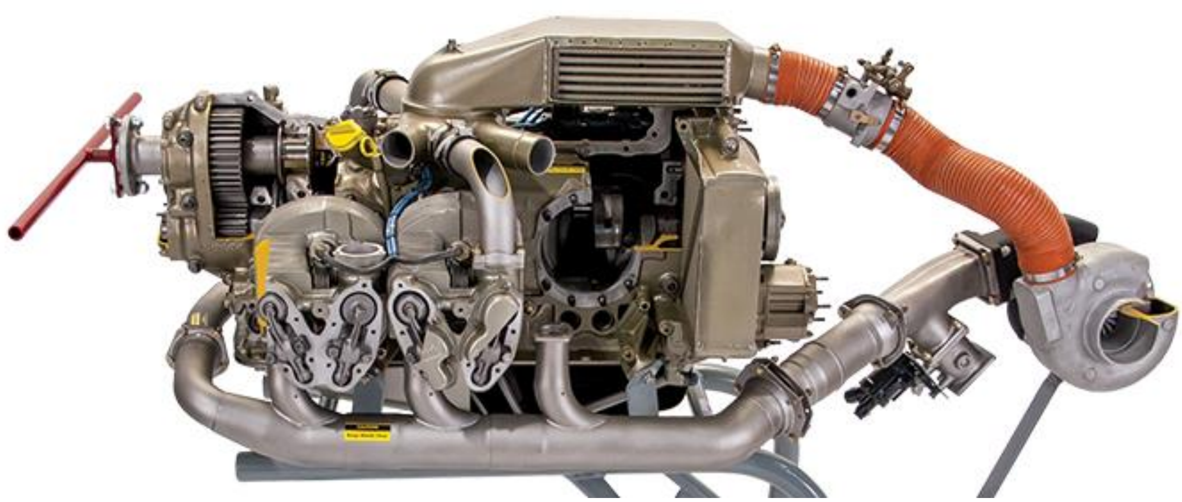

Figure 13-1 Continental GSIO-520-D [32]

13.3 Fuel System Layout Design

As all the fuel will be stored in the wings, the fuel system will be centered about this area. Fuel lines will be used to transport the fuel from the tanks to the engine. Each wing will house a fuel pump, fuel tank, valves, and filters. These will remain consistent among the four configurations aside from the fuel tank, which will vary in size. Due to the amount of fuel needed for the mission, the fuel in the wings were separated into two different tanks per wing. To balance the fuel in each wing, the valves and pumps will work in tandem with each other to prevent an imbalance.

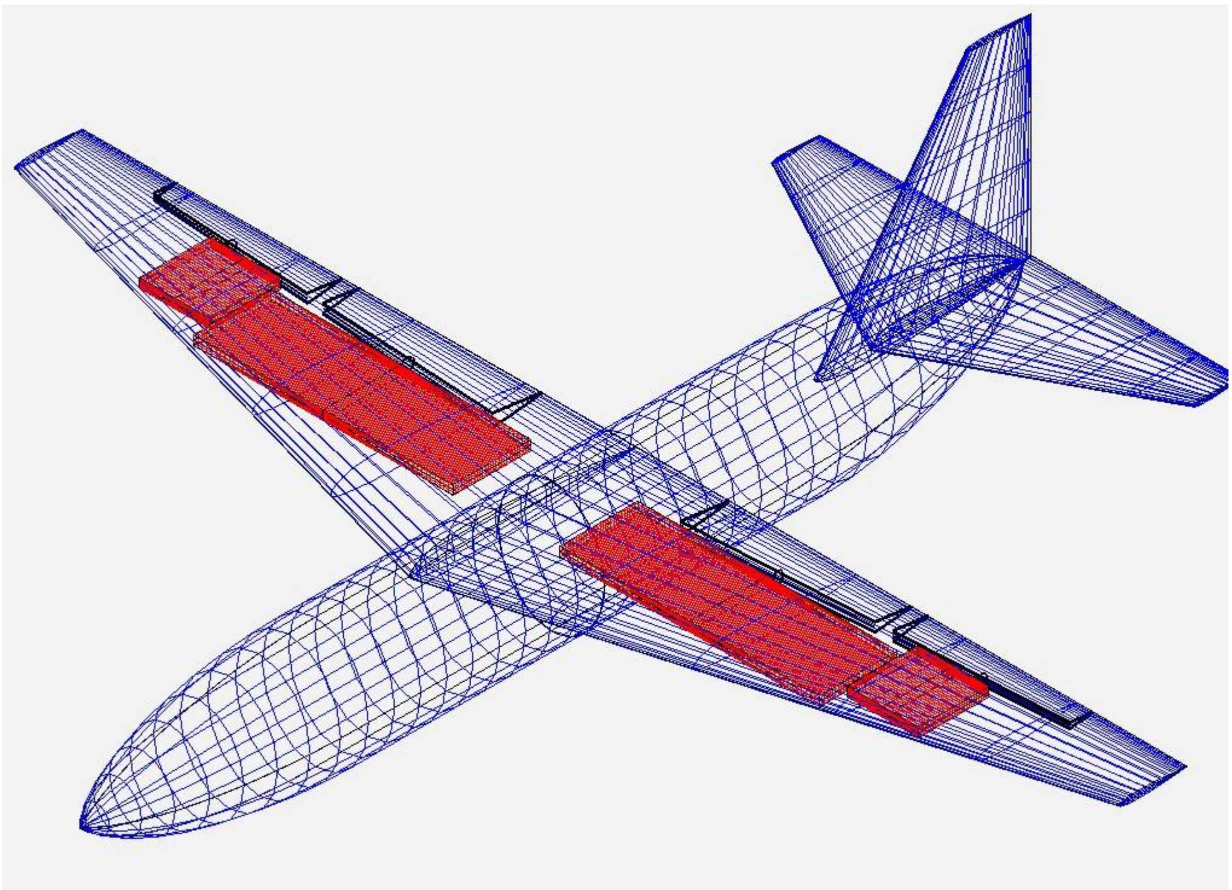

Figure 13-2 Fuel tanks for the cargo configuration

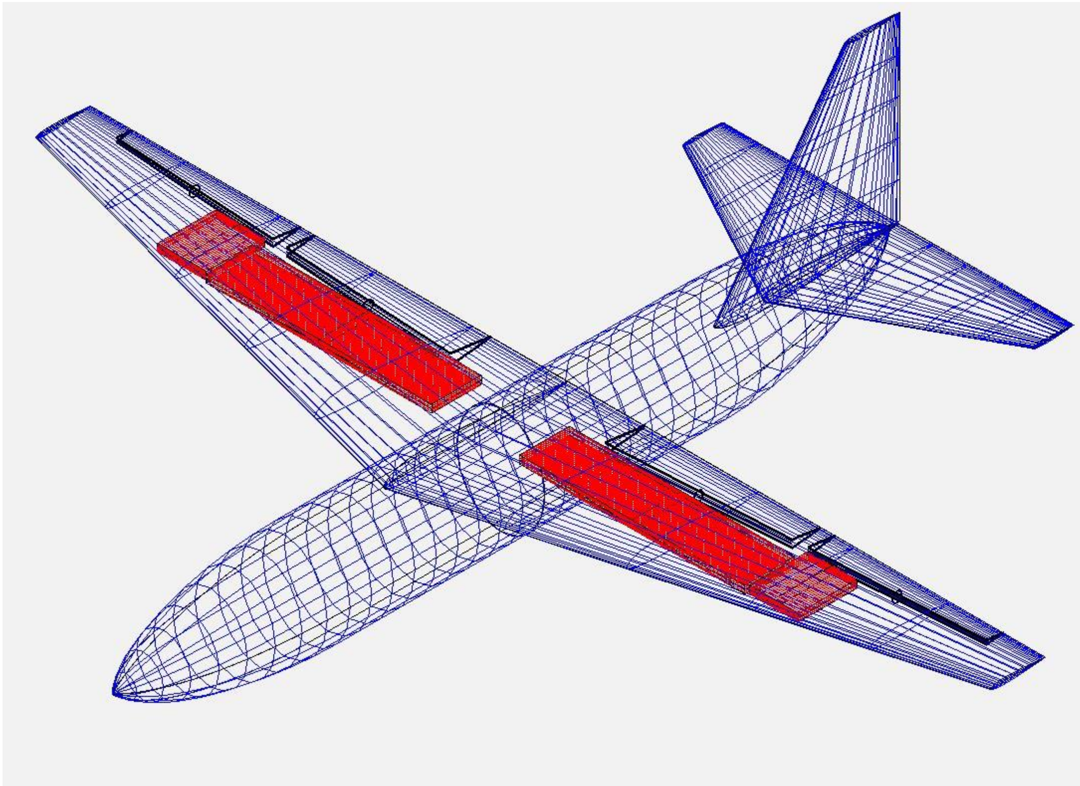

Figure 13-3 Fuel tanks for the combat configuration

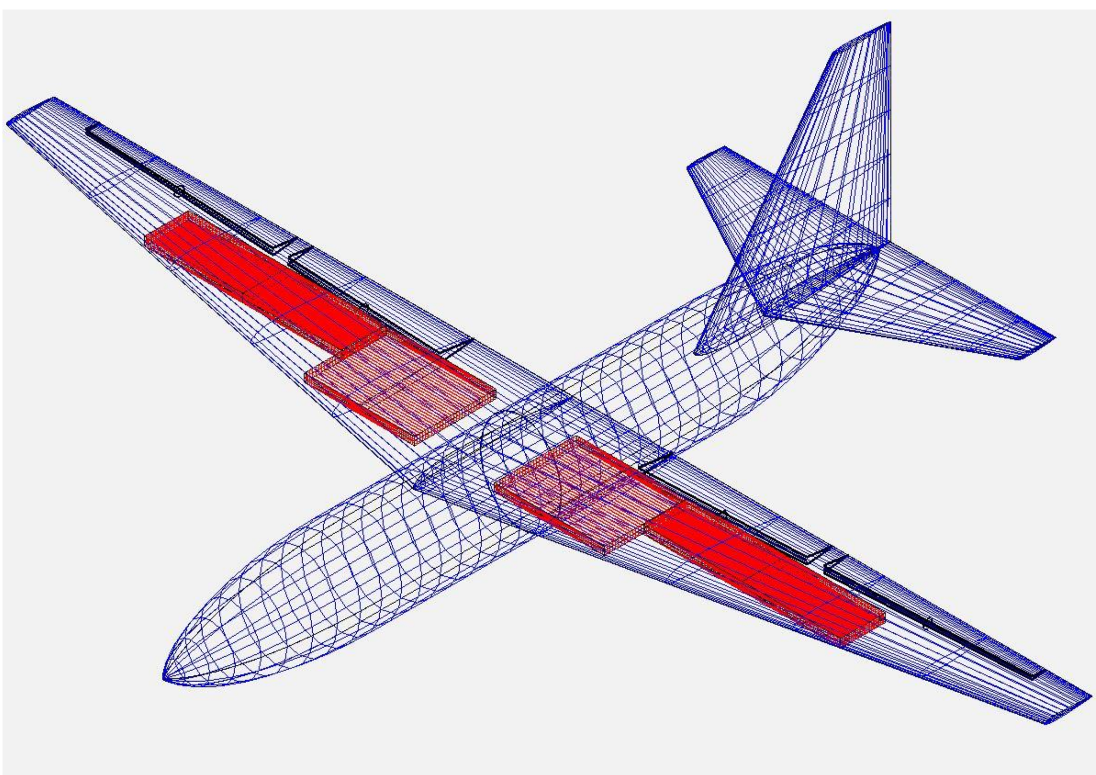

Figure 13-4 Fuel tanks for the surveillance configuration

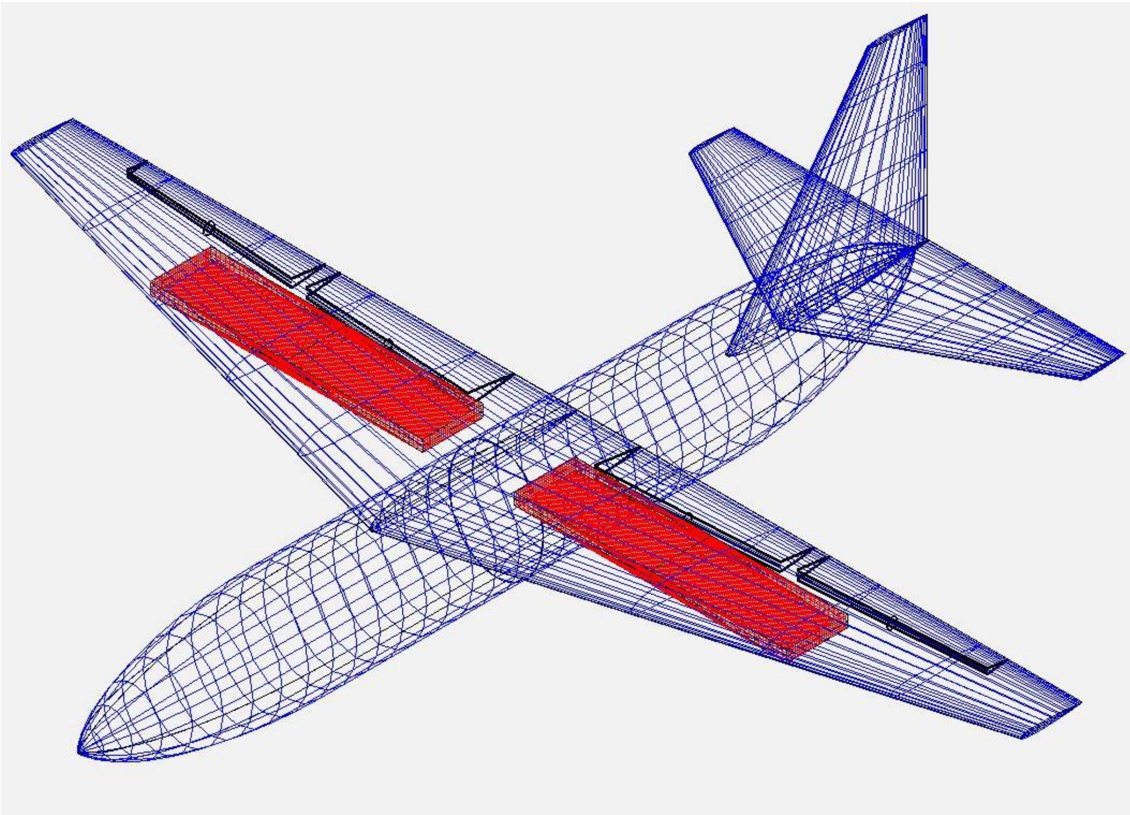

Figure 13-5 Fuel tanks for the decoy configuration

13.4 Hydraulic System Layout Design

The hydraulics will be used in the landing gear, brakes, and control surfaces. This will be accomplished through the use of pumps, reservoirs, heat exchangers, sensors, valves, and actuators. To prevent pinching or cutting of hydraulic lines, the lines will be kept away from the control surfaces. Each wing will have a separate hydraulic system to increase redundancy in case of an emergency. MIL-H-87257 will be used since this fluid is fire resistant.

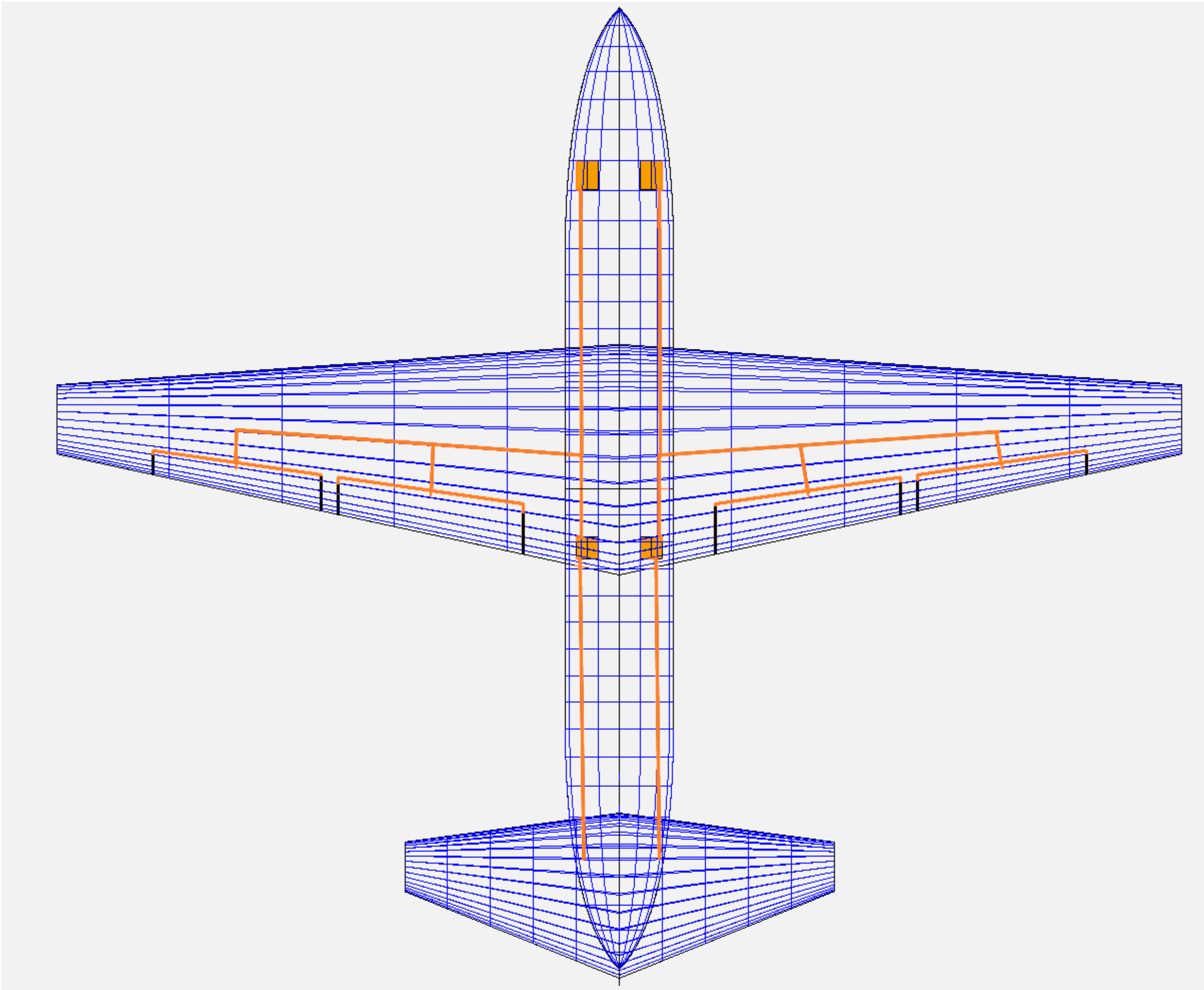

Figure 13-6 Hydraulic Lines

13.5 Electrical System Layout Design

To power the aircraft and start the engines, two separate batteries will be used. Both will be located near the nose where the cockpit would typically be. Each battery will power its respective side of the aircraft. The batteries were sized so that if one becomes inoperable, the other will be able to provide enough power to temporarily support the other side. This redundancy will reduce the chances of a mission failure. The wiring for the electrical system is small enough that managing the cables would not pose an issue when arranging the other subsystems.

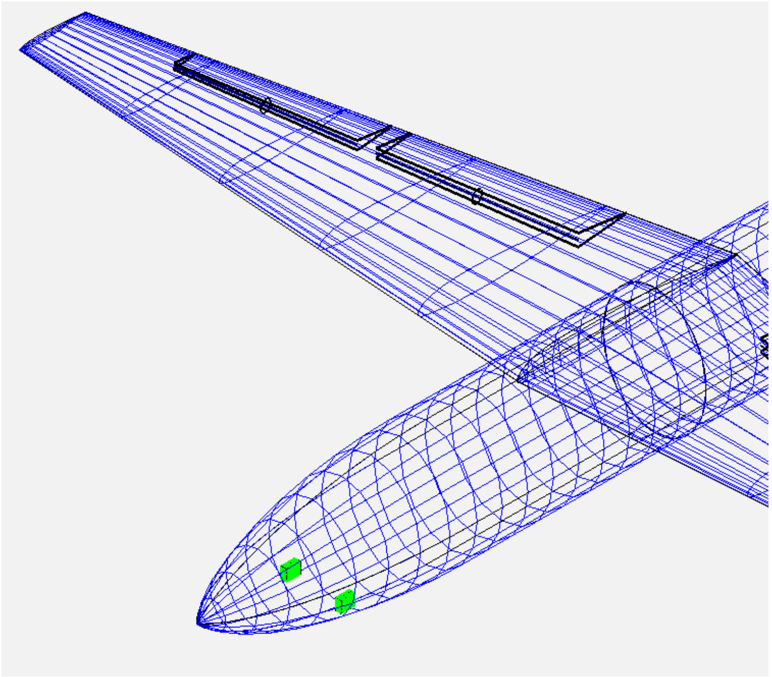

Figure 13-7 Battery locations

13.6 Environmental Control System

The cargo configuration will be the only aircraft that carries humans, so it will be the only configuration with A/C. This system will be centered on the paratroopers in the center of the fuselage. Since the aircraft is unmanned, the cockpit will only contain the avionics and not require A/C.

13.7 Ground Station Instrumentation and Avionics System

There will be no pilot onboard, so all the displays and other visual indicators will be at a ground station. There will still be avionics onboard, but all the information will be transmitted to the ground station. To accomplish this, both radio and satellite antennas will be used. To keep latency down and improve bandwidth, the avionics will need a stable, high frequency satellite connection. For more accurate tracking, a GPS system will be incorporated. Since the missions will be military in nature, all communications will need to be encrypted to prevent the enemy from intercepting the data. All data stored onboard will be encrypted as well.

Since the combat configuration will not be able to compete with other combat aircraft, it will be equipped with air to ground missiles. With a stationary target, this configuration will not need an advanced targeting system. The surveillance configuration will need additional avionics to store and transmit the data collected during missions. These additional avionics have been accounted for in the form of the 500 lb (227 kg) payload.

13.8 Escape System/Emergency System

Since the cargo configuration is the only aircraft that will carry people, this subsystem is only applicable to the cargo configuration. For the purposes of the mission, the paratroopers will have a main door upon which they will enter and exit the aircraft. In the case of an emergency, there is another door on the opposite side of the fuselage. Since it's not the main door, it will be slightly smaller in size. This is the only necessary escape system as the aircraft will be unmanned.

13.9 Discussion

If additional time was devoted to this section of the design, each subsystem would've been further detailed to include aspects such as specific components used, or to optimize the overall layout design. The fuel tanks were designed using a box shape for simplicity, but this could've been defined further to show the fuel shape with the internal spars and ribs in mind. This would most likely slightly decrease the overall volume of the fuel tanks, as they would be shaped according to the internals of the wing. The hydraulic system was designed in 2-D, but with additional time the hydraulic system layout could've been modeled in the CAD software so an isometric view of the subsystem could be included. The internal wires connecting the various subsystems was not modeled due to time constraints, but this could've been further detailed to show the total wire length required in addition to ways to use the shortest wire length possible.

14. Initial Structural Arrangement

14.1 Introduction

OpenVSP was used to create the internal structure of the aircraft. Using the FEA structure tab, the CAD drawings from previous chapters could be further detailed through the definition of spars, ribs, and skins. These definitions were applied to the fuselage, wings, and empennages. By first defining the number of ribs and the distance between them, the program would detail the specified structure from one end to the other. The spars had to be manually defined and placed within the structure. Using the reference aircraft as an example, two main spars were used for the wings and empennages. This process was repeated across the four variations except for the fuselage which was kept the same throughout the variations.

14.2 Structural Drawings

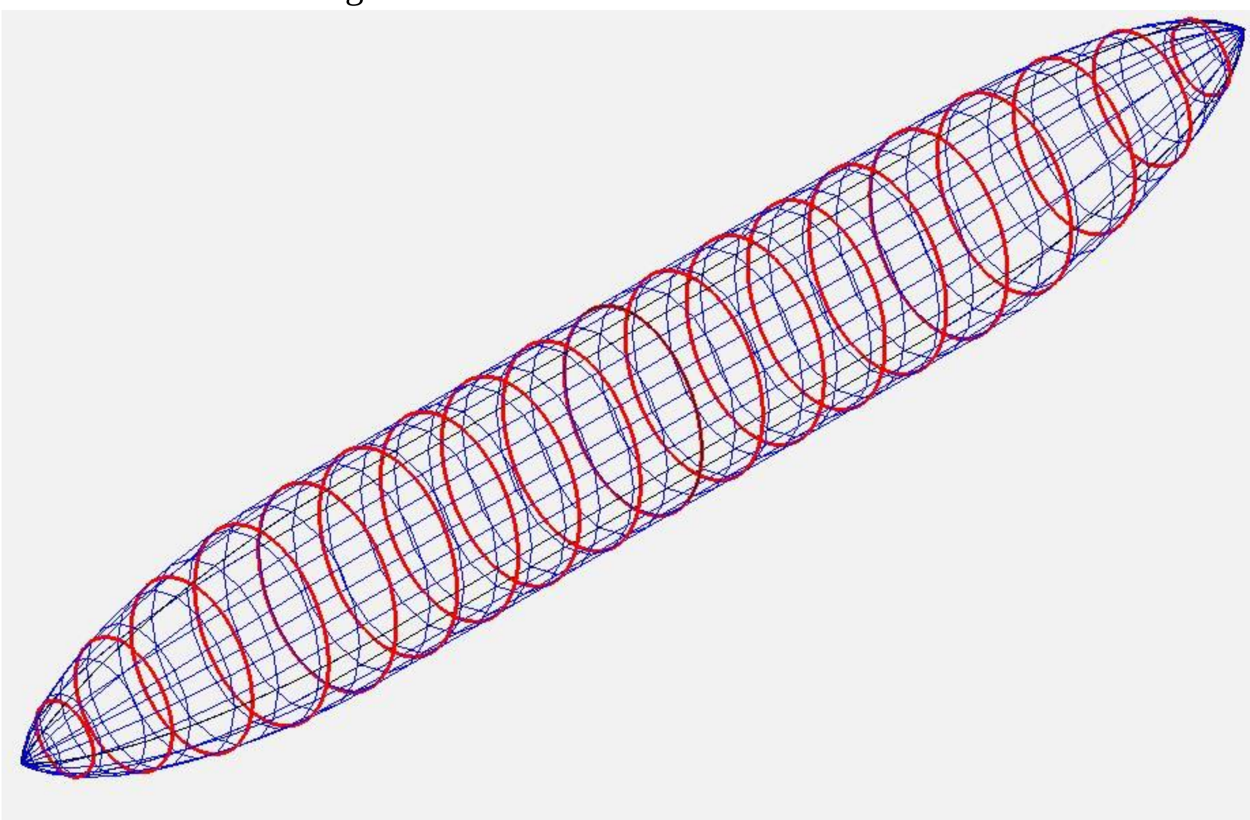

Figure 14-1 Fuselage internal array layout

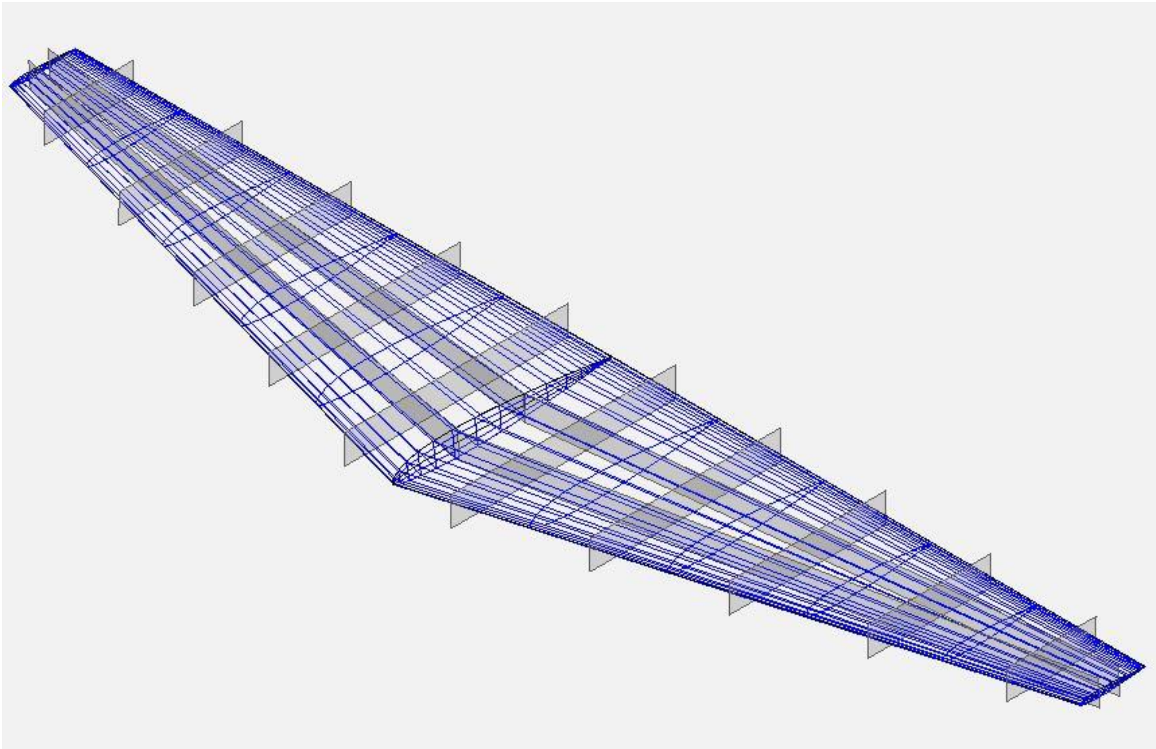

Figure 14-2 Wing internal spar and rib layout

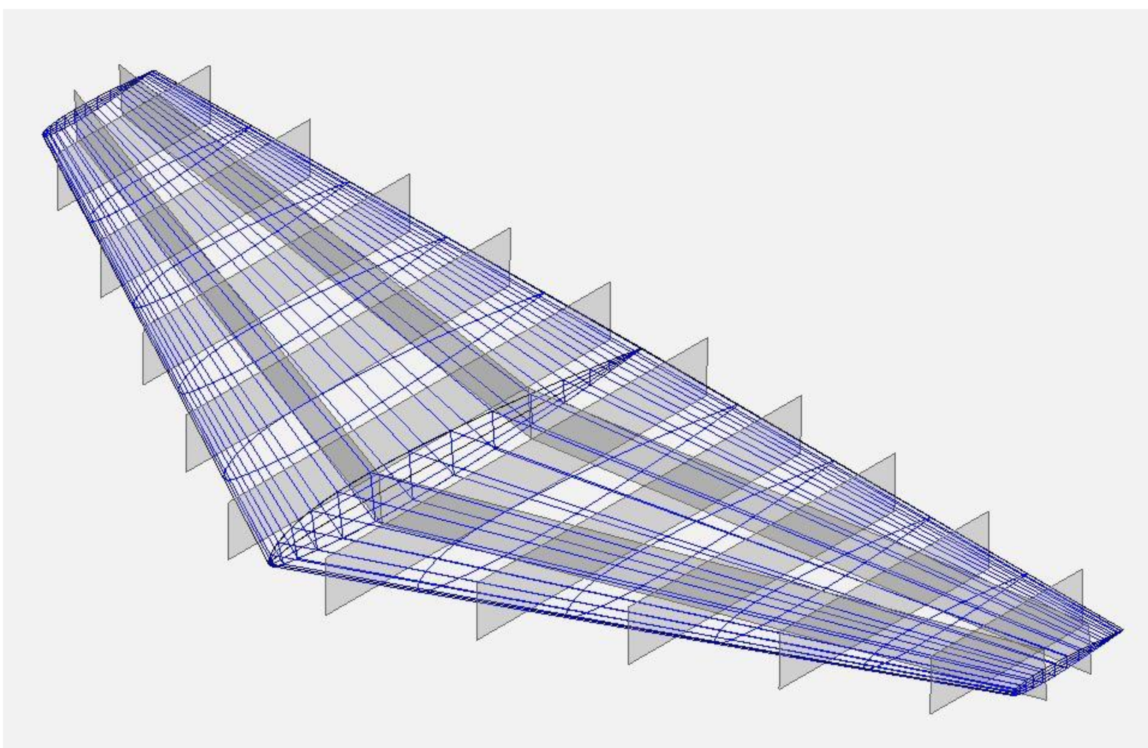

Figure 14-3 Horizontal stabilizer spar and rib layout

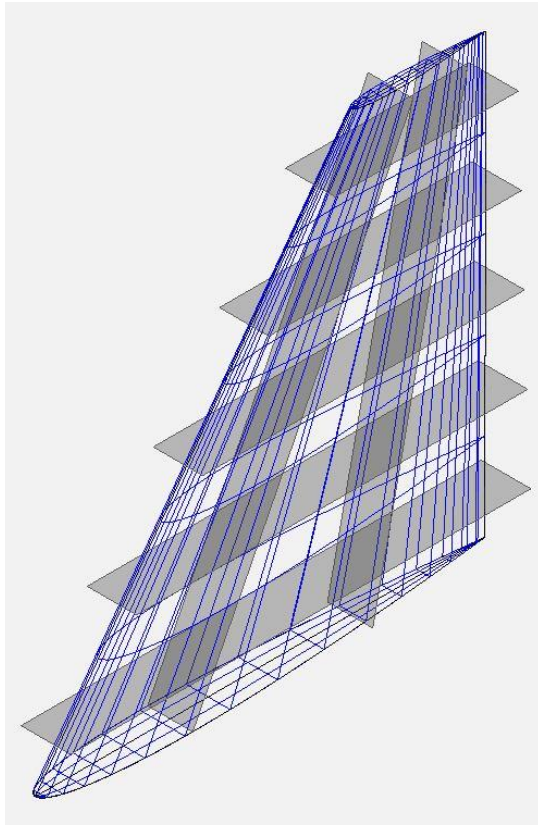

Figure 14-4 Vertical stabilizer spar and rib layout

14.3 Discussion

Due to the simplified nature of the structural program in OpenVSP, certain aspects of the internal structure could not be modified to accurately depict the intended layout. A fuselage in OpenVSP can only model the internals as an array of rings. These rings can only be modified in number and distance between each other. The thickness of the rings could not be adjusted to accurately depict the real volume required. This was not true of the wing as the internal layout of the wing was able to be properly adjusted in OpenVSP. The spars and ribs were able to be constrained by the dimensions of the wing. With additional time, the internal layout could've been further modeled with the end goal of having a cut away view of the structural layout imposed over the outside shell.

15. V-n Diagram

15.1 Introduction

In order to create a V-n diagram, the following parameters were necessary: maximum takeoff weight, wing reference area, air density, C_{L_max} and C_{D0} all of which have been previously calculated. Roskam was used as a reference to create the plots. From these starting values, the stall speed, design cruise speed, design diving speed, and design maneuvering speed can be calculated. Afterwards, the positive and negative load limits are determined, which are the highest and lowest horizontal lines. From these values, it's possible to get an idea of the design limits of the aircraft. The Excel formulas and calculations for this section can be found in Appendix F.

15.2 V-n Diagrams

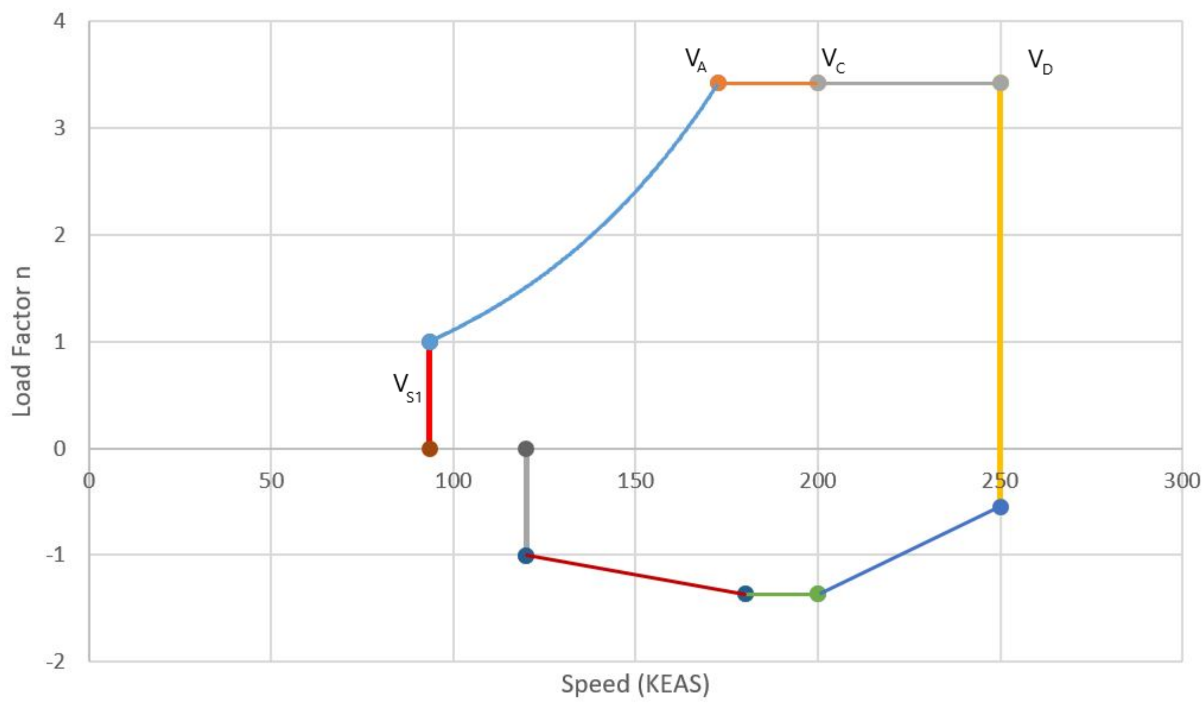

Figure 15-1 V-n diagram for cargo configuration

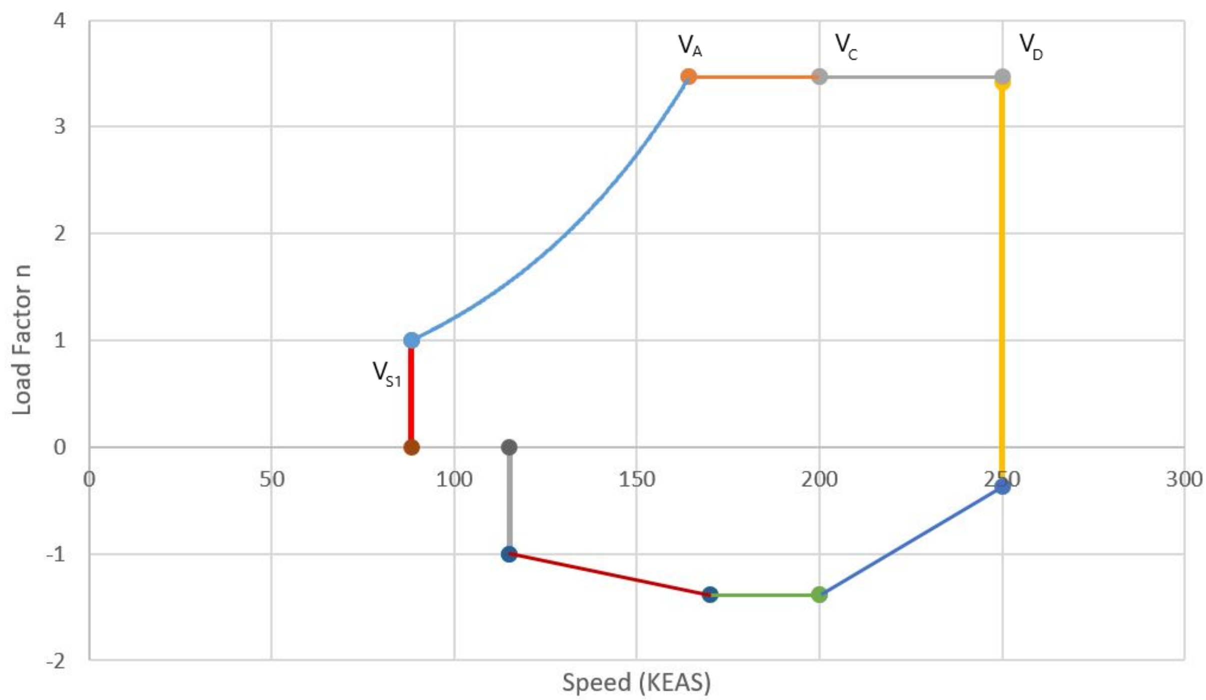

Figure 15-2 V-n diagram for combat configuration

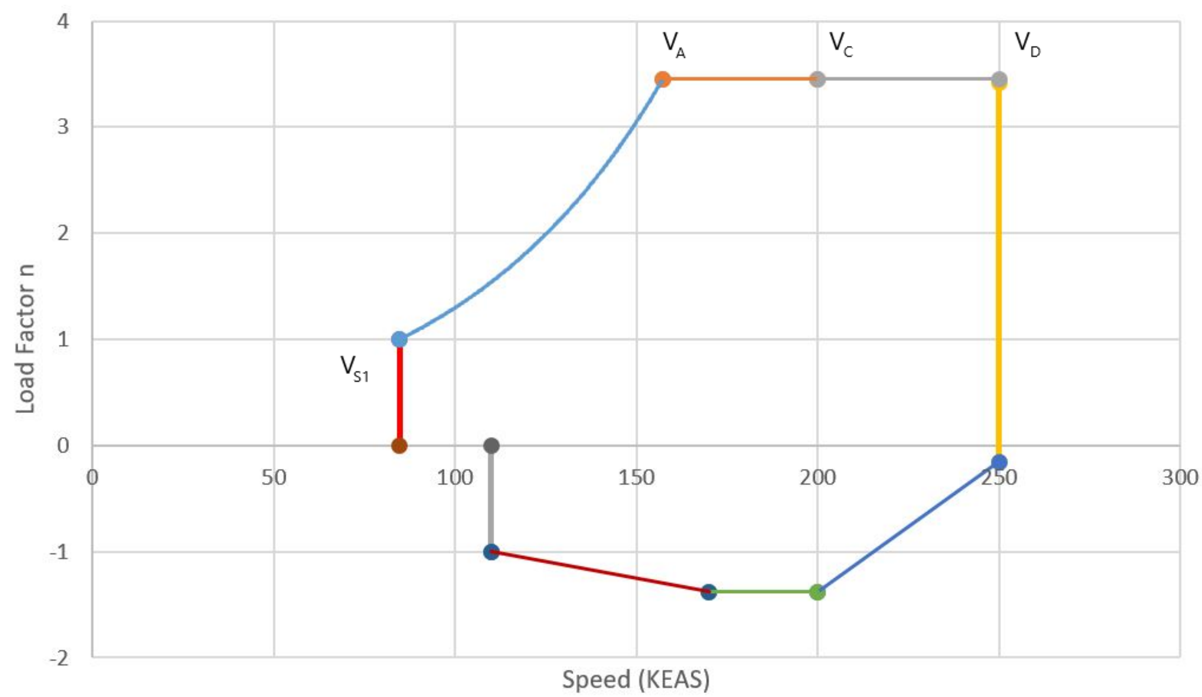

Figure 15-3 V-n diagram for surveillance configuration

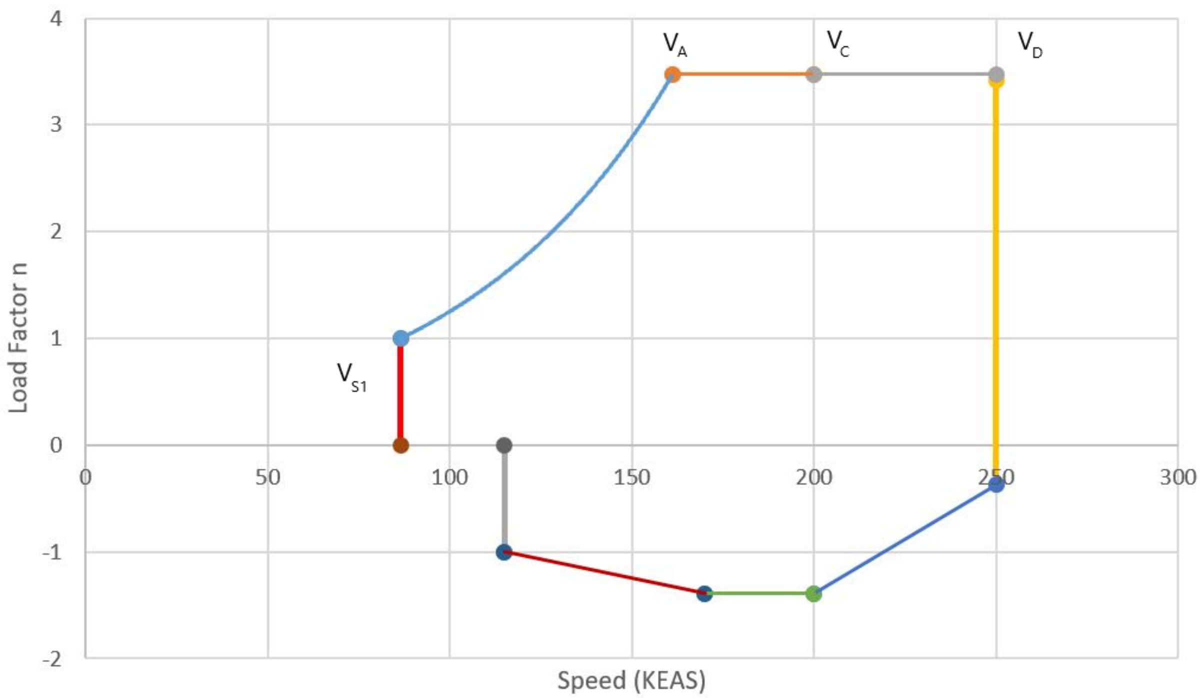

Figure 15-4 V-n diagram for decoy configuration

15.3 Discussion

In the V-n diagrams, the subscript S1 was used to denote the stall speed, the subscript A was used to denote the design maneuvering speed, the subscript C was used to denote the design cruising speed, and the subscript D was used to denote the design diving speed. The maneuvering and diving speed were not particularly relevant to the design, but included to complete the V-n diagram. The methods described in Roskam showed two different ways to depict the V-n diagram, with one method using the stall speed as the leftmost part of the diagram while the other showed the origin as the leftmost part [27]. Since the load factor wasn't relevant until the stall speed was reached, the first method was used. Comparing the V-n diagrams of the four configurations, there were only slight differences between each one. Even with these slight differences, all four were included to provide a full picture of the aircraft.

16. Weight and Balance Analysis – Class II

16.1 Introduction

Since the design has been iterated upon multiple times since the previous weight analysis, another more detailed analysis will occur. This will account for the changes to the engine, wing, empennages, landing gears, and fuselage. For consistency, the calculated empty weights will be compared with the known empty weights with a 5% tolerance being accepted. The previous weight analysis assumed an avionics weight of 100 lb (45 kg), this has been updated to a more acceptable value of 300 lb (136 kg). Using the necessary equations, this resulted in a total avionics weight of 390 lb (177 kg), or roughly 8% of the overall empty weight. The Excel formulas and calculations for this section can be found in Appendix G.

16.2 Component Weight Breakdown

Table 16.1 Weight breakdown of cargo configuration

Component	**Weight**
Wing	539 lb (244 kg)
Horizontal tail	85 lb (39 kg)
Vertical tail	54 lb (24 kg)
Fuselage	654 lb (296 kg)
Main landing gear	362 lb (164 kg)
Nose landing gear	98 lb (44 kg)
Installed engine	1385 lb (628 kg)
Fuel system	135 lb (61 kg)
Flight controls	103 lb (47 kg)
Hydraulics	72 lb (33 kg)
Electrical	291 lb (132 kg)
Avionics	390 lb (177 kg)
A/C and anti-ice	209 lb (95 kg)
Furnishings	321 lb (146 kg)
Total	4698 lb (2131 kg)

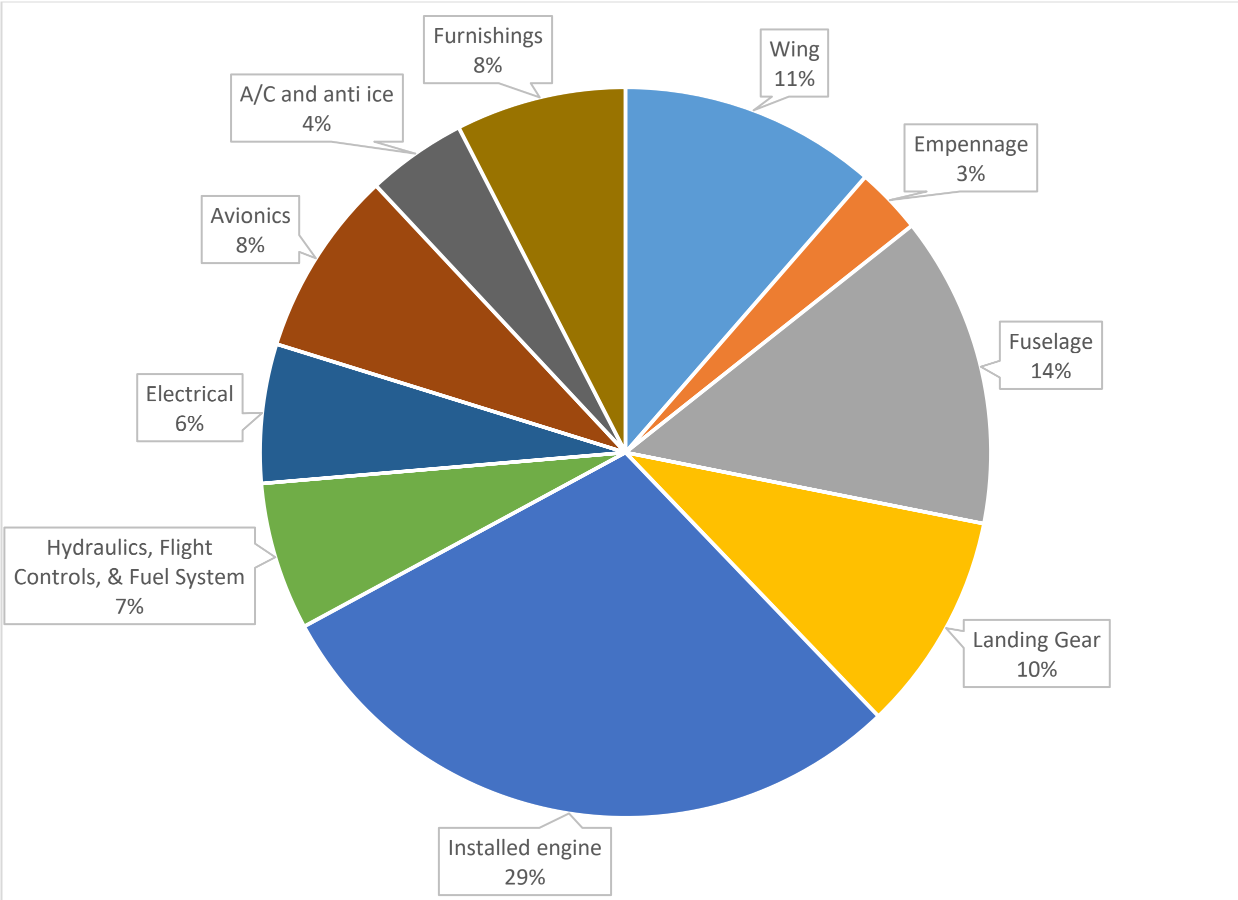

Figure 16-1 Component breakdown by weight (cargo)

Table 16.2 Weight breakdown of combat configuration

Component	**Weight**
Wing	557 lb (253 kg)
Horizontal tail	84 lb (38 kg)
Vertical tail	57 lb (26 kg)
Fuselage	655 lb (297 kg)
Main landing gear	246 lb (112 kg)
Nose landing gear	73 lb (33 kg)
Installed engine	1385 lb (628 kg)
Fuel system	116 lb (53 kg)
Flight controls	100 lb (45 kg)
Hydraulics	69 lb (31 kg)
Electrical	286 lb (130 kg)
Avionics	390 lb (177 kg)
Total	4018 lb (1823 kg)

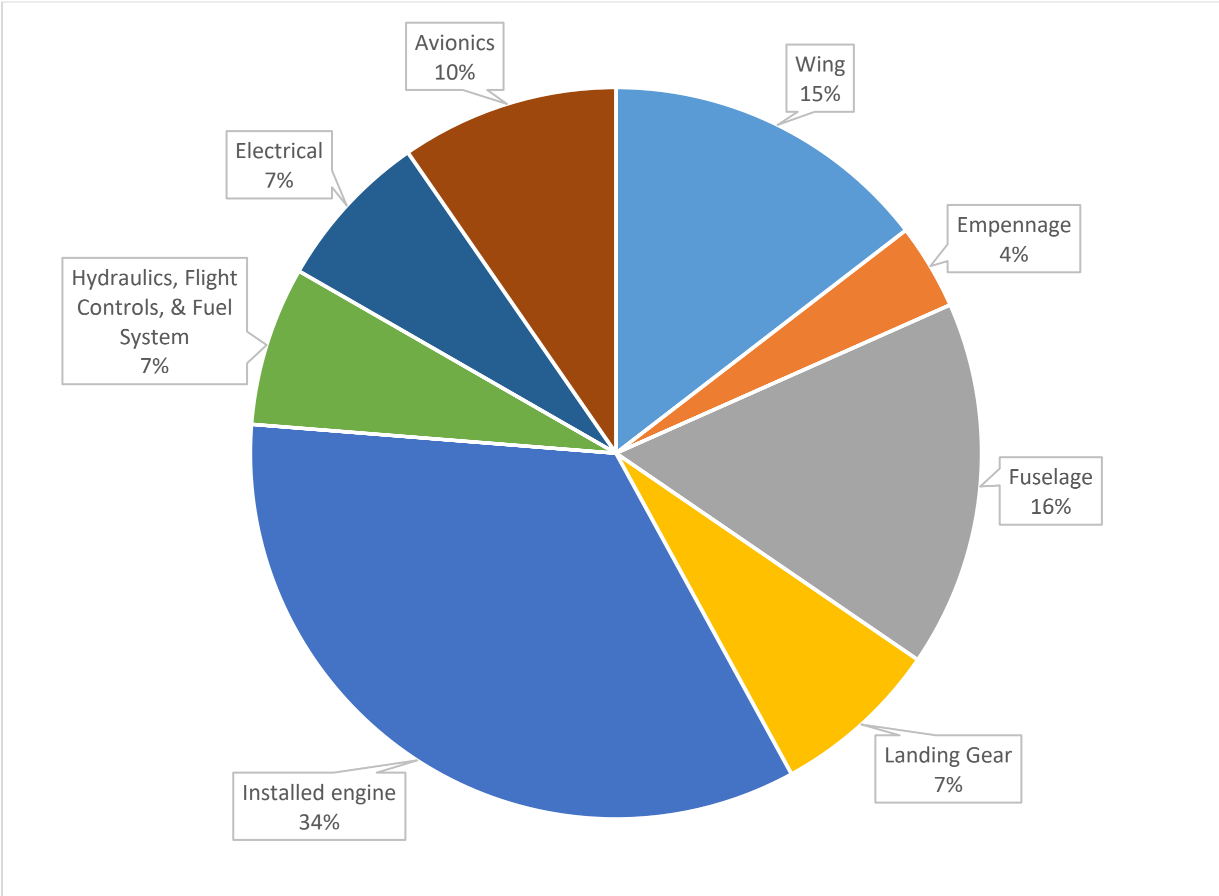

Figure 16-2 Component breakdown by weight (combat)

Table 16.3 Weight breakdown of surveillance configuration

Component	**Weight**
Wing	751 lb (341 kg)
Horizontal tail	86 lb (39 kg)
Vertical tail	71 lb (33 kg)
Fuselage	650 lb (295 kg)
Main landing gear	247 lb (112 kg)
Nose landing gear	74 lb (34 kg)
Installed engine	1385 lb (628 kg)
Fuel system	172 lb (78 kg)
Flight controls	101 lb (46 kg)
Hydraulics	66 lb (30 kg)
Electrical	302 lb (137 kg)
Avionics	390 lb (177 kg)
Total	4295 lb (1948 kg)

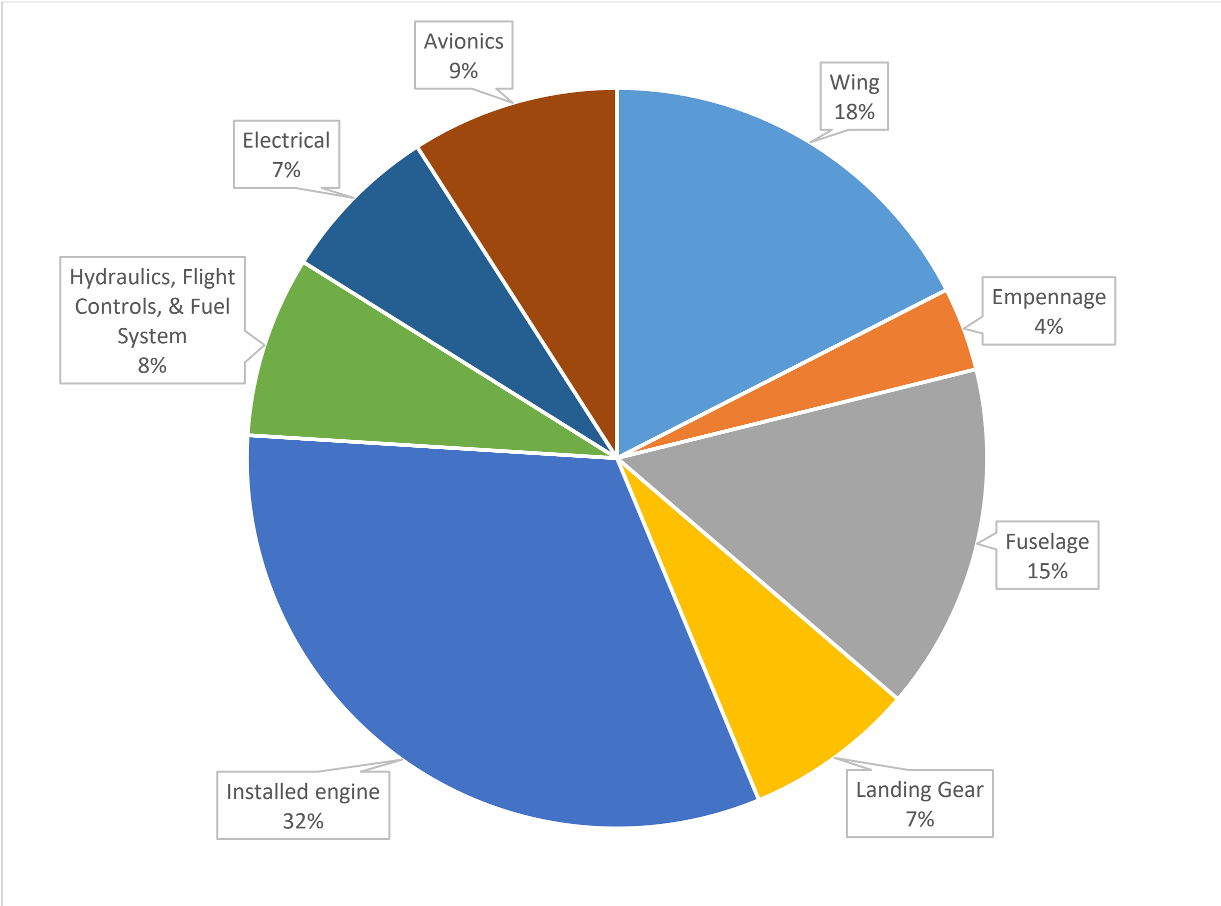

Figure 16-3 Component breakdown by weight (surveillance)

Table 16.4 Weight breakdown of decoy configuration

Component	**Weight**
Wing	512 lb (232 kg)
Horizontal tail	85 lb (39 kg)
Vertical tail	55 lb (25 kg)
Fuselage	642 lb (291 kg)
Main landing gear	234 lb (106 kg)
Nose landing gear	71 lb (32 kg)
Installed engine	1385 lb (628 kg)
Fuel system	193 lb (88 kg)
Flight controls	89 lb (40 kg)
Hydraulics	62 lb (28 kg)
Electrical	307 lb (139 kg)
Avionics	390 lb (177 kg)
Total	4025 lb (1826 kg)

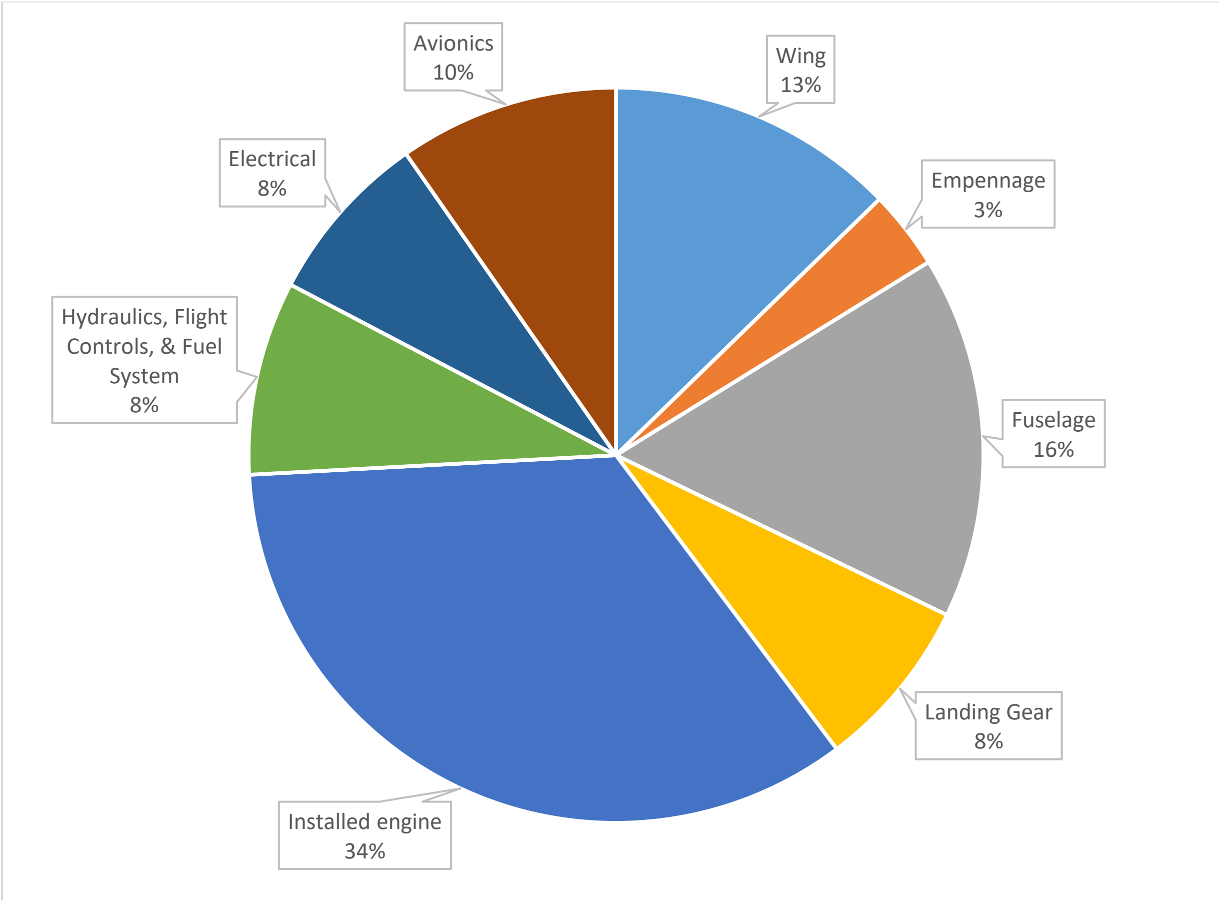

Figure 16-4 Component breakdown by weight (decoy)

Table 16.5 CG of various loading scenarios for cargo configuration

Load Scenario	Weight	CG_X	CG_Z
Takeoff	8165 lb (3704 kg)	16.6 ft (5.1 m)	7.9 ft (2.4 m)
With payload	6335 lb (2874 kg)	16.6 ft (5.1 m)	7.4 ft (2.3 m)
With fuel	6364 lb (2887 kg)	15.6 ft (4.8 m)	8.4 ft (2.6 m)
Empty	4536 lb (2057 kg)	15.3 ft (4.7 m)	7.9 ft (2.4 m)

Table 16.6 CG of various loading scenarios for combat configuration

Load Scenario	Weight	CG_X	CG_Z
Takeoff	7545 lb (3422 kg)	15.8 ft (4.8 m)	8.5 ft (2.6 m)
With payload	6051 lb (2745 kg)	15.5 ft (4.7 m)	8.2 ft (2.5 m)
With fuel	5445 lb (2470 kg)	16.1 ft (4.9 m)	8.5 ft (2.6 m)
Empty	3951 lb (1792 kg)	15.6 ft (4.8 m)	8.2 ft (2.5 m)

Table 16.7 CG of various loading scenarios for surveillance configuration

Load Scenario	Weight	CG_X	CG_Z
Takeoff	7722 lb (3503 kg)	16.2 ft (4.9 m)	8.4 ft (2.6 m)
With payload	5159 lb (2340 kg)	16.4 ft (5.0 m)	7.6 ft (2.3 m)
With fuel	6722 lb (3049 kg)	15.8 ft (4.8 m)	8.4 ft (2.6 m)
Empty	4169 lb (1891 kg)	15.7 ft (4.8 m)	7.6 ft (2.3 m)

Table 16.8 CG of various loading scenarios for decoy configuration

Load Scenario	Weight	CG_X	CG_Z
Takeoff	7434 lb (3372 kg)	15.9 ft (4.8 m)	8.6 ft (2.6 m)
With payload	4436 lb (2012 kg)	15.8 ft (4.8 m)	7.7 ft (2.3 m)
With fuel	6934 lb (3145 kg)	15.6 ft (4.8 m)	8.6 ft (2.6 m)
Empty	3936 lb (1785 kg)	15.3 ft (4.7 m)	7.7 ft (2.3 m)

16.3 CG Excursion Diagrams

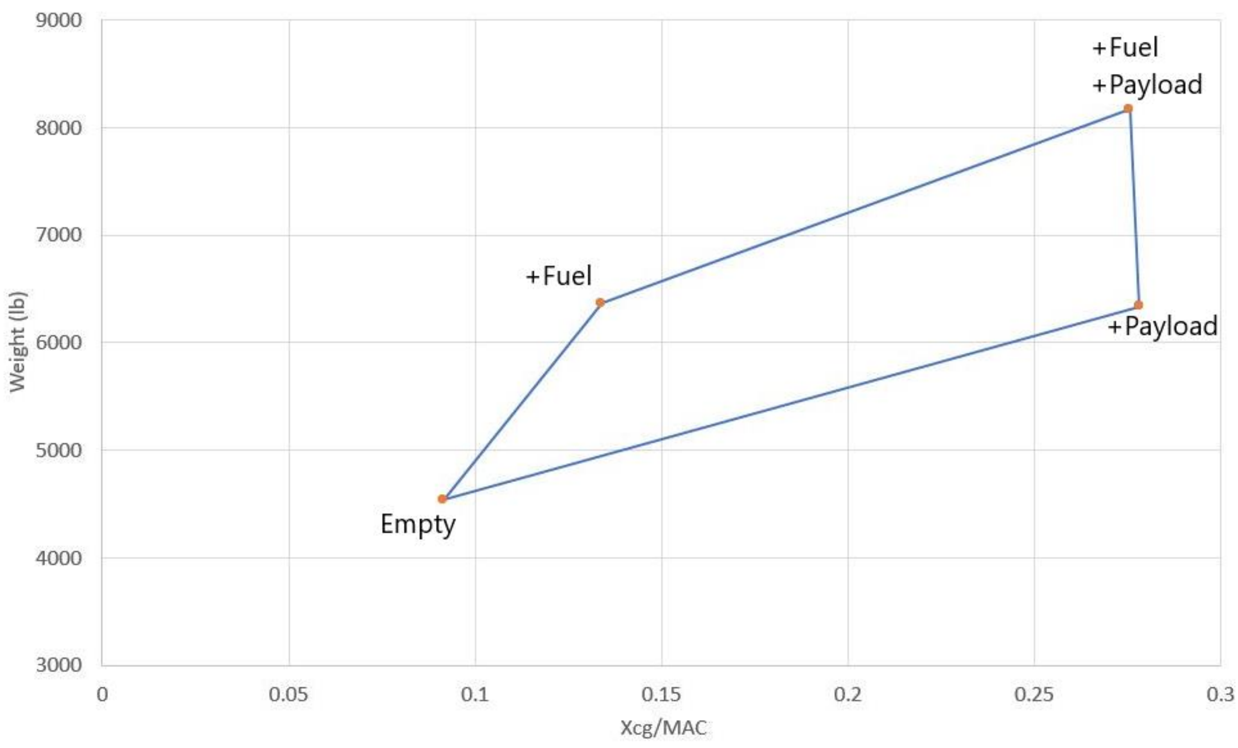

Figure 16-5 CG excursion diagram for the cargo configuration

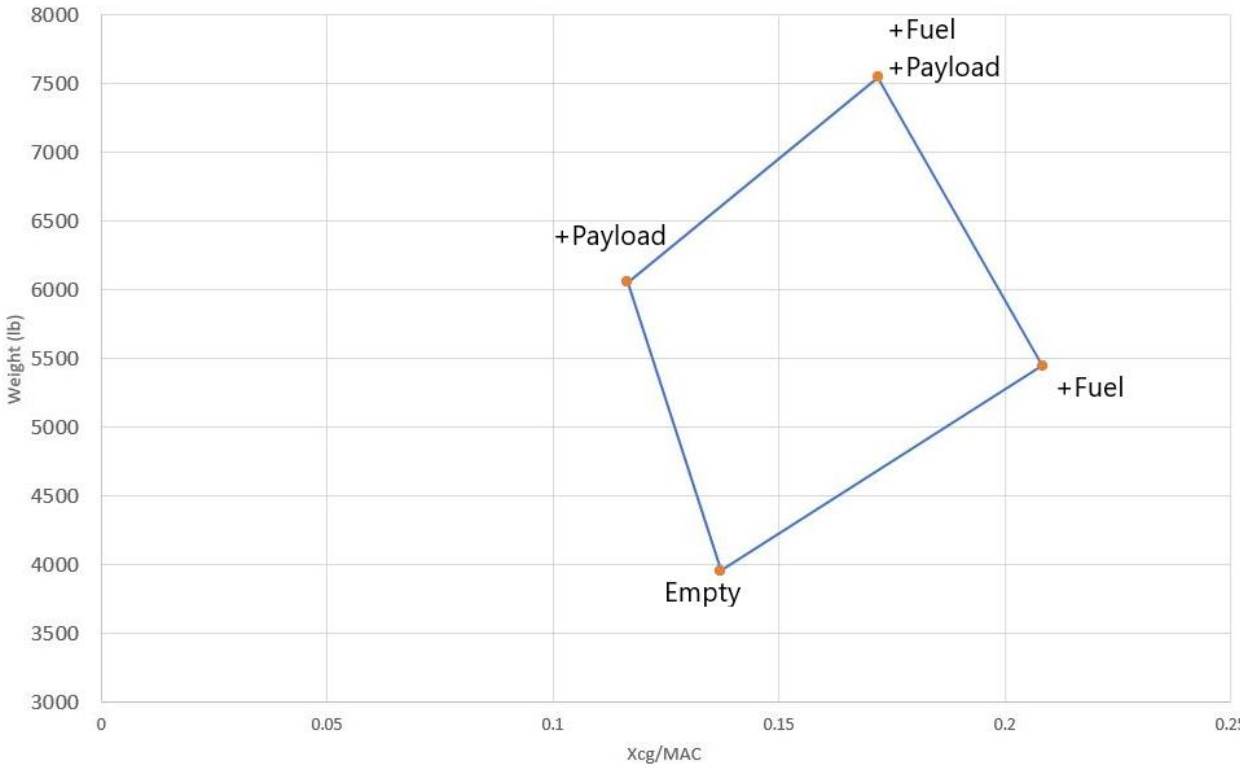

Figure 16-6 CG excursion diagram for the combat configuration

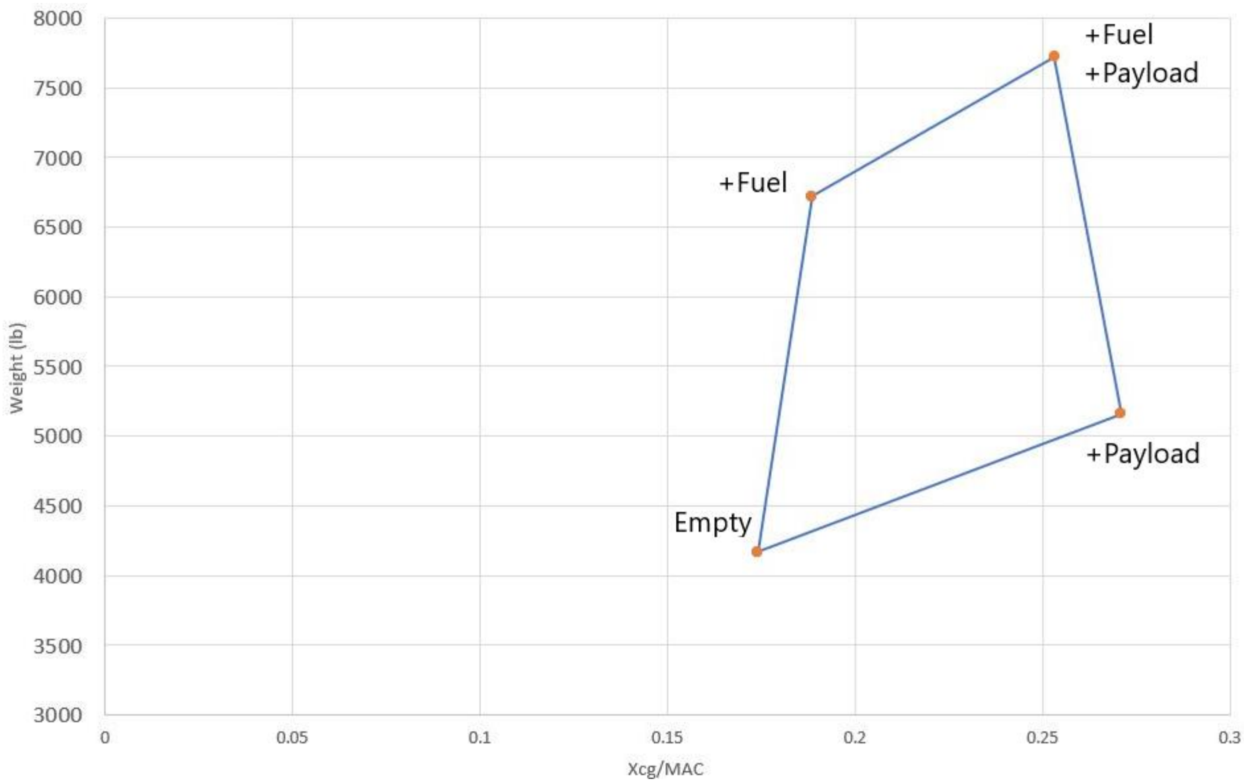

Figure 16-7 CG excursion diagram for the surveillance configuration

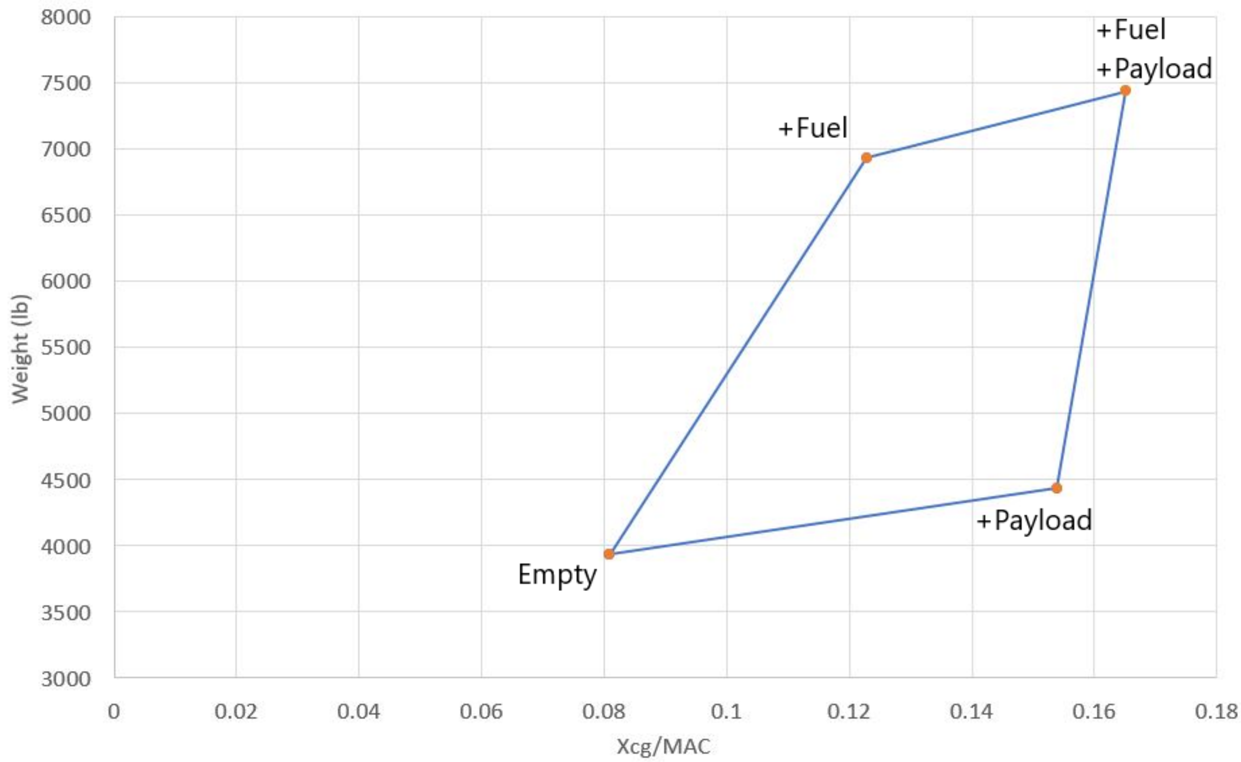

Figure 16-8 CG excursion diagram for the decoy configuration

16.4 Discussion

While the methods to define the weight breakdown in this chapter were more detailed than the previous calculation, the weights were still close in value. The accepted tolerance for the weight difference was 5%, with the highest difference being the cargo configuration with a difference of 3.44%. This took into account some of the fudge factors provided by Roskam [27]. These fudge factors ranged from 10-15% percent reduction in weight to account for composites or other materials. With additional time, some of the weight calculations could be replaced with the weights of specifically chosen components. While this was only done with the engine, it could've been further expanded to include specific avionics instead of an estimated value of the avionics weight. This most likely would've reduced the avionics weight as avionics weight was expressed as a fraction of the overall empty weight. This additional time could also have been devoted to adjusting the CG excursion diagram so the four plots could have been closer in terms of shape. The cargo configuration had a much narrower diagram due to the CG shifting the furthest in this configuration. While still acceptable, it would've been ideal to optimize the payload and fuel locations while not moving them around too much to negatively affect the clearance and stability angles.

17. Stability and Control Analysis – Class II

17.1 Trim Diagram

To create a trim diagram of the aircraft, Roskam and Raymer were used as a reference [27] [26]. Roskam was used to better understand the process of creating a trim diagram, while the equations and general process used was from Raymer. The Excel formulas and calculations for this section can be found in Appendix H.

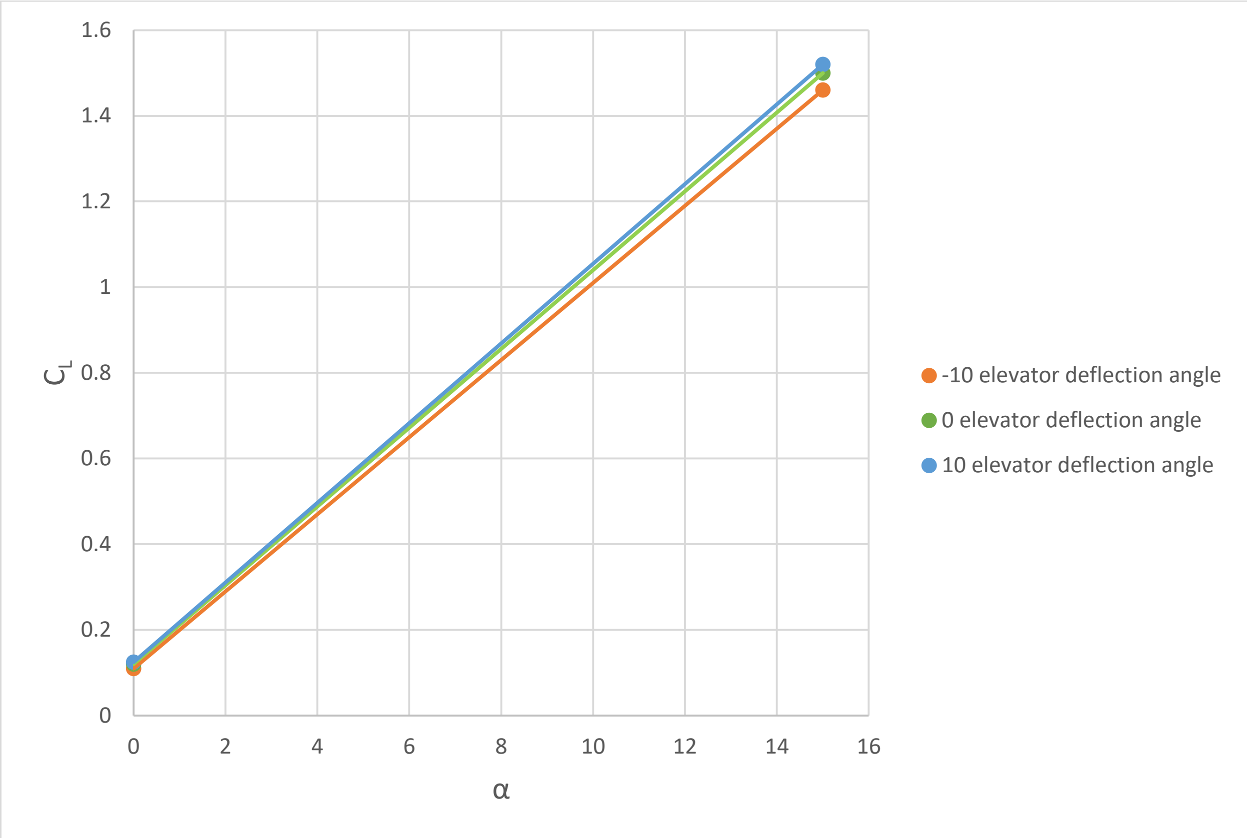

Figure 17-1 Trim diagram

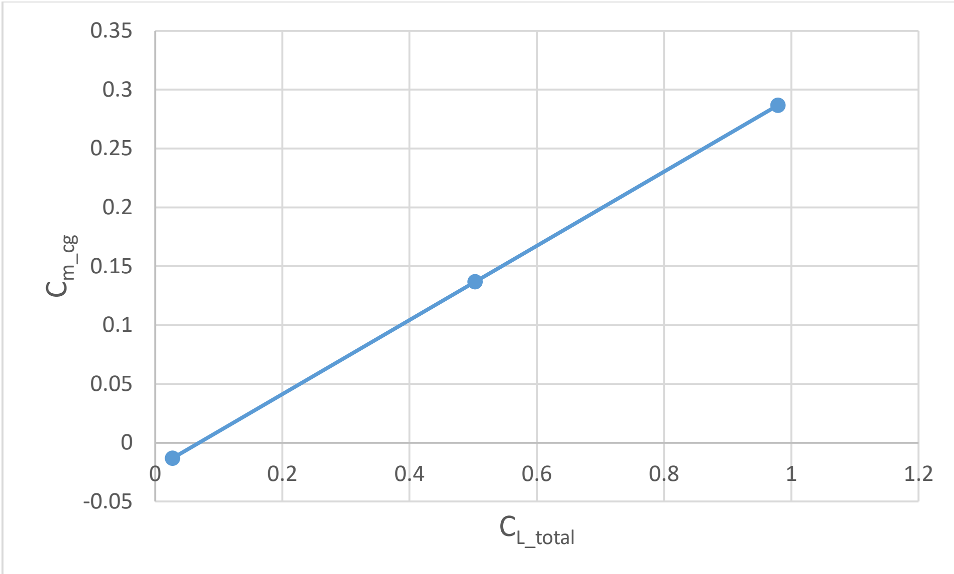

Figure 17-2 C_{m_cg} vs C_L plot

17.2 Discussion

A complete trim diagram plot was not generated, but what has been completed is shown in the previous section. The process of creating a trim diagram was not clearly defined in either Raymer or Roskam so both references had to be used to get a general idea of the process. Through Raymer, most of the process was straightforward, but when it came to creating the trim diagram, some details were vague in how they were calculated. One of the last steps in the process involves varying the deflection angle to create three parallel lines to represent the change in angle. The issue with this comes from the deflection angle not being used in any of the equations defined in the chapter. While a single plot was generated, this assumes a deflection angle of 0°. Another issue that arose is that the plot shown above did not line up with the example in the text. The example plot shows a negative slope for the plot while the one generated above shows a positive slope. This process was repeated multiple times, but the results were not similar to the provided example.

18. Drag Polar Estimation – Class II

18.1 Introduction

Building off of the previously calculated drag polar estimation, a more accurate analysis can be completed as more aspects of the aircraft have been clearly defined. By calculating the drag buildup of each component, a better understanding of each components overall impact to the drag can be seen. This also allows for adjustment factors (such as interference drag or leakage) to be applied to singular components instead of an overall adjustment.

18.2 Component Drag Polar Buildup

A dynamic viscosity of $3.53*10^{-7}$ slug/ft*s ($1.69*10^{-5}$ N s/m^2) was assumed due the respective altitude of 10,000 ft (3048 m). The Mach number was kept to 0.3 across all components. The drag polar for each component was calculated separately and totaled in the end to determine the overall CD0.The Excel formulas and calculations for this section can be found in Appendix I.

Table 18.1 Class I drag estimation for cargo configuration

Parameter	Raymer	Roskam
Cfe	0.0045	N/A
cf	N/A	0.007
CD_0 clean	0.0198	0.0308
C_L cruise	0.24	0.24
L/D cruise	10.4	7

Table 18.2 Component drag build up for cargo configuration

	Wing	Fuselage	Horizontal Stabilizer	Vertical Stabilizer	Engine	TOTAL
Length	6.84 ft (2.08 m)	40 ft (12.2 m)	4.90 ft (1.49 m)	6.52 ft (1.98m)	5.3 ft (1.6m)	
RE	11.5e6	67e6	8.21e6	10.9e6	8.87e6	
C_f Laminar skin friction coefficient	0.000392	0.000162	0.000464	0.000402	0.000446	
C_f Turbulent skin friction coefficient	0.00291	0.00223	0.00308	0.00294	0.00304	
Fraction laminar	0.1	0	0.1	0.1	0	
Fraction turbulent	0.9	1	0.9	0.9	1	
C_f Weighted average skin friction	0.00266	0.00223	0.00281	0.00268	0.00304	
x/c	2.052		1.47	1.956		
Form Factor	1.140	1.055	1.154	1.141	1.125	
Interference drag	1.05	1	1.04	1.04	1.5	
S_{wet}	559 ft^2 (51.9 m^2)	510 ft^2 (47.4 m^2)	129 ft^2 (12.0 m^2)	85.9 ft^2 (8.0 m^2)	15 ft^2 (1.4 m^2)	
$CD_{0,c}$	0.00610	0.00412	0.00149	0.000937	0.000527	0.0132
Leakage	10	5				15
CD_0						0.0151

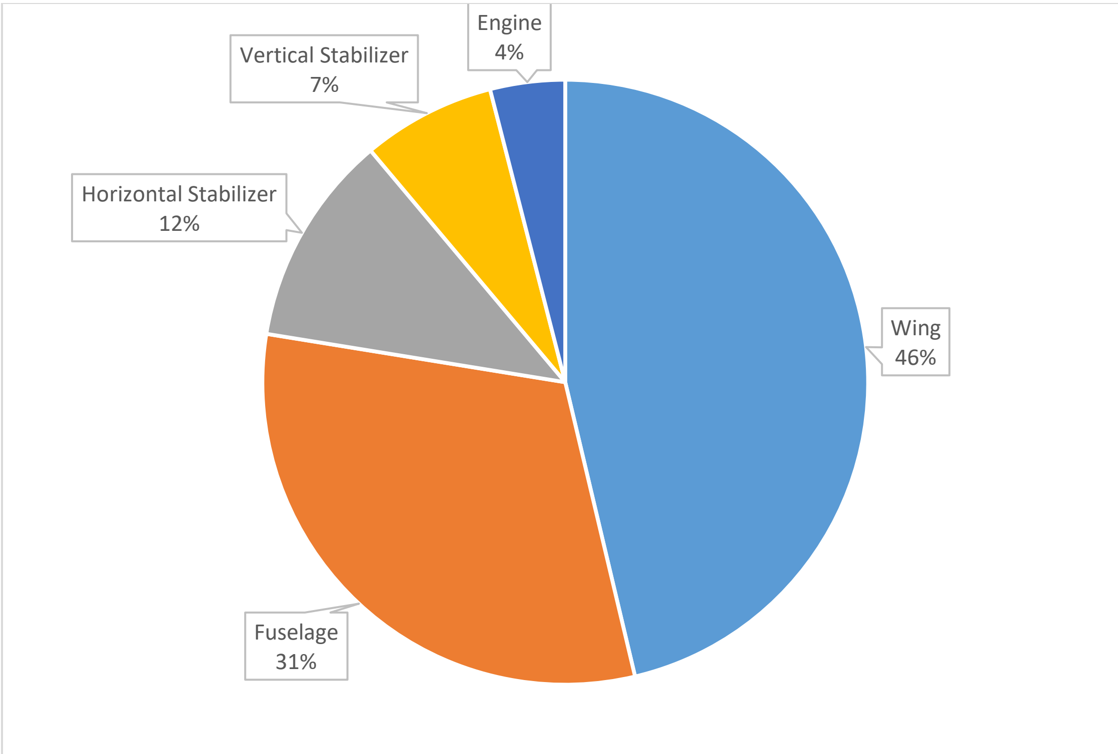

Figure 18-1 Component breakdown by drag for cargo configuration

Table 18.3 Class I drag estimation for combat configuration

Parameter	Raymer	Roskam
Cfe	0.0045	N/A
cf	N/A	0.007
CD_0 clean	0.0196	0.0305
C_L cruise	0.2	0.2
L/D cruise	9.2	6.1

Table 18.4 Component drag build up for combat configuration

	Wing	Fuselage	Horizontal Stabilizer	Vertical Stabilizer	Engine	TOTAL
Length	6.74 ft (2.05 m)	40 ft (12.2 m)	4.95 ft (1.51 m)	6.8 ft (2.07 m)	5.3 ft (1.6 m)	
RE	11.3e6	67e6	8.29e6	11.4e6	8.87e6	
C_f Laminar skin friction coefficient	0.000395	0.000162	0.000461	0.000394	0.0004458	
C_f Turbulent skin friction coefficient	0.00292	0.00223	0.00307	0.00292	0.00304	
Fraction laminar	0.1	0	0.1	0.1	0	
Fraction turbulent	0.9	1	0.9	0.9	1	
C_f Weighted average skin friction	0.00267	0.00223	0.00281	0.00267	0.00304	
x/c	2.022		1.485	2.04		
Form Factor	1.140	1.0552	1.1536	1.139	1.125	
Interference drag	1.25	1	1.04	1.04	1.5	
S_{wet}	579 ft^2 (53.8 m^2)	510 ft^2 (47.4 m^2)	132 ft^2 (12.3 m^2)	93.1 ft^2 (8.6 m^2)	15 ft^2 (1.4 m^2)	
$CD_{0,c}$	0.00729	0.00398	0.00147	0.000974	0.000509	0.0142
Leakage	10	5				15
CD_0						0.0164

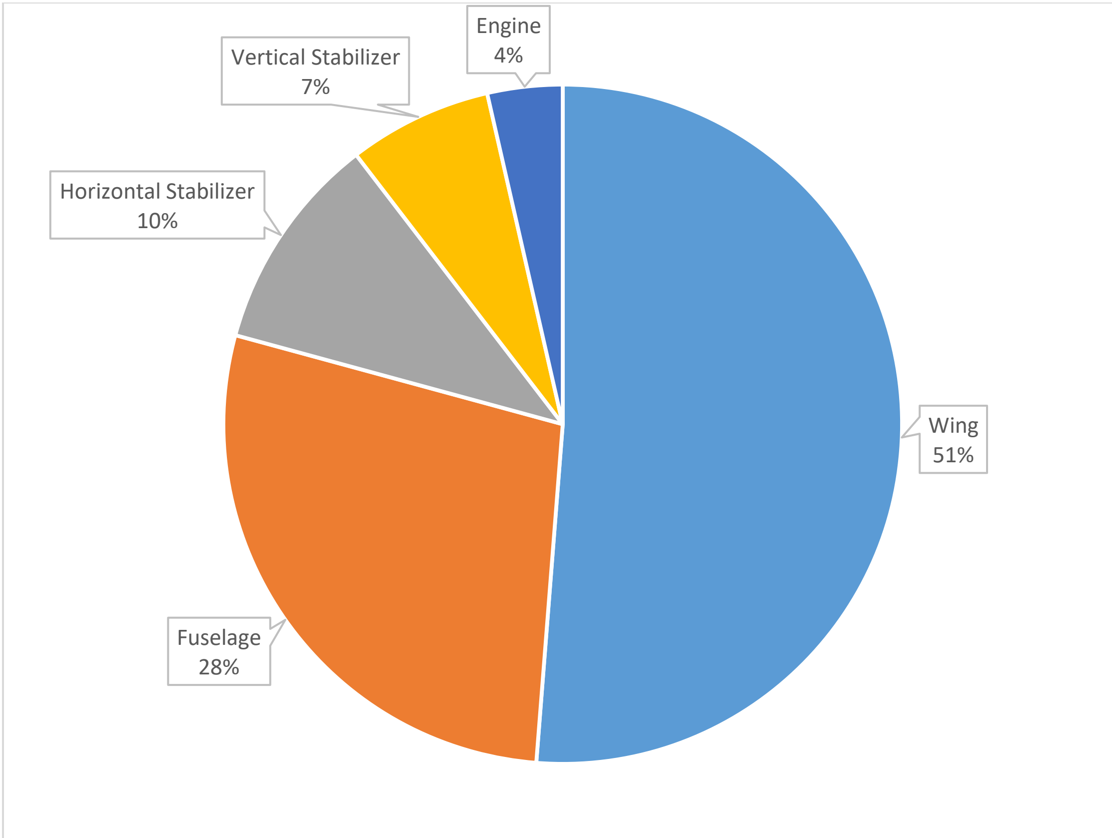

Figure 18-2 Component breakdown by drag for combat configuration

Table 18.5 Class I drag estimation for surveillance configuration

Parameter	Raymer	Roskam
Cfe	0.0045	N/A
cf	N/A	0.007
CD_0 clean	0.0197	0.0306
C_L cruise	0.2	0.2
L/D cruise	9.5	6.2

Table 18.6 Component drag build up for surveillance configuration

	Wing	Fuselage	Horizontal Stabilizer	Vertical Stabilizer	Engine	TOTAL
Length	6.35 ft (1.94 m)	40 ft (12.2 m)	5.06 ft (1.54 m)	7.78 ft (2.37 m)	5.3 ft (1.6 m)	
RE	11e6	67e6	8.5e6	13e6	8.9e6	
C_f Laminar skin friction coefficient	0.000407	0.000162	0.000456	0.000368	0.000446	
C_f Turbulent skin friction coefficient	0.00295	0.00223	0.00306	0.00286	0.00304	
Fraction laminar	0.1	0	0.1	0.1	0	
Fraction turbulent	0.9	1	0.9	0.9	1	
C_f Weighted average skin friction	0.00270	0.00223	0.00280	0.00261	0.00304	
x/c	1.905		1.518	2.334		
Form Factor	1.142	1.055	1.152	1.135	1.125	
Interference drag	1.05	1	1.04	1.04	1.5	
S_{wet}	649 ft^2 (60.3 m^2)	510 ft^2 (47.4 m^2)	140 ft^2 (13 m^2)	122 ft^2 (11.3 m^2)	15 ft^2 (1.4 m^2)	
$CD_{0,c}$	0.00626	0.00359	0.00140	0.00112	0.000459	0.0128
Leakage	10	5				15
CD_0						0.0151

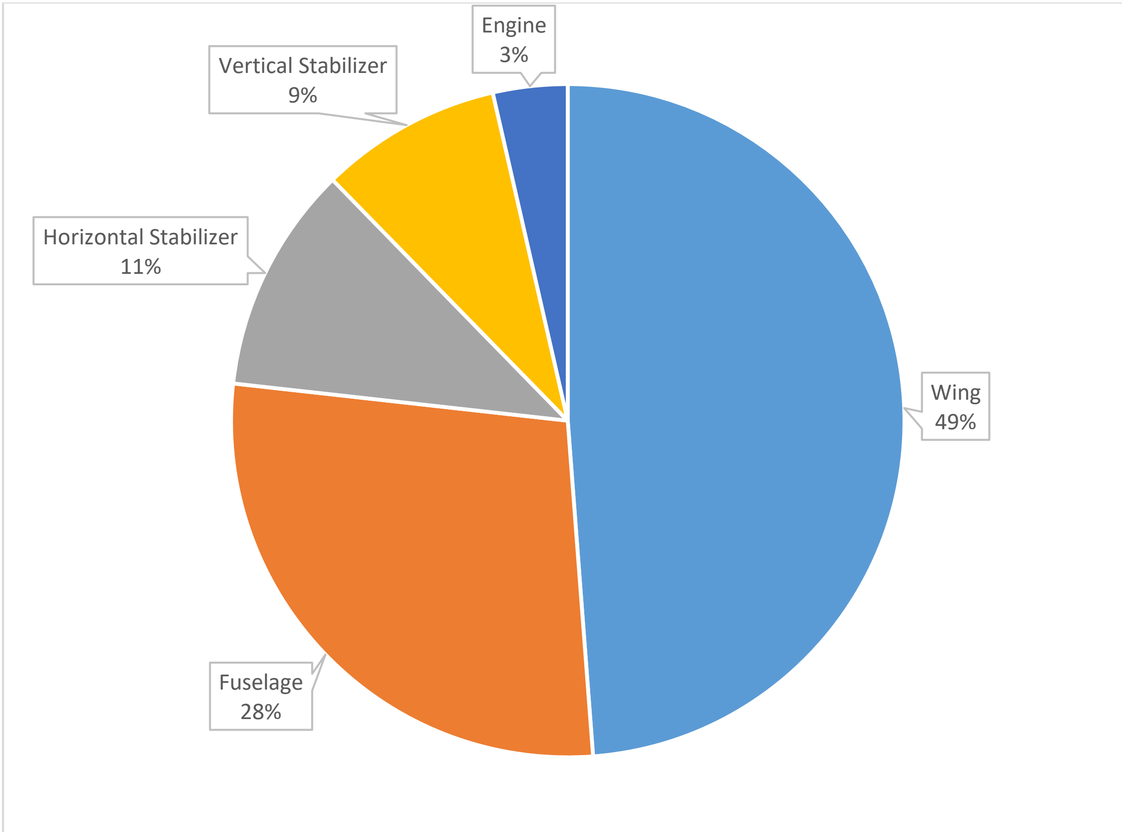

Figure 18-3 Component breakdown by drag for surveillance configuration

Table 18.7 Class I drag estimation for decoy configuration

Parameter	Raymer	Roskam
Cfe	0.0045	N/A
cf	N/A	0.007
CD_0, clean	0.0196	0.0304
C_L cruise	0.2	0.2
L/D cruise	9.4	6.2

Table 18.8 Component drag build up for decoy configuration

	Wing	Fuselage	Horizontal Stabilizer	Vertical Stabilizer	Engine	TOTAL
Length	7.05 ft (2.15 m)	40 ft (12.2 m)	5.12 ft (1.56 m)	6.82 ft (2.08 m)	5.3 ft (1.6 m)	
RE	12e6	67e6	8.6e6	11e6	8.9e6	
C_f Laminar skin friction coefficient	0.000387	0.000162	0.000454	0.000393	0.000446	
C_f Turbulent skin friction coefficient	0.00290	0.00223	0.00305	0.00292	0.00304	
Fraction laminar	0.1	0	0.1	0.1	0	
Fraction turbulent	0.9	1	0.9	0.9	1	
C_f Weighted average skin friction	0.00265	0.00223	0.00279	0.00266	0.00304	
x/c	2.115		1.536	2.046		
Form Factor	1.138	1.055	1.152	1.139	1.125	
Interference drag	1.05	1	1.04	1.04	1.5	
S_{wet}	594 ft^2 (55.2 m^2)	510 ft^2 (47.4 m^2)	145 ft^2 (13.5 m^2)	94 ft^2 (8.7 m^2)	15 ft^2 (1.4 m^2)	
$CD_{0,c}$	0.00609	0.00389	0.00157	0.000960	0.000498	0.0130
Leakage	10	5				15
CD_0						0.0150

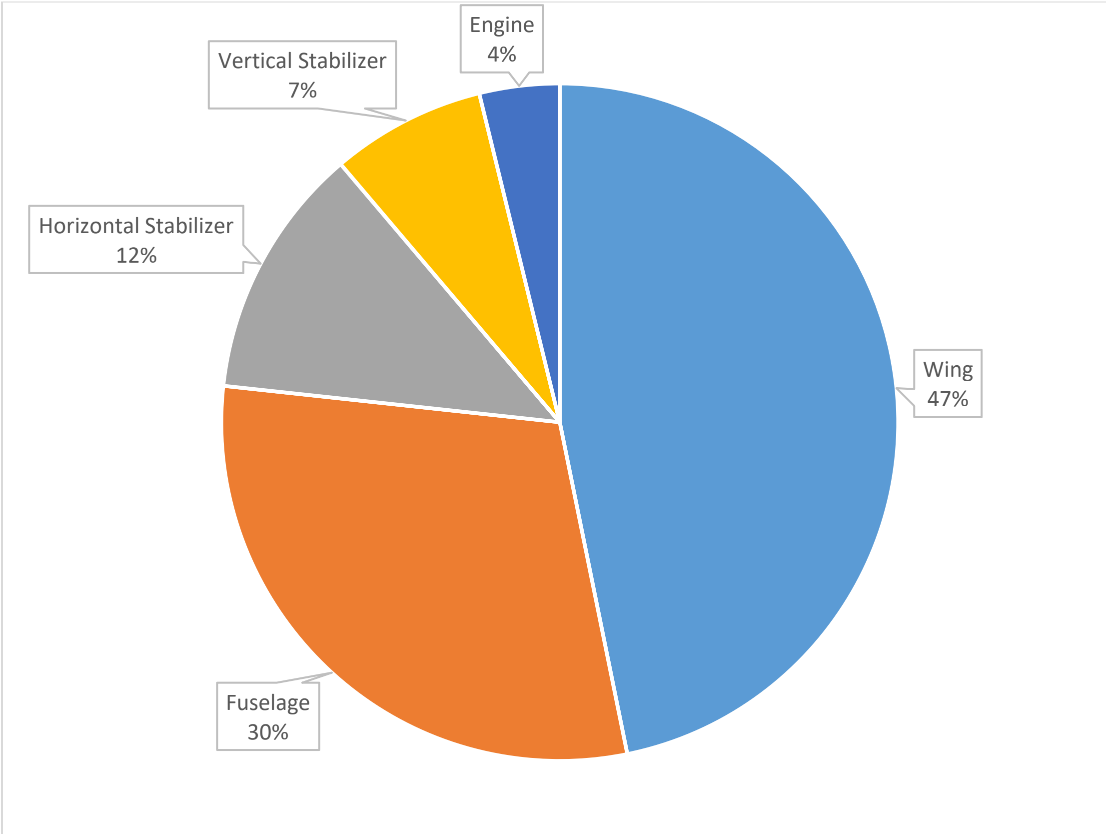

Figure 18-4 Component breakdown by drag for decoy configuration

18.3 Discussion

Across the four configurations, the zero lift drag coefficient was nearly identical for the cargo, surveillance, and decoy configurations. The combat had a slightly higher drag coefficient due to the presence of the missiles on the wing. With additional time, the placement of the missiles and hardpoints could have been optimized by calculating different combinations until one with the lowest drag coefficient was found. This additional time could also have be used to accurately define the leakage. These values were included as it is realistic to assume there could be a slight leakage in the fuselage or wings due to their modularity. Computational fluid dynamics could've been used to model this leakage which could then be applied to the calculations used in this chapter.

19. Installed Power Characteristics

19.1 Introduction

By adding the electrical power requirement with the mechanical power requirement, the total power available can be determined. The electrical power requirement relies on electric power load profile and the efficiency of the generators. The mechanical power requirement relies on power required by the fuel pumps and hydraulic pumps. Since all the configurations have the same requirements, it was not necessary to repeat the calculations for each design.

19.2 Installed Power

According to the recommendations from Roskam, the power requirement from the electrical systems was kept near 4 HP (3 KW). This was also true for the mechanical power requirement, which was kept between 5-10 HP (3.7-7.5 KW). The Excel formulas and calculations for this section can be found in Appendix J.

Table 19.1 Installed power per engine

Parameter	Power
P_{el}	3.0 HP (2.2 KW)
P_{fp}	0.032 HP (0.024 KW)
P_{hydr}	6.0 HP (4.5 KW)
P_{mech}	6.03 HP (4.5 KW)
P_{extr}	9.01 HP (6.72 KW)
P_{av}	309.5 HP (230.8 KW)

Table 19.2 Power available compared to power required

Parameter	Power per engine
Available	309.5 HP (230.8 KW)
Cargo requirement	308 HP (229 KW)
Combat requirement	309 HP (230 KW)
Surveillance requirement	222 HP (166 KW)
Decoy requirement	236 HP (176 KW)

19.3 Discussion

With 375 HP (280 KW) available at sea level, 310 HP (231 KW) is what is available after the considering the operating conditions. With a twin engine setup, the horsepower requirement is satisfied as the surveillance and decoy power requirements were 222 HP (166 KW) and 236 HP (176 KW) each respectively. The cargo and combat requirements were slightly higher at 308 HP (229 KW) and 309 HP (230 KW) each.

20. Critical Performance Requirements

20.1 Mission Requirements

Using the mission requirements defined at the beginning of the report, these values can be compared to the actual calculated performance of the aircraft. The mission requirements are as follows:

- Cargo Transport
  - Carry 6 paratroopers (300 lb or 136 kg each) or an equivalent payload
  - Range: 1500 nmi (2778 km)
  - Cruise: 200 knots (371 km/h)
  - Service ceiling: 15000 ft (4570 m)
- Combat
  - 2 hardpoints
  - 4 AGM missiles (525 lb or 238 kg each)
  - Range: 1000 nmi (1852 km)
  - Cruise: 200 knots (371 km/h)
  - Service ceiling: 15000 ft (4570 m)
- Surveillance
  - Transmit collected data to command center
  - Endurance: 20 hours
  - Range: 2000 nmi (3704 km)
  - Cruise: 200 knots (371 km/h)
  - Service ceiling: 15000 ft (4570 m)
- Decoy
  - Jamming/interference capabilities
  - Range: 2000 nmi (3704 km)
  - Cruise: 200 knots (371 km/h)
  - Service ceiling: 15000 ft (4570 m)

20.2 Performance Calculations

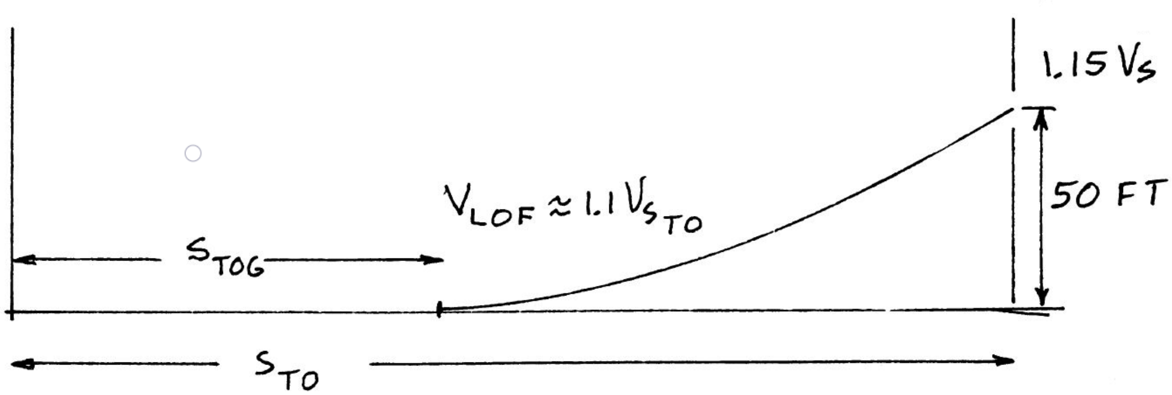

Figure 20-1 Takeoff distance [27]

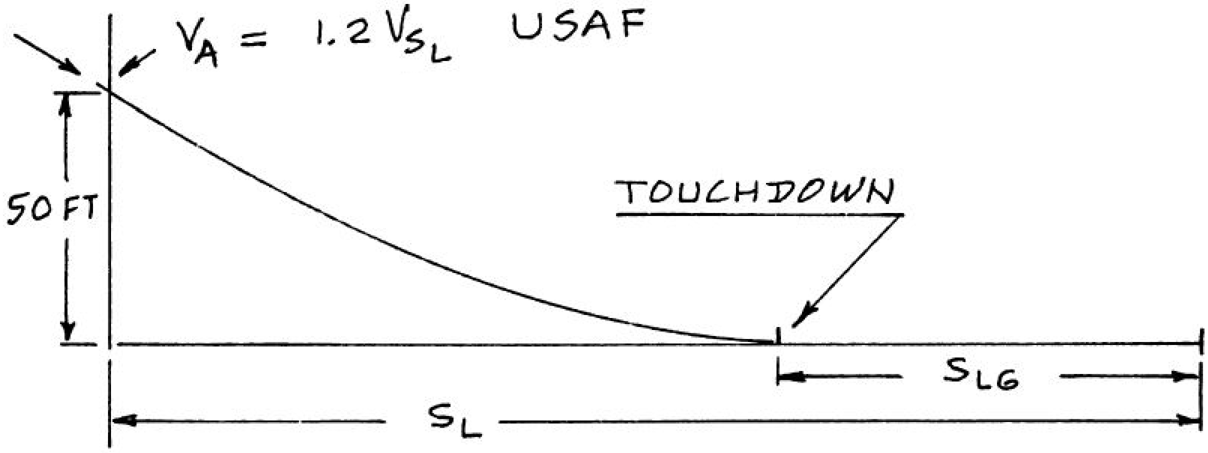

Figure 20-2 Landing distance [27]

Table 20.1 Performance of cargo configuration

Parameter	Value	Requirement
S_{TO}	1634 ft (498 m)	
BFL	2602 ft (793 m)	
V_{LOF}	138 knot (71 m/s)	
S_{TOG}	1173 ft (358 m)	1500 ft (457 m)
Range	2415 nmi (4473 km)	1500 nmi (2778 km)
V_{SL}	96 knot (49 m/s)	
V_A	115 knot (59 m/s)	
V_{TD}	109 knot (56 m/s)	
s_{AIR}	707 ft (215 m)	
s_{LG}	621 ft (189 m)	
s_L	1328 ft (405 m)	

Table 20.2 Performance of combat configuration

Parameter	Value	Requirement
S_{TO}	1348 ft (411 m)	
BFL	2262 ft (689 m)	
V_{LOF}	130 knot (67 m/s)	
S_{TOG}	963 ft (294 m)	1500 ft (457 m)
Range	2354 nmi (4360 km)	1000 nmi (1852 km)
V_{SL}	88 knot (45 m/s)	
V_A	106 knot (55 m/s)	
V_{TD}	100 knot (51 m/s)	
s_{AIR}	674 ft (205 m)	
s_{LG}	521 ft (159 m)	
s_L	1195 ft (364 m)	

Table 20.3 Performance of surveillance configuration

Parameter	Value	Requirement
S_{TO}	1266 ft (386 m)	
BFL	2219 ft (676 m)	
V_{LOF}	125 knot (64 m/s)	
S_{TOG}	906 ft (276 m)	1500 ft (457 m)
Range	2144 nmi (3971 km)	2000 nmi (3704 km)
V_{SL}	87 knot (45 m/s)	
V_A	105 knot (54 m/s)	
V_{TD}	99 knot (51 m/s)	
s_{AIR}	670 ft (204 m)	
s_{LG}	510 ft (155 m)	
s_L	1180 ft (360 m)	

Table 20.4 Performance of decoy configuration

Parameter	Value	Requirement
S_{TO}	1291 ft (393 m)	
BFL	2184 ft (666 m)	
V_{LOF}	128 knot (66 m/s)	
S_{TOG}	907 ft (276 m)	1500 ft (457 m)
Range	2134 nmi (3952 km)	2000 nmi (3704 km)
V_{SL}	89 knot (46 m/s)	
V_A	107 knot (55 m/s)	
V_{TD}	101 knot (52 m/s)	
s_{AIR}	678 ft (207 m)	
s_{LG}	534 ft (163 m)	
s_L	1211 ft (369 m)	

20.3 Discussion

For all four configurations, the mission requirements were met or exceeded. The mission requirements were reasonably defined using similarly sized aircraft. The service ceiling and cruise speed requirements were shared among the four aircraft, while the range was individually defined as each configuration was sized according to the range. The takeoff and landing requirements were not critical to the mission, but defined as necessary to complete some of the earlier calculations. Even with this in mind, both requirements were met. The Excel formulas and calculations for this section can be found in Appendix K.

21. Final 3-View and Subsystem Drawings

21.1 Final 3-View

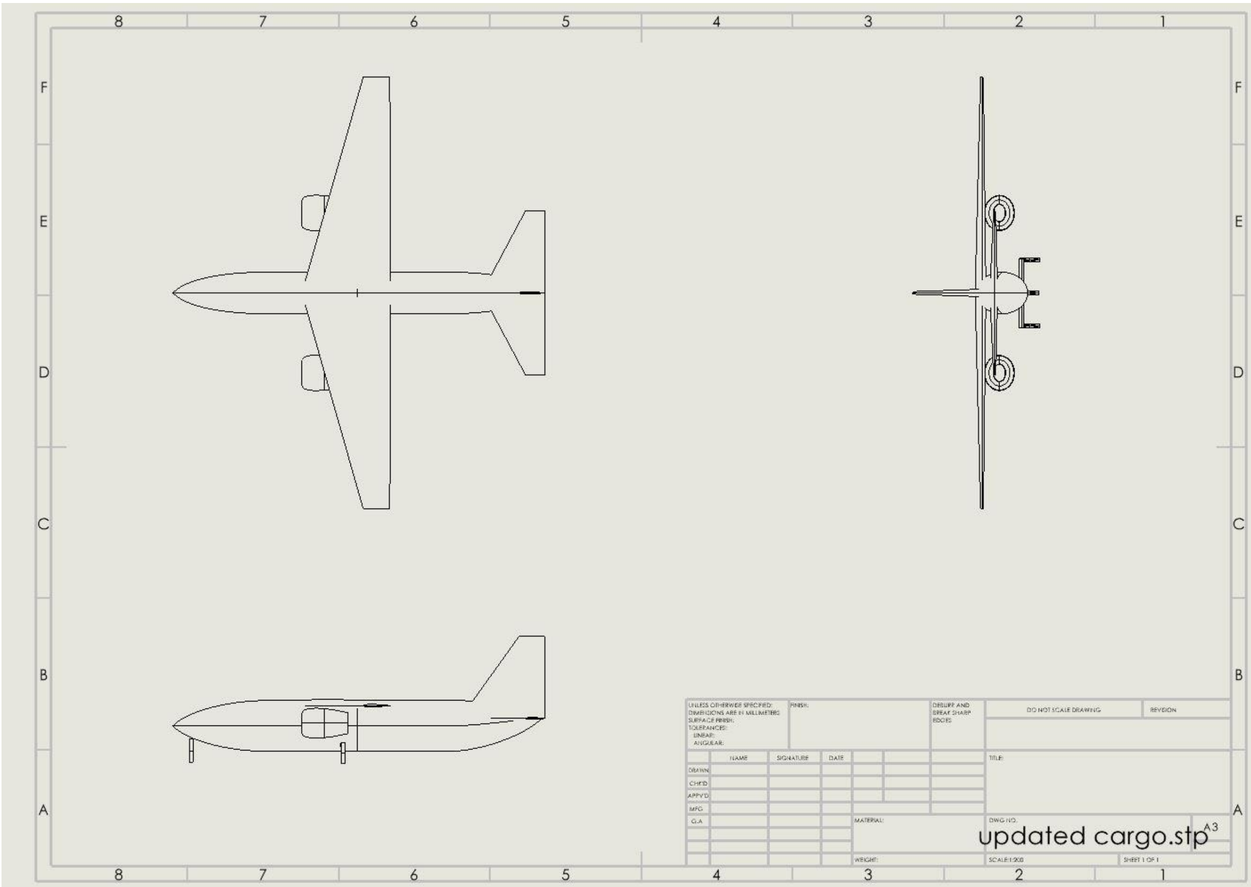

Figure 21-1 Final 3-view of the cargo configuration

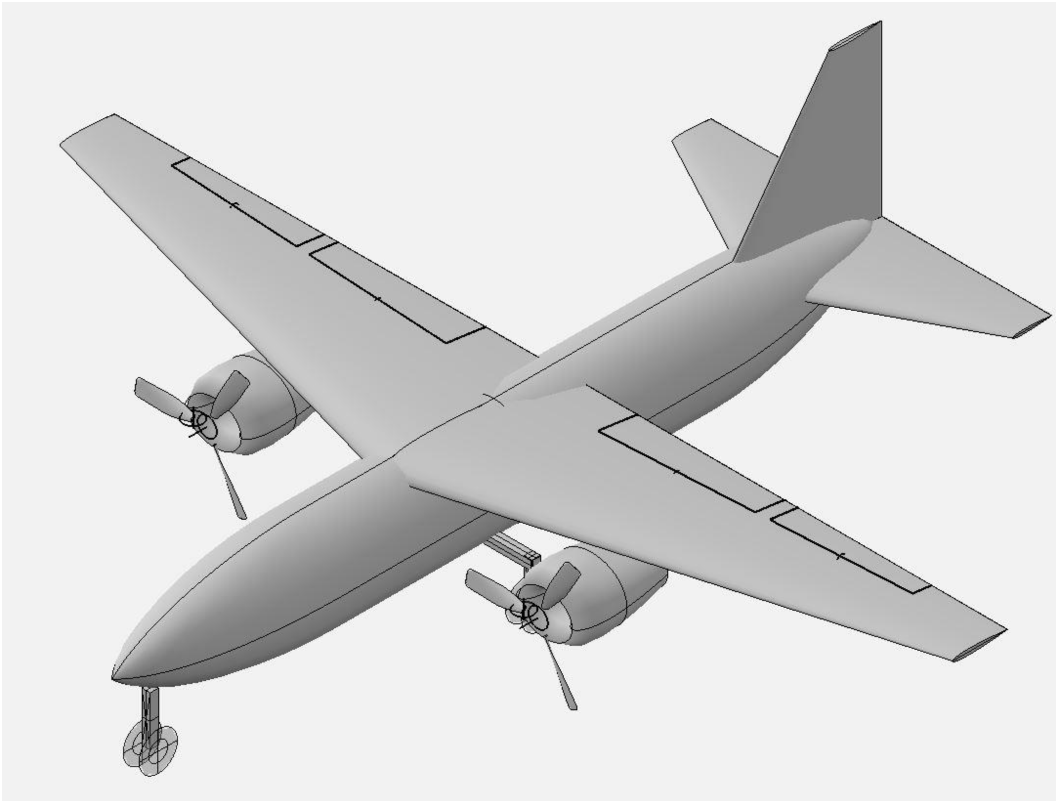

Figure 21-2 Final CAD model for the cargo configuration

Table 21.1 Cargo configuration information

Parameter	Value
W (weight)	8165 lb (3704 kg)
W/S (wing loading)	28 lb/ft^2 (137 kg/m^2)
A (aspect ratio)	7.5
λ (taper ratio)	0.3
S_{REF} (reference wing area)	292 ft^2 (27.1 m^2)
b (span)	46.8 ft (14.3 m)
C_{root}	9.59 ft (2.92 m)
C_{tip}	2.88 ft (0.88 m)
MAC	6.84 ft (2.08 m)
Fuel weight	1830 lb (830 kg)
Empty weight	4536 lb (2057 kg)
Payload weight	1800 lb (816 kg)
Range	1388 nmi (2571 km)

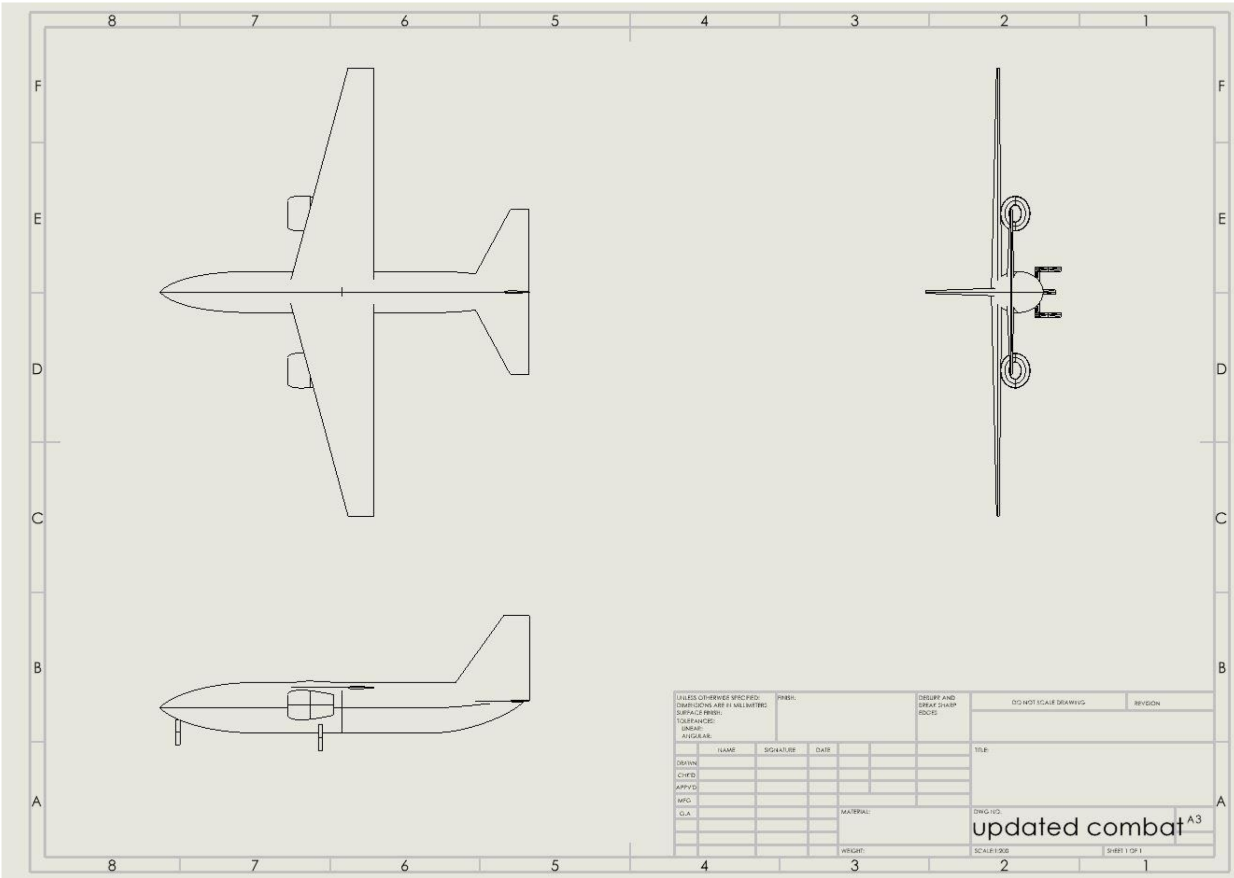

Figure 21-3 Final 3-view of the combat configuration

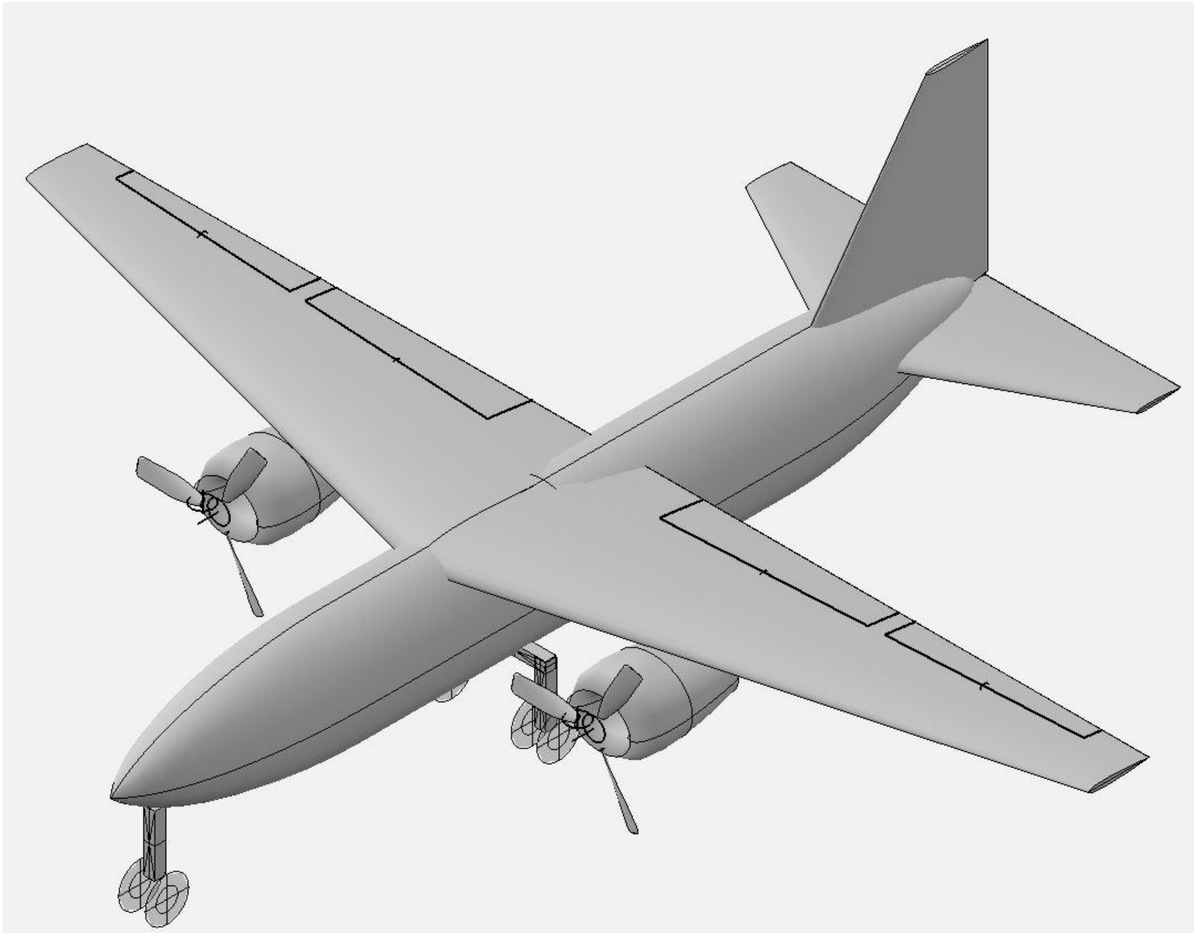

Figure 21-4 Final CAD model for the combat configuration

Table 21.2 Combat configuration information

Parameter	Value
W (weight)	7545 lb (3422 kg)
W/S (wing loading)	25 lb/ft^2 (122 kg/m^2)
A (aspect ratio)	8
λ (taper ratio)	0.3
S_{REF} (reference wing area)	302 ft^2 (28.1 m^2)
b (span)	49.1 ft (15.0 m)
C_{root}	9.45 ft (2.88 m)
C_{tip}	2.83 ft (0.86 m)
MAC	6.74 ft (2.05 m)
Fuel weight	1494 lb (678 kg)
Empty weight	3951 lb (1792 kg)
Payload weight	2100 lb (953 kg)
Range	1079 nmi (1998 km)

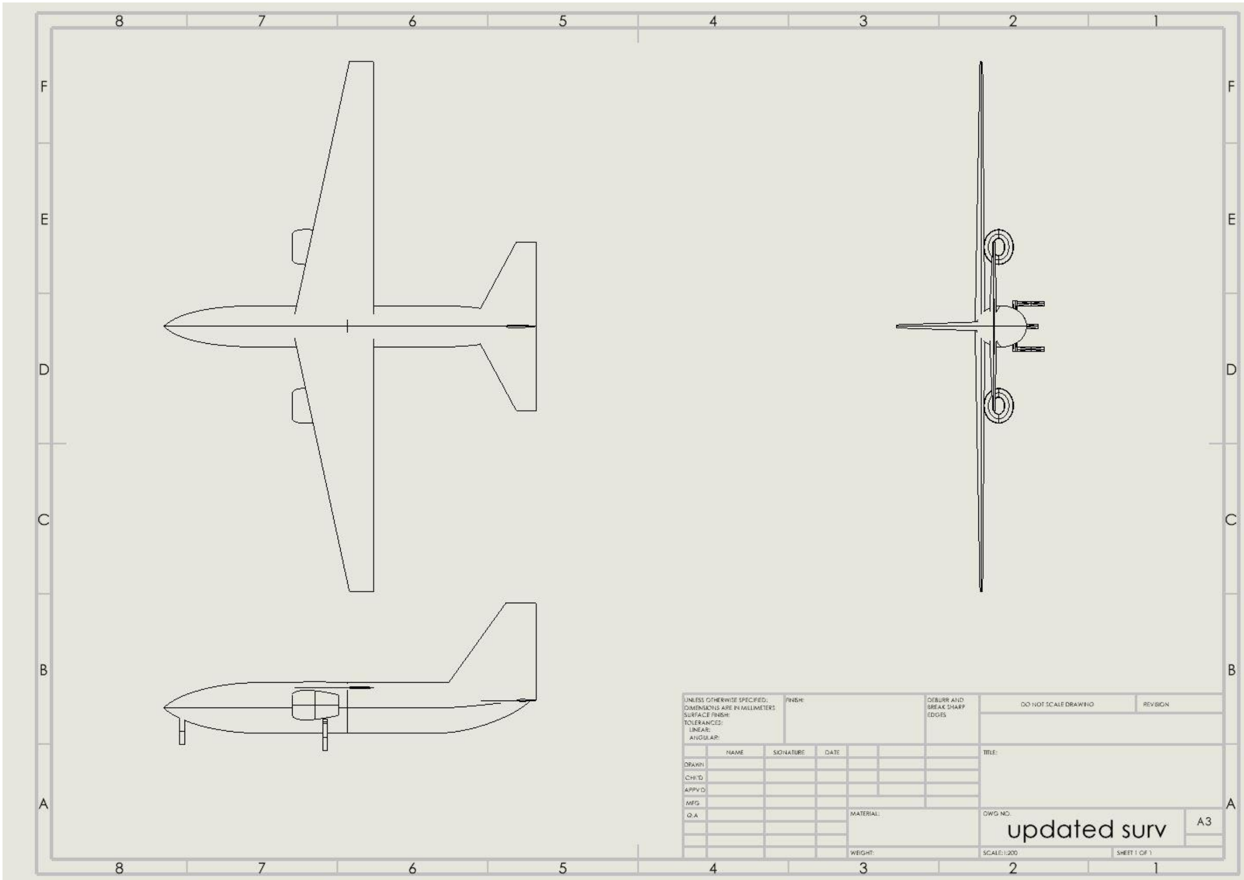

Figure 21-5 Final 3-view of the surveillance configuration

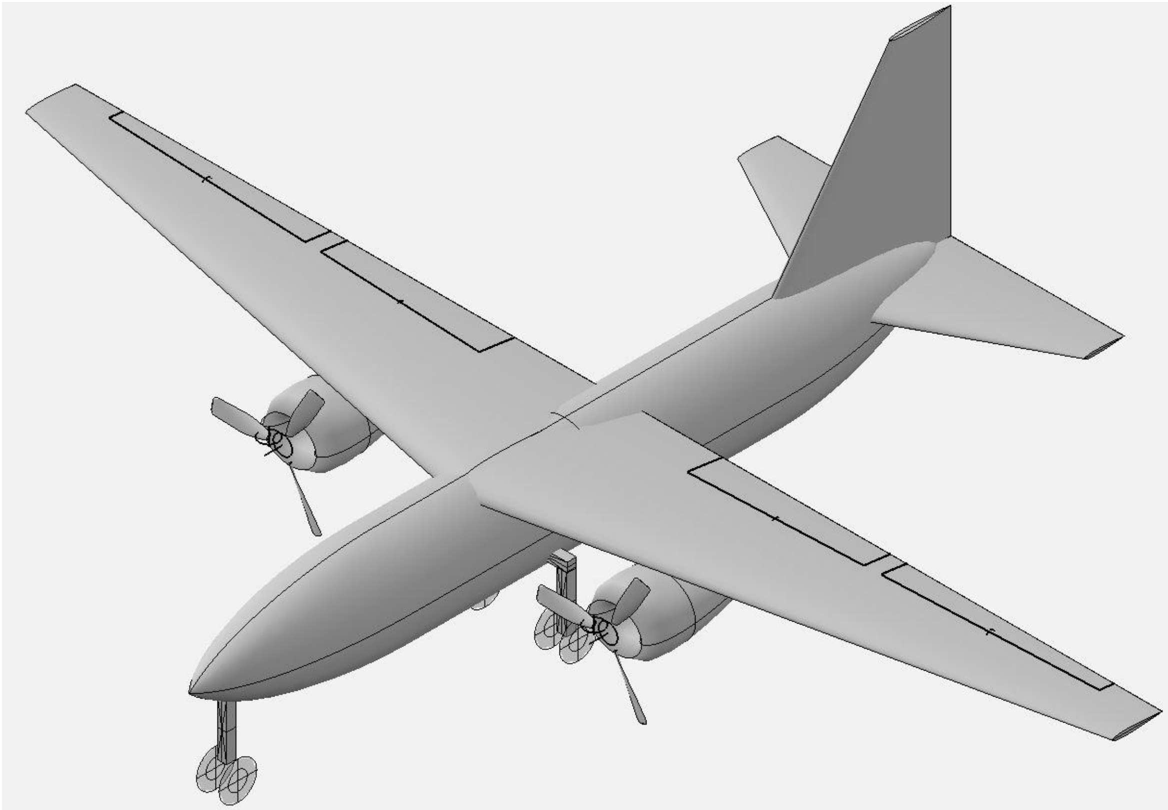

Figure 21-6 Final CAD model for the surveillance configuration

Table 21.3 Surveillance configuration information

Parameter	Value
W (weight)	7722 lb (3503 kg)
W/S (wing loading)	23 lb/ft^2 (112 kg/m^2)
A (aspect ratio)	10
λ (taper ratio)	0.3
S_{REF} (reference wing area)	336 ft^2 (31.2 m^2)
b (span)	57.9 ft (17.6 m)
C_{root}	8.91 ft (2.72 m)
C_{tip}	2.67 ft (0.81 m)
MAC	6.35 ft (1.94 m)
Fuel weight	2563 lb (1163 kg)
Empty weight	4169 lb (1891 kg)
Payload weight	1000 lb (454 kg)
Range	2536 nmi (4697 km)

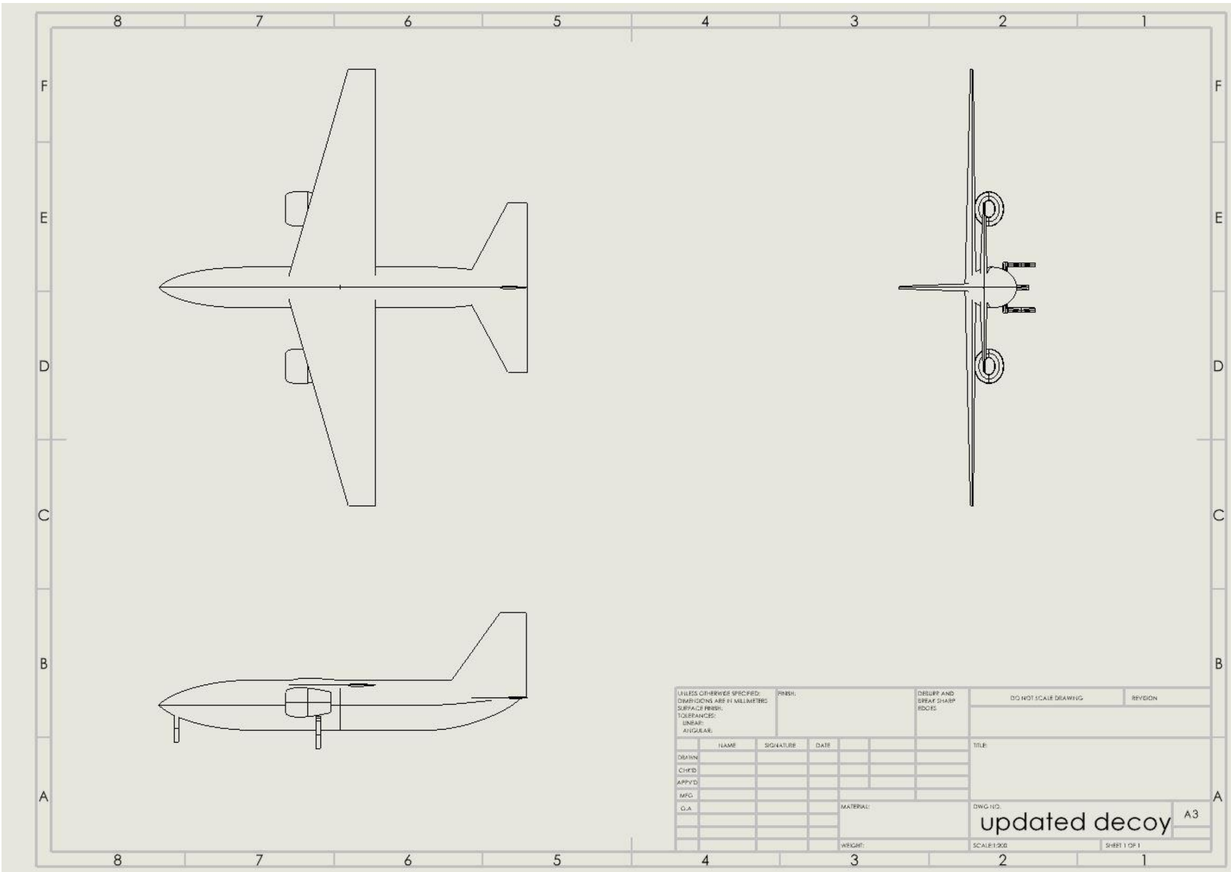

Figure 21-7 Final 3-view of the decoy configuration

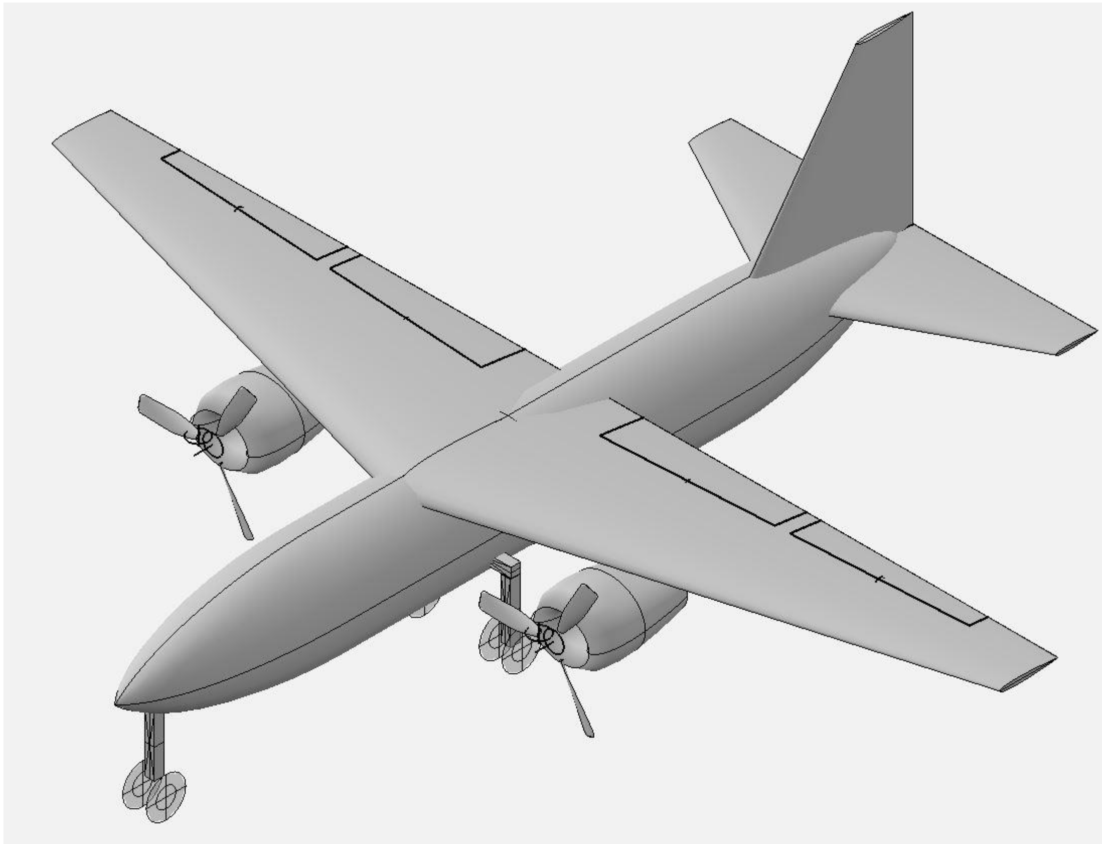

Figure 21-8 Final CAD model for the decoy configuration

Table 21.4 Decoy configuration information

Parameter	Value
W (weight)	7434 lb (3372 kg)
W/S (wing loading)	24 lb/ft^2 (117 kg/m^2)
A (aspect ratio)	7.5
λ (taper ratio)	0.3
S_{REF} (reference wing area)	310 ft^2 (28.8 m^2)
b (span)	48.2 ft (14.7 m)
C_{root}	9.89 ft (3.01 m)
C_{tip}	2.97 ft (0.91 m)
MAC	7.05 ft (2.15 m)
Fuel weight	2998 lb (1360 kg)
Empty weight	3936 lb (1785 kg)
Payload weight	500 lb (227 kg)
Range	2961 nmi (5484 km)

22. Cost Analysis

22.1 Introduction

Since cost is a vital selling point of the aircraft, various methods and references were used to complete the cost analysis. To ensure consistency across the four cost estimations, the monetary values were adjusted to 2024 values. The hourly rates for the various fields were adjusted as well. The number of units produced was kept the same across all the cost estimations. While Raymer, Snorri, and Nicolai were used to get an idea of the price per unit, Roskam was used to determine the direct operating cost [26] [33] [34] [27].

22.2 Design and Development Cost

Table 22.1 Developmental cost estimation from Roskam

Parameter	Value
C_{POL} (total)	$8,665,155,225
C_{POL} each year	$288,838,507
C_{POL} each year per aircraft	$577,677
C_{crewpr} (total)	$18,225,000,000
C_{crewpr} each year	$607,500,000
$C_{mpersdir}$ (total)	$21,870,000,000
$C_{mpersdir}$ per year	$729,000,000
C_{conmat} (total)	$3,159,000,000
C_{conmat} per year	$105,300,000

22.3 Manufacturing Cost

Table 22.2 Manufacturing cost estimation from Snorri

	Total Cost	**Cost per unit**	
Engineering	$945,807,838	$945,808	
Development support	$39,392,968	$39,393	
Flight test operations	$785,896	$786	
Tooling	$49,477,876	$49,478	
Certification Cost	**$1,035,464,578**		
Manufacturing labor	$484,608,801	$484,609	
Quality control	$ 62,999,144	$62,999	
Materials/equipment	$72,251,388	$72,251	
Quantity Discount Factor			0.6
		Without QDF	With QDF
Engines		$174,870	$104,885
Propellers		$8,429	$5,055
Avionics		$20,100	$12,056
Total Cost to Produce		**$1,858,723**	**$1,777,320**

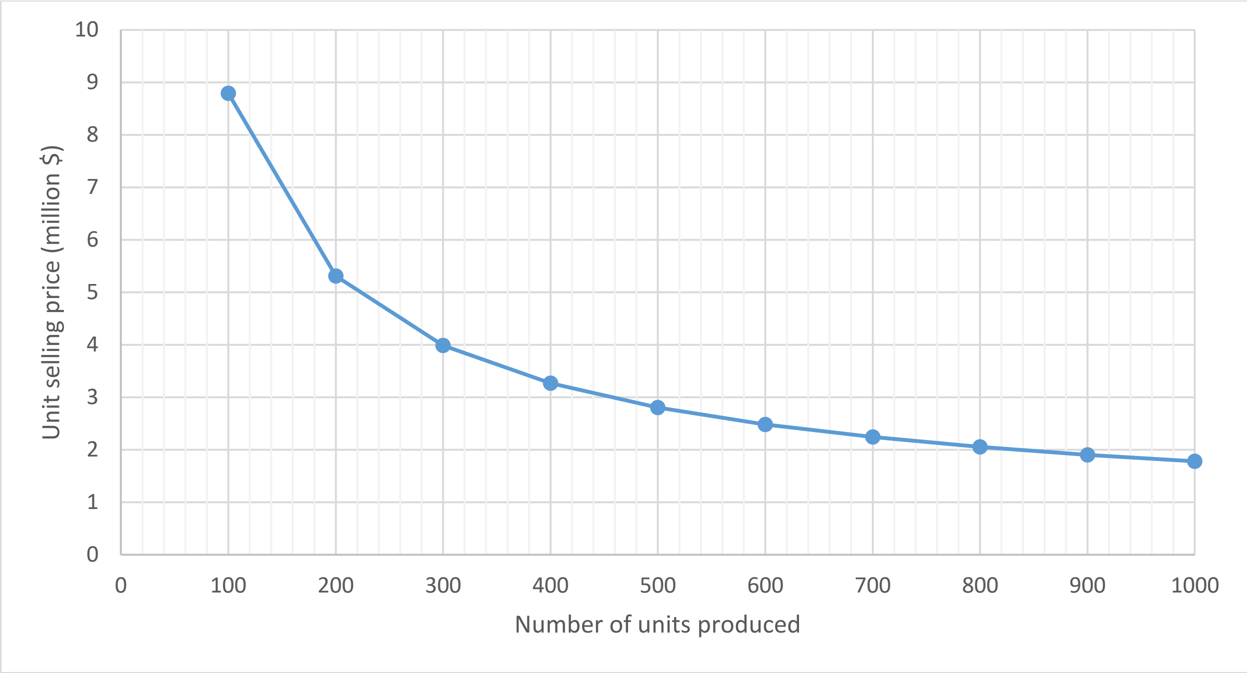

Figure 22-1 Selling price vs units produced (Raymer method)

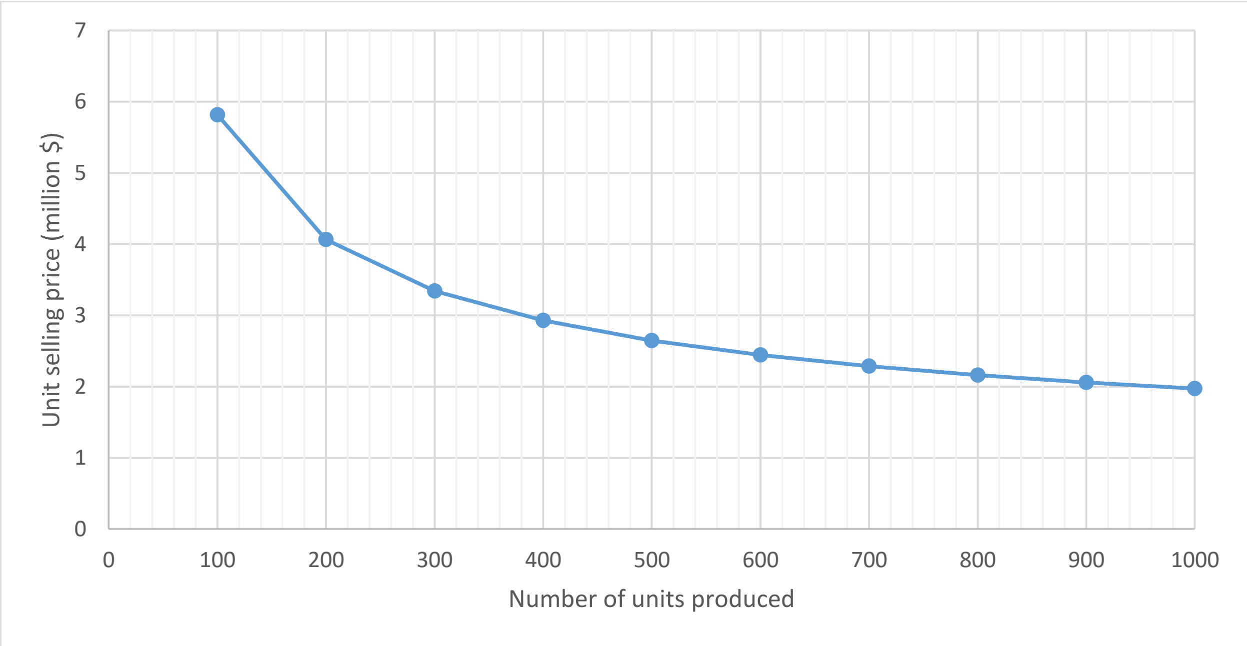

Figure 22-2 Selling price vs units produced (Snorri method)

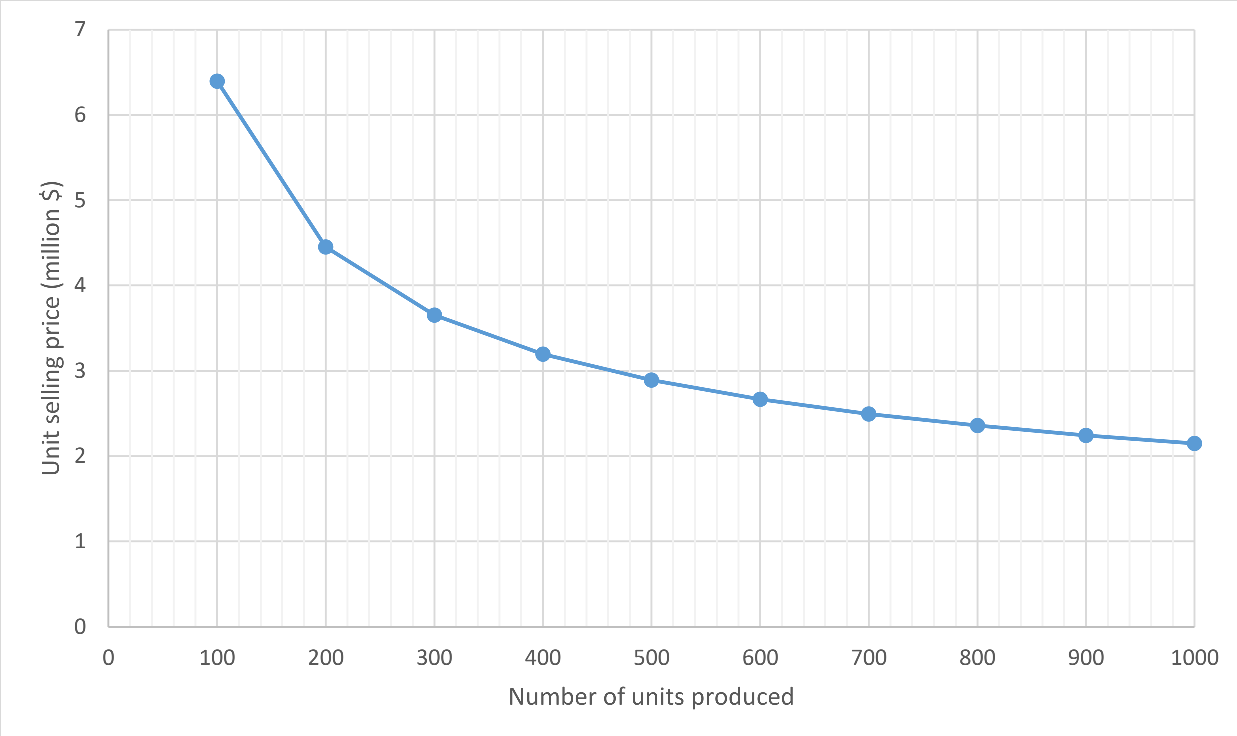

Figure 22-3 Selling price vs units produced (Nicolai method)

22.4 Operating Cost

Table 22.3 Direct operating cost estimation from Roskam

C_{OPS}	$ 63,573,877,783
$C_{OPS/hr}$	$ 3,924

Table 22.4 Direct operating cost comparison

Compared with	Value
Fighter Example [27]	**$ 10,286**
Average for passenger carrier (2018) [33]	$ 8,916
Average for passenger carrier (2024)	**$ 11,094**
Average for cargo carrier (2018) [35]	$ 28,744
Average for cargo carrier (2024)	**$ 35,766**
Average military DOC/hr for UAV (2018) [35]	$ 3,030
Average military DOC/hr for UAV (2024)	**$ 3,770**
Cessna Caravan DOC/Flyaway	$ 1,400
Predator Operating Cost (2012) [36]	$ 3,624
Predator Operating Cost (2024)	**$ 4,909**

22.5 Discussion

Each reference had different values for the hourly rates of each field, but this ultimately didn't have wide-reaching effects as the cost per unit was nearly the same across all the estimations. The three estimations all showed a selling price of $2 million per unit at 1000 units sold. This is most likely due to each cost estimation having different ways of calculating the various costs. The maximum takeoff weight, cruise speed, and number of units produced were used across all the cost estimations and had the biggest impact on the final cost estimates. To further illustrate the similarities between the cost estimation models, a plot showing the number of units produced compared to the selling cost of each aircraft was created for each model. Since each reference was published in a different year, all of the costs were scaled up to the year 2024 using a CPI conversion.

The direct operating cost of the project's design was compared with values presented in Raymer's text in addition to other references found online. These direct operating costs were then adjusted to 2024 values using the date in which the references were published as the adjustment factor. The direct operating cost was lower in every case except for the Cessna Caravan and the average military UAV. The specifications of the military UAVs was not stated, and is assumed to be based on smaller UAV that can't carry paratroopers. The Excel formulas and calculations for this section can be found in Appendix L.

23. Conclusions

23.1 Discussion

The goal of this project was to design an aircraft that could complete various types of missions by changing modular aspects of the aircraft. This ranged from changing the wings, to changing the avionics or storage bay layout in the fuselage. While the modular wings are a unique idea, the actual feasibility of it was not within the scope of this project. The project idea was more focused on whether sharing common aspects while changing other aspects among four configurations would allow for widely varying missions. If there was additional time to work on the project, this would've been used to complete the trim diagram. A significant amount of time was devoted to this section, but a completed trim diagram was still not possible. Even with multiple references being used, it was unclear how to proceed with the analysis. Additional time could also have been used to further iterate each section of the design. Some aspects were only iterated upon a couple of times while others were iterated over 10 times. The CAD model could've also been further detailed as OpenVSP did not allow for specific details that would've been possible through another program like Solidworks.

While not present in the report, some aspects of the design were iterated upon numerous times, sometimes for just a 5% improvement in performance. This could have been included in the report to show the full progress of the design across the full year the project was worked on, but this would've doubled the report size and resulted in some cluttered sections. In some chapters, there were references to the iterations, but a single sentence can't convey the time and effort spent to maximize aspects of the aircraft.

References

[1] *Aerospace Global Market Report 2023*. The Business Research Company, 2023.

[2] Dahlgren, R., Alonso, J., and Fladeland, M., "Progress on Modular Unmanned Aircraft Technology ," *ASPRS 3rd UAS Symposium*, Moffett Field, CA, Sep. 2016.

[3] Hanna, M., Schwenke, J., Schwede, L.-N., Laukotka, F., and Krause, D., "Model-based application of the methodical process for modular lightweight design of aircraft cabins," *Procedia CIRP*, Vol. 100, No. 1, 2021, pp. 637–642.

[4] Rivero, A. E., Fournier, S., Heeb, R. M., and Woods, B. K., "Design, manufacture and wind tunnel test of a modular FISHBAC wing with novel 3D printed skins," *Applied Sciences*, Vol. 12, No. 2, 2022, p. 652.

[5] Fichera, S., Jiffr, S., and Mottershead, J. E., "Design and wind tunnel test of a MODular aeroelastic FLEXible wing (MODFLEX)," *ISMA*, Ieuven, Belgium, July 2016, pp. 445–456.

[6] Modular Unmanned Air-Vehicle, by R. Colgren. (2011, Apr. 12). *US20080149758A1*. [Online]. Available: https://patents.google.com/patent/US20080149758A1/en

[7] Sachs, F., "Configurational aspects and vehicle specific investigations for future unmanned cargo aircraft," *Automated Low-Altitude Air Delivery*, Vol. 2021, No. 1, pp. 133–157.

[8] Hasan, Y. J., and Sachs, F., "Performance-based preliminary design and selection of aircraft configurations for unmanned cargo operations," *Automated Low-Altitude Air Delivery*, Vol. 2021, No. 1, pp. 107–131.

[9] Hasan, Y. J., Sachs, F., and Dauer, J. C., "Preliminary design study for a future unmanned cargo aircraft configuration," *CEAS Aeronautical Journal*, Vol. 9, No. 1, 2018, pp. 571–586.

[10] Celek, O. E., Yurdakul, M., and Ic, Y. T., "A computer-aided design and analysis of a modular flexible fixturing system for Aircraft Fuselage Panel Assembly," *International Journal on Interactive Design and Manufacturing (IJIDeM)*, Vol. 17, No. 4, May 2023, pp. 2005–2018.

[11] Fujita, K., "Product variety optimization under Modular Architecture," *Computer-Aided Design*, Vol. 34, No.12, 2002, pp. 953–965.

[12] Kohli, L., Saurabh, M., Bhatia, I., Sindhwani, N., and Vijh, M., "Design and development of modular and multifunctional UAV with amphibious landing, processing and surround sense module," *Unmanned Aerial Vehicles for Internet of Things (IoT)*, Wiley, Hoboken, NJ, 2021, pp. 207–230.

[13] Hert, D., Baca, T., Petracek, P., Kratky, V., Spurny, V., Petrlik, M., Vrba, M., Zaitlik, D., Stoudek, P., Walter, V., Stepan, P., Horyna, J., Pritzl, V., Silano, G., Bonilla Licea, D., Stibinger, P., Penicka, R., Nascimento, T., and Saska, M., "MRS Modular UAV hardware platforms for supporting research in real-world outdoor and indoor environments," *2022 International Conference on Unmanned Aircraft Systems (ICUAS)*, Dubrovnik, Croatia, June 2022.

[14] Tezza, D., "A Modular Framework for Multi-Rotor Unmanned Aerial Vehicles for Military Operations ," dissertation, University of South Florida, 2021.

[15] Gaska, T., Watkin, C., and Chen, Y., "Integrated Modular Avionics – Past, present, and future," *IEEE Aerospace and Electronic Systems Magazine*, Vol. 30, No. 9, Sep. 2015, pp. 12–23.

[16] Evers, L., Dollevoet, T., Barros, A. I., and Monsuur, H., "Robust UAV mission planning," *Annals of Operations Research*, Vol. 222, No. 1, 2012, pp. 293–315.

[17] Zhai, Q., Ye, Z.-S., "How reliable should military uavs be?," *IISE Transactions*, Vol. 52, No. 11, 2020, pp. 1234–1245.

[18] Morgan, M. J., "Integrated Modular Avionics for next-generation commercial airplanes," *IEEE AES Systems Magazine,* Vol. 6, No. 8, Aug. 1991, pp. 9–12.

[19] Boniol, F., Wiels, V., "Towards Modular and Certified Avionics for UAV ," *Aerospace Lab Journal*, Vol. 8, No. 2, Dec. 2014, pp. 1–7.

[20] Zheng, W., Mehbodniya, A., Neware, R., Wawale, S. G., Ganthia, B. P., and Shabaz, M., "Modular Unmanned Aerial Vehicle Platform Design: Multi-objective evolutionary system method," *Computers and Electrical Engineering*, Vol. 99, No. 1, 2022, p. 107838.

[21] Wang, I., Gibbs, S., and Dowell, E. "Aeroelastic Model of Multisegmented Folding Wings: Theory and Experiment." Journal of Aircraft, Vol. 49, No. 3, 2012, pp. 911–921.

[22] Wang, I., and Dowell, E. H. "Structural Dynamics Model of Multisegmented Folding Wings: Theory and Experiment." Journal of Aircraft, Vol. 48, No. 6, 2011, pp. 2149–2160.

[23] Qi, W., Zhao, C., Liu, B., and Tian, S. "Flutter and Discrete Gust Load Alleviation Characteristics of Multi-Segment Folding Wings with Constant Cross Section." *Journal of Sound and Vibration*, Vol. 540, No.1, 2022, pp. 1–21.

[24] Lu, X., Yang, R., Qian, W., and Sun, S. "Design and Manufacture of Similar Model of Folding Wings and Study on Dynamic Characteristics." *Machines*, Vol. 10, No. 12, 2022, pp. 1–13.

[25] Taylor, J. W. R., *Jane's All the World's Aircraft 1988-89*. Jane's Information Group, UK, 1988.

[26] Raymer, D., *Aircraft Design : A Conceptual Approach*. AIAA, Washington, D.C, 1992.

[27] Roskam, J., *Airplane Design*. Darcorporation, Lawrence, KS, 1985.

[28] Airfoil Tools. http://airfoiltools.com/.

[29] Wood, A. Wing Plotting Tool. AeroToolbox. https://aerotoolbox.com/wing-plot-tool/

[30] Scheelhaase, J., Müller, L., Ennen, D., and Grimme, W. "Economic and Environmental Aspects of Aircraft Recycling." *Transportation Research Procedia*, Vol. 65, 2022, pp. 3–12.

[31] Pamplona, D., and Alves, C. "Does a Fighter Pilot Live in the Danger Zone? A Risk Assessment Applied to Military Aviation." *Transportation Research Interdisciplinary Perspectives*, Vol. 5, 2020, p. 100114.

[32] Teledyne Continental Motors GTSIO-520 Cutaway Model E50. Avotek.

[33] Snorri Gudmundsson. *General Aviation Aircraft Design*. Elsevier, 2016.

[34] Nicolai Leland M, and Carichner Grant E. *Fundamentals of Aircraft and Airship Design Volume 1 - Aircraft Design*. American Institute Of Aeronautics And Astronautics, 2010.

[35] 4. AIRCRAFT OPERATING COSTS. *Federal Aviation Administration*. https://www.faa.gov/sites/faa.gov/files/regulations_policies/policy_guidance/benefit_cost/econ-value-section-4-op-costs.pdf.

[36] Wheeler, W. 2. The MQ-9'S Cost and Performance. *Time*. https://nation.time.com/2012/02/28/2-the-mq-9s-cost-and-performance/.

Appendix A – Constraint Diagram

A.1 Equations

GIVEN			Solve	
LANDING				
S_{LG}	1500	ft	V_{SL}^2 (kt^2)	=B3/0.265
ρ	0.002378	slug/ft^3	V_{SL} (kt)	=SQRT(E3)
$C_{L\_MAX\_Landing1}$	1.7		V_{SL} (ft/s)	=E4*1.688
$C_{L\_MAX\_Landing2}$	2		$C_{L\_MAX\_Landing}$	=(E5^2)*B4/2
$C_{L\_MAX\_Landing3}$	2.3		CL_MAX_Landing (including 95% TO	=E6/0.95
$C_{L\_MAX\_Landing\_1}$	=E7*B5			
$C_{L\_MAX\_Landing\_2}$	=E7*B6			
$C_{L\_MAX\_Landing\_3}$	=E7*B7			
TAKEOFF				
TOP_{23}	218.46	hp/ft^2		
$C_{L\_MAX\_TO}$	1.4	1.7	2	
W/S	W/P	W/P	W/P	
Lb/ft^2	lb/HP	lb/HP	lb/HP	
20	=B14*B15/A18	=B14*C15/A18	=B14*D15/A18	
30	=B14*B15/A19	=B14*C15/A19	=B14*D15/A19	
40	=B14*B15/A20	=B14*C15/A20	=B14*D15/A20	
50	=B14*B15/A21	=B14*C15/A21	=B14*D15/A21	
60	=B14*B15/A22	=B14*C15/A22	=B14*D15/A22	
CRUISE				
h	10000	ft		
v	200	knots		
v	=B25*1.151	mph		
σ	0.7386			
I_P	1.3		0	0
	=(B28^3)*B27		10	=B30*D29
	=1/B29		20	=B30*D30
			30	=B30*D31
			40	=B30*D32
			50	=B30*D33
			60	=B30*D34
			70	=B30*D35
			80	=B30*D36
			90	=B30*D37
			100	=B30*D38
CLIMB				
W_0	8165		S_{wet}	=10^(B42+B43*LOG10(B41))
c	0.8635		f	=10^(B46+LOG((E41)))
d	0.5632		C_{D0}	=E42/B49
			C_{DMAX}	=E43*4
c_f	0.007		C_{LMAX}	=SQRT(3*E43*PI()*B52*B53)
a	-2.1549		(C_{LMAX})^(3/2)/C_D	=E45^(3/2)/E44
b	1			
S_{ref}	306		RC_0 (ft/min)	=B57/B58*LN(1-(B56/B57))*-1
			RCP	=E49/33000
A	7.5		(C_{LMAX})^(3/2)/C_D	=(1.345*(B52*B53)^(3/4))/(E43^(1/
e	0.8		Denominator	=E52*19
η_p	0.8			
h	10000	ft		
h_{abs}	25000	ft		
t_{climb}	10	min		
Lb/ft^2	RCP	(W/S)^(1/2)/258	1/(W/P)	W/P
20	=E50	=A61^0.5/E53	=(B61+C61)/B54	=1/D61
30	=E50	=A62^0.5/E53	=(B62+C62)/B54	=1/D62
40	=E50	=A63^0.5/E53	=(B63+C63)/B54	=1/D63
50	=E50	=A64^0.5/E53	=(B64+C64)/B54	=1/D64
60	=E50	=A65^0.5/E53	=(B65+C65)/B54	=1/D65

AEO					
C_{D0}	=E43		$C_{D0\ W/FLAPS}$	=B71+0.0134	
A	7.5				
e	0.8				
$C_{L\_MAX\_TO}$	C_{L_TO}	C_D	L/D		
1.4	1.2	=E71+(B75^2)/(PI()*E	=B75/C75		
1.7	1.5	=E71+(B76^2)/(PI()*E	=B76/C76		
2	1.8	=E71+(B77^2)/(PI()*E	=B77/C77		
Constant	18.97		Nominator (LHS)	=B80*B81	
η_p	0.8		RHS (1.4)	=(0.0833+(1/D75))/(B75^0.5)	
			RHS (1.7)	=(0.0833+(1/D76))/(B76^0.5)	
			RHS (2.0)	=(0.0833+(1/D77))/(B77^0.5)	
$C_{L\_MAX\_TO}$	1.4	1.7	2		
W/S	W/P	W/P	W/P		
Lb/ft^2					
20	=E80/E81/SQRT(A88)	=E80/E82/SQRT(A88)	=E80/E83/SQRT(A88)		
30	=E80/E81/SQRT(A89)	=E80/E82/SQRT(A89)	=E80/E83/SQRT(A89)		
40	=E80/E81/SQRT(A90)	=E80/E82/SQRT(A90)	=E80/E83/SQRT(A90)		
50	=E80/E81/SQRT(A91)	=E80/E82/SQRT(A91)	=E80/E83/SQRT(A91)		
60	=E80/E81/SQRT(A92)	=E80/E82/SQRT(A92)	=E80/E83/SQRT(A92)		
OEI					
e (flaps up)	0.85				
e (flaps takeoff)	0.8				
C_{D0}	=E43				
C_{DMAX}	=B100*4				
C_{LMAX}	=SQRT(3*E43*PI()*B				
(C_L)^(3/2)/C_D	=B102^(3/2)/B101				
W/S	V_{S0}	V_{S0}	RC	RCP	
Lb/ft^2	ft/s	kts	ft/min		
20	=23.96*(A108^0.5)	=B108/1.688	=0.027*C108^2	=D108/33000	
30	=23.96*(A109^0.5)	=B109/1.688	=0.027*C109^2	=D109/33000	
40	=23.96*(A110^0.5)	=B110/1.688	=0.027*C110^2	=D110/33000	
50	=23.96*(A111^0.5)	=B111/1.688	=0.027*C111^2	=D111/33000	
60	=23.96*(A112^0.5)	=B112/1.688	=0.027*C112^2	=D112/33000	
W/S	(W/S)^(1/2)/258	RCP			
Lb/ft^2					
20	=(A116^0.5)/E53	=E108	=1/(C116+B116/0.8)	=D116/1.19	
30	=(A117^0.5)/E53	=E109	=1/(C117+B117/0.8)	=D117/1.19	
40	=(A118^0.5)/E53	=E110	=1/(C118+B118/0.8)	=D118/1.19	
50	=(A119^0.5)/E53	=E111	=1/(C119+B119/0.8)	=D119/1.19	
60	=(A120^0.5)/E53	=E112	=1/(C120+B120/0.8)	=D120/1.19	
CEILING					
RoC	100	ft/min	RCP (HP/lb)	=(33000^-1)*B124	
h	20000	ft	C_D	=0.04+(B127^2)/20.1	
Sigma (air density)	0.533		(C_{LMAX})^(3/2)/C_D	=(B127^(3/2))/E125	
C_L	1.7		Denom	=19*E126*B126^0.5	
η_p	0.8				
W/S	RCP	(W/S)^(1/2)/167	(W/S)^(1/2)/167 + RCP	1/(W/P)	
Lb/ft^2					
20	=(33000^-1)*B124	=A132^(1/2)/E127	=C132+B132	=D132/B128	=1/E132
30	=(33000^-1)*B124	=A133^(1/2)/E127	=C133+B133	=D133/B128	=1/E133
40	=(33000^-1)*B124	=A134^(1/2)/E127	=C134+B134	=D134/B128	=1/E134
50	=(33000^-1)*B124	=A135^(1/2)/E127	=C135+B135	=D135/B128	=1/E135
60	=(33000^-1)*B124	=A136^(1/2)/E127	=C136+B136	=D136/B128	=1/E136

A.2 Cargo

GIVEN			Solve				
LANDING							
S_{LG}	1500	ft	$V_{SL}{}^2$	5660.377358	kt^2		
ρ	0.002378	$slug/ft^3$	V_{SL}	75.23547939	kt		
$C_{L\_MAX\_Landing1}$	1.7		V_{SL}	126.9974892	ft/s		
$C_{L\_MAX\_Landing2}$	2		$C_{L\_MAX\_Landing}$	19.17662273			
$C_{L\_MAX\_Landing3}$	2.3		CL_MAX_Landing (in	20.18591867			
			$C_{L\_MAX\_Landing\_1}$	34.31606173	10		
			$C_{L\_MAX\_Landing\_2}$	40.37183733			
			$C_{L\_MAX\_Landing\_3}$	46.42761293			
TAKEOFF							
TOP_{23}	218.46	hp/ft^2	$C_{L\_MAX\_TO}$	1.4	1.7	2	
			W/S	W/P	W/P	W/P	
			Lb/ft^2	lb/HP	lb/HP	lb/HP	
			20	15.2922	18.5691	21.846	
			30	10.1948	12.3794	14.564	
			40	7.6461	9.28455	10.923	
			50	6.11688	7.42764	8.7384	
			60	5.0974	6.1897	7.282	
CRUISE							
h	10000	ft					
v	200	knots					
v	230.2	mph					
σ	0.7386						
I_P	1.3		0	0			
	1.622704		10	6.162552608			
	0.616255		20	12.32510522			
			30	18.48765782			
			40	24.65021043			
			50	30.81276304			
			60	36.97531565			
			70	43.13786826			
			80	49.30042087			
			90	55.46297347			
			100	61.62552608			
CLIMB							
W_0	8165		S_{wet}	1166.040743			
c	0.8635		f	8.162322041			
d	0.5632		C_{D0}	0.026674255			
			C_{DMAX}	0.10669702			
c_f	0.007		C_{LMAX}	1.228166758			
a	-2.1549		(C_{LMAX})^(3/2)/C_D	12.75656415			
b	1						
S_{ref}	306		RC_0	1277.064059	ft/min		
			RCP	0.038698911			
A	7.5		(C_{LMAX})^(3/2)/C_D	12.75888278			
e	0.8		Denominator	242.4187728			
η_p	0.8		Lb/ft^2	RCP	(W/S)^(1/2)/258	1/(W/P)	W/P
			20	0.038698911	0.018447977	0.07143361	13.99901
h	10000	ft	30	0.038698911	0.022594065	0.07661622	13.05207
h_{abs}	25000	ft	40	0.038698911	0.026089379	0.080985363	12.34791
t_{climb}	10	min	50	0.038698911	0.029168813	0.084834655	11.78764
			60	0.038698911	0.031952834	0.088314681	11.32315

AEO								
C_{D0}	0.026674		$C_{D0\ W/FLAPS}$	0.040074255				
A	7.5							
e	0.8							
			$C_{L\_MAX\_TO}$	C_{L_TO}	C_D	L/D		
			1.4	1.2	0.116468628	10.30320373		
			1.7	1.5	0.159440462	9.407900465		
			2	1.8	0.211961594	8.492104488		
Constant	18.97							
η_p	0.8		Nominator (LHS)	15.176				
			RHS (1.4)	0.164642835				
			RHS (1.7)	0.15480256				
			RHS (2.0)	0.149858623				
			$C_{L\_MAX\_TO}$	1.4	1.7	2		
			W/S	W/P	W/P	W/P		
			Lb/ft^2					
			20	20.61101993	21.92119278	22.64438772		
			30	16.82882731	17.89857895	18.48906515		
			40	14.57419196	15.50062407	16.01200011		
			50	13.03555358	13.86417964	14.32156828		
			60	11.89977791	12.65620655	13.07374334		
OEI								
e (flaps up)	0.85		e (flaps takeoff)	0.8				
C_{D0}	0.026674							
C_{DMAX}	0.106697							
C_{LMAX}	1.265965			1.228166758				
(C_L)^(3/2)/C_D	13.34997		12.75656415					
			W/S	V_{S0}	V_{S0}	RC	RCP	
			Lb/ft^2	ft/s	kts	ft/min		
			20	107.1523775	63.47889661	108.7983985	0.003297	
			30	131.2343248	77.74545307	163.1975978	0.004945	
			40	151.5363455	89.77271651	217.596797	0.006594	
			50	169.4227848	100.3689483	271.9959963	0.008242	
			60	185.593362	109.9486741	326.3951955	0.009891	
			W/S	(W/S)^(1/2)/258	RCP			
			Lb/ft^2					
			20	0.018447977	0.003296921	37.94073983	31.88297	
			30	0.022594065	0.004945382	30.13140607	25.32051	
			40	0.026089379	0.006593842	25.50658208	21.4341	
			50	0.029168813	0.008242303	22.36970371	18.79807	
			60	0.031952834	0.009890764	20.06750491	16.86345	
CEILING								
RoC	100	ft/min	RCP	0.003030303	HP/lb			
h	20000	ft	C_D	0.183781095				
Sigma (air densit	0.533		(C_{LMAX})^(3/2)/C_D	12.06070093				
C_L	1.7		Denom	167.2976166				
η_p	0.8							
			W/S	RCP	(W/S)^(1/2)/167	(W/S)^(1/2)/167 + RCP	1/(W/P)	
			Lb/ft^2					
			20	0.003030303	0.026731618	0.029761921	0.037202	26.87999
			30	0.003030303	0.032739412	0.035769715	0.044712	22.36529
			40	0.003030303	0.037804217	0.04083452	0.051043	19.59127
			50	0.003030303	0.042266399	0.045296702	0.056621	17.66133
			60	0.003030303	0.04630052	0.049330823	0.061664	16.21704

A.3 Combat

GIVEN			Solve				
LANDING							
S_{LG}	1500	ft	V_{SL}^{2}	5660.377	kt^2		
ρ	0.002378	$slug/ft^3$	V_{SL}	75.23548	kt		
$C_{L\_MAX\_Landing1}$	1.7		V_{SL}	126.9975	ft/s		
$C_{L\_MAX\_Landing2}$	2		$C_{L\_MAX\_Landing}$	19.17662			
$C_{L\_MAX\_Landing3}$	2.3		CL_MAX_Landir	20.18592			
			$C_{L\_MAX\_Landing\_1}$	34.31606	10		
			$C_{L\_MAX\_Landing\_2}$	40.37184			
			$C_{L\_MAX\_Landing\_3}$	46.42761			
TAKEOFF							
TOP_{23}	218.46	hp/ft^2	$C_{L\_MAX\_TO}$	1.4	1.7	2	
			W/S	W/P	W/P	W/P	
			Lb/ft^2	lb/HP	lb/HP	lb/HP	
			20	15.2922	18.5691	21.846	
			30	10.1948	12.3794	14.564	
			40	7.6461	9.28455	10.923	
			50	6.11688	7.42764	8.7384	
			60	5.0974	6.1897	7.282	
CRUISE							
h	10000	ft					
v	200	knots					
v	230.2	mph					
σ	0.7386						
I_P	1.4		0	0			
	2.026718		10	4.934085			
	0.493408		20	9.868169			
			30	14.80225			
			40	19.73634			
			50	24.67042			
			60	29.60451			
			70	34.53859			
			80	39.47268			
			90	44.40676			
			100	49.34085			
CLIMB							
W_0	7545		S_{wet}	1115.315			
c	0.8635		f	7.807243			
d	0.5632		C_{D0}	0.021627			
			C_{DMAX}	0.086507			
c_f	0.007		C_{LMAX}	1.142144			
a	-2.1549		(C_{LMAX})^(3/2)/C	14.11012			
b	1						
S_{ref}	361		RC_0	1277.064	ft/min		
			RCP	0.038699			
A	8		(C_{LMAX})^(3/2)/C	14.11268			
e	0.8		Denominator	268.141			
η_p	0.8		Lb/ft^2	RCP	(W/S)^(1/	1/(W/P)	W/P
			20	0.038699	0.016678	0.069222	14.44638
h	10000	ft	30	0.038699	0.020427	0.073907	13.53052
h_{abs}	25000	ft	40	0.038699	0.023587	0.077857	12.84406
t_{climb}	10	min	50	0.038699	0.026371	0.081337	12.29452
			60	0.038699	0.028888	0.084483	11.83667

AEO								
C_{D0}	0.021627		$C_{D0\ W/FLAPS}$	0.035027				
A	8							
e	0.8							
			$C_{L\_MAX\_TO}$	C_{L_TO}	C_D	L/D		
			1.4	1.2	0.106646	11.25213		
			1.7	1.5	0.146933	10.20877		
			2	1.8	0.196171	9.175664		
Constant	18.97							
η_p	0.8		Nominator (LHS	15.176				
			RHS (1.4)	0.157171				
			RHS (1.7)	0.147994				
			RHS (2.0)	0.14332				
			$C_{L\_MAX\_TO}$	1.4	1.7	2		
			W/S	W/P	W/P	W/P		
			Lb/ft^2					
			20	21.59088	22.92968	23.67748		
			30	17.62888	18.722	19.33259		
			40	15.26706	16.21373	16.74251		
			50	13.65527	14.502	14.97496		
			60	12.4655	13.23845	13.6702		
OEI								
e (flaps up)	0.85		e (flaps takeoff	0.8				
C_{D0}	0.021627							
C_{DMAX}	0.086507							
C_{LMAX}	1.177295							
(C_L)^(3/2)/C_D	14.76649		14.11012021					
			W/S	V_{S0}	V_{S0}	RC	RCP	
			Lb/ft^2	ft/s	kts	ft/min		
			20	107.1524	63.4789	108.7984	0.003297	
			30	131.2343	77.74545	163.1976	0.004945	
			40	151.5363	89.77272	217.5968	0.006594	
			50	169.4228	100.3689	271.996	0.008242	
			60	185.5934	109.9487	326.3952	0.009891	
			W/S	(W/S)^(1/	RCP	W/P	W/P (S.L)	
			Lb/ft^2			lb/HP	lb/HP	
			20	0.016678	0.003297	41.41679	34.80403	
			30	0.020427	0.004945	32.80979	27.57125	
			40	0.023587	0.006594	27.71835	23.29273	
			50	0.026371	0.008242	24.2685	20.39369	
			60	0.028888	0.009891	21.73897	18.26804	
CEILING								
RoC	100	ft/min	RCP	0.00303	HP/lb			
h	30000	ft	C_D	0.183781				
Sigma (air de	0.3747		(C_{LMAX})^(3/2)/C	12.0607				
C_L	1.7		Denom	140.271				
η_p	0.8							
			W/S	RCP	(W/S)^(1/	(W/S)^(1/	1/(W/P)	
			Lb/ft^2					
			20	0.00303	0.031882	0.034912	0.043641	22.91449
			30	0.00303	0.039047	0.042078	0.052597	19.01242
			40	0.00303	0.045088	0.048118	0.060148	16.62565
			50	0.00303	0.05041	0.05344	0.0668	14.96996
			60	0.00303	0.055221	0.058252	0.072815	13.7335

A.4 Surveillance

GIVEN			Solve					
LANDING								
S_{LG}	1500	ft	V_{SL}^2	5660.377	kt^2			
ρ	0.002378	$slug/ft^3$	V_{SL}	75.23548	kt			
$C_{L\_MAX\_Landing1}$	1.7		V_{SL}	126.9975	ft/s			
$C_{L\_MAX\_Landing2}$	2		$C_{L\_MAX\_Landing}$	19.17662				
$C_{L\_MAX\_Landing3}$	2.3		CL_MAX_Landir	20.18592				
			$C_{L\_MAX\_Landing\_1}$	34.31606	10			
			$C_{L\_MAX\_Landing\_2}$	40.37184				
			$C_{L\_MAX\_Landing\_3}$	46.42761				
TAKEOFF								
TOP_{23}	218.46	hp/ft^2	$C_{L\_MAX\_TO}$	1.4	1.7	2		
			W/S	W/P	W/P	W/P		
			Lb/ft^2	lb/HP	lb/HP	lb/HP		
			20	15.2922	18.5691	21.846		
			30	10.1948	12.3794	14.564		
			40	7.6461	9.28455	10.923		
			50	6.11688	7.42764	8.7384		
			60	5.0974	6.1897	7.282		
CRUISE								
h	10000	ft						
v	200	knots						
v	230.2	mph						
σ	0.7386							
I_P	1.4		0	0				
	2.026718		10	4.934085				
	0.493408		20	9.868169				
			30	14.80225				
			40	19.73634				
			50	24.67042				
			60	29.60451				
			70	34.53859				
			80	39.47268				
			90	44.40676				
			100	49.34085				
CLIMB								
W_0	7722		S_{wet}	1129.977				
c	0.8635		f	7.909871				
d	0.5632		C_{D0}	0.037136				
			C_{DMAX}	0.148542				
c_f	0.007		C_{LMAX}	1.673306				
a	-2.1549		(C_{LMAX})^(3/2)/C	14.57181				
b	1							
S_{ref}	213		RC_0	1277.064	ft/min			
			RCP	0.038699				
A	10		(C_{LMAX})^(3/2)/C	14.57445				
e	0.8		Denominator	276.9146				
η_p	0.8		Lb/ft^2	RCP	(W/S)^(1/	1/(W/P)	W/P	
			20	0.038699	0.01615	0.068561	14.58556	
h	10000	ft	30	0.038699	0.019779	0.073098	13.68027	
h_{abs}	25000	ft	40	0.038699	0.022839	0.076923	13.00004	
t_{climb}	10	min	50	0.038699	0.025535	0.080293	12.45444	
			60	0.038699	0.027972	0.083339	11.99916	

AEO								
C_{D0}	0.037136		$C_{D0\ W/FLAPS}$	0.050536				
A	10							
e	0.8							
			$C_{L\_MAX\_TO}$	C_{L_TO}	C_D	L/D		
			1.4	1.2	0.107831	11.12849		
			1.7	1.5	0.14006	10.70968		
			2	1.8	0.179451	10.03059		
Constant	18.97							
η_p	0.8		Nominator (LHS	15.176				
			RHS (1.4)	0.158072				
			RHS (1.7)	0.144253				
			RHS (2.0)	0.136396				
			$C_{L\_MAX\_TO}$	1.4	1.7	2		
			W/S	W/P	W/P	W/P		
			Lb/ft^2					
			20	21.46776	23.52429	24.87936		
			30	17.52835	19.20751	20.31392		
			40	15.18	16.63419	17.59237		
			50	13.5774	14.87807	15.73509		
			60	12.39442	13.58176	14.36411		
OEI								
e (flaps up)	0.85		e (flaps takeoff	0.8				
C_{D0}	0.037136							
C_{DMAX}	0.148542							
C_{LMAX}	1.724805							
(C_L)^(3/2)/C_D	15.24966		14.57180631					
			W/S	V_{S0}	V_{S0}	RC	RCP	
			Lb/ft^2	ft/s	kts	ft/min		
			20	107.1524	63.4789	108.7984	0.003297	
			30	131.2343	77.74545	163.1976	0.004945	
			40	151.5363	89.77272	217.5968	0.006594	
			50	169.4228	100.3689	271.996	0.008242	
			60	185.5934	109.9487	326.3952	0.009891	
			W/S	(W/S)^(1/	RCP	W/P	W/P (S.L)	
			Lb/ft^2			lb/HP	lb/HP	
			20	0.01615	0.003297	42.58171	35.78295	
			30	0.019779	0.004945	33.70439	28.32302	
			40	0.022839	0.006594	28.45513	23.91187	
			50	0.025535	0.008242	24.8996	20.92403	
			60	0.027972	0.009891	22.29343	18.73398	
CEILING								
RoC	100	ft/min	RCP	0.00303	HP/lb			
h	30000	ft	C_D	0.183781				
Sigma (air de	0.3747		(C_{LMAX})^(3/2)/C	12.0607				
C_L	1.7		Denom	140.271				
η_p	0.8							
			W/S	RCP	(W/S)^(1/	(W/S)^(1/	1/(W/P)	
			Lb/ft^2					
			20	0.00303	0.031882	0.034912	0.043641	22.91449
			30	0.00303	0.039047	0.042078	0.052597	19.01242
			40	0.00303	0.045088	0.048118	0.060148	16.62565
			50	0.00303	0.05041	0.05344	0.0668	14.96996
			60	0.00303	0.055221	0.058252	0.072815	13.7335

A.5 Decoy

GIVEN			Solve					
LANDING								
S_{LG}	1500	ft	V_{SL}^2	5660.377	kt^2			
ρ	0.002378	$slug/ft^3$	V_{SL}	75.23548	kt			
$C_{L\_MAX\_Landing1}$	1.7		V_{SL}	126.9975	ft/s			
$C_{L\_MAX\_Landing2}$	2		$C_{L\_MAX\_Landing}$	19.17662				
$C_{L\_MAX\_Landing3}$	2.3		CL_MAX_Landir	20.18592				
			$C_{L\_MAX\_Landing\_1}$	34.31606	10			
			$C_{L\_MAX\_Landing\_2}$	40.37184				
			$C_{L\_MAX\_Landing\_3}$	46.42761				
TAKEOFF								
TOP_{23}	218.46	hp/ft^2	$C_{L\_MAX\_TO}$	1.4	1.7	2		
			W/S	W/P	W/P	W/P		
			Lb/ft^2	lb/HP	lb/HP	lb/HP		
			20	15.2922	18.5691	21.846		
			30	10.1948	12.3794	14.564		
			40	7.6461	9.28455	10.923		
			50	6.11688	7.42764	8.7384		
			60	5.0974	6.1897	7.282		
CRUISE								
h	10000	ft						
v	200	knots						
v	230.2	mph						
σ	0.7386							
I_P	1.4		0	0				
	2.026718		10	4.934085				
	0.493408		20	9.868169				
			30	14.80225				
			40	19.73634				
			50	24.67042				
			60	29.60451				
			70	34.53859				
			80	39.47268				
			90	44.40676				
			100	49.34085				
CLIMB								
W_0	7434		S_{wet}	1106.044				
c	0.8635		f	7.742345				
d	0.5632		C_{D0}	0.02325				
			C_{DMAX}	0.093001				
c_f	0.007		C_{LMAX}	1.146635				
a	-2.1549		(C_{LMAX})^(3/2)/C	13.2023				
b	1							
S_{ref}	333		RC_0	1277.064	ft/min			
			RCP	0.038699				
A	7.5		(C_{LMAX})^(3/2)/C	13.2047				
e	0.8		Denominator	250.8894				
η_p	0.8		Lb/ft^2	RCP	(W/S)^(1/	1/(W/P)	W/P	
			20	0.038699	0.017825	0.070655	14.15327	
h	10000	ft	30	0.038699	0.021831	0.075663	13.21655	
h_{abs}	25000	ft	40	0.038699	0.025209	0.079884	12.5181	
t_{climb}	10	min	50	0.038699	0.028184	0.083604	11.9612	
			60	0.038699	0.030874	0.086966	11.49872	

AEO								
C_{D0}	0.02325		$C_{D0\ W/FLAPS}$	0.03665				
A	7.5							
e	0.8							
			$C_{L\_MAX\_TO}$	C_{L_TO}	C_D	L/D		
			1.4	1.2	0.113045	10.61527		
			1.7	1.5	0.156016	9.614368		
			2	1.8	0.208538	8.631536		
Constant	18.97							
η_p	0.8		Nominator (LHS	15.176				
			RHS (1.4)	0.162038				
			RHS (1.7)	0.152939				
			RHS (2.0)	0.148441				
			$C_{L\_MAX\_TO}$	1.4	1.7	2		
			W/S	W/P	W/P	W/P		
			Lb/ft^2					
			20	20.94233	22.18833	22.86067		
			30	17.09934	18.1167	18.66566		
			40	14.80847	15.68952	16.16494		
			50	13.2451	14.03313	14.45836		
			60	12.09106	12.81044	13.19862		
OEI								
e (flaps up)	0.85		e (flaps takeoff	0.8				
C_{D0}	0.02325							
C_{DMAX}	0.093001							
C_{LMAX}	1.181925							
(C_L)^(3/2)/C_D	13.81645		13.20230356					
			W/S	V_{S0}	V_{S0}	RC	RCP	
			Lb/ft^2	ft/s	kts	ft/min		
			20	107.1524	63.4789	108.7984	0.003297	
			30	131.2343	77.74545	163.1976	0.004945	
			40	151.5363	89.77272	217.5968	0.006594	
			50	169.4228	100.3689	271.996	0.008242	
			60	185.5934	109.9487	326.3952	0.009891	
			W/S	(W/S)^(1/	RCP	W/P	W/P (S.L)	
			Lb/ft^2			lb/HP	lb/HP	
			20	0.017825	0.003297	39.09558	32.85343	
			30	0.021831	0.004945	31.02273	26.06952	
			40	0.025209	0.006594	26.2436	22.05345	
			50	0.028184	0.008242	23.00315	19.33038	
			60	0.030874	0.009891	20.62566	17.33248	
CEILING								
RoC	100	ft/min	RCP	0.00303	HP/lb			
h	15000	ft	C_D	0.183781				
Sigma (air de	0.6295		(C_{LMAX})^(3/2)/C	12.0607				
C_L	1.7		Denom	181.8126				
η_p	0.8							
			W/S	RCP	(W/S)^(1/	(W/S)^(1/	1/(W/P)	
			Lb/ft^2					
			20	0.00303	0.024598	0.027628	0.034535	28.95634
			30	0.00303	0.030126	0.033156	0.041445	24.12839
			40	0.00303	0.034786	0.037816	0.047271	21.15483
			50	0.00303	0.038892	0.041922	0.052403	19.08289
			60	0.00303	0.042604	0.045634	0.057043	17.53063

Appendix B - Wing Design

B.1 Wing Design Equations

S_{REF}	=B2/B3	
b (span)	=SQRT(B4*B7)	
C root	=(2*B7)/(B8*(1+B5))	
C tip	=B5*B9	
MAC	=(2/3)*B9*((B5^2+B5	
MAC y position	=(B8/6)*((1+2*B5)/(1	
LE Sweep		=B13*PI()/180
MAC x position	=B12*TAN(C13)	

B.2 Cargo

Weight	8165	
Wing Loading	28	
Aspect Ratio	7.5	
Taper Ratio	0.3	
S_{REF}	291.6071	
b (span)	46.76594	23.38297
C root	9.593014	
C tip	2.877904	
MAC	6.838097	
MAC y position	9.593014	
LE Sweep	4.11	0.071733
MAC x position	0.689319	

B.3 Combat

Weight	7545	
Wing Loading	25	
Aspect Ratio	8	
Taper Ratio	0.3	
S_{REF}	301.8	
b (span)	49.13654	24.56827
C root	9.449335	
C tip	2.834801	
MAC	6.73568	
MAC y position	10.07929	
LE Sweep	3.86	0.06737
MAC x position	0.680068	

B.4 Surveillance

Weight	7722	
Wing Loading	23	
Aspect Ratio	10	
Taper Ratio	0.3	
S_{REF}	335.7391	
b (span)	57.943	28.9715
C root	8.914308	
C tip	2.674292	
MAC	6.354301	
MAC y position	11.88574	
LE Sweep	3.09	0.053931
MAC x position	0.641628	

B.5 Decoy

Weight	7434	
Wing Loading	24	
Aspect Ratio	7.5	
Taper Ratio	0.3	
S_{REF}	309.75	
b (span)	48.19881	24.0994
C root	9.886935	
C tip	2.96608	
MAC	7.04761	
MAC y position	9.886935	
LE Sweep	4.11	0.071733
MAC x position	0.710439	

B.6 High Lift Devices Equations

Raymer	
Flaps	
ΔCL_{max} (Fowler)	=1.3*1.1
S_{ref}	292
Taper ratio	0.3
Hinge sweep (°)	12.15
Hinge sweep (rad)	=B6*PI()/180
Wingspan	46.8
Flap start	4
Flap end	12
n_i	=B9/(B8/2)
n_0	=B10/(B8/2)
S_f/S_{ref}	=(B12-B11)*((2-(1-B5)))*(B11+B12)/(1+B5)
S_f	=B13*B4
Landing ΔCL_{max}	=0.9*B3*B13*COS(B7)
Takeoff ΔCL_{max}	=B15*0.6

Aileron	
Wingspan	=B8/2
Chord	6.84
Aileron Span	8
Aileron Chord	2
Aileron Span	=F6/F3
Aileron Chord	=F7/F4

B.7 Cargo

Raymer	
Flaps	
ΔCL_{max} (Fowler)	1.43
S_{ref}	292
Taper ratio	0.3
Hinge sweep (°)	12.15
Hinge sweep (rad)	0.212058
Wingspan	46.8
Flap start	4
Flap end	12
n_i	0.17094
n_0	0.512821
S_f/S_{ref}	0.233764
S_f	68.25919
Landing ΔCL_{max}	0.294116
Takeoff ΔCL_{max}	0.176469

Aileron	
Wingspan	23.4
Chord	6.84
Aileron Span	8
Aileron Chord	2
Aileron Span	0.34188
Aileron Chord	0.292398

B.8 Combat

Raymer	
Flaps	
ΔCL_{max} (Fowler)	1.43
S_{ref}	302
Taper ratio	0.3
Hinge sweep (°)	11.43
Hinge sweep (rad)	0.199491
Wingspan	49.1
Flap start	4.5
Flap end	13
n_i	0.183299
n_0	0.529532
S_f/S_{ref}	0.246805
S_f	74.53511
Landing ΔCL_{max}	0.311339
Takeoff ΔCL_{max}	0.186803

Aileron	
Wingspan	24.55
Chord	6.74
Ailerson Span	9
Ailerson Chord	2
Ailerson Span	0.366599
Ailerson Chord	0.296736

B.9 Surveillance

Raymer	
Flaps	
ΔCL_{max} (Fowler)	1.43
S_{ref}	336
Taper ratio	0.3
Hinge sweep (°)	9.19
Hinge sweep (rad)	0.160396
Wingspan	57.9
Flap start	5.5
Flap end	15
n_i	0.189983
n_0	0.518135
S_f/S_{ref}	0.23237
S_f	78.07637
Landing ΔCL_{max}	0.295222
Takeoff ΔCL_{max}	0.177133

Aileron	
Wingspan	28.95
Chord	6.35
Ailerson Span	11
Ailerson Chord	2
Ailerson Span	0.379965
Ailerson Chord	0.314961

B.10 Decoy

Raymer	
Flaps	
ΔCL_{max} (Fowler)	1.43
S_{ref}	310
Taper ratio	0.3
Hinge sweep (°)	12.16
Hinge sweep (rad)	0.212232
Wingspan	48.2
Flap start	4
Flap end	12
n_i	0.165975
n_0	0.497925
S_f/S_{ref}	0.220382
S_f	68.31838
Landing ΔCL_{max}	0.277268
Takeoff ΔCL_{max}	0.166361

Aileron	
Wingspan	24.1
Chord	7.05
Ailerson Span	8
Ailerson Chord	2
Ailerson Span	0.33195
Ailerson Chord	0.283688

Appendix C - Weight and Balance Analysis

C.1 Cargo

	Weight lbs or kg	X-Location ft or m	Z-Location ft or m	Moment ft-lbs or kg-m	Moment ft-lbs or kg-m
STRUCTURES GROUP	=SUM(B9:B20)	=E8/B8	=F8/B8	=SUM(E9:E20)	=SUM(F9:F20)
Wing	634	17.4	10	=B9*C9	=B9*D9
Horiz. Tail	102	35.5	8	=B10*C10	=B10*D10
Vert. Tail	65	36.1	10	=B11*C11	=B11*D11
Fuselage	725	15.6	7.75	=B12*C12	=B12*D12
Main Lndg Gear	381	22	1.3	=B13*C13	=B13*D13
Nose Lndg Gear	103	9	1.3	=B14*C14	=B14*D14
Engine Mounts	30	16.9	10	=B15*C15	=B15*D15
Firewall	5	16.9	10	=B16*C16	=B16*D16
Engine Section				=B17*C17	=B17*D17
Air Induction				=B18*C18	=B18*D18
				=B19*C19	=B19*D19
				=B20*C20	=B20*D20
PROPULSION GROUP	=SUM(B22:B30)	=E21/B21	=F21/B21	=SUM(E22:E30)	=SUM(F22:F30)
Engine(s)	968	16.9	8	=B22*C22	=B22*D22
Tailpipe				=B23*C23	=B23*D23
Engine Cooling	50	16.9	10	=B24*C24	=B24*D24
Oil Cooling	40	16.9	10	=B25*C25	=B25*D25
Engine Controls	20	16.9	10	=B26*C26	=B26*D26
Starter				=B27*C27	=B27*D27
Fuel System	150	16.9	10	=B28*C28	=B28*D28
				=B29*C29	=B29*D29
				=B30*C30	=B30*D30
EQUIPMENT GROUP	=SUM(B32:B45)	=E31/B31	=F31/B31	=SUM(E32:E45)	=SUM(F32:F45)
Flight Controls	114	4	6	=B32*C32	=B32*D32
Instruments				=B33*C33	=B33*D33
Hydraulics	81	22	6	=B34*C34	=B34*D34
Electrical	324	4	10	=B35*C35	=B35*D35
Avionics	403	5	6	=B36*C36	=B36*D36
Furnishings & Misc	357	20	6	=B37*C37	=B37*D37
Air Conditioning	207	5	10	=B38*C38	=B38*D38
Handling Gear	5	18	6	=B39*C39	=B39*D39
APU installed	0	0	0	=B40*C40	=B40*D40
Misc Empty Weight				=B41*C41	=B41*D41
				=B42*C42	=B42*D42
				=B43*C43	=B43*D43
				=B44*C44	=B44*D44
				=B45*C45	=B45*D45
(% We Allowance)	10	%	%		
We-Allowance	=(B46/100)*(B8+B21+SUM(B32:B4	=(E31+E21+E8)/(B31+B21+B8	=(F31+F21+F8)/(B31+B21+B8)	=B47*C47	=B47*D47
EMPTY WEIGHT	**=B31+B21+B8**	**=E48/B48**	**=F48/B48**	**=E31+E21+E8**	**=F31+F21+F8**
USEFUL LOAD GROUP	=B58-B31-B21-B8	=E49/B49	=F49/B49	=SUM(E50:E57)	=SUM(F50:F57)
Crew				=B50*C50	=B50*D50
Passengers	1800	20	6	=B51*C51	=B51*D51
Payload				=B52*C52	=B52*D52
Fuel (weight available)	=B49-B50-B51-B52-B54-B55-B56-E	16.5	10	=B53*C53	=B53*D53
Oil	40	20	10	=B54*C54	=B54*D54
				=B55*C55	=B55*D55
				=B56*C56	=B56*D56
				=B57*C57	=B57*D57
TAKEOFF GROSS WEIGHT	**8165**	**=E58/B58**	**=F58/B58**	**=E49+E31+E21+E8**	**=F49+F31+F21+F8**
	With Payload CG	=(E58-E53)/(B58-B53)	=(F58-F53)/(B58-B53)		
	With Fuel CG	=(E58-E51)/(B58-B51)	=(F58-F51)/(B58-B51)		
	Empty CG	=(E58-E51-E53)/(B58-B51-B5	=(F58-F51-F53)/(B58-B51-B53)		

C.2 Combat

	Weight lbs or kg	X-Location ft or m	Z-Location ft or m	Moment ft-lbs or kg-m	Moment ft-lbs or kg-m
STRUCTURES GROUP	=SUM(B9:B20)	=E8/B8	=F8/B8	=SUM(E9:E20)	=SUM(F9:F20)
Wing	654	17.4	10	=B9*C9	=B9*D9
Horiz. Tail	102	35.5	8	=B10*C10	=B10*D10
Vert. Tail	69	36.2	10	=B11*C11	=B11*D11
Fuselage	728	15.6	7.75	=B12*C12	=B12*D12
Main Lndg Gear	259	22	1.3	=B13*C13	=B13*D13
Nose Lndg Gear	77	9	1.3	=B14*C14	=B14*D14
Engine Mounts	30	16.9	10	=B15*C15	=B15*D15
Firewall				=B16*C16	=B16*D16
Engine Section				=B17*C17	=B17*D17
Air Induction				=B18*C18	=B18*D18
				=B19*C19	=B19*D19
				=B20*C20	=B20*D20
PROPULSION GROUP	=SUM(B22:B30)	=E21/B21	=F21/B21	=SUM(E22:E30)	=SUM(F22:F30)
Engine(s)	968	16.9	8	=B22*C22	=B22*D22
Tailpipe				=B23*C23	=B23*D23
Engine Cooling	50	16.9	10	=B24*C24	=B24*D24
Oil Cooling	40	16.9	10	=B25*C25	=B25*D25
Engine Controls	20	16.9	10	=B26*C26	=B26*D26
Starter				=B27*C27	=B27*D27
Fuel System	129	16.9	10	=B28*C28	=B28*D28
				=B29*C29	=B29*D29
				=B30*C30	=B30*D30
EQUIPMENT GROUP	=SUM(B32:B45)	=E31/B31	=F31/B31	=SUM(E32:E45)	=SUM(F32:F45)
Flight Controls	111	4	6	=B32*C32	=B32*D32
Instruments				=B33*C33	=B33*D33
Hydraulics	76	22	6	=B34*C34	=B34*D34
Electrical	218	4	6	=B35*C35	=B35*D35
Avionics	403	5	6	=B36*C36	=B36*D36
Furnishings & Misc	0		6	=B37*C37	=B37*D37
Air Conditioning	0		6	=B38*C38	=B38*D38
Handling Gear	5.3	18	6	=B39*C39	=B39*D39
APU installed	0	0	0	=B40*C40	=B40*D40
Misc Empty Weight				=B41*C41	=B41*D41
				=B42*C42	=B42*D42
				=B43*C43	=B43*D43
				=B44*C44	=B44*D44
				=B45*C45	=B45*D45
(% We Allowance)	10	%	%		
We-Allowance	=(B46/100)*(B8+B21+SUM(B32:B4	=(E31+E21+E8)/(B31+B21+B8	=(F31+F21+F8)/(B31+B21	=B47*C47	=B47*D47
EMPTY WEIGHT	**=B31+B21+B8**	**=E48/B48**	**=F48/B48**	**=E31+E21+E8**	**=F31+F21+F8**
USEFUL LOAD GROUP	=B58-B31-B21-B8	=E49/B49	=F49/B49	=SUM(E50:E57)	=SUM(F50:F57)
Crew				=B50*C50	=B50*D50
Passengers					=B51*D51
Payload	2100	15.2	8.6	=B52*C52	=B52*D52
Fuel (weight available)	=B49-B50-B51-B52-B54-B55-B56-E	17.4	10	=B53*C53	=B53*D53
Oil	50	20	10	=B54*C54	=B54*D54
				=B55*C55	=B55*D55
				=B56*C56	=B56*D56
				=B57*C57	=B57*D57
TAKEOFF GROSS WEIGHT	**7545**	**=E58/B58**	**=F58/B58**	**=E49+E31+E21+E8**	**=F49+F31+F21+F8**
	With Payload CG	=(E58-E53)/(B58-B53)	=(F58-F53)/(B58-B53)		
	With Fuel CG	=(E58-E52)/(B58-B52)	=(F58-F51)/(B58-B51)		
	Empty CG	=(E58-E52-E53)/(B58-B52-B5	=(F58-F51-F53)/(B58-B51		

C.3 Surveillance

	Weight lbs or kg	X-Location ft or m	Z-Location ft or m	Moment ft-lbs or kg-m	Moment ft-lbs or kg-m
STRUCTURES GROUP	=SUM(B9:B20)	=E8/B8	=F8/B8	=SUM(E9:E20)	=SUM(F9:F20)
Wing	883	17.2	10	=B9*C9	=B9*D9
Horiz. Tail	104	35.5	8	=B10*C10	=B10*D10
Vert. Tail	85	36.6	10	=B11*C11	=B11*D11
Fuselage	722	15.6	7.75	=B12*C12	=B12*D12
Main Lndg Gear	259	22	1.3	=B13*C13	=B13*D13
Nose Lndg Gear	77	9	1.3	=B14*C14	=B14*D14
Engine Mounts	30	16.9	10	=B15*C15	=B15*D15
Firewall		33.3	10	=B16*C16	=B16*D16
Engine Section				=B17*C17	=B17*D17
Air Induction				=B18*C18	=B18*D18
				=B19*C19	=B19*D19
				=B20*C20	=B20*D20
PROPULSION GROUP	=SUM(B22:B30)	=E21/B21	=F21/B21	=SUM(E22:E30)	=SUM(F22:F30)
Engine(s)	968	16.9	8	=B22*C22	=B22*D22
Tailpipe	0	16.9		=B23*C23	=B23*D23
Engine Cooling	50	16.9	10	=B24*C24	=B24*D24
Oil Cooling	40	16.9	10	=B25*C25	=B25*D25
Engine Controls	20	16.9	10	=B26*C26	=B26*D26
Starter		16.9		=B27*C27	=B27*D27
Fuel System	191	16.9	10	=B28*C28	=B28*D28
				=B29*C29	=B29*D29
				=B30*C30	=B30*D30
EQUIPMENT GROUP	=SUM(B32:B45)	=E31/B31	=F31/B31	=SUM(E32:E45)	=SUM(F32:F45)
Flight Controls	112	4	6	=B32*C32	=B32*D32
Instruments				=B33*C33	=B33*D33
Hydraulics	73	22	6	=B34*C34	=B34*D34
Electrical	225	4	6	=B35*C35	=B35*D35
Avionics	403	5	6	=B36*C36	=B36*D36
Furnishings & Misc			6	=B37*C37	=B37*D37
Air Conditioning			6	=B38*C38	=B38*D38
Handling Gear	5	18	6	=B39*C39	=B39*D39
APU installed	0	0	0	=B40*C40	=B40*D40
Misc Empty Weight				=B41*C41	=B41*D41
				=B42*C42	=B42*D42
				=B43*C43	=B43*D43
				=B44*C44	=B44*D44
				=B45*C45	=B45*D45
(% We Allowance)	10	%	%		
We-Allowance	=(B46/100)*(B8+B21+SUM(B32:B4	=(E31+E21+E8)/(B31+B21+B8	=(F31+F21+F8)/(B31+B2	=B47*C47	=B47*D47
EMPTY WEIGHT	**=B31+B21+B8**	**=E48/B48**	**=F48/B48**	**=E31+E21+E8**	**=F31+F21+F8**
USEFUL LOAD GROUP	=B58-B31-B21-B8	=E49/B49	=F49/B49	=SUM(E50:E57)	=SUM(F50:F57)
Crew				=B50*C50	=B50*D50
Passengers					=B51*D51
Payload	1000	19	5.5	=B52*C52	=B52*D52
Fuel (weight available)	=B49-B50-B51-B52-B54-B55-B56-E	16	10	=B53*C53	=B53*D53
Oil	50	20	10	=B54*C54	=B54*D54
				=B55*C55	=B55*D55
				=B56*C56	=B56*D56
				=B57*C57	=B57*D57
TAKEOFF GROSS WEIGHT	**7722**	**=E58/B58**	**=F58/B58**	**=E49+E31+E21+E8**	**=F49+F31+F21+F8**
	With Payload CG	=(E58-E53)/(B58-B53)	=(F58-F53)/(B58-B53)		
	With Fuel CG	=(E58-E52)/(B58-B52)	=(F58-F51)/(B58-B51)		
	Empty CG	=(E58-E52-E53)/(B58-B52-B5	=(F58-F51-F53)/(B58-B5		

C.4 Decoy

	Weight lbs or kg	X-Location ft or m	Z-Location ft or m	Moment ft-lbs or kg-m	Moment ft-lbs or kg-m
STRUCTURES GROUP	=SUM(B9:B20)	=E8/B8	=F8/B8	=SUM(E9:E20)	=SUM(F9:F20)
Wing	603	17.6	10	=B9*C9	=B9*D9
Horiz. Tail	102	35.6	8	=B10*C10	=B10*D10
Vert. Tail	66	36.2	10	=B11*C11	=B11*D11
Fuselage	714	15.6	7.75	=B12*C12	=B12*D12
Main Lndg Gear	247	22	1.3	=B13*C13	=B13*D13
Nose Lndg Gear	75	9	1.3	=B14*C14	=B14*D14
Engine Mounts	20	16.9	10	=B15*C15	=B15*D15
Firewall		33.3	10	=B16*C16	=B16*D16
Engine Section				=B17*C17	=B17*D17
Air Induction				=B18*C18	=B18*D18
				=B19*C19	=B19*D19
				=B20*C20	=B20*D20
PROPULSION GROUP	=SUM(B22:B30)	=E21/B21	=F21/B21	=SUM(E22:E30)	=SUM(F22:F30)
Engine(s)	968	16.9	8	=B22*C22	=B22*D22
Tailpipe	0	16.9		=B23*C23	=B23*D23
Engine Cooling	50	16.9	10	=B24*C24	=B24*D24
Oil Cooling	40	16.9	10	=B25*C25	=B25*D25
Engine Controls	20	16.9	10	=B26*C26	=B26*D26
Starter		16.9		=B27*C27	=B27*D27
Fuel System	214	16.9	10	=B28*C28	=B28*D28
				=B29*C29	=B29*D29
				=B30*C30	=B30*D30
EQUIPMENT GROUP	=SUM(B32:B45)	=E31/B31	=F31/B31	=SUM(E32:E45)	=SUM(F32:F45)
Flight Controls	99	4	6	=B32*C32	=B32*D32
Instruments				=B33*C33	=B33*D33
Hydraulics	69	22	6	=B34*C34	=B34*D34
Electrical	341	4	6	=B35*C35	=B35*D35
Avionics	403	5	6	=B36*C36	=B36*D36
Furnishings & Misc			6	=B37*C37	=B37*D37
Air Conditioning			6	=B38*C38	=B38*D38
Handling Gear	5.3	18	6	=B39*C39	=B39*D39
APU installed	0	0	0	=B40*C40	=B40*D40
Misc Empty Weight				=B41*C41	=B41*D41
				=B42*C42	=B42*D42
				=B43*C43	=B43*D43
				=B44*C44	=B44*D44
				=B45*C45	=B45*D45
(% We Allowance)	10	%	%		
We-Allowance	=(B46/100)*(B8+B21+SUM(B32:B4	=(E31+E21+E8)/(B31+B21+B8	=(F31+F21+F8)/(B31+B21	=B47*C47	=B47*D47
EMPTY WEIGHT	**=B31+B21+B8**	**=E48/B48**	**=F48/B48**	**=E31+E21+E8**	**=F31+F21+F8**
USEFUL LOAD GROUP	=B58-B31-B21-B8	=E49/B49	=F49/B49	=SUM(E50:E57)	=SUM(F50:F57)
Crew				=B50*C50	=B50*D50
Passengers					=B51*D51
Payload	500	20	5.5	=B52*C52	=B52*D52
Fuel (weight available)	=B49-B50-B51-B52-B54-B55-B56-E	16	10	=B53*C53	=B53*D53
Oil	50	20	10	=B54*C54	=B54*D54
				=B55*C55	=B55*D55
				=B56*C56	=B56*D56
				=B57*C57	=B57*D57
TAKEOFF GROSS WEIGHT	**7434**	**=E58/B58**	**=F58/B58**	**=E49+E31+E21+E8**	**=F49+F31+F21+F8**
	With Payload CG	=(E58-E53)/(B58-B53)	=(F58-F53)/(B58-B53)		
	With Fuel CG	=(E58-E52)/(B58-B52)	=(F58-F51)/(B58-B51)		
	Empty CG	=(E58-E53-E52)/(B58-B53-B5	=(F58-F51-F53)/(B58-B51		

Appendix D - Stability and Control Analysis

D.1 Cargo

XNP	17.6
XCG_f	15.2
XCG_a	16.8
MAC	6.84
SM_{f1}	=(B2-B3)/B5*100
SM_{a1}	=(B2-B4)/B5*100
X_0 (reference to nose)	0
X_1 (nose to wing apex)	14
X_{bar}	0.69
X_{NP_MAC} (MAC to NP)	2.91
$X_0 + X_1 + X_{bar} + X_{NP\_MAC} = XNP$	=B8+B9+B10+B11
$X_{CG\_MAC\_f}$ (MAC to CG_f)	=B3-B9-B10
$X_{CG\_MAC\_a}$ (MAC to CG_a)	=B4-B9-B10
$NP_{MAC} = X_{NP\_MAC}/MAC*100\%$	=B11/B5*100
$CG_{MAC\_f} = X_{CG\_MAC\_f}/MAC*100\%$	=B13/B5*100
$CG_{MAC\_a} = X_{CG\_MAC\_a}/MAC*100\%$	=B14/B5*100
$SM_{f2} = NP_{MAC} - CG_{MAC\_f}$	=B15-B16
$SM_{a2} = NP_{MAC} - CG_{MAC\_a}$	=B15-B17

X_1 (main gear to aft cg)	1.7	
Z_1 (aft cg to ground)	7.1	
Z_2 (rear to ground)	6.5	
X_2 (rear to main gear)	21.7	
Z_3 (lateral to ground)	2.07	
Y_3 (lateral to main gear)	22	
Y_4 (main gear)	4.3	
X_4 (main gear to nose gear)	16.3	
Z_5 (forward cg to ground)	5.9	
D_5 (perpendicular to forward cg)	4.157759	
		Degrees
θ_1 (longitudinal tip over angle)	0.235012	13.46521
θ_2 (longitudinal ground clearance angle)	0.291034	16.67502
θ_3 (lateral ground clearance angle)	0.093815	5.375187
θ_4 (semi-apex angle)	0.257928	14.77816
Ψ (lateral tip over angle)	0.95692	54.82746

D.2 Combat

XNP	17.3
XCG_f	15.3
XCG_a	16.3
MAC	6.74
SM_{f1}	=(B2-B3)/B5*100
SM_{a1}	=(B2-B4)/B5*100
X_0 (reference to nose)	0
X_1 (nose to wing apex)	14
X_{bar}	0.68
X_{NP_MAC} (MAC to NP)	2.62
$X_0 + X_1 + X_{bar} + X_{NP\_MAC} = XNP$	=B8+B9+B10+B11
$X_{CG\_MAC\_f}$ (MAC to CG_f)	=B3-B9-B10
$X_{CG\_MAC\_a}$ (MAC to CG_a)	=B4-B9-B10
$NP_{MAC} = X_{NP\_MAC}/MAC*100\%$	=B11/B5*100
$CG_{MAC\_f} = X_{CG\_MAC\_f}/MAC*100\%$	=B13/B5*100
$CG_{MAC\_a} = X_{CG\_MAC\_a}/MAC*100\%$	=B14/B5*100
$SM_{f2} = NP_{MAC} - CG_{MAC\_f}$	=B15-B16
$SM_{a2} = NP_{MAC} - CG_{MAC\_a}$	=B15-B17

X_1 (main gear to aft cg)	2.2	
Z_1 (aft cg to ground)	8.3	
Z_2 (rear to ground)	6.5	
X_2 (rear to main gear)	21.7	
Z_3 (lateral to ground)	2.07	
Y_3 (lateral to main gear)	23.2	
Y_4 (main gear)	5.1	
X_4 (main gear to nose gear)	16.3	
Z_5 (forward cg to ground)	6.2	
D_5 (perpendicular to forward cg)	4.867316	
		Degrees
θ_1 (longitudinal tip over angle)	0.259102	14.84545
θ_2 (longitudinal ground clearance angle)	0.291034	16.67502
θ_3 (lateral ground clearance angle)	0.088988	5.098665
θ_4 (semi-apex angle)	0.303234	17.37404
Ψ (lateral tip over angle)	0.905237	51.86628

D.3 Surveillance

XNP	17.27
XCG_f	15.4
XCG_a	16.5
MAC	6.35
SM_{f1}	=(B2-B3)/B5*100
SM_{a1}	=(B2-B4)/B5*100
X_0 (reference to nose)	0
X_1 (nose to wing apex)	14
X_{bar}	0.64
X_{NP_MAC} (MAC to NP)	2.63
$X_0 + X_1 + X_{bar} + X_{NP\_MAC}$ = XNP	=B8+B9+B10+B11
$X_{CG\_MAC\_f}$ (MAC to CG_f)	=B3-B9-B10
$X_{CG\_MAC\_a}$ (MAC to CG_a)	=B4-B9-B10
$NP_{MAC} = X_{NP\_MAC}$/MAC*100%	=B11/B5*100
$CG_{MAC\_f} = X_{CG\_MAC\_f}$/MAC*100%	=B13/B5*100
$CG_{MAC\_a} = X_{CG\_MAC\_a}$/MAC*100%	=B14/B5*100
$SM_{f2} = NP_{MAC} - CG_{MAC\_f}$	=B15-B16
$SM_{a2} = NP_{MAC} - CG_{MAC\_a}$	=B15-B17

X_1 (main gear to aft cg)	1.9	
Z_1 (aft cg to ground)	7.3	
Z_2 (rear to ground)	6.5	
X_2 (rear to main gear)	21.7	
Z_3 (lateral to ground)	2.07	
Y_3 (lateral to main gear)	28.9	
Y_4 (main gear)	5	
X_4 (main gear to nose gear)	16.3	
Z_5 (forward cg to ground)	5.6	
D_5 (perpendicular to forward cg)	4.780161	
		Degrees
θ_1 (longitudinal tip over angle)	0.254625	14.58892
θ_2 (longitudinal ground clearance angle)	0.291034	16.67502
θ_3 (lateral ground clearance angle)	0.071504	4.096888
θ_4 (semi-apex angle)	0.297636	17.05331
Ψ (lateral tip over angle)	0.864216	49.51592

D.4 Decoy

XNP	17.48
XCG_f	15.2
XCG_a	16.4
MAC	7.05
SM_{f1}	=(B2-B3)/B5*100
SM_{a1}	=(B2-B4)/B5*100
X_0 (reference to nose)	0
X_1 (nose to wing apex)	14
X_{bar}	0.71
X_{NP_MAC} (MAC to NP)	2.77
$X_0 + X_1 + X_{bar} + X_{NP\_MAC} = XNP$	=B8+B9+B10+B11
$X_{CG\_MAC\_f}$ (MAC to CG_f)	=B3-B9-B10
$X_{CG\_MAC\_a}$ (MAC to CG_a)	=B4-B9-B10
$NP_{MAC} = X_{NP\_MAC}/MAC*100\%$	=B11/B5*100
$CG_{MAC\_f} = X_{CG\_MAC\_f}/MAC*100\%$	=B13/B5*100
$CG_{MAC\_a} = X_{CG\_MAC\_a}/MAC*100\%$	=B14/B5*100
$SM_{f2} = NP_{MAC} - CG_{MAC\_f}$	=B15-B16
$SM_{a2} = NP_{MAC} - CG_{MAC\_a}$	=B15-B17

X_1 (main gear to aft cg)	2.4	
Z_1 (aft cg to ground)	8.3	
Z_2 (rear to ground)	6.5	
X_2 (rear to main gear)	21.7	
Z_3 (lateral to ground)	2.07	
Y_3 (lateral to main gear)	24.1	
Y_4 (main gear)	5	
X_4 (main gear to nose gear)	16.3	
Z_5 (forward cg to ground)	5.7	
D_5 (perpendicular to forward cg)	4.780161424	
		Degrees
θ_1 (longitudinal tip over angle)	0.281479299	16.12758
θ_2 (longitudinal ground clearance angle)	0.291033962	16.67502
θ_3 (lateral ground clearance angle)	0.085681824	4.909207
θ_4 (semi-apex angle)	0.297636491	17.05331
Ψ (lateral tip over angle)	0.872943327	50.01597

D.5 Landing gear tire sizing equation

Tire Sizing	
Weight (lb)	8165
Weight on main gear (lb)	=B2*0.9
Weight on each wheel (lb)	=B3/4
A Diameter	1.51
B Diameter	0.349
A Width	0.715
B Width	0.312
Diameter (in)	=B6*B4^B7
Width (in)	=B9*B4^B10
Radius (in)	9.8
Contact Area (in^2)	=2.3*SQRT(B13*B12)
Pressure (psi)	=B4/B16

D.6 Landing gear tire sizing for cargo

Weight (lb)	8165
Weight on main gear (lb)	7348.5
Weight on each wheel (lb)	1837.125
A Diameter	1.51
B Diameter	0.349
A Width	0.715
B Width	0.312
Diameter (in)	20.8047
Width (in)	7.459631
Radius (in)	9.8
Contact Area (in^2)	17.25895
Pressure (psi)	106.4448

D.7 Landing gear tire sizing for combat

Weight (lb)	7545
Weight on main gear (lb)	6790.5
Weight on each wheel (lb)	1697.625
A Diameter	1.51
B Diameter	0.349
A Width	0.715
B Width	0.312
Diameter (in)	20.23912
Width (in)	7.278077
Radius (in)	9.55
Contact Area (in^2)	15.89913
Pressure (psi)	106.7747

D.8 Landing gear tire sizing for surveillance

Weight (lb)	7722
Weight on main gear (lb)	6949.8
Weight on each wheel (lb)	1737.45
A Diameter	1.51
B Diameter	0.349
A Width	0.715
B Width	0.312
Diameter (in)	20.40358
Width (in)	7.330923
Radius (in)	9.62
Contact Area (in^2)	16.36538
Pressure (psi)	106.1662

D.9 Landing gear tire sizing for decoy

Weight (lb)	7434
Weight on main gear (lb)	6690.6
Weight on each wheel (lb)	1672.65
A Diameter	1.51
B Diameter	0.349
A Width	0.715
B Width	0.312
Diameter (in)	20.13471
Width (in)	7.2445
Radius (in)	9.5
Contact Area (in^2)	15.76008
Pressure (psi)	106.132

Appendix E - Drag Polar Estimation

E.1 Equations

Kc	=1/(PI()*B32*B37)
Kl	=1/(PI()*B32*B38)
Kt	=1/(PI()*B32*B39)
CD0 clean	=B43*B44
CD0 clean t	=B49+B40+B41
CD0 clean l	=B49+B40+B42
CD clean	=B49+B46+B34^2
CD t	=B50+B47+B35^2
CD l	=B51+B48+B36^2
L/D	=B34/B53
	=B35/B54
	=B36/B55
L/D Max	=B57/B46
	=B58/B47
	=B59/B48

E.2 Cargo

W0	8165
A	7.5
Sref	292
Cl max clean	1.1
Cl max takeoff	1.4
Cl max landing	1.7
e	0.8
e	0.75
e	0.7
CD0 landing gear	0.02
CD0 takeoff flaps	0.015
CD0 landing flaps	0.065
Cfe	0.0045
Swet/Sref	4.4
K_clean	0.053051648
K_landing	0.056588424
K_takeoff	0.060630455
CD0 clean	0.0198
CD0 takeoff	0.0548
CD0 landing	0.1048
CD clean	1.282851648
CD takeoff	2.071388424
CD landing	3.055430455
L/D clean	0.857464697
L/D takeoff	0.675875168
L/D landing	0.556386416
L/D Max clean	16.16282877
L/D Max takeoff	11.94370011
L/D Max landing	9.176682255

E.3 Combat

W0	7545
A	8
Sref	302
Cl max clean	1.1
Cl max takeoff	1.4
Cl max landing	1.7
e	0.8
e	0.75
e	0.7
CD0 landing gear	0.02
CD0 takeoff flaps	0.015
CD0 landing flaps	0.065
Cfe	0.0045
Swet/Sref	4.35
K_clean	0.04973592
K_landing	0.053051648
K_takeoff	0.056841051
CD0 clean	0.019575
CD0 takeoff	0.054575
CD0 landing	0.104575
CD clean	1.27931092
CD takeoff	2.067626648
CD landing	3.051416051
L/D clean	0.859837889
L/D takeoff	0.677104835
L/D landing	0.557118391
L/D Max clean	17.28806652
L/D Max takeoff	12.76312545
L/D Max landing	9.801338645

E.4 Surveillance

W0	7722
A	10
Sref	336
Cl max clean	1.1
Cl max takeoff	1.4
Cl max landing	1.7
e	0.8
e	0.75
e	0.7
CD0 landing gear	0.02
CD0 takeoff flaps	0.015
CD0 landing flaps	0.065
Cfe	0.0045
Swet/Sref	4.37
K_clean	0.039788736
K_landing	0.042441318
K_takeoff	0.045472841
CD0 clean	0.019665
CD0 takeoff	0.054665
CD0 landing	0.104665
CD clean	1.269453736
CD takeoff	2.057106318
CD landing	3.040137841
L/D clean	0.866514446
L/D takeoff	0.680567644
L/D landing	0.559185172
L/D Max clean	21.77788333
L/D Max takeoff	16.03549733
L/D Max landing	12.29712419

E.5 Decoy

W0	7434
A	7.5
Sref	310
Cl max clean	1.1
Cl max takeoff	1.4
Cl max landing	1.7
e	0.8
e	0.75
e	0.7
CD0 landing gear	0.02
CD0 takeoff flaps	0.015
CD0 landing flaps	0.065
Cfe	0.0045
Swet/Sref	4.35
K_clean	0.053051648
K_landing	0.056588424
K_takeoff	0.060630455
CD0 clean	0.019575
CD0 takeoff	0.054575
CD0 landing	0.104575
CD clean	1.282626648
CD takeoff	2.071163424
CD landing	3.055205455
L/D clean	0.857615115
L/D takeoff	0.675948592
L/D landing	0.556427391
L/D Max clean	16.16566407
L/D Max takeoff	11.94499761
L/D Max landing	9.17735807

Appendix F - V-n Diagram

F.1 Equations

C_D	=B6+(B5^2)/(PI()*B36*B44)
$C_{N\_max\_pos}$	=((B5^2)+(B7^2))^0.5
V_S (ft/s)	=((2*B2/B3)/(B4*B8))^0.5
V_S (knots)	=B10/1.688
K_c	32.56
$V_c >$	=B13*((B2/B3)^0.5)
V_c	200
V_D	=B15*1.25
n_{lim_pos}	=2.1+24000/(B2+10000)
n_{lim_neg}	=B19*0.4
V_A	=B11*B19^0.5
$C_{L\_max\_neg}$	-1
$C_{D\_max\_neg}$	=B6+(B23^2)/(PI()*B36*B44)
$C_{N\_max\_neg}$	=((B23^2)+(B24^2))^0.5
V_{S_neg}	=((2*B2/B3)/(B4*B25))^0.5
V_{S_neg} (knots)	=B26/1.688
U_{de_vc}	50
U_{de_vd}	25
U_{de_vb}	66
g	32.17
c (ft)	6.84
A	7.5
M	0.3
β^2	=1-B37^2
$S_{exposed}$	220
d	5
b	46.8
F	=1.07*(1+B41/B42)^2
η	0.8
Λ	4.11
Λ (deg)	=B45*PI()/180
C_{L_α}	=2*PI()*B36*(B39/B3)*B43/(2+(SQRT(4+((B36^2)*(B38)/(B44^2))*(1+(TAN(B46)^2)/B38))))
μ_g	=2*(B2/B3)/(B4*B34*B33*B48)
K_g	=0.88*B51/(5.3+B51)
$n_{lim\_gust\_c}$	=1+(B52*B29*B15*B48)/(498*B2/B3)
$n_{lim\_gust\_d}$	=1+(B52*B30*B17*B48)/(498*B2/B3)

F.2 Cargo

GW (lb)	8165
S (ft^2)	292
ρ ($slug/ft^3$)	1.50E-03
C_{L_max}	1.5
C_{D0}	0.015145
C_D	0.134511
$C_{N\_max\_pos}$	1.506019
V_S (ft/s)	157.5508
V_S (knots)	93.33579
K_c	32.56
V_c >	172.1754
V_c	200
V_D	250
n_{lim_pos}	3.421222
n_{lim_neg}	1.368489
V_A	172.639
$C_{L\_max\_neg}$	-1
$C_{D\_max\_neg}$	0.068196
$C_{N\_max\_neg}$	1.002323
V_{S_neg}	193.1222
V_{S_neg} (knots)	114.4089
U_{de_vc}	50
U_{de_vd}	25
U_{de_vb}	66
g	32.17
c (ft)	6.84
A	7.5
M	0.3
β^2	0.91
$S_{exposed}$	220
d	5
b	46.8
F	1.310846
η	0.8
Λ	4.11
Λ (deg)	0.071733
C_{L_α}	4.159571
μ_g	40.84285
K_g	0.778923
$n_{lim\_gust\_c}$	3.326699
$n_{lim\_gust\_d}$	2.454187

F.3 Combat

GW (lb)	7545
S (ft^2)	302
ρ ($slug/ft^3$)	1.50E-03
C_{L_max}	1.5
C_{D0}	0.01636
C_D	0.135727
$C_{N\_max\_pos}$	1.506128
V_S (ft/s)	148.917
V_S (knots)	88.221
K_c	32.725
V_c >	163.5708
V_c	200
V_D	250
n_{lim_pos}	3.467911
n_{lim_neg}	1.387164
V_A	164.288
$C_{L\_max\_neg}$	-1
$C_{D\_max\_neg}$	0.066096
$C_{N\_max\_neg}$	1.002182
V_{S_neg}	182.5585
V_{S_neg} (knots)	108.1508
U_{de_vc}	50
U_{de_vd}	25
U_{de_vb}	66
g	32.17
c (ft)	6.74
A	8
M	0.3
$β^2$	0.91
$S_{exposed}$	230
d	5
b	49.1
F	1.299018
η	0.8
Λ	3.86
Λ (deg)	0.06737
$C_{L\_α}$	4.224985
$μ_g$	36.45982
K_g	0.768314
$n_{lim\_gust\_c}$	3.609048
$n_{lim\_gust\_d}$	2.630655

F.4 Surveillance

GW (lb)	7722
S (ft^2)	336
ρ ($slug/ft^3$)	1.50E-03
C_{L_max}	1.5
C_{D0}	0.014756
C_D	0.134122
$C_{N\_max\_pos}$	1.505984
V_S (ft/s)	142.8349
V_S (knots)	84.61781
K_c	32.835
V_c >	157.41
V_c	200
V_D	250
n_{lim_pos}	3.454249
n_{lim_neg}	1.3817
V_A	157.2674
$C_{L\_max\_neg}$	-1
$C_{D\_max\_neg}$	0.054545
$C_{N\_max\_neg}$	1.001486
V_{S_neg}	175.1547
V_{S_neg} (knots)	103.7647
U_{de_vc}	50
U_{de_vd}	25
U_{de_vb}	66
g	32.17
c (ft)	6.35
A	10
M	0.3
$β^2$	0.91
$S_{exposed}$	265
d	5
b	57.9
F	1.262781
η	0.8
Λ	3.09
Λ (deg)	0.053931
$C_{L\_α}$	4.435057
$μ_g$	33.9129
K_g	0.76106
$n_{lim\_gust\_c}$	3.949157
$n_{lim\_gust\_d}$	2.843223

F.5 Decoy

GW (lb)	7434
S (ft^2)	310
ρ ($slug/ft^3$)	1.50E-03
C_{L_max}	1.5
C_{D0}	0.014955
C_D	0.134321
$C_{N\_max\_pos}$	1.506002
V_S (ft/s)	145.9039
V_S (knots)	86.43595
K_c	32.78
V_c >	160.5238
V_c	200
V_D	250
n_{lim_pos}	3.47662
n_{lim_neg}	1.390648
V_A	161.1659
$C_{L\_max\_neg}$	-1
$C_{D\_max\_neg}$	0.068007
$C_{N\_max\_neg}$	1.00231
V_{S_neg}	178.8458
V_{S_neg} (knots)	105.9513
U_{de_vc}	50
U_{de_vd}	25
U_{de_vb}	66
g	32.17
c (ft)	7.05
A	7.5
M	0.3
$β^2$	0.91
$S_{exposed}$	230
d	5
b	48.2
F	1.303506
η	0.8
Λ	4.11
Λ (deg)	0.071733
$C_{L\_α}$	4.073205
$μ_g$	34.70426
K_g	0.763412
$n_{lim\_gust\_c}$	3.603786
$n_{lim\_gust\_d}$	2.627366

Appendix G - Weight and Balance Analysis Class II

G.1 Equations

Weights		**Fudge Factors**	**Final Weight**
Wing	=0.036*(B40^0.758)*(B47^0.0035)*((B19/(COS(B52)^2))^0.6)*(B36^0.006)*(B57^0.04)*((100*B41/(COS(B52)))^-0.3)*((B35*B45)^0.49)	0.85	=G17*I17
Horizontal Tail	=0.016*((B35*B45)^0.414)*(B36^0.168)*(B38^0.896)*((100*B41/COS(B52))^-0.12)*((B20/(COS(B54)^2))^0.043)*(B58^-0.02)	0.83	=G18*I18
Vertical Tail	=0.073*(1+0.2*C32)*((B35*B45)^0.376)*(B36^0.122)*(B39^0.873)*((100*B41/COS(B56))^-0.49)*((B21/(COS(B56)^2))^0.357)*(B59^0.039)	0.83	=G19*I19
Fuselage	=0.052*(B37^1.086)*((B35*B45)^0.177)*(B28^-0.051)*((B25/B23)^-0.072)*(B36^0.241)+B49	0.9	=G20*I20
Main landing gear	=0.095*((B32*B48)^0.768)*((B26/12)^0.409)	0.95	=G21*I21
Nose landing gear	=0.125*((B32*B48)^0.566)*((B27/12)^0.845)	0.95	=G22*I22
Installed engine	=2.575*(B46^0.922)*B31	0.9	=G23*I23
Fuel system	=2.49*(B44^0.726)*((1/(1+B42/B44))^0.363)*(B34^0.242)*(B31^0.157)	0.9	=G24*I24
Flight controls	=(0.053*(B25^1.536)*(B22^0.371))*(B35*B45*0.0001)^0.8	0.9	=G25*I25
Hydraulics	=B24*(B45^0.8)*(B29^0.5)	0.9	=G26*I26
Electrical	=12.57*(G24+G28)^0.51	0.9	=G27*I27
Avionics	=2.117*B50^0.933	0.9	=G28*I28
A/c and anti ice	=(0.265*B45^0.52)*(B33^0.68)*(G28^0.17)*(B29^0.08)	0.9	=G29*I29
Furnishings	=0.0582*B45-65	0.9	=G30*I30
	=SUM(G17:G30)		=SUM(J17:J30)

G.2 Cargo

Inputs	
Wing	291
Horizontal Tail	79.8
Vertical Tail	53.1
Fuselage	471
TOGW	8165
Engine Weight	968
Variable	
A (aspect ratio)	7.5
A_h (aspect ratio)	4
A_v (aspect ratio)	1.5
B_w (wing span)	45
D (fuselage structural depth)	4
K_h (hydraulic)	0.12
L (fuselage structural length)	35
L_m (extended length of main landing gear, in)	36
L_n (extended nose gear length, in)	36
L_t (tail length)	20
M (mach number)	0.3
N_c (number of crew)	0.5
N_{en} (number of engines)	2
N_l (ultimate landing load factor)	4.5
N_p (number of personnel onboard)	6
N_t (number of fuel tanks)	2
N_z (ultimate load factor)	3.75
q (dynamic pressure at cruise, lb/ft^2)	135
S_f (fuselage wetted area)	=B14
S_{ht} (horizontal tail area)	=B12
S_{vt} (vertical tail area)	=B13
S_w (trapezoidal wing area)	=B11
t/c (thickness to chord ratio)	0.12
V_i (integral tanks volume, gal)	273
V_{pr} (volume of pressurized section, ft^3)	605
V_t (total fuel volume, gal)	273
W_{dg} (flight design gross weight)	=B15-B47*0.5
W_{en} (engine weight, each)	=B16/2
W_{fw} (weight of fuel in wings)	1830
W_l (landing design gross weight)	=B15-1800-B47*0.15
W_{press} (weight penalty due to pressurization)	=11.9*(B43*8)^0.271
W_{uav} (uninstalled avionics weight)	300
Λ (wing sweep, °)	4.11
Λ (wing sweep)	=B51*PI()/180
$Λ_{ht}$ (wing sweep, °)	7.67
$Λ_{ht}$ (wing sweep)	=B53*PI()/180
$Λ_{vt}$ (wing sweep, °)	19.76
$Λ_{vt}$ (wing sweep)	=B55*PI()/180
λ (taper ratio)	0.3
$λ_{ht}$ (taper ratio)	0.3
$λ_{vt}$ (taper ratio)	0.3

G.3 Combat

Inputs	
Wing	301
Horizontal Tail	81.4
Vertical Tail	57.6
Fuselage	471
TOGW	7545
Engine Weight	968
Variable	
A (aspect ratio)	8
A_h (aspect ratio)	4.5
A_v (aspect ratio)	1.5
B_w (wing span)	48
D (fuselage structural depth)	5
H_t/H_v	0
K_h (hydraulic)	0.12
L (fuselage structural length)	35
L_m (extended length of main landing gear, in)	36
L_n (extended nose gear length, in)	36
L_t (tail length)	20
M (mach number)	0.3
N_c (number of crew)	0.5
N_{en} (number of engines)	2
N_l (ultimate landing load factor)	3
N_p (number of personnel onboard)	0
N_t (number of fuel tanks)	2
N_z (ultimate load factor)	3.75
q (dynamic pressure at cruise, lb/ft^2)	135
S_f (fuselage wetted area)	471
S_{ht} (horizontal tail area)	81.4
S_{vt} (vertical tail area)	57.6
S_w (trapezoidal wing area)	301
t/c (thickness to chord ratio)	0.12
V_i (integral tanks volume, gal)	222
V_{pr} (volume of pressurized section, ft^3)	605
V_t (total fuel volume, gal)	222
W_{dg} (flight design gross weight)	6798
W_{en} (engine weight, each)	484
W_{fw} (weight of fuel in wings)	1494
W_l (landing design gross weight)	5520.9
W_{press} (weight penalty due to pressurization)	118.6151
W_{uav} (uninstalled avionics weight)	300
Λ (wing sweep, °)	3.86
Λ (wing sweep)	0.06737
Λ_{ht} (wing sweep, °)	6.82
Λ_{ht} (wing sweep)	0.119031
Λ_{vt} (wing sweep, °)	19.74
Λ_{vt} (wing sweep)	0.344528
λ (taper ratio)	0.3
λ_{ht} (taper ratio)	0.3
λ_{vt} (taper ratio)	0.3

G.4 Surveillance

Inputs	
Wing	335
Horizontal Tail	85.3
Vertical Tail	75.6
Fuselage	471
TOGW	7722
Engine Weight	968
Variable	
A (aspect ratio)	12
A_h (aspect ratio)	4.5
A_v (aspect ratio)	1.5
B_w (wing span)	56
D (fuselage structural depth)	5
H_t/H_v	0
K_h (hydraulic)	0.12
L (fuselage structural length)	35
L_m (extended length of main landing gear, in)	36
L_n (extended nose gear length, in)	36
L_t (tail length)	20
M (mach number)	0.3
N_c (number of crew)	0.5
N_{en} (number of engines)	2
N_l (ultimate landing load factor)	3
N_p (number of personnel onboard)	0
N_t (number of fuel tanks)	2
N_z (ultimate load factor)	3.75
q (dynamic pressure at cruise, lb/ft^2)	135
S_f (fuselage wetted area)	471
S_{ht} (horizontal tail area)	85.3
S_{vt} (vertical tail area)	75.6
S_w (trapezoidal wing area)	335
t/c (thickness to chord ratio)	0.12
V_i (integral tanks volume, gal)	382
V_{pr} (volume of pressurized section, ft^3)	605
V_t (total fuel volume, gal)	382
W_{dg} (flight design gross weight)	6440.5
W_{en} (engine weight, each)	484
W_{fw} (weight of fuel in wings)	2563
W_l (landing design gross weight)	5537.55
W_{press} (weight penalty due to pressurization)	118.6151
W_{uav} (uninstalled avionics weight)	300
Λ (wing sweep, °)	3.09
Λ (wing sweep)	0.053931
Λ_{ht} (wing sweep, °)	6.82
Λ_{ht} (wing sweep)	0.119031
Λ_{vt} (wing sweep, °)	19.76
Λ_{vt} (wing sweep)	0.344877
λ (taper ratio)	0.3
λ_{ht} (taper ratio)	0.3
λ_{vt} (taper ratio)	0.3

G.5 Decoy

Inputs	
Wing	309
Horizontal Tail	87.2
Vertical Tail	58.1
Fuselage	471
TOGW	7434
Engine Weight	968
Variable	
A (aspect ratio)	7.5
A_h (aspect ratio)	4.5
A_v (aspect ratio)	1.5
B_w (wing span)	47
D (fuselage structural depth)	5
H_t/H_v	0
K_h (hydraulic)	0.12
L (fuselage structural length)	35
L_m (extended length of main landing gear, in)	36
L_n (extended nose gear length, in)	36
L_t (tail length)	20
M (mach number)	0.3
N_c (number of crew)	0.5
N_{en} (number of engines)	2
N_l (ultimate landing load factor)	3
N_p (number of personnel onboard)	0
N_t (number of fuel tanks)	2
N_z (ultimate load factor)	3.75
q (dynamic pressure at cruise, lb/ft^2)	135
S_f (fuselage wetted area)	471
S_{ht} (horizontal tail area)	87.2
S_{vt} (vertical tail area)	58.1
S_w (trapezoidal wing area)	309
t/c (thickness to chord ratio)	0.12
V_i (integral tanks volume, gal)	446
V_{pr} (volume of pressurized section, ft^3)	605
V_t (total fuel volume, gal)	446
W_{dg} (flight design gross weight)	5935
W_{en} (engine weight, each)	484
W_{fw} (weight of fuel in wings)	2998
W_l (landing design gross weight)	5184.3
W_{press} (weight penalty due to pressurization)	118.6151
W_{uav} (uninstalled avionics weight)	300
Λ (wing sweep, °)	4.11
Λ (wing sweep)	0.071733
Λ_{ht} (wing sweep, °)	6.82
Λ_{ht} (wing sweep)	0.119031
Λ_{vt} (wing sweep, °)	19.73
Λ_{vt} (wing sweep)	0.344353
λ (taper ratio)	0.3
λ_{ht} (taper ratio)	0.3
λ_{vt} (taper ratio)	0.3

Appendix H - Stability and Control Analysis

H.1 Equations

l_f	40
d_f	5
l_f/d_f	=B2/B3
$k_2 - k_1$	0.91
S	292
c	6.84
w_{f_i}	4.3
Δx_i	=40/13
i_w	0
α_{O_1} ()	-1.4
$\Delta\alpha_O/\varepsilon_t$	-0.43
ε_t	0
α_{O_1}/α@M ()	1
$\alpha_{O\_L\_w}$ ()	=(B11*B14)
i_{Cl_f}	0
A	7.5
$c_{m\_o\_r}$	-0.014
$c_{m\_o\_t}$	-0.014
Δc_m	0
$c_{m\_o\_w}$	=(B17*COS(H22)^2)/(B17+2*COS(H22))*(B18+B19)/2
$(C_{m\_0@M})/(C_{m\_0@M=0})$	1
i	=(B8^2)*(B10+B15+B16)*B9
Sum	=B23*13
$c_{m\_o\_f}$	=(B5/(36.5*B6*B7))*B24
$c_{m\_o\_wf}$	=(B21+B25)*B22
x_{ref}	17.48
x_{ref_bar}	=B27/B7
x_{ac_h}	34
$x_{ac\_h\_bar}$	=B29/6.99
$C_{L\_o\_h}$	0.18
$C_{m\_o\_h}$	=(B30-B28)*B31
C_{m_o}	=B26+B32
Λ_{LE}	4.11
Λ_{LE}	=B34*PI()/180
tan Λ_{LE}	=TAN(B35)
A*tan Λ_{LE}	=B36*B17

A	=B17
Λ (°)	=H22
i_w (°)	=B10
i_w (rad)	=E4*PI()/180
η_h	0.9
C_{L_a}	4.16
$C_{L\_a\_h}$	4.91
L_f (ft)	40
L_h (ft)	18.5
c (ft)	=B7
c_h (ft)	4.9
Λ_{LE} (°)	=B34
Λ_{LE} (rad)	=B35
tan Λ_{LE}	=B36
A*tan Λ_{LE}	=B37
X (ft)	14
X_{cg}	=16.8-E17
X_{cg_bar}	=E18/E11
X_{np}	=17.6-E17
X_{np_bar}	=E20/E11
X_{acw}	=14.69-E17
X_{acw_bar}	=E22/E11
X_{ach}	=34-33.5
X_{ach_bar}	=E24/E11
X_{cp}	3.25
X_{cp_bar}	=E26/E11
S_w	=B6
S_h	85.6
$c_{m\_o\_airfoil}$	-0.01
c_{m_w}	=E30*(E2*(COS(E3))^2/(E2+2*COS(E3)))
	=14.69/40
K_{fuse}	0.012
W_f (ft)	4.5
$c_{m\_fuselage}$	=(E33*(E34^2)*E9)/(E11*E28)
α_{0_L}	-1.2
	=E36*PI()/180
α (°)	10
α (rad)	=E38*PI()/180
i_h (°)	0
i_h (rad)	=E40*PI()/180
ε (°)	0
ε (rad)	=E42*PI()/180
C_L	=E7*(E39+E4-E37)
C_{L_h}	=E8*(E39+E41-E43-E37)

Z_t	4
Z_{t_bar}	=E46/E11
T	1447.5
C_{m_cg}	=E44*(E19-E23)+E31+E35-E6*(E29/E28)*E45*(E25-E19)-E48*E47/(H46*E28)
T*zt	=E48*E47/(H46*E28)
Cl*x	=E44*(E19-E23)
nh*sh	=E6*(E29/E28)
	=E52*(E25-E19)
c_f/c	0.1
$\Delta\alpha_{0l}$ / δ_e	=1.576*(E54^3)-3.458*(E54^2)+2.882*E54
δC_L / δd_f	=E55*E7
δf (deg)	30
δf (rad)	=E57*PI()/180
$C_{m\_w\delta f}$	=-E58*(E27-E19)
C_{m_cg}	=E49+E59*E58
d_{prop}	3.65
A_{prop} (ft^2)	=PI()*((E61/2)^2)
N_B	3
V (knot)	200
n	3
D (ft)	=E61
J	=E64/(E65*E66)
dC_{N_blade}/dα	0.04
ρ	0.001756
	=E48/(E69*(E64^2)*(E66^2))
f(T)	1.7
F_p	=H46*E63*E61*E68*E71
X_p	=14.5-E17
X_{p_bar}	=E73/E11
F_p/q	=E72/(H46*E28)*(E19-E74)
C_{m_cg}	=E75+E60
C_{L_total}	=E7*(E39+E5)+E6*E29/E28*E45

c	=B7
ref center	12
x_{cg_a}	=16.4-H3
$x_{cg\_a\_bar}$	=H4/H2
x_{cg_f}	=15.2-H3
$x_{cg\_f\_bar}$	=H6/H2
x_{ref}	=(14.69-H3)*-1
x_{ref_bar}	=H8/H2
$x_{cg\_a} - x_{ref}$	=H5-H9
$\Delta C_{M\_cg\_a\_ref}$	=-1*H10
$x_{cg\_f} - x_{ref}$	=H7-H9
$\Delta C_{M\_cg\_a\_ref}$	=-1*H12
A	7.5
M	0.3
β	=(1-(H15^2))^0.5
β M=0	1
C_{L_α}	0.107
$C_{L\_\alpha\ M=0.3}$	=H18/((1-H15^2)^0.5)
k	=H19/(2*PI()/H16)
k M=0	=H18/(2*PI())
Λ	0
$C_{L\_a\_w\ M=0.3}$	=2*PI()*H14/((2+((H14^2)*(H16^2)/(H20^2)*(1+(TAN(H22)^2)/(H16^2))+4)^0.5))
$C_{L\_a\_w\ M=0}$	=2*PI()*H14/((2+((H14^2)*(H17^2)/(H21^2)*(1+(TAN(H22)^2)/(H17^2))+4)^0.5))
K_A	=(1/H14)-(1/(1+H14^1.7))
λ	0.3
K_λ	=(10-3*H26)/7
h_h	=2.2-0.82
b	46.8
h_h/b	=H28/H29
l_h	=34-14.7
l_h/b	=H31/H29
k_h	=(1-H30)/((2*H32)^1/3)
d_ε/d_α	=4.44*((H25*H27*H33*(COS(H22)^0.5))^1.19)*(H23/H24)
ε_{0_h}	0

α	α_h
-10	=G39+H36-G39*H34
0	=G40+H36-G40*H34
10	=G41+H36-G41*H34
S	=B6
W_{TO}	8165
W_L	=H44-1830*0.85
q (lb/ft^2)	100
C_{L_cr}	=H44/(H46*H43)
C_{L_land}	=(H45/(H43*H46))
η_h	=E6
S_h	79.8
$C_{L\_i\_h}$	=H51*(H52/H43)*H23

Appendix I - Drag Polar Estimation Class II

I.1 Equations

Component Build Up					
	Wing	Fuselage	Horizontal Stabilizer	Vertical Stabilizer	Engine
ρ (slug/ft^3)	1.756e-3	1.756e-3	1.756e-3	1.756e-3	1.756e-3
Velocity (ft/s)	337	337	337	337	337
Length (ft)	6.84	40	4.9	6.52	5.3
Dynamic Viscosity (slug/ft*s)	3.534e-7	3.534e-7	3.534e-7	3.534e-7	3.534e-7
RE	=B32*B33*B34/B35	=C32*C33*C34/C35	=D32*D33*D34/D35	=E32*E33*E34/E35	=F32*F33*F34/F35
Cf Laminar skin friction coefficient	=(1.328/(SQRT(B36)))	=(1.328/(SQRT(C36)))	=(1.328/(SQRT(D36)))	=(1.328/(SQRT(E36)))	=(1.328/(SQRT(F36)))
M	0.3	0.3	0.3	0.3	0.3
Cf Turbulent skin friction coefficient	=0.455/(((LOG10(B36))^2.58)*(1+0.144*(B43^2))^0.65)	=0.455/(((LOG10(C36))^2.58)*(1+0.144*(C43^2))^0.65)	=0.455/(((LOG10(D36))^2.58)*(1+0.144*(D43^2))^0.65)	=0.455/(((LOG10(E36))^2.58)*(1+0.144*(E43^2))^0.65)	=0.455/(((LOG10(F36))^2.58)*(1+0.144*(F43^2))^0.65)
Frct lam	0.1	0	0.1	0.1	0
Frct turb	0.9	1	0.9	0.9	1
Cf Weighted average skin friction	=B46*B41+B47*B44	=C46*C41+C47*C44	=D46*D41+D47*D44	=E46*E41+E47*E44	=F46*F41+F47*F44
t/c	0.12		0.12	0.12	
x/c	=B34*0.3		=D34*0.3	=E34*0.3	
M cruise	0.3	0.3	0.3	0.3	0.3
Quarter chord sweep angle	0		0	0	
Length		40			5.3

Cross section area		5.5			2.83
f		=C54/(SQRT(4/PI()*C55))			=F54/(SQRT(4/PI()*F55))
Form Factor	=(1+0.6/B51*B50+100*(B50^4))*((1.34*B52^0.18)*COS(B53)^0.28)	=1+(60/C56^3)+(C56/400)	=(1+0.6/D51*D50+100*(D50^4))*((1.34*D52^0.18)*COS(D53)^0.28)	=(1+0.6/E51*E50+100*(E50^4))*((1.34*E52^0.18)*COS(E53)^0.28)	=1+0.35/F56
Form Factor Adjustments					
Interference drag	1.05	1	1.04	1.04	1.5
Swet	=D2	=D5	=D3	=D4	15
Sref	292	292	292	292	292
CD0,c	=B48*B57*B61*B63/B64	=C48*C57*C61*C63/C64	=D48*D57*D61*D63/D64	=E48*E57*E61*E63/E64	=F48*F57*F61*F63/F64*2
Leakage	10	5			

I.2 Cargo

Component Build Up					
	Wing	Fuselage	Horizontal Stabilizer	Vertical Stabilizer	Engine
ρ (slug/ft^3)	0.001756	0.001756	0.001756	0.001756	0.001756
Velocity (ft/s)	337	337	337	337	337
Length (ft)	6.84	40	4.9	6.52	5.3
Dynamic Viscosity (slug/ft*s)	3.53E-07	3.53E-07	3.53E-07	3.53E-07	3.53E-07
RE	11453651.61	66980418.79	8205101.302	10917808.26	8874905.49
Cf Laminar skin friction coefficient	0.000392397	0.000162265	0.000463614	0.000401911	0.000445776
M	0.3	0.3	0.3	0.3	0.3
Cf Turbulent skin friction coefficient	0.002914928	0.002233835	0.003075113	0.002937215	0.003036349
Frct lam	0.1	0	0.1	0.1	0
Frct turb	0.9	1	0.9	0.9	1
Cf Weighted average skin friction	0.002662675	0.002233835	0.002813963	0.002683685	0.003036349
t/c	0.12		0.12	0.12	
x/c	2.052		1.47	1.956	
M cruise	0.3	0.3	0.3	0.3	0.3
Quarter chord sweep angle	0		0	0	
Length		40			5.3
Cross section area		5.5			2.83
f		15.11553723			2.792078295
Form Factor	1.139142456	1.05516207	1.154130585	1.14100045	1.125354651

Interference drag	1.05	1	1.04	1.04	1.5
Swet	559	510	129	85.9	15
Sref	292	292	292	292	292
CD0,c	0.006096976	0.004116779	0.001492153	0.00093683	0.000526588
Leakage	10	5			

CD0	0.015144726

I.3 Combat

	Wing	Fuselage	Horizontal Stabilizer	Vertical Stabilizer	Engine
ρ (slug/ft^3)	0.001756	0.001756	0.001756	0.001756	0.001756
Velocity (ft/s)	337	337	337	337	337
Length (ft)	6.74	40	4.95	6.8	5.3
Dynamic Viscosity (slug/ft*s)	3.53E-07	3.53E-07	3.53E-07	3.53E-07	3.53E-07
RE	11286200.57	66980418.79	8288826.825	11386671.19	8874905.49
k (skin roughness)	5.00E-06	5.00E-06	5.00E-06	5.00E-06	5.00E-06
RE cutoff	108827961.5	709791499.6	78628664.2	109848342.5	84493658.25
Cf Laminar skin friction coefficient	0.000395298	0.000162265	0.000461266	0.00039355	0.000445776
M	0.3	0.3	0.3	0.3	0.3
Cf Turbulent skin friction coefficient	0.002921754	0.002233835	0.003070059	0.002917644	0.003036349
Frct lam	0.1	0	0.1	0.1	0
Frct turb	0.9	1	0.9	0.9	1
Cf Weighted average skin friction	0.002669108	0.002233835	0.00280918	0.002665234	0.003036349
t/c	0.12		0.12	0.12	
x/c	2.022		1.485	2.04	
M cruise	0.3	0.3	0.3	0.3	0.3
Quarter chord sweep angle	0		0	0	
Length		40			5.3
Cross section area		5.5			2.83
f		15.11553723			2.792078295
Form Factor	1.139704127	1.05516207	1.1535968	1.139365142	1.125354651

Interference drag	1.25	1	1.04	1.04	1.5
Swet	579	510	132	93.1	15
Sref	302	302	302	302	302
CD0,c	0.007290208	0.003980462	0.001473106	0.000973586	0.000509151
Leakage	10	5			

CD0	0.01636049

I.4 Surveillance

Component Build Up					
	Wing	Fuselage	Horizontal Stabilizer	Vertical Stabilizer	Engine
ρ (slug/ft^3)	0.001756	0.001756	0.001756	0.001756	0.001756
Velocity (ft/s)	337	337	337	337	337
Length (ft)	6.35	40	5.06	7.78	5.3
Dynamic Viscosity (slug/ft*s)	3.53E-07	3.53E-07	3.53E-07	3.53E-07	3.53E-07
RE	10633141.48	66980418.79	8473022.977	13027691.45	8874905
k (skin roughness)	5.00E-06	5.00E-06	5.00E-06	5.00E-06	5.00E-06
RE cutoff	102207403.6	709791499.6	80469650.92	126579430.9	84493658
Cf Laminar skin friction coefficient	0.000407256	0.000162265	0.000456225	0.000367929	0.000446
M	0.3	0.3	0.3	0.3	0.3
Cf Turbulent skin friction coefficient	0.002949605	0.002233835	0.003059158	0.002856183	0.003036
Frct lam	0.1	0	0.1	0.1	0
Frct turb	0.9	1	0.9	0.9	1
Cf Weighted average skin friction	0.00269537	0.002233835	0.002798864	0.002607358	0.003036
t/c	0.12		0.12	0.12	
x/c	1.905		1.518	2.334	
M cruise	0.3	0.3	0.3	0.3	0.3
Quarter chord sweep angle	0		0	0	
Length		40			5.3
Cross section area		5.5			2.83
f		15.11553723			2.792078
Form Factor	1.142063675	1.05516207	1.152459605	1.134568521	1.125355

Interference drag	1.05	1	1.04	1.04	1.5
Swet	649	510	140	122	15
Sref	335	335	335	335	335
CD0,c	0.006261782	0.003588357	0.001401923	0.001120417	0.000459
Leakage	10	5			

CD0	0.014756196

I.5 Decoy

Component Build Up					
	Wing	Fuselage	Horizontal Stabilizer	Vertical Stabilizer	Engine
ρ (slug/ft^3)	0.001756	0.001756	0.001756	0.001756	0.001756
Velocity (ft/s)	337	337	337	337	337
Length (ft)	7.05	40	5.12	6.82	5.3
Dynamic Viscosity (slug/ft*s)	3.53E-07	3.53E-07	3.53E-07	3.53E-07	3.53E-07
RE	11805298.81	66980418.79	8573493.605	11420161.4	8874905
k (skin roughness)	5.00E-06	5.00E-06	5.00E-06	5.00E-06	5.00E-06
RE cutoff	114105023.1	709791499.6	81474722.89	110188575.8	84493658
Cf Laminar skin friction coefficient	0.000386509	0.000162265	0.000453544	0.000392972	0.000446
M	0.3	0.3	0.3	0.3	0.3
Cf Turbulent skin friction coefficient	0.002900983	0.002233835	0.003053333	0.002916284	0.003036
Frct lam	0.1	0	0.1	0.1	0
Frct turb	0.9	1	0.9	0.9	1
Cf Weighted average skin friction	0.002649536	0.002233835	0.002793354	0.002663953	0.003036
t/c	0.12		0.12	0.12	
x/c	2.115		1.536	2.046	
M cruise	0.3	0.3	0.3	0.3	0.3
Quarter chord sweep angle	0		0	0	
Length		40			5.3
Cross section area		5.5			2.83
f		15.11553723			2.792078
Form Factor	1.138014813	1.05516207	1.151859913	1.139253473	1.125355
Interference drag	1.05	1	1.04	1.04	1.5
Swet	594	510	145	94	15
Sref	309	309	309	309	309
CD0,c	0.006086042	0.00389029	0.001570249	0.000960173	0.000498
Leakage	10	5			

CD0	0.014955027

Appendix J - Installed Power

J.1 Equations

η_{gen}	0.9
VA	2000
P_{el}	=0.00134*B2/B1
c_p (sfc)	0.4
SHP	375
η_{fp}	0.65
P_{fp}	=0.00014*B6*B7/B8
Δp_{hydr} (psi)	1500
V_{hydr} (gal/min)	5
η_{hp}	0.75
P_{hydr}	=0.0006*B12*B13/B14
P_{other}	0
P_{mech}	=B10+B16+B18
P_{extr}	=B4+B20
$\eta_{inl/inc}$	1
SHP_{av}	375
η_{gear}	1
η_p	0.8
T_s (°F)	23.36
Ts (K)	268.35
T_{inlet} (°F)	250
T_{inlet} (K)	394
HP chart	375
Actual	=B37*SQRT(B33/B36)

J.2 Values

η_{gen}	0.9
VA	2000
P_{el}	2.9777778
c_p (sfc)	0.4
SHP	375
η_{fp}	0.65
P_{fp}	0.0323077
Δp_{hydr} (psi)	1500
V_{hydr} (gal/min)	5
η_{hp}	0.75
P_{hydr}	6
P_{other}	0
P_{mech}	6.0323077
P_{extr}	9.0100855
$\eta_{inl/inc}$	1
SHP_{av}	375
η_{gear}	1
η_p	0.8
T_s (°F)	23.36
Ts (K)	268.35
T_{inlet} (°F)	250
T_{inlet} (K)	394
HP chart	375
Actual	309.48098

Appendix K - Performance Calculations

K.1 Equations

Stall	
W (lb)	8165
ρ (slug/ft^3)	0.001756
C_{LMax}	1.5
S (ft^2)	292
V_s (knots)	=((2*B3)/(B15*B5*B6))^(1/2)
Takeoff	pg 139
V_3/V_{STO}	1.15
f_{TO}	1
h_{TO} (ft)	50
μ_g	0.02
C_{D0}	0.0151447258963347
C_{LmaxTO}	1.7
ρ (slug/ft^3)	0.002377
μ'	=B12+0.72*(B13/B14)
Vcr (knots)	200
P_{TO} (HP)	750
P_{TO}/D_p^2	7
σ	1
A	7.5
N (# of engines)	2
T	=4.6*B18*((B20*B22/B19)^(1/3))
γ_{LOF}	=0.9*(B23/B3)-0.3/(B21^0.5)
S_{TO} (ft)	=B10*B11*((1/B24)+((B9^2)*(B3/B6)*(1/((B23/B3)-B16)+1.414)/((B11*B15*32.12*B14)*(1+1.414*B24))))
T/W OEI	=(B23/2)/B3
γ_{2min}	0.024
C_L OEI	1.27
C_D OEI	0.11
$(C_L/C_D)_{TO\_OEI}$^-1	=1/(B28/B29)
γ_2	=B26-B30
BFL (ft)	=(655/(B20^0.5))+(0.863/(1+2.3*(B31-B27)))*((B3/B6)/(0.694*B15*32.12*B14)+B11)*(1/((B23/B3)-B16)+2.7)
V_{LOF} (knot)	=B7*1.1
S_{TOG} (ft) (groundrun)	=((B33^2)/(2*32.12))/((B23/B3)-B16)
Climb	
η_p	0.8
C_L	1.23
C_D	0.11
RC (ft/min)	=33000*(B36/(B3/B18)-((B3/B6)^0.5/(19*((B37^1.5)/(B38))*B20^0.5)))
t_{cl} (min)	=1/B39*10000
Cruise	
q (lb/ft^2)	100
C_{L_cr}	=B3/(B42*B6)
η_p	0.8
L/D cruise	7
$(T/W)_{CR}$	=1/B45
f_{mp}	326
cp	0.4
Wf (lb)	4810
Range (nmi)	=B47*(B44/B48)*(B45)*LN(B3/B49)

Endurance/Loiter	
C_{L_ltr}	=B49/(B6*B42)
L/D loiter	12.4
$(T/W)_{ltr}$	=1/B53
C_{D_ltr}	0.04957
E (hours)	=778*(B44/B48)*((B4*B6)^(0.5))*((B52^(3/2))/B55)*((B49^-0.5)-(B3^-0.5))
Descent	
C_{L_dsc}	=B52
C_{D_dsc}	=B55
tan γ	=-B59/B58
γ	=ATAN(B60)
cos γ	=COS(B61)
h (ft)	10000
R_{GL} (ft)	=-B63/B60
RD (ft/min)	=SQRT((B49/B6)*(2/B4)*((B59^2)/(B58^3))*(B62^3))
t_{GL} (s)	=B63/B65
Landing	
V_{SL} (knots)	=((2*B49)/(B15*B5*B6))^(1/2)
V_A (knots)	=B69*1.2
Δn	0.1
γ_{bar}	=0.1
V_{TD} (knots)	=B70*SQRT((1-(B72^2)/B71))
h_L (ft)	50
s_{AIR} (ft)	=(1/B72)*(((B70^2)-(B73^2))/(2*32.12)+B74)
a/g	=0.3
s_{LG} (ft)	=(B73^2)/(2*B76*32.12)
s_L (ft)	=B75+B77

K.2 Cargo

Stall	
W (lb)	8165
ρ (slug/ft^3)	1.76E-03
C_{LMax}	1.5
S (ft^2)	292
V_s (knots)	125.2395349
Takeoff	pg 139
V_3/V_{STO}	1.15
f_{TO}	1
h_{TO} (ft)	50
μ_g	0.02
C_{D0}	0.015144726
C_{LmaxTO}	1.7
ρ (slug/ft^3)	2.38E-03
μ'	0.026414237
Vcr (knots)	200
P_{TO} (HP)	750
P_{TO}/D_p^2	7
σ	1
A	7.5
N (# of engines)	2
T	2272.286458
γ_{LOF}	0.140921846
S_{TO} (ft)	1633.93838
T/W OEI	0.139147977
γ_{2min}	0.024
C_L OEI	1.27
C_D OEI	0.11
$(C_L/C_D)_{TO\_OEI}$^-1	0.086614173
γ_2	0.052533803
BFL (ft)	2601.958574
V_{LOF} (knot)	137.7634884
S_{TOG} (ft) (groundrun)	1172.913774
Climb	
η_p	0.8
C_L	1.23
C_D	0.11
RC (ft/min)	1684.387559
t_{cl} (min)	5.936875956
Cruise	
q (lb/ft^2)	100
C_{L_cr}	0.279623288
η_p	0.8
L/D cruise	7
$(T/W)_{CR}$	0.142857143
f_{mp}	326
cp	0.4
Wf (lb)	4810
Range (nmi)	2415.084607

Endurance/Loiter	
C_{L_ltr}	0.164726027
L/D loiter	12.4
$(T/W)_{ltr}$	0.080645161
C_{D_ltr}	0.04957
E (hours)	5.037152436
Descent	
C_{L_dsc}	0.164726027
C_{D_dsc}	0.04957
tan γ	-0.300923909
γ	-0.292304201
cos γ	0.957582441
h (ft)	10000
R_{GL} (ft)	33230.99201
RD (ft/min)	95.16422097
t_{GL} (s)	105.0815096
Landing	
V_{SL} (knots)	96.12489754
V_A (knots)	115.3498771
Δn	0.1
γ_{bar}	0.1
V_{TD} (knots)	109.4305018
h_L (ft)	50
s_{AIR} (ft)	707.1231964
a/g	0.3
s_{LG} (ft)	621.3695891
s_L (ft)	1328.492786

K.3 Combat

Stall	
W (lb)	7545
ρ (slug/ft^3)	1.76E-03
C_{LMax}	1.5
S (ft^2)	302
V_s (knots)	118.3807
Takeoff	pg 139
V_3/V_{STO}	1.15
f_{TO}	1
h_{TO} (ft)	50
μ_g	0.02
C_{D0}	0.01636
C_{LmaxTO}	1.7
ρ (slug/ft^3)	2.38E-03
μ'	0.026929
Vcr (knots)	200
P_{TO} (HP)	750
P_{TO}/D_p^2	7
σ	1
A	8
N (# of engines)	2
T	2272.286
γ_{LOF}	0.164982
S_{TO} (ft)	1347.602
T/W OEI	0.150582
γ_{2min}	0.024
C_L OEI	1.18
C_D OEI	0.09
$(C_L/C_D)_{TO\_OEI}$^-1	0.076271
γ_2	0.074311
BFL (ft)	2261.991
V_{LOF} (knot)	130.2188
S_{TOG} (ft) (groundrun)	962.5387
Climb	
η_p	0.8
C_L	1.14
C_D	0.09
RC (ft/min)	1982.348
t_{cl} (min)	5.044523
Cruise	
q (lb/ft^2)	100
C_{L_cr}	0.249834
η_p	0.8
L/D cruise	6.1
$(T/W)_{CR}$	0.163934
f_{mp}	326
cp	0.4
Wf (lb)	4175
Range (nmi)	2353.591

Endurance/Loiter	
C_{L_ltr}	0.138245
L/D loiter	12.8
$(T/W)_{ltr}$	0.078125
C_{D_ltr}	0.04957
E (hours)	4.657559
Descent pg 161	
C_{L_dsc}	0.138245
C_{D_dsc}	0.04957
tan γ	-0.35857
γ	-0.34429
cos γ	0.941317
h (ft)	10000
R_{GL} (ft)	27888.85
RD (ft/min)	110.5162
t_{GL} (s)	90.4845
Landing	
V_{SL} (knots)	88.06018
V_A (knots)	105.6722
Δn	0.1
γ_{bar}	0.1
V_{TD} (knots)	100.2495
h_L (ft)	50
s_{AIR} (ft)	673.8265
a/g	0.3
s_{LG} (ft)	521.4796
s_L (ft)	1195.306

K.4 Surveillance

Stall	
W (lb)	7722
ρ (slug/ft^3)	1.76E-03
C_{LMax}	1.5
S (ft^2)	336
V_s (knots)	**113.5403**
Takeoff	pg 139
V_3/V_{STO}	1.15
f_{TO}	1
h_{TO} (ft)	50
μ_g	0.02
C_{D0}	0.014756
C_{LmaxTO}	1.7
ρ (slug/ft^3)	2.38E-03
μ'	0.02625
Vcr (knots)	200
P_{TO} (HP)	750
P_{TO}/D_p^2	7
σ	1
A	10
N (# of engines)	2
T	2272.286
γ_{LOF}	0.169967
S_{TO} (ft)	1265.567
T/W OEI	0.147131
γ_{2min}	0.024
C_L OEI	1.72
C_D OEI	0.15
$(C_L/C_D)_{TO\_OEI}$^-1	0.087209
γ_2	0.059921
BFL (ft)	2219.314
V_{LOF} (knot)	124.8943
S_{TOG} (ft) (groundrun)	905.9957
Climb	
η_p	0.8
C_L	1.67
C_D	0.14
RC (ft/min)	2023.959
t_{cl} (min)	4.940811
Cruise	
q (lb/ft^2)	100
C_{L_cr}	0.229821
η_p	0.8
L/D cruise	6.2
$(T/W)_{CR}$	0.16129
f_{mp}	326
cp	0.4
Wf (lb)	4543
Range (nmi)	2144.436

Endurance/Loiter	
C_{L_ltr}	0.135208
L/D loiter	14.2
$(T/W)_{ltr}$	0.070423
C_{D_ltr}	0.04957
E (hours)	4.14358
Descent pg 161	
C_{L_dsc}	0.135208
C_{D_dsc}	0.04957
tan γ	-0.36662
γ	-0.3514
cos γ	0.938891
h (ft)	10000
R_{GL} (ft)	27276.24
RD (ft/min)	112.5617
t_{GL} (s)	88.84015
Landing	
V_{SL} (knots)	87.08764
V_A (knots)	104.5052
Δn	0.1
γ_{bar}	0.1
V_{TD} (knots)	99.1423
h_L (ft)	50
s_{AIR} (ft)	670.0082
a/g	0.3
s_{LG} (ft)	510.0247
s_L (ft)	1180.033

K.5 Decoy

Stall	
W (lb)	7434
ρ (slug/ft^3)	1.76E-03
C_{LMax}	1.5
S (ft^2)	310
V_s (knots)	115.9806
Takeoff	pg 139
V_3/V_{STO}	1.15
f_{TO}	1
h_{TO} (ft)	50
μ_g	0.02
C_{D0}	0.014955
C_{LmaxTO}	1.7
ρ (slug/ft^3)	2.38E-03
μ'	0.026334
Vcr (knots)	200
P_{TO} (HP)	750
P_{TO}/D_p^2	7
σ	1
A	7.5
N (# of engines)	2
T	2272.286
γ_{LOF}	0.165551
S_{TO} (ft)	1290.82
T/W OEI	0.152831
γ_{2min}	0.024
C_L OEI	1.18
C_D OEI	0.09
$(C_L/C_D)_{TO\_OEI}$^-1	0.076271
γ_2	0.076559
BFL (ft)	2183.994
V_{LOF} (knot)	127.5786
S_{TOG} (ft) (groundrun)	907.0613
Climb	
η_p	0.8
C_L	1.15
C_D	0.09
RC (ft/min)	2042.731
t_{cl} (min)	4.895406
Cruise	
q (lb/ft^2)	100
C_{L_cr}	0.239806
η_p	0.8
L/D cruise	6.2
$(T/W)_{CR}$	0.16129
f_{mp}	326
cp	0.4
Wf (lb)	4385
Range (nmi)	2133.88

Endurance/Loiter	
C_{L_ltr}	0.141452
L/D loiter	12.4
$(T/W)_{ltr}$	0.080645
C_{D_ltr}	0.04957
E (hours)	4.316265
Descent	
C_{L_dsc}	0.141452
C_{D_dsc}	0.04957
tan γ	-0.35044
γ	-0.33706
cos γ	0.943729
h (ft)	10000
R_{GL} (ft)	28535.73
RD (ft/min)	108.4264
t_{GL} (s)	92.22847
Landing	
V_{SL} (knots)	89.07559
V_A (knots)	106.8907
Δn	0.1
γ_{bar}	0.1
V_{TD} (knots)	101.4054
h_L (ft)	50
s_{AIR} (ft)	677.8584
a/g	0.3
s_{LG} (ft)	533.5752
s_L (ft)	1211.434

Appenndix L - Cost Analysis

L.1 Equations

Raymer		
W_e (lb)	4536	
V (knots)	200	
Q (# produced)	1000	
FTA	2	
N_{eng}	2	
T_{max}	1448	
M_{max}	0.3	
$T_{turbine\_inlet}$ (°R)	2460	
$C_{avionics}$	=4000*(B2*0.1)	
	2012	2024
Engineering rate	115	153.12
Tooling rate	118	157.12
QC rate	108	143.8
Manufacturing rate	98	130.49
	2012	2024
Engineering hours	=4.86*(B2^0.777)*(B3^0.894)*(B4^0.163)	
Tooling hours	=5.99*(B2^0.777)*(B3^0.696)*(B4^0.263)	
Mfg hours	=7.37*(B2^0.82)*(B3^0.484)*(B4^0.641)	
QC hours	=0.076*B19	
Devel support cost	=91.3*(B2^0.63)*(B3^1.3)	=B21*L27
Flight test cost	=2498*(B2^0.325)*(B3^0.822)*(B5^1.21)	=B22*L27
Mfg materials cost	=22.1*(B2^0.921)*(B3^0.621)*(B4^0.799)	=B23*L27
Engine production cost	=3112*(0.043*B7+243.25*B8+0.969*B9-2228)	=B24*L27
RDT&E + flyaway	=B17*B12+B18*B13+B19*B15+B20*B14+B21+B22+B23+B24*B6+B10	=B17*C12+B18*C13+B19*C15+B20*C14+C21+C22+C23+C24*B6+B10
Cost per unit	=B25/B4	=C25/B4

Nicolai	
W (lb)	4536
S (knots)	200
Q_D (# produced)	2
Q_P (# produced)	1000
Q (# produced)	=S4+S5
E (hours)	=4.86*(S2^0.777)*(S3^0.894)*(S6^0.163)
D ($ in 1998)	=66*(S2^0.63)*(S3^1.3)
D ($)	=S8*S26
F ($ in 1998)	=1852*(S2^0.325)*(S3^0.822)*(S4^1.21)
F ($)	=S10*S26
T (hours)	=5.99*(S2^0.777)*(S3^0.696)*(S6^0.263)
L (hours)	=7.37*(S2^0.82)*(S3^0.484)*(S6^0.641)
QC (hours)	=S13*0.076
M ($ in 1998)	=16.39*(S2^0.921)*(S3^0.621)*(S6^0.799)
M ($)	=S15*S26
T (lb)	1448
M_{max}	0.3
T_R (°R)	2460
P ($ in 1998)	=2306*(0.043*S17+243.3*S18+0.969*S19-2228)
P ($)	=S20*S26
R_{eng} (1998 $/hour)	88.85
R_{tool} (1998 $/hour)	94.23
R_{MFG} (1998 $/hour)	75.37
R_{QC} (1998 $/hour)	82.8
CPI_{1998}	1.9
R_{eng} ($/hour)	=S22*S26
R_{tool} ($/hour)	=S23*S26
R_{MFG} ($/hour)	=S24*S26
R_{QC} ($/hour)	=S25*S26
C_{eng} ($)	=S7*S27
C_{tool} ($)	=S12*S28
C_{mfg} ($)	=S13*S29
C_{qc} ($)	=S14*S30
Total cost	=S9+S11+S16+S21+S31+S32+S33+S34
Cost per unit	=S35/S5

Snorri	
$W_{airframe}$ (lb)	4536
V_H (knots)	200
N (# produced over 5 years)	1000
$N_{prototype}$	2
N_{eng}	2
P_{BHP}	375
F_{cert}	1
F_{cf}	1
f_{COMP}	
F_{COMP}	=L10+1
F_{press}	1.03
H_{eng} (hours)	=0.396*(L2^0.791)*(L3^1.526)*(L4^0.183)*(L8)*L11*L12
Q_m (# produced per month)	=L4/60
F_{taper}	0.95
F_{press}	1.01
H_{tool} (hours)	=1.0032*(L2^0.764)*(L3^0.899)*(L4^0.178)*(L14^0.066)*L15*L9*L11*L16
H_{MFG} (hours)	=9.6613*(L2^0.74)*(L3^0.543)*(L4^0.524)*L8*L9*L11
R_{eng} ($/hour)	92
R_{tool} ($/hour)	61
R_{MFG} ($/hour)	53
CPI_{2012}	1.34
C_{eng} ($)	=2.0969*L13*L19*L22
C_{dev} ($)	=0.6458*(L2^0.873)*(L3^1.89)*(L5^0.346)*L22*L8*L9*L12*L11
C_{ft} ($)	=0.009646*(L2^1.16)*(L3^1.3718)*(L5^1.281)*L22*L8
C_{tool} ($)	=2.0969*L17*L20*L22
C_{mfg} ($)	=2.0969*L18*L21*L22
C_{qc} ($)	=0.13*L27*L8*L11
C_{mat} ($)	=24.896*(L2^0.689)*(L3^0.624)*(L4^0.792)*L22*L8*L9*L16
C_{cert} ($)	=L23+L24+L25+L26
$C_{avionics}$ ($ each AC)	=15000*L22
C_{engine} ($ each AC)	=174*L6*L7*L22
C_{prop} ($)	=3145*L6*L22

Roskam	
Airframe and Design Cost	
V_{max} (knots)	200
N_{rdte}	2
F_{diff}	1.5
F_{cad}	1
W_{ampr} (lb)	=F9-SUM(F10:F20)
W_{TO} (lb)	8165
W_e (lb)	4536
W_1 wheels, brakes, tires(lb)	
W_2 engine (lb)	=484*2
W_3 starter (lb)	
W_4 cooling fluid(lb)	
W_5 fuel cells(lb)	
W_6 batteries (lb)	
W_7 avionics (lb)	766
W_8 (lb)	0
W_9 A/C (lb)	232
W_{10} APU (lb)	
W_{11} trapped fuel (lb)	
Engineering hours (phase 1-3)	=0.0396*(I7^0.791)*(F3^1.526)*(F4^0.183)*(F5*F6)
$R_{e\_r\_1989}$ (\$/hour)	60
CEF_{1989}	3
CEF_{2024}	6
$R_{e\_r\_2024}$ (\$/hour)	=F22*F24/F23
C_{aed_r}	=F21*F25
Development and Testing Cost	
C_{dst_r}	=0.008325*(I7^0.873)*(F3^1.89)*(F4^0.346)*F24*F5
Flight test	
C_{e_r}	=19000*F24
N_e	2
C_{p_r}	=10000
N_p	3
$C_{avionics\_r}$	100000
N_{st}	1
$C_{(e+a)\_r}$	=(F30*F31+F32*F33+F34)*(F4-F35)
MHR_{man_r} (hours)	=28.984*(I7^0.74)*(F3^0.543)*(F4^0.524)*F5
$R_{m\_r\_1989}$	35
$R_{m\_r\_2024}$	=F38*F24/F23
C_{man_r}	=F37*F39
F_{mat}	1
C_{mat_r}	=37.632*F41*(I7^0.689)*(F3^0.624)*(F4^0.792)*F24
N_{r_r}	0.33
MHR_{tool_r} (hours)	=4.0127*(I7^0.764)*(F3^0.899)*(F4^0.178)*(F43)*(F5)
$R_{t\_r\_2024}$	=44*F24/F23
C_{tool_r}	=F44*F45
C_{qc_r}	=0.13*F40
C_{fta_r}	=F36+F40+F42+F46+F47
Flight test	
C_{fto_r} (\$)	=0.001244*(I7^1.16)*(F3^1.371)*((F4-F35)^1.281)*F24*F5
Test and Simulation	
C_{tsf_r}	=0

RDTE Profit	
F_{pro_r}	0.1
C_{pro_r}	=75526314.472027*F54
Cost to Finance RDTE	
F_{fin_r}	0.1
C_{fin_r}	=75526314.472027*F57
Total RDTE Cost	
C_{RDTE}	=F26+F28+F48+F50+F52+F55+F58
Prototype Program Cost	
N_{prot}	2
CEF_{1973}	1.14
C_{prot}	=(1115.4*10^3)*(I7^0.35)*(F62^0.99)*F24/F63
Fuel, Oil, Lubricant Cost	
F_{OL}	1.005
W_{f_used} (lb)	1830
FP	6.98
FD	6
U_{ann_flt}	1200
t_{mis}	4
$N_{mission}$	=F70/F71
N_m	500
N_{rdte}	6
$N_{program}$	=F73+F74
N_{acq}	=F73
N_{res}	=F76*0.1
L_R	=5/10^5
N_{yr}	30
N_{serv}	=F76-F77-0.5*F96
N_{loss}	=F78*450*F70*F79
C_{POL} (total)	=((F66*F67)*(F68/F69)*(F72*F80*F79))
C_{POL} each year	=F82/F79
C_{POL} each year per aircraft	=F83/F73
C_{POL} hourly	=F83/F70/F80
Direct Personnel Cost	
N_{crew}	3
R_{CR}	1.5
Pay_{crew}	100000
OHR_{crew}	3
C_{crewpr} (total)	=F80*F87*F88*F89*F90*F79
C_{crewpr} each year	=F91/F79
	=F92/F70/F80

Maintenance Personnel Cost	
MHR_{flthr}	=15
$R_{m\_ml\_1989}$	=45
CEF_{1989}	=3
CEF_{2024}	=6
$R_{m\_ml\_2024}$	=F114*F116/F115
$C_{mpersdir}$ (total)	=F80*F79*F70*F113*F117
$C_{mpersdir}$ per year	=F119/F79
	=F120/F70/F80
Indirect Personnel Cost	
$f_{persind}$	0.13
$C_{persind}$	=F144*F123
Consumable Materials Cost	
R_{conmat}	=6.5*F116/F115
C_{conmat} (total)	=F80*F79*F70*F113*F128
C_{conmat} per year	=F130/F79
Spare Cost	
f_{spares}	0.17
C_{spares}	=F144*F134
Depot Cost	
f_{depot}	0.17
C_{depot}	=F144*F139
Program Operating Cost	
C_{OPS}	=(F82+F119+F130)/(1-F123-F134-F139)
$C_{OPS/hr}$	**=F144/(F80*F79*F70)**
Compared with	
Fighter EX	**10286.2**
Average for passenger carrier (2018)	8916
Average for passenger carrier (2024)	**11094.04**
Average for cargo carrier (2018)	28744
Average for cargo carrier (2024)	**35765.71**
Average military DOC/hr for UAV (2018)	3030
Average military DOC/hr for UAV (2024)	**3770.18**
Cessna Caravan DOC/Flyaway	1400
Predator Operating Cost (2012)	3624
Predator Operating Cost (2024)	**4909.46**

L.2 Results

Raymer		
W_e (lb)	4536	
V (knots)	200	
Q (# produced)	1000	
FTA	2	
N_{eng}	2	
T_{max}	1448	
M_{max}	0.3	
$T_{turbine\_inlet}$ (°R)	2460	
$C_{avionics}$	$1,814,400.00	
	2012	2024
Engineering rate	115	153.12
Tooling rate	118	157.12
QC rate	108	143.8
Manufacturing rate	98	130.49
	2012	2024
Engineering hours	1.19E+06	
Tooling hours	1.02E+06	
Mfg hours	7.99E+06	
QC hours	6.07E+05	
Devel support cost	$ 18,010,003.23	$ 24,133,404.33
Flight test cost	$ 6,945,509.75	$ 9,306,983.06
Mfg materials cost	$ 345,245,300.98	$ 462,628,703.31
Engine production cost	$ 905,526.65	$ 1,213,405.71
RDT&E + flyaway	$ 1,479,487,595.19	$ 1,972,521,220.28
Cost per unit	$ 1,479,487.60	$ 1,972,521.22

Nicolai	
W (lb)	4536
S (knots)	200
Q_D (# produced)	2
Q_P (# produced)	1000
Q (# produced)	1002
E (hours)	1186133.251
D ($ in 1998)	$ 13,019,279.45
D ($)	$ 24,736,630.95
F ($ in 1998)	$ 5,149,353.10
F ($)	$ 9,783,770.90
T (hours)	1021896.394
L (hours)	8001918.3
QC (hours)	608145.7908
M ($ in 1998)	$ 256,452,989.26
M ($)	$ 487,260,679.59
T (lb)	1448
M_{max}	0.3
T_R (°R)	2460
P ($ in 1998)	$ 671,032.16
P ($)	$ 1,274,961.11
R_{eng} (1998 $/hour)	88.85
R_{tool} (1998 $/hour)	94.23
R_{MFG} (1998 $/hour)	75.37
R_{QC} (1998 $/hour)	82.8
CPI_{1998}	1.9
R_{eng} ($/hour)	168.815
R_{tool} ($/hour)	179.037
R_{MFG} ($/hour)	143.203
R_{QC} ($/hour)	157.32
C_{eng} ($)	$ 200,237,084.74
C_{tool} ($)	$ 182,957,264.75
C_{mfg} ($)	$ 1,145,898,706.29
C_{qc} ($)	$ 95,673,495.81
Total cost	$ 2,147,822,594.14
Cost per unit	$ 2,147,822.59

Snorri	
$W_{airframe}$ (lb)	4536
V_H (knots)	200
N (# produced over 5 years)	1000
$N_{prototype}$	2
N_{eng}	2
P_{BHP}	375
F_{cert}	1
F_{cf}	1
f_{COMP}	
F_{COMP}	1
F_{press}	1.03
H_{eng} (hours)	3.66E+06
Q_m (# produced per month)	16.66666667
F_{taper}	0.95
F_{press}	1.01
H_{tool} (hours)	2.89E+05
H_{MFG} (hours)	3.25E+06
R_{eng} ($/hour)	92
R_{tool} ($/hour)	61
R_{MFG} ($/hour)	53
CPI_{2012}	1.34
C_{eng} ($)	$ 945,807,837.96
C_{dev} ($)	$ 39,392,967.99
C_{ft} ($)	$ 785,896.15
C_{tool} ($)	$ 49,477,875.82
C_{mfg} ($)	$ 484,608,801.07
C_{qc} ($)	$ 62,999,144.14
C_{mat} ($)	$ 72,251,387.79
C_{cert} ($)	$ 1,035,464,577.92
$C_{avionics}$ ($ each AC)	$ 20,100.00
C_{engine} ($ each AC)	$ 174,870.00
C_{prop} ($)	$ 8,428.60

Roskam	
Airframe and Design Cost	
V_{max} (knots)	200
N_{rdte}	2
F_{diff}	1.5
F_{cad}	1
W_{ampr} (lb)	2570
W_{TO} (lb)	8165
W_e (lb)	4536
W_1 wheels, brakes, tires(lb)	
W_2 engine (lb)	968
W_3 starter (lb)	
W_4 cooling fluid(lb)	
W_5 fuel cells(lb)	
W_6 batteries (lb)	
W_7 avionics (lb)	766
W_8 (lb)	0
W_9 A/C (lb)	232
W_{10} APU (lb)	
W_{11} trapped fuel (lb)	
Engineering hours (phase 1-3)	147386.0001
$R_{e\_r\_1989}$ ($/hour)	60
CEF_{1989}	3
CEF_{2024}	6
$R_{e\_r\_2024}$ ($/hour)	120
C_{aed_r}	$ 17,686,320.02
Development and Testing Cost	
C_{dst_r}	$ 2,812,737.54
Flight test	
C_{e_r}	$ 114,000.00
N_e	2
C_{p_r}	$ 10,000.00
N_p	3
$C_{avionics\_r}$	$ 100,000.00
N_{st}	1
$C_{(e+a)\_r}$	$ 358,000.00
MHR_{man_r} (hours)	491256.5097
$R_{m\_r\_1989}$	35
$R_{m\_r\_2024}$	70
C_{man_r}	$ 34,387,955.68
F_{mat}	1
C_{mat_r}	$ 3,100,822.91
N_{r_r}	0.33
MHR_{tool_r} (hours)	141880.4627
$R_{t\_r\_2024}$	88
C_{tool_r}	$ 12,485,480.72
C_{qc_r}	$ 4,470,434.24
C_{fta_r}	$ 54,802,693.55
Flight test	
C_{fto_r} ($)	$ 224,563.37
Test and Simulation	
C_{tsf_r}	$ -

RDTE Profit	
F_{pro_r}	0.1
C_{pro_r}	7552631.447
Cost to Finance RDTE	
F_{fin_r}	0.1
C_{fin_r}	7552631.447
Total RDTE Cost	
C_{RDTE}	$ 90,631,577.37
Prototype Program Cost	
N_{prot}	2
CEF_{1973}	1.14
C_{prot}	$ 208,025,645.75
Fuel, Oil, Lubricant Cost	
F_{OL}	1.005
W_{f_used} (lb)	1830
FP	6.98
FD	6
U_{ann_flt}	1200
t_{mis}	4
$N_{mission}$	300
N_m	500
N_{rdte}	6
$N_{program}$	506
N_{acq}	500
N_{res}	50
L_R	0.00005
N_{yr}	30
N_{serv}	450
N_{loss}	810
C_{POL} (total)	$ 8,665,155,225.00
C_{POL} each year	$ 288,838,507.50
C_{POL} each year per aircraft	$ 577,677.02
C_{POL} hourly	$ 534.89
Direct Personnel Cost	
N_{crew}	3
R_{CR}	1.5
Pay_{crew}	$ 100,000.00
OHR_{crew}	3
C_{crewpr} (total)	$ 18,225,000,000.00
C_{crewpr} each year	$ 607,500,000.00
	$ 1,125.00

Maintenance Personnel Cost	
MHR_{flthr}	15
$R_{m\_ml\_1989}$	45
CEF_{1989}	3
CEF_{2024}	6
$R_{m\_ml\_2024}$	90
$C_{mpersdir}$ (total)	$ 21,870,000,000.00
$C_{mpersdir}$ per year	$ 729,000,000.00
	$ 1,350.00
Indirect Personnel Cost	
$f_{persind}$	0.13
$C_{persind}$	$ 8,264,604,111.79
Consumable Materials Cost	
R_{conmat}	13
C_{conmat} (total)	$ 3,159,000,000.00
C_{conmat} per year	$ 105,300,000.00
Spare Cost	
f_{spares}	0.17
C_{spares}	$ 10,807,559,223.11
Depot Cost	
f_{depot}	0.17
C_{depot}	$ 10,807,559,223.11
Program Operating Cost	
C_{OPS}	$ 63,573,877,783.02
$C_{OPS/hr}$	**$ 3,924.31**
Compared with	
Fighter EX	**$ 10,286.20**
Average for passenger carrier (2018)	$ 8,916.00
Average for passenger carrier (2024)	**$ 11,094.04**
Average for cargo carrier (2018)	$ 28,744.00
Average for cargo carrier (2024)	**$ 35,765.71**
Average military DOC/hr for UAV (2018)	$ 3,030.00
Average military DOC/hr for UAV (2024)	**$ 3,770.18**
Cessna Caravan DOC/Flyaway	$ 1,400.00
Predator Operating Cost (2012)	$ 3,624.00
Predator Operating Cost (2024)	**$ 4,909.46**